USGS
science for a changing world

Understanding Contaminants Associated with Mineral Deposits

Circular 1328

U.S. Department of the Interior
U.S. Geological Survey

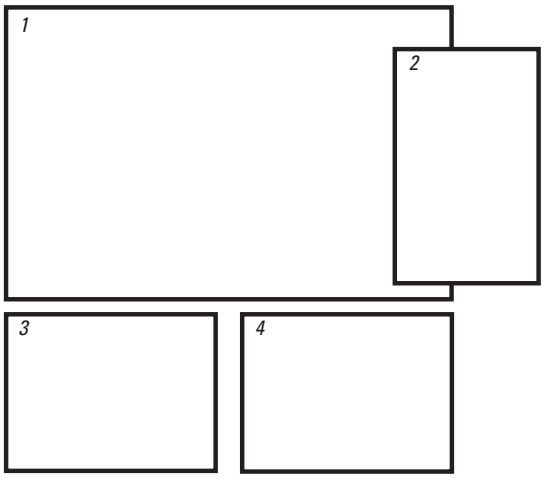

COVER

1 View of Red Mountain mining district, Silverton, Colorado.

2 U.S. Geological Survey scientist performing a stream survey, Red Mountain Creek, Colorado.

3 Silver Ledge mine, Silverton, Colorado.

4 U.S. Geological Survey scientist sampling natural acid spring, Crested Butte, Colorado.

All photographs by Philip L. Verplanck

Understanding Contaminants Associated with Mineral Deposits

Edited by Philip L. Verplanck

Circular 1328

U.S. Department of the Interior
U.S. Geological Survey

U.S. Department of the Interior
DIRK KEMPTHORNE, Secretary

U.S. Geological Survey
Mark D. Myers, Director

U.S. Geological Survey, Reston, Virginia: 2008

This and other USGS information products are available at http://store.usgs.gov/
U.S. Geological Survey
Box 25286, Denver Federal Center
Denver, CO 80225

To learn about the USGS and its information products visit http://www.usgs.gov/
1-888-ASK-USGS

Suggested citation:
Verplanck, P.L., ed., 2008, Understanding contaminants associated with mineral deposits: U.S. Geological Survey Circular 1328, 96 p.

CONTENTS

Understanding Contaminants Associated with Mineral Deposits

Edited By Philip L. Verplanck

Introduction

Interdisciplinary studies by the U.S. Geological Survey (USGS) have resulted in substantial progress in understanding the processes that control

- the release of metals and acidic water from inactive mines and mineralized areas,
- the transport of metals and acidic water to streams, and
- the fate and effect of metals and acidity on downstream ecosystems.

The potential environmental effects associated with abandoned and inactive mines, resulting from the complex interaction of a variety of chemical and physical processes, is an area of study that is important to the USGS Mineral Resources Program. Understanding the processes contributing to the environmental effects of abandoned and inactive mines is also of interest to a wide range of stakeholders, including both those responsible for managing lands with historically mined areas and those responsible for anticipating environmental consequences of future mining operations. The recently completed (2007) USGS project entitled "Process Studies of Contaminants Associated with Mineral Deposits" focused on abandoned and inactive mines and mineralized areas in the Rocky Mountains of Montana, Colorado, New Mexico, Utah, and Arizona, where there are thousands of abandoned mines.

Results from these studies provide new information that advances our understanding of the physical and biogeochemical processes causing the mobilization, transport, reaction, and fate of potentially toxic elements (including aluminum, arsenic, cadmium, copper, iron, lead, and zinc) in mineralized

near-surface systems and their effects on aquatic and riparian habitat. These interdisciplinary studies provide the basis for scientific decisionmaking and remedial action by local, State, and Federal agencies charged with minimizing the effects of potentially toxic elements on the environment.

Current (2007) USGS research highlights the need to understand (1) the geologic sources of metals and acidity and the geochemical reactions that release them from their sources, (2) the pathways that facilitate transport from those sources, and (3) the processes that control the fate of the elements once released from the sources. Experts in the fields of economic geology, structural geology, mineralogy, geophysics, geochemistry, hydrology, ground-water modeling, microbiology, and toxicology came together for a series of studies that address these relationships on scales ranging from the microscopic to the watershed.

This Circular presents results and highlights from the detailed, interdisciplinary studies that include investigations in both mining-affected areas and mineralized but unmined areas. The first section of the Circular describes laboratory and site-scale field investigations that primarily focus on mineralogic and biologic controls on the source and release of metals and acidity from mine-waste rock and hydrothermally altered areas. The second section describes a set of basin- to watershed-scale studies that not only investigate the source and release of metals and acidity but also the transport of these constituents away from the source areas. The third section is a summary of results from postremediation ecosystem monitoring. For more information on these and other project-related studies, please visit the project Web site at *http://minerals.cr.usgs.gov/projects/contaminants/index.html*. The Web site includes a complete bibliography and detailed descriptions of each interdisciplinary study.

Part 1—Laboratory- and Site-Scale Studies of the Sources and Release of Metals

One objective of this project was to better understand the mineralogical controls of metals and acidity in the acid weathering environment of hard-rock mining waste-rock piles and in mineralized but unmined areas. This section includes detailed mineralogical studies highlighting (1) the importance that mineral chemistry has concerning the sources of metals and acidity and (2) how mineral chemistry can be used to determine the potential for the release of metals and acidity from mine-waste material. Furthermore, detailed work on a weathering profile in an extensively hydrothermally altered area documents the change in mineralogy as a result of weathering in an acidic environment and the potential for a once-stable area to become unstable. Bacterial processes serve as another potentially important control on the release of metals and acidity in the acid weathering environment. This section includes results of recent field and laboratory investigations on the function of bacteria in the release and removal of metals from sulfide-rich rocks. To complement these field and laboratory studies, results of an evaluation of a new field screening test of water toxicity from the leaching of mine-waste rock are presented.


USGS
USGS
USGS
science for a changing world

Chapter A: What is weathering in mine waste? Mineralogic Evidence for Sources of Metals in Leachates

by Sharon F. Diehl, Philip L. Hageman, and Kathleen S. Smith

Overview

Mine waste is discarded, uneconomical rock from active and inactive mine sites, and it covers hundreds of thousands of acres in the United States. Case studies of mine waste in the Colorado Rocky Mountains demonstrated a link between the weathering of trace-element-bearing sulfide minerals in mine waste and resulting metal contamination and acidity in receiving streams (Diehl and others, 2006). This study compares mineralogy, weathering textures, and leachate chemistry between the Dinero and Lower Chatauqua mine-waste piles, and the Saints John mine tailings-affected wetland to determine the source of leachable metals. Leaching experiments are a commonly used technique to identify metals that are released from mine waste and enter the environment, thereby affecting ecosystems.

This study identifies mineralogic sources of potentially hazardous metals such as lead, zinc, cobalt, and copper and explains why concentrations of different metals are elevated in surface water at different mine-waste sites. Metals in USGS Field Leach Test (FLT) leachates show a relationship between weathering and mobility of elements from minerals in the mine waste and leachate geochemistry. The two waste piles and wetland are close to timberline, at about 10,500 feet, situated on steep slopes where they are subject to rapid runoff and erosion during precipitation events. The weathering of minerals in mine waste is evidenced by oxidation by-products such as secondary sulfate minerals and dissolution textures such as etch pits on surfaces of sulfide grains.

Introduction

Sulfide minerals such as pyrite (iron sulfide) commonly contain trace metals such as arsenic, lead, zinc, cobalt, and nickel. Sphalerite (zinc sulfide) commonly contains cadmium, and galena (lead sulfide) commonly contains silver. These trace metals render the lattice unstable and increase the solubility of the host sulfide mineral. This chapter describes how metals leaching into the environment at each locality are a result of mineralogic controls such as the residence of trace elements in sulfide minerals, weathering of these minerals, and formation of soluble secondary evaporative salts.

Two abandoned mine waste sites (Dinero, Lower Chatauqua) and one mine-waste-affected wetland site (Saints John) were sampled and subjected to the USGS FLT (U.S. Geological Survey Fact Sheet 2005–3100; Hageman, 2007). The elements that were leached from the samples exhibited a unique geochemical fingerprint that is related to their ore deposit mineralogy (fig. 1).

The Dinero and Lower Chatauqua mine-waste piles are composed of hydrothermally altered and mineralized granite, schist, and gneiss rock fragments, ranging from boulder to silt sized. Two waste-rock piles at Dinero were sources of contaminant metals and acid drainage that negatively affected the downstream ecosystem, including fish populations (Walton-Day and others, 2005). Zinc, cadmium, and lead are major metals of concern in drainages from Dinero waste and an open adit.

The abandoned mine waste in the Lower Chatauqua site is in a similar geological setting as the Dinero waste. The Lower Chatauqua mine-waste pile remains a potential source of zinc, lead, cadmium, cobalt, and nickel contaminants to a downstream drainage, Deer Creek, where aquatic life had high uptake of metals (Yang, 2006). The reason we see high lead content in the Lower Chatauqua mine waste is because galena at this site is not a pure mineral; it contains silver. Figures 2*C* and 4*C* show that galena has weathered to anglesite in the mine waste, and the anglesite has undergone partial dissolution, resulting in releasing lead into the environment.

The Saints John wetland received fluvial tailings from an upstream mill site. The tailings have been deposited as sandbars composed of layered, crossbedded, sand-size grains. Mercury, lead, and zinc are the primary elements of concern in the wetland.

Methods and Techniques

Microanalytical techniques, such as optical mineralogy, scanning electron microscopy, electron microprobe, and laser ablation inductively coupled mass spectrometer (LA–ICP–MS), were used to identify minerals, weathering textures, and the distribution of trace elements in minerals. These microanalytical techniques provide insight into why some minerals are more soluble than others.

In addition, the USGS FLT, which is designed to rapidly characterize the water reactive, readily soluble, mobile phases of mineralogic materials, was used to identify metals in solution (U.S. Geological Survey, 2005; Hageman, 2007). Using FLT leachates, researchers have described geochemical fingerprints for different mined areas (fig. 1).

Weathering of Minerals in Mine Waste and Leachate Geochemistry

Exposure to weathering processes (for example, freeze-thaw cycles, solar radiation, atmospheric oxygen, meteoric precipitation, and microbial activity) causes the breakdown of mineral grains and the formation of reactive, readily soluble secondary mineral phases (figs. 2 and 3). Metals in these soluble mineral phases are released as the mineral dissolves in rainwater or snowmelt.

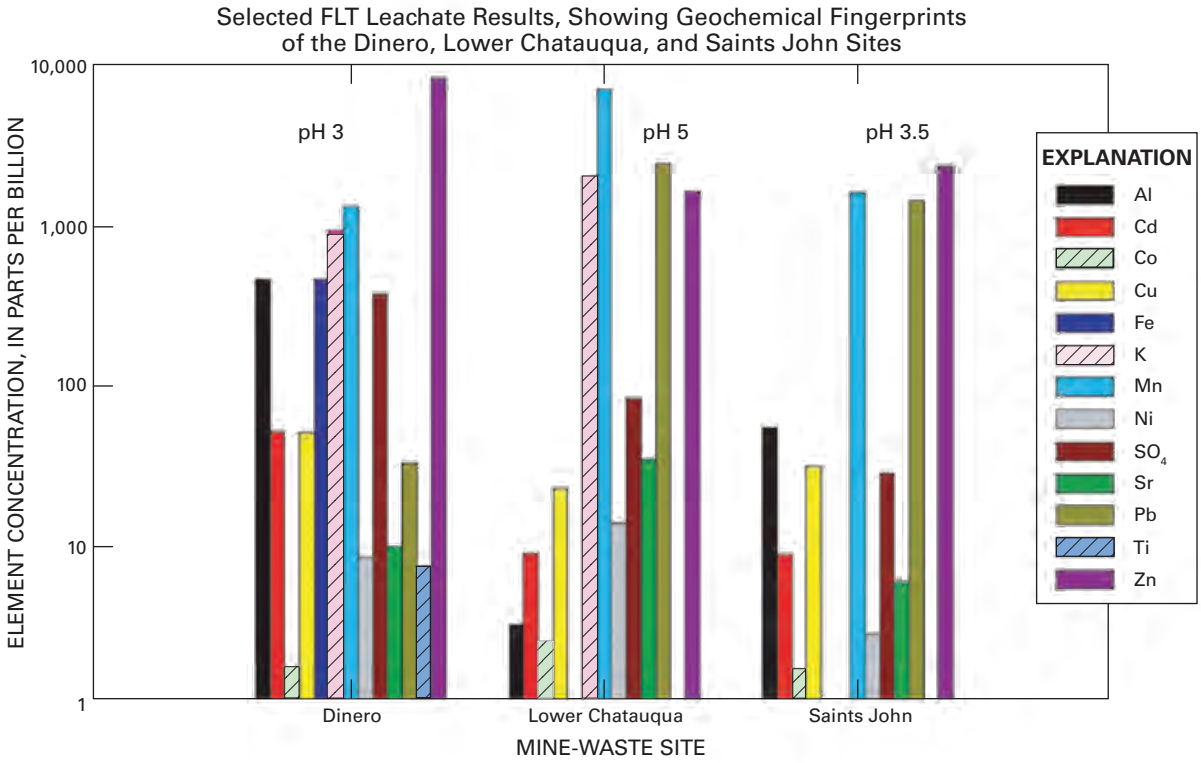

Figure 1. Metals in high concentration leached from Dinero mine waste are zinc, manganese, potassium, iron, and aluminum. In contrast to results from Dinero, lead is high in concentration in solution in Lower Chatauqua waste, and iron is not detected in the leachate. In Saints John leachate, neither potassium nor iron is detected in solution, but elevated levels of manganese, lead, and zinc are going into solution.

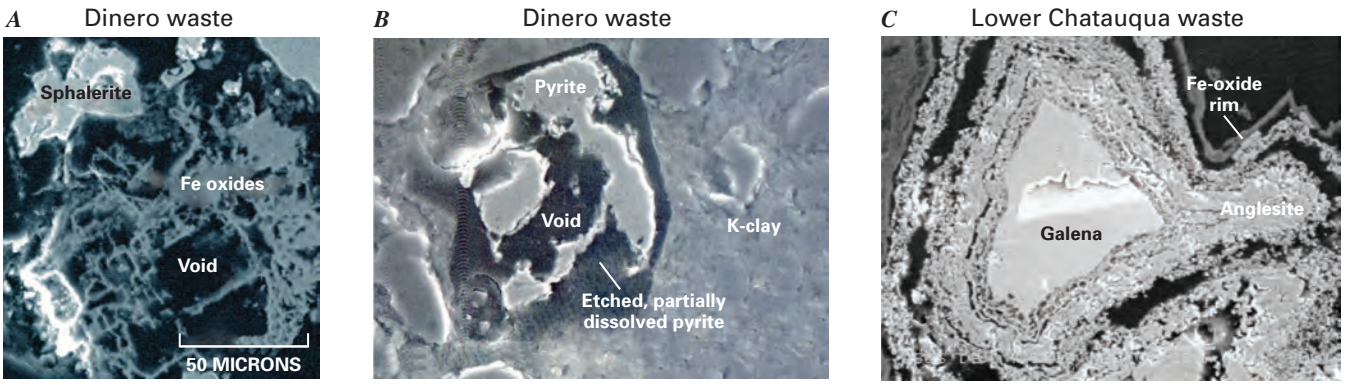

Figure 2. Trace-element-rich sulfide minerals commonly show partial to total dissolution in mine-waste piles. (*A*) Sphalerite ([Zn,Fe]S) shows partial dissolution and remnant iron-oxide rims. (*B*) Pyrite (FeS) is deeply embayed and etched by dissolution processes. (*C*) Galena (PbS) has partially altered to anglesite ($PbSO_4$). Fine-grained, porous anglesite rinds show partial to total dissolution, indicating that weathering of galena and the subsequent dissolution of the secondary weathering product, anglesite, is the primary source for lead in solution.

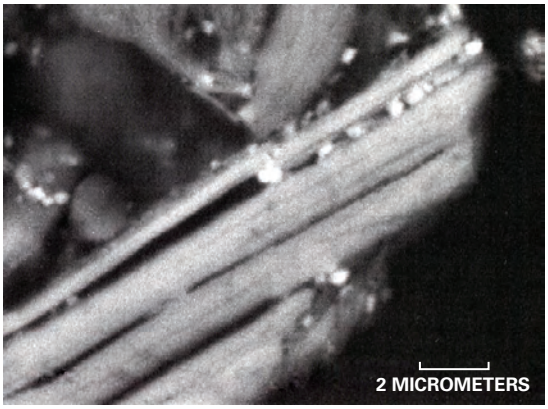

Figure 3. Silicate minerals undergo weathering and dissolution, thereby contributing cations to the formation of secondary minerals. Here, mica [$KAl_3(Si_3Al)O_{10}(OH,F)_2$] from the Saints John tailings has altered by splitting along cleavage planes. Bright spots of lead-bearing jarosite [lead substitutes for potassium in $KFe^{3+}(SO_4)_2(OH)_6$)] have formed between the cleavage planes.

Element distribution maps, also called element intensity maps, show that sulfide minerals such as galena, sphalerite, and pyrite contain varying amounts of trace metals that increase the mineral's susceptibility to dissolution (fig. 4). Warm, yellow-green to red colors in figure 4 indicate relatively high concentrations of an element, and cool, blue colors indicate low concentrations. Figure 4 shows element distribution maps of cadmium in sphalerite, silver in galena, and metals such as cobalt and arsenic in pyrite. Figure 4*A* shows a cadmium-rich sphalerite grain from Dinero mine waste that is highly etched and has undergone partial dissolution. In comparison, a cadmium-poor sphalerite grain from the Saints John tailings (fig. 4*B*) does not show deep etch embayments or the high degree of weathering as the grain in 4*A*.

During dry periods, secondary evaporative minerals form at seeps on the surfaces of mine-waste piles (fig. 5). Element distribution maps show that these highly soluble secondary minerals have a preferred order of precipitation, from early magnesium- and zinc-rich minerals to later manganese-rich minerals and gypsum ($CaSO_4$).

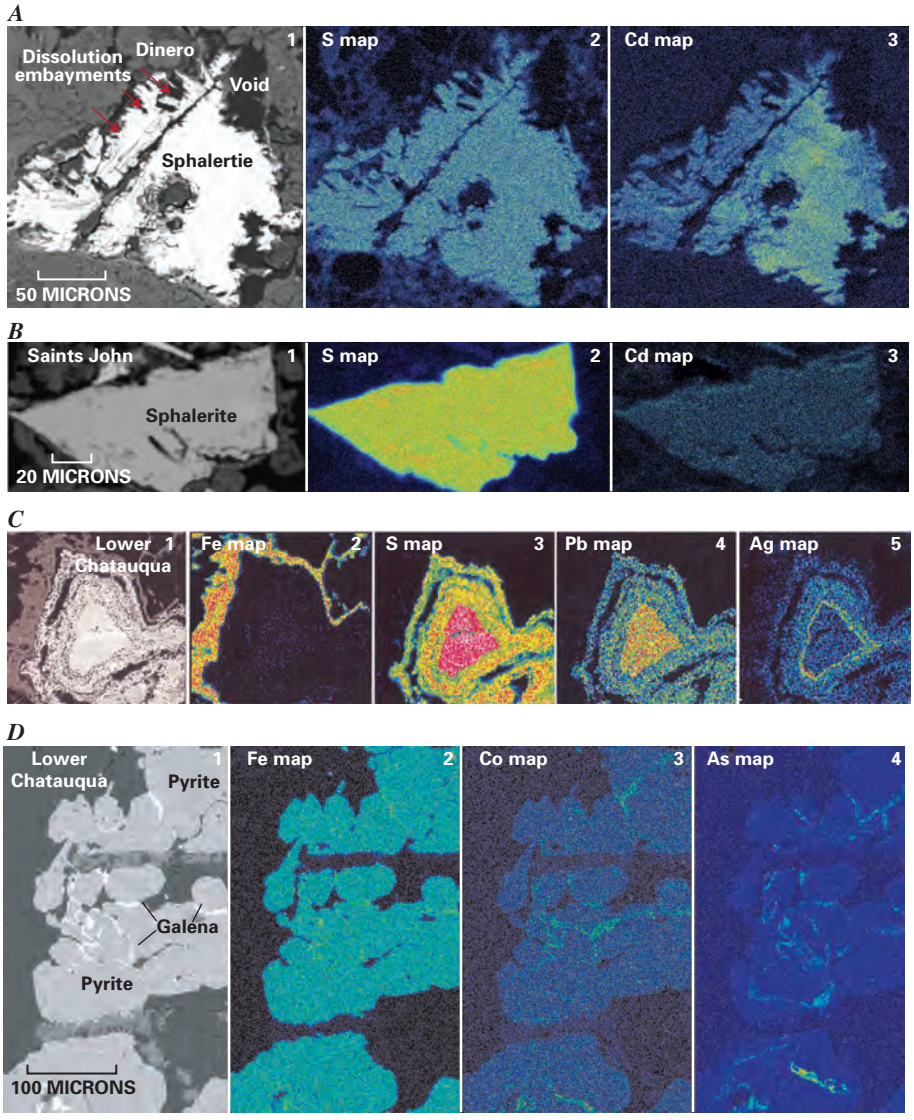

Figure 4. Element distribution maps gathered by electron microprobe show trace-metal enrichment and residence sites in sulfide minerals. (*A*) Sphalerite that hosts cadmium is deeply etched and embayed by dissolution processes. (*B*) Sphalerite that lacks cadmium has not undergone the pitting and deep weathering as its cadmium-rich counterpart in (*A*). (*C*) Silver-rich galena, a sulfide, has undergone partial alteration to anglesite, a sulfate. In turn, the rinds of anglesite have undergone partial dissolution. (*D*) Cobalt and nickel are concentrated in a pyrite within healed fractures (green areas in image 3). The elements arsenic (image 4) and cobalt do not overlap in area, suggesting that these elements precipitated during different times in the deformation history of the ore deposit.

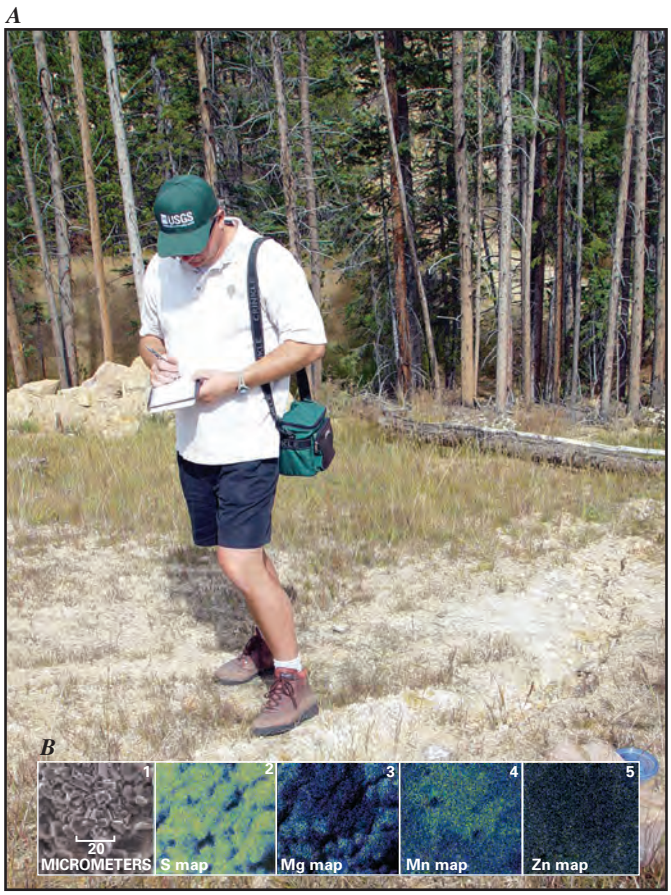

Figure 5. (*A*) U.S. Geological Survey scientist notes development of secondary salts at seep on reclaimed mine-waste material. During dry periods, soluble secondary minerals form on the surfaces and in pore spaces in mine-waste piles. (*B*) Secondary minerals (1) readily dissolve during precipitation events. Yellow color indicates high concentration as shown in the sulfur (S) map (2). The minerals have a preferred order of metal precipitation; magnesium-rich zinc-bearing minerals precipitate first (3), followed by manganese-rich minerals (4). Zinc (5) preferentially precipitates early with magnesium. During wet periods, these minerals will readily dissolve, and magnesium, manganese, and zinc will be flushed downstream.

Effects

Leachate analytical data produced during this study show that metals from the three mine-waste samples are mobilized and may become bioavailable (fig. 1). The FLT leachates produced as part of this study were also the source leachate for bioavailable toxicity studies (Choate and others, this volume.) The uptake of leached metals by flora and fauna was observed in a study of benthic invertebrates in Deer Creek downstream from the Lower Chatauqua mine-waste pile (Yang, 2006). An interesting finding during that study was that no swallows nested along the stream where the highest metal content in aquatic food sources was recorded.

Summary

This study documents that the microscale alteration of mineral grains due to weathering leads directly to the leaching and mobility of acid and metals from the waste materials into the environment upon exposure to and leaching by water. Geochemical fingerprints derived from the FLT leachates, along with the etched, partially dissolved minerals observed in these samples, serve as evidence of this weathering process. The geochemical fingerprints of a waste pile can be used to assess and profile the release and mobility of potential toxic elements into the environment.

In addition, secondary mineral precipitates are observed to be more soluble than original sulfide minerals, as evidenced by the dissolution and reprecipitation of sulfates during wetting and drying cycles. The study also verifies that the USGS FLT is an effective tool to characterize or predict water-reactive, readily soluble phases of mine-waste samples.

References Cited

Diehl, S.F., Hageman, P.L., and Smith, K.S., 2006, What's weathering? Mineralogy and field leach studies in mine waste, Leadville and Montezuma Mining Districts, Colorado, *in* Barnhisel, R.I., ed., Gateway to the future: Society for Mining, Metallurgy, and Exploration (SME) Annual Meeting and 7th International Conference on Acid Rock Drainage (ICARD), March 26–30, St. Louis, Mo. CD–ROM, p. 508–527.

Hageman, P.L., 2007, U.S. Geological Survey field leach test for assessing water reactivity and leaching potential of mine wastes, soils, and other geologic and environmental material: U.S. Geological Survey Techniques and Methods, book 5, chap. D3, 14 p.

U.S. Geological Survey, 2005, A simple field leach test to assess potential leaching of soluble constituents from mine wastes, soils, and other geologic materials: U.S. Geological Survey Fact Sheet 2005–3100 (Contact: P.L. Hageman). *http://pubs.usgs.gov/fs/2005/3100/*

Walton-Day, K., Flynn, J.L., Kimball, B.A., and Runkel, R.L., 2005, Mass loading of selected major and trace elements in Lake Fork Creek near Leadville, Colorado, September–October 2001: U.S. Geological Survey Scientific Investigations Report 2005–5151, 52 p.

Yang, Chi, 2006, Effects of acid mine drainage on nesting tree swallows: Boulder, University of Colorado, Master's thesis, 94 p.

Chapter B: Understanding Jarosite—From Mine Waste to Mars

by Gregg A. Swayze, George A. Desborough, Kathleen S. Smith, Heather A. Lowers, Jane M. Hammarstrom, Sharon F. Diehl, Reinhard W. Leinz, and Rhonda L. Driscoll

Overview

The presence of jarosite, an iron-sulfate mineral, in soil or in mining waste is an indicator of acidic, sulfate-rich conditions. Physical and chemical properties of synthetically prepared jarosites are commonly used as analogs in laboratory studies to determine solubility and acid-generation potential of naturally occurring jarosites. In our work we have mineralogically and chemically characterized both natural and synthetic jarosites. Analyses of natural potassium (K)- and sodium (Na)-jarosites from hydrothermal and weathering environments indicate that there is little solid solution (chemical mixing); instead, they revealed that samples consist of discrete mixtures of potassium- and sodium-endmembers. Hydronium (H_3O^+)-bearing jarosite was detected in only one relatively young natural sample, suggesting that terrestrial H_3O-bearing jarosites are unstable over geologic timescales. Although the presence of H_3O^+ in jarosite is very difficult to measure directly with traditional analytical methods, we found that heating H_3O-bearing samples at high temperatures (greater than 200 to 300 degrees Celsius) produces an $Fe(OH)SO_4$ compound. $Fe(OH)SO_4$ is easily detected by X-ray diffraction and reflectance spectroscopy; hence, it can be used as a "post-mortem" indicator of the presence of H_3O^+ in jarosite. Results from our synthetic jarosite studies indicate that natural H_3O-bearing jarosite, alkali-site deficient, and iron-deficient forms of natural jarosite are metastable and likely are significant factors in acid generation of some mining wastes, but that these natural phases are not accurately represented by synthetic jarosite prepared by commonly used methods. The widespread practice of heating synthetic jarosites to at least 110 degrees Celsius (°C) after synthesis appears to drive off structural water, resulting in samples with crystal structures similar to those of the hydrothermal jarosites, which are a much more stable form of jarosite. Therefore, synthetic jarosite should not be heated above 60°C if it is to be used as an analog for low-temperature natural jarosite found in mine waste. An extension of our work on jarosite reveals that reflectance spectroscopy can be used in remote sensing studies to identify H_3O-bearing and iron-deficient jarosites on the surface of the Earth and Mars.

Introduction

In 1852, a German mineralogist named August Breithaupt discovered a yellowish-brown mineral in Barranco del Jaroso (Jaroso Ravine) in the Sierra Almagrera along the southeastern coast of Spain. He named this potassium-iron-sulfate-hydroxide mineral "jarosite" (Anthony and others, 1990). Jarosite has the chemical formula $KFe_3(SO_4)_2(OH)_6$ but its "garbage can"-like structure can accommodate many other elements to produce chemically diverse varieties like natrojarosite [$NaFe_3(SO_4)_2(OH)_6$], hydronium jarosite [$H_3OFe_3(SO_4)_2(OH)_6$], ammoniojarosite [$NH_4Fe_3(SO_4)_2(OH)_6$], and plumbojarosite [$PbFe_6(SO_4)_4(OH)_{12}$], among others. These are examples of endmember jarosites; intermediate jarosites consist of mixtures of alkali-site cations (for example, K^+ and Na^+, or H_3O^+ and K^+).

Jarosite has been in the headlines as one of the hydrated minerals discovered using the Mossbauer spectrometer on the Opportunity Rover at Eagle Crater on Mars (Klingelhöfer and others, 2004). Here on Earth jarosite is common in acidic soils, in mine waste formed by oxidation of sulfide minerals, or as a product of iron precipitation prior to electrolytic refining of zinc. Because of its association with sulfide minerals, acidic conditions, and heavy metals in mine waste, jarosite can be used as a proxy in remote-sensing studies to locate areas of high acidity and metal leachability (Swayze and others, 2000), thereby providing a rapid way to screen mined areas for potential sources of acidic drainage (fig. 1).

Jarosite's function as a potential source of acid in mine waste is not completely understood. The traditional view is that acid can be generated in mine waste due to the oxidation of sulfide minerals, the dissolution of highly soluble sulfate salts, and the dissolution of less-soluble sulfate minerals, such as jarosite. In waste where all of these materials are mixed together, it is difficult to decipher which ones contribute the most to acid generation. As a further complication, jarosite's compositional variability allows multiple levels of chemical reactivity. Because natural endmember jarosites are very difficult to physically segregate, synthetic jarosites have been used as analogs to determine solubility and dissolution properties of the natural jarosites. Solubility data from synthetic jarosites are used to predict the acid-generation potential of mine-waste materials. Hydronium-bearing jarosite, in particular, is thought to contribute to acid generation in mine wastes because the hydronium ion (H_3O^+) accelerates jarosite dissolution (Gasharova and others, 2005, and references therein).

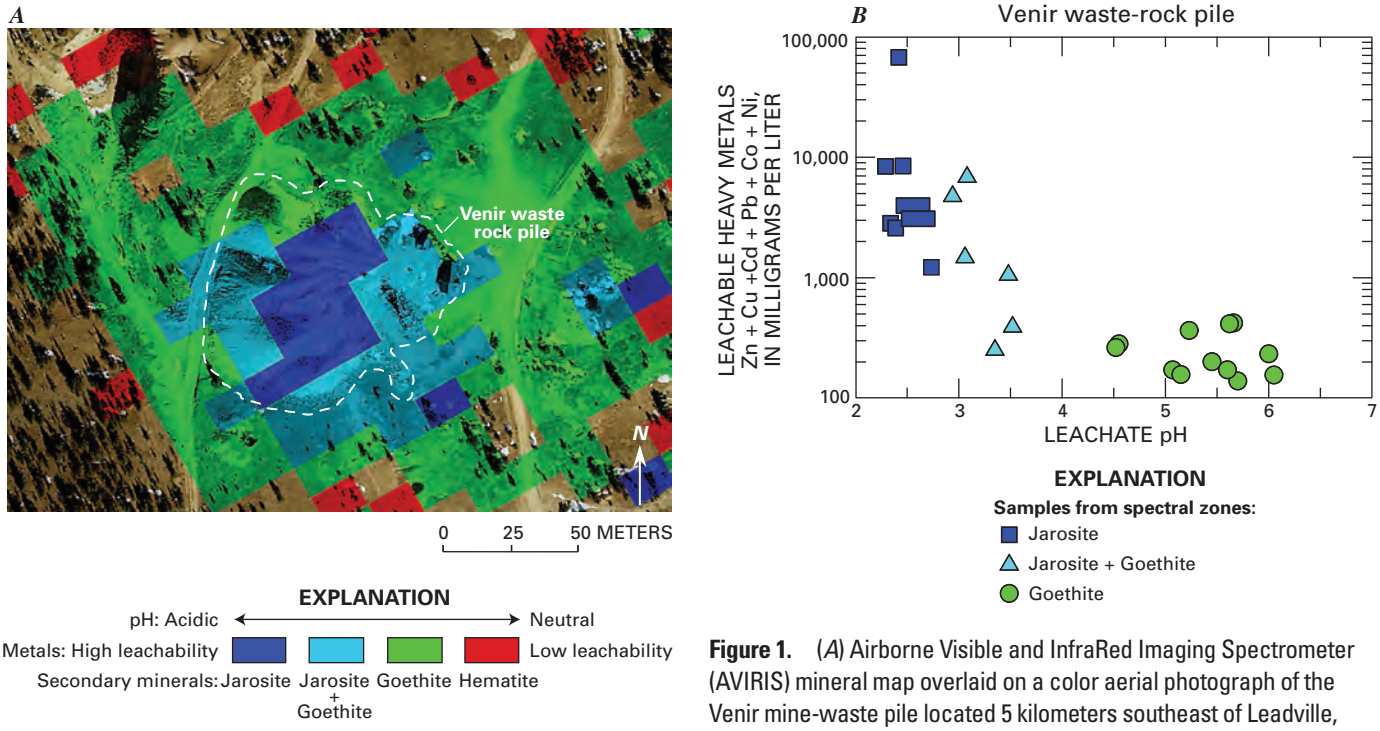

Figure 1. (*A*) Airborne Visible and InfraRed Imaging Spectrometer (AVIRIS) mineral map overlaid on a color aerial photograph of the Venir mine-waste pile located 5 kilometers southeast of Leadville, Colorado. In the aerial photograph white areas are snow, rectangular objects are abandoned mine structures, and dark green objects are lodgepole pines casting shadows. The mineral map overlay shows the spectrally dominant iron-bearing secondary minerals, jarosite, goethite, hematite, and mixtures, for each 20-by-15-meter pixel on the ground. (*B*) Comparison of field and laboratory measurements with AVIRIS mapping demonstrates that jarosite-bearing areas have low pH and higher metal leachability and goethite-bearing areas have more neutral pH and lower metal leachability. Because imaging spectroscopy measures reflected sunlight, it cannot be used to detect minerals deeper than can typically be seen with the human eye; hence, the data can only provide information on minerals exposed in the top few millimeters of the surface.

In this study, a detailed laboratory examination of the mineralogical, microscopic, thermal, and spectral characteristics of jarosite was conducted in order to find clues to its place in the acid-mine drainage story. We studied both natural and synthetic jarosites to see if lessons learned from past research on synthetic jarosites can be used to accurately predict the geochemical behavior of natural ones and to define the environmental conditions under which their comparison to natural samples is valid. While conducting this research we were mindful of how these findings might be used to better understand jarosite formation on Mars and how its presence there constrains Martian surface chemistry.

Jarosite Geochemistry

Jarosites found in mining wastes generally are very fine grained (<5 micrometers), making it very difficult to determine the composition of individual grains. The unit cell of a mineral is the smallest group of atoms that possess the crystallographic symmetry and chemical properties of the mineral. Changes in unit cell parameters can be diagnostic of element substitutions or vacancies within the unit cell, which can lead to decreased stability of a mineral phase. The a- and c-cell dimensions of natural jarosites were examined using X-ray diffraction (XRD) analysis, and it was found that both hydrothermal and low-temperature samples consisted of single K- or Na-jarosite endmembers or pairs of endmembers. This is in contrast to the existence of complete solid solution (chemical mixing) across the sodium-potassium compositional series in jarosites synthesized at hydrothermal temperatures (>100°C). We concluded from these observations that natural jarosites rarely, if at all, form crystals with intermediate composition.

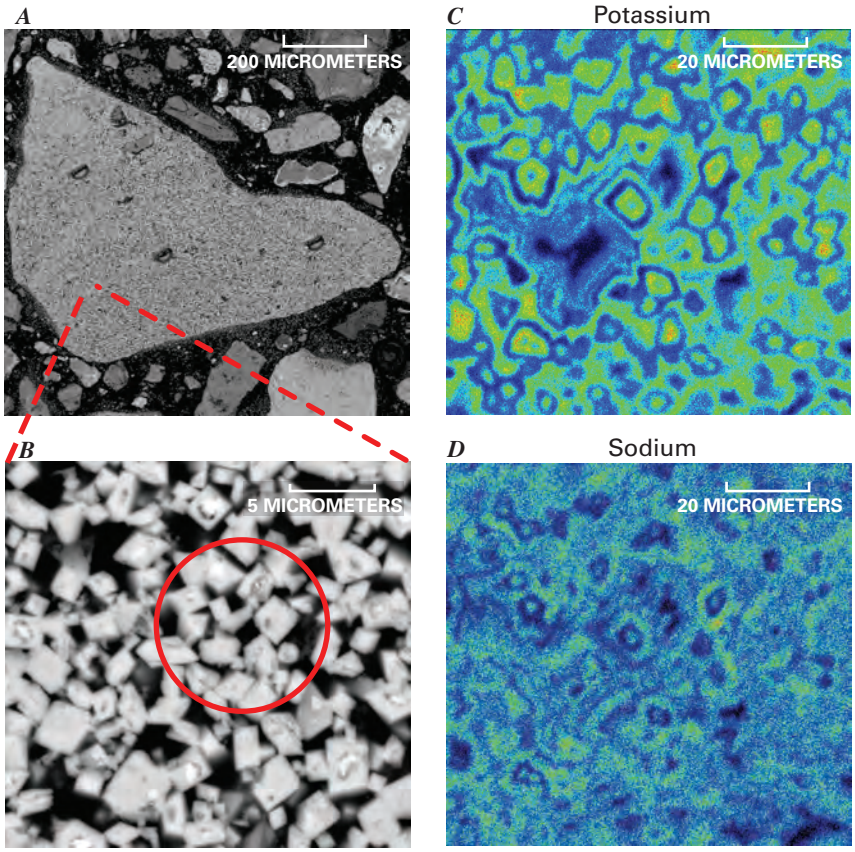

Figure 2. (*A*) Backscattered electron image of a potassium-jarosite sample, originally identified by X-ray diffraction, from a waste-rock pile showing the typical small grain size of low-temperature jarosite minerals observed in mine waste. (*B*) Blowup of (*A*) where the circle represents the diameter of the electron beam defocused to 10 micrometers (μm) for electron microprobe analysis of jarosite, which illustrates the difficulty of obtaining an elemental analysis of compositional zoning within individual grains. (*C*) and (*D*) Electron microprobe X-ray intensity maps of potassium (K) (top) and sodium (Na) (bottom) of about 5- to 10-micrometer jarosite crystals from the Richmond Mine at Iron Mountain in California. Green and orange areas depict regions with greater elemental intensity than blue regions. Note the K- and Na-zoning is less than 2 micrometers across, which suggests that potassium- and sodium-jarosites grew at different times and have limited solid solution (chemical mixing).

Quantitative electron probe microanalysis data of several natural hydrothermal jarosite samples show only endmember compositions for individual grains or zones, and no detectable alkali-site deficiencies, which indicates that there is no H_3O^+ substitution within the analytical uncertainty of the method (fig. 2). In addition, there is no evidence of deficiencies in the natural hydrothermal jarosite samples. X-ray diffraction data for the natural low-temperature (<100°C) K- and Na-jarosites we studied have cell dimensions similar to the "mature" high-temperature hydrothermal jarosites. Hence, it is inferred that these samples also lack alkali- or iron-site vacancies, lack an H_3O^+ component, and instead consist of a mixture of potassium- and sodium-jarosite endmembers. In other words, they chemically resemble the more stable hydrothermal jarosites and do not resemble low-temperature synthetic jarosites.

There is an explanation for the apparent discrepancy between low-temperature synthetic jarosites and natural low-temperature jarosites. A series of five synthetic jarosites were prepared in pressure vessels at 95°C and dried at 60°C for one hour. These samples vary from H_3O-poor and iron-deficient to H_3O-rich (fig. 3). After heating these samples at 110°C for 20 and 40 hours, respectively, structural water losses ranged from 3.5 to 9 weight percent and cell dimensions were reduced significantly. Post-synthesis heating is a common practice used to remove "excess" water from nonstoichiomeric (non-ideal chemical formula) jarosite samples. Heating these samples causes some H_3O^+ in alkali sites near iron vacancies to permanently transfer protons to hydroxyls surrounding these iron vacancies, thereby converting this H_3O^+ to H_2O and the hydroxyls to protonated hydroxyls (OH_2), which are then both lost as water vapor at temperatures near 200°C. Samples with little to no H_3O^+ tend to gradually lose their protonated hydroxyl component as H_2O vapor at temperatures lower than 200°C. Both water-loss processes produce relatively stable stoichiometric (ideal chemical formula) jarosite that may no longer be representative of the chemically reactive type of nonstoichiometric jarosite, which can potentially contribute to acid-mine drainage.

Identification of Hydronium-Bearing Jarosite

Heating synthetic H_3O-bearing jarosite samples up to 240°C results in the production of an XRD-detectable compound with the chemical formula $Fe(OH)SO_4$. The loss of H_3O^+ from the jarosite crystal structure is accompanied by a small but significant change in cell dimensions, which coincides with the development of endmember K-jarosite (Desborough and others, 2006). Formation of crystalline $Fe(OH)SO_4$ from H_3O-bearing jarosite requires the loss of water and formation of amorphous iron hydroxide, as shown in the reaction equation:

$$\underset{\text{hydronium-jarosite}}{(H_3O)Fe_3(SO_4)_2(OH)_6} \rightarrow 2Fe(OH)SO_4 + 2H_2O + \underset{\text{amorphous Fe-hydroxide}}{Fe(OH)_3},$$

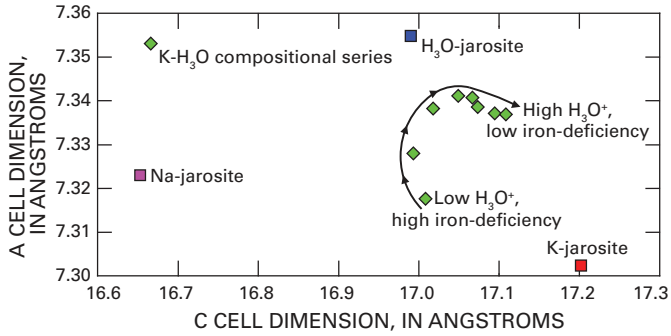

Figure 3. Crystallographic unit-cell dimensions for eight synthetic jarosites with variable hydronium (H_3O^+) content prepared in a pressure vessel at 95 degrees Celsius and then dried in air at 60 degrees Celsius for one hour. Unit-cell dimensions refer to the lengths, usually given in Angstroms (one ten-millionth of a millimeter), of the sides of a unit cell, the smallest group of atoms whose arrangement produces a crystal's symmetry and whose repetition in three dimensions produces a crystal's lattice. Unit-cell values for endmember H_3O-jarosite, sodium (Na)-jarosite, and potassium (K)-jarosite are also shown for reference. Arrow shows trend of unit-cell dimension changes as samples become H_3O-rich. Unit-cell dimensions calculated from X-ray diffraction analysis can be used to measure the H_3O^+ content of natural jarosites, thus helping scientists predict how much acidity and leachable metals they can potentially contribute to acidic mine drainage.

with the remaining jarosite recrystallizing to endmember K-jarosite. Thermogravimetric analysis of synthetic H_3O-bearing jarosite shows evidence of rapid H_2O loss near 200°C (fig. 4), although there is no evidence of rapid H_2O loss at this temperature when H_3O^+ is absent. There is also no XRD-detectable $Fe(OH)SO_4$ produced by heating when H_3O^+ is absent from jarosite samples. Therefore, we conclude that H_3O^+ loss from jarosite is the cause of $Fe(OH)SO_4$ production. Consequently, the easily XRD-detectable $Fe(OH)SO_4$ phase can be used as a "post-mortem" indicator of the presence of H_3O^+ in jarosite.

In the natural jarosites studied, no $Fe(OH)SO_4$ was detected after heating, in agreement with the quantitative electron probe microanalysis results that show no detectable alkali-site deficiencies or H_3O^+ substitution. The sole exception is a sample from the Richmond mine in California, where jarosite-rich stalactites are actively forming from dripping acidic water (Jamieson and others, 2005). These samples yield $Fe(OH)SO_4$ after thermal treatment at 240°C, which indicates that their jarosite contains H_3O^+.

Spectroscopic Studies of Jarosite

Reflectance spectroscopy can be a useful tool for jarosite identification in remote-sensing studies and for detecting the presence of H_3O^+ and iron-deficiencies in jarosite with portable field spectrometers. In the spectral region spanning the ultraviolet to the near-infrared wavelengths (about 0.35 to 2.5 micrometers [μm]), jarosite has many diagnostic absorptions (fig. 5). Most notable is the wide absorption band near 0.9 μm caused by an Fe^{3+}-electronic transition. This spectral feature was used to map for the presence of jarosite in mine waste near Leadville, Colorado (fig. 1*A*). Variations in the wavelength position and shape of vibrational absorptions near 1.4, 1.85, and 2.26 μm can be used to differentiate potassium- from sodium-jarosite and assess the temperature of jarosite formation (Swayze and others, 2006). Hydronium-bearing and iron-deficient jarosites have relatively weak spectral features compared to those of the potassium- and sodium-endmembers, thus allowing them to be recognized using airborne and orbital imaging spectrometers. The relative proportion of protonated hydroxyl (OH_2) to H_3O^+ can be directly measured based on the depth of absorption bands at 1.93 and 1.96 μm, respectively (see vertical arrows in fig. 5). Using this information, it may now be possible to spectrally identify which areas of mine waste have the highest concentrations of H_3O-bearing jarosite and are thus more likely contribute to acidic drainage.

Is synthetic jarosite a suitable analog for natural jarosite in mine waste?

The chemical composition, cell dimensions, and other properties of synthetic jarosites formed at low temperature (<100°C) may simulate relatively young jarosites in mining wastes. Most of the low-temperature synthetic jarosites seem to be metastable (easily changed and more chemically reactive) due to either substitution of H_3O^+ in the mineral's structure or to iron- and

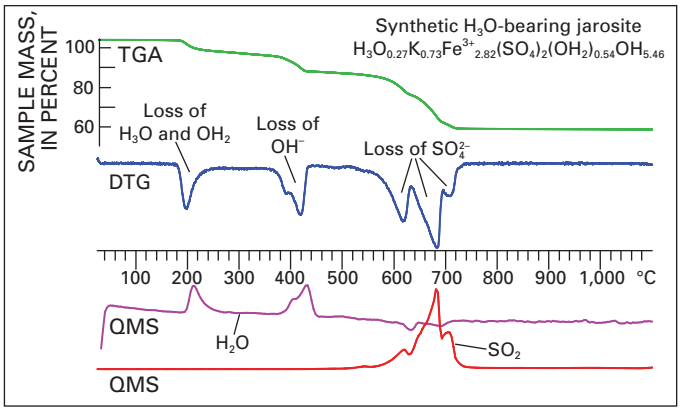

Figure 4. Top: Thermogravimetric Analysis (TGA) curve shows the mass loss as a function of heating a synthetic H_3O-bearing jarosite at a rate of 10 degrees Celsius per minute up to 1,100 degrees Celsius in an inert gas. Middle: Derivative thermogravimetry (DTG) curve shows the first derivative of the TGA curve highlighting changes in the rate-of-mass-loss during heating. Bottom: Quadrupole Mass Spectrometer (QMS) curves record the ion current associated with masses 18 (H_2O) and 64 (SO_2) released during heating. In this jarosite sample, progressive heating drives off H_3O^+ and OH_2 at about 200 degrees Celsius. Near 400 degrees Celsius hydroxyl (OH) is converted to H_2O, and near 680 degrees Celsius SO_4 is converted to SO_2. These kinds of measurements help scientists understand the composition of jarosite.

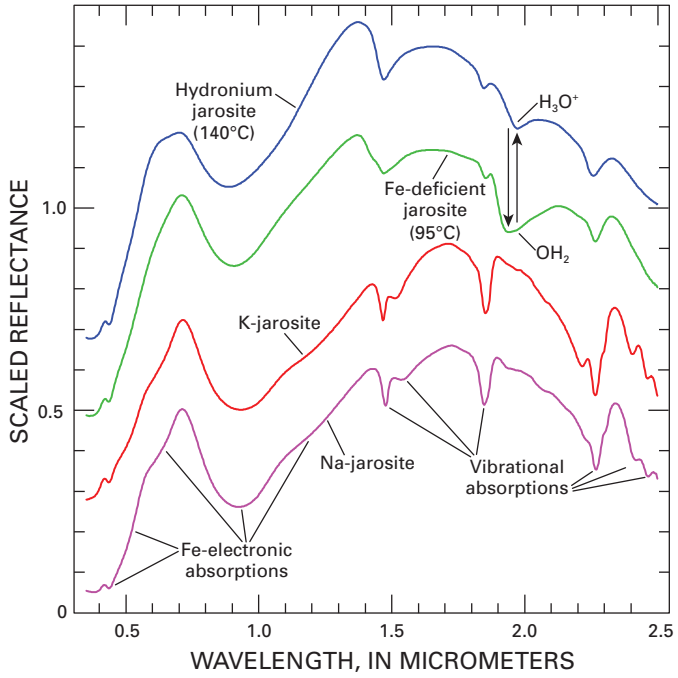

Figure 5. Reflectance spectra of synthetic jarosites (upper two curves) and natural jarosites (lower two curves). Hydronium (H_3O^+)-bearing jarosites have a diagnostic H_3O^+ spectral absorption at 1.96 micrometers. The iron (Fe)-deficient jarosite is potassium (K)-rich with about 10 percent vacancies in the iron site and a diagnostic H_2O spectral absorption at 1.93 micrometers. Synthesis temperatures are listed in parentheses for synthetic samples. Spectra of the natural samples have stronger vibrational absorptions than spectra of the synthetic samples because they do not contain H_3O^+ or protonated hydroxyl (OH_2). Spectra are offset vertically for clarity.

alkali-site deficiencies in the mineral structure. Heating synthetic jarosite samples drives off "excess" water (OH_2) and changes the properties of the jarosites. Over time, recrystallization and desiccation may do the same thing to natural jarosites (fig. 6). Metastable or "modern" low-temperature natural jarosites and synthetic jarosites have larger a- and smaller c-unit-cell dimensions than do "mature" natural jarosites. In addition, mature natural jarosites do not appear to have the site vacancies, iron-deficiencies, or significant H_3O^+ substitutions in the mineral structure that are observed in some synthetic and modern natural jarosites. Recognition of metastable jarosite phases is important because they tend to have different solubility and acid-generation properties than mature or high-temperature synthetic jarosites. In order for synthetic jarosites to be representative of young jarosites from mining wastes, the synthetic jarosites should not be dried at temperatures above 60°C.

What can jarosite tell us about Mars?

As mentioned previously, one of the Mars exploration rovers found jarosite in what many interpret as sedimentary rocks on Mars (fig. 7). A remaining question about this jarosite occurrence is the type of geochemical environment in which it was deposited. One hypothesis suggests that this jarosite may have been deposited in shallow, acid-saline water, but another hypothesis suggests that hydrothermal fluids may have been instrumental in the formation of the jarosite (Golden and others, 2008). In 2007, jarosite was observed on Mars from orbit by the CRISM imaging spectrometer in layered materials south of the Valles Marineris Canyon System (Milliken and others, 2008). A spectrum of this jarosite shows H_3O^+ and protonated hydroxyl (OH_2) absorptions near 1.9 μm, which is consistent with formation of this mineral in an acidic, low-temperature environment. This observation supports an emerging picture of Mars as an initially wet planet that dried up over time. The ability to differentiate spectrally between low-temperature lake sediments and relict high-temperature hydrothermal deposits from Martian orbit can help focus future rover deployment and sample collection on areas with the highest potential of having preserved possible evidence of ancient life. In summary, our studies have led to the recognition that jarosite can, under the right conditions, preserve evidence of the geochemical and thermal conditions in which it formed.

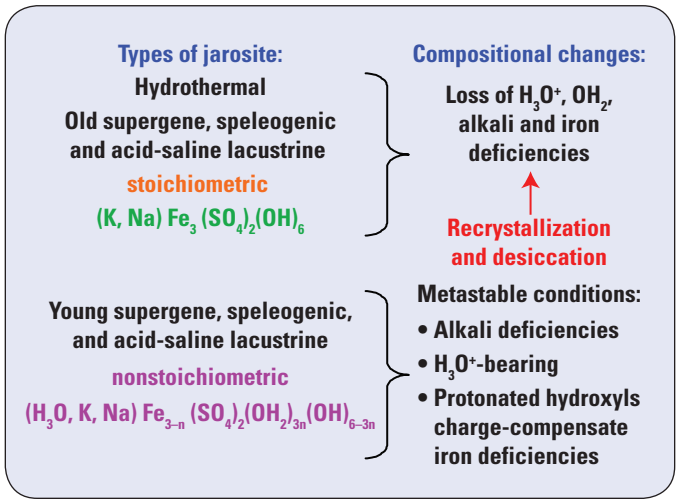

Figure 6. Terrestrial environments in which jarosites are known to form. Hydrothermal formation of jarosite usually involves precipitation from hot (greater than 100 degrees Celsius) fluids. Low-temperature (less than 100 degrees Celsius) sulfide oxidation is responsible for most supergene jarosite formation. Sulfuric acid associated with hydrocarbons may form speleogenic jarosite in caves, whereas highly acidic-saline fluids can cause precipitation of jarosite in lakes. Most hydrothermal jarosites are stoichiometric, having ideal jarosite chemical formulas. The other types of jarosite may be nonstoichiometric initially, but through long-term desiccation they usually recrystallize to stoichiometric forms. In the nonstoichiometric jarosite formula the letter "n" indicates the level of iron deficiency, and if this value is known it can be used to calculate the amount of protonated hydroxyl (OH_2) and normal hydroxyl (OH).

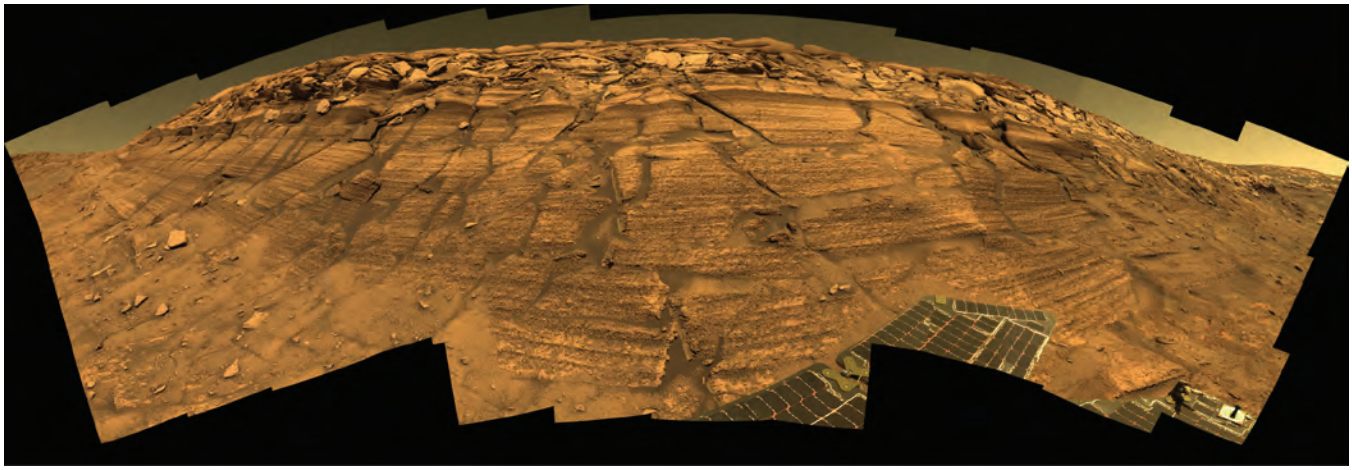

NASA/JPL/Cornell

Figure 7. Approximate true-color mosaic of "Burns Cliff" along the southeastern inner wall of Endurance Crater in Meridiani Planum on Mars. Images were collected by the panoramic camera on the Opportunity Rover. *In-situ* Mossbauer analyses of these crossbedded sediments indicate that they contain spherical hematite-rich concretions known as "blue berries," magnesium sulfates, and jarosite. The mosaic spans more than 180 degrees from side to side.

References Cited

Anthony, J.W., Bideaux, R.A., Bladh, K.W., and Nichols, M.C., 1990, Handbook of mineralogy, volume I. Elements, sulfides, sulfosalts: Tucson, Arizona, Mineral Data Publishing, 588 p.

Desborough, G.A., Smith, K.S., Lowers, H.A., Swayze, G.A., Hammarstrom, J.M., Diehl, S.F., Driscoll, R.L., and Leinz, R.W., 2006, The use of synthetic jarosite as an analog for natural jarosite: Proceedings of the Seventh International Conference on Acid Rock Drainage (ICARD 7), St. Louis, Missouri, March 26–30, 2006, p. 458–475.

Gasharova, B., Gottlicher, J., and Becker, U., 2005, Dissolution at the surface of jarosite—An in situ AFM study: Chemical Geology, v. 215, p. 499–516.

Golden, D.C., Ming, D.W., Morris, R.V., and Graff, T.G., 2008, Hydrothermal synthesis of hematite spherules and jarosite—Implications for diagenesis and hematite spherule formation in sulphate outcrops at Meridiani Planum, Mars: American Mineralogist, v. 93, p. 1201–1214.

Jamieson, H.E., Robinson, C., Alpers, C.N., Nordstrom, D.K., Poustovetov, A., and Lowers, H.A., 2005, The composition of coexisting jarosite-group minerals and water from the Richmond Mine, California: Canadian Mineralogist, v. 43, no. 4, p. 1225–1242.

Klingelhöfer, G., Morris, R.V., Bernhardt, B., Schröder, C., Rodionov, D.S., de Souza, Jr., P.A., Yen, A., Gellert, R., Evlanov, E.N., Zubkov, B., Foh, J., Bonnes, U., Kankeleit, E., Gütlich, P., Ming, D.W., Renz, F., Wdowiak, T., Squyres, S.W., and Arvidson, R.E., 2004, Jarosite and hematite at Meridiani Planum from Opportunity's Mössbauer spectrometer: Science, v. 306, p. 1740–1745.

Milliken, R.E., Swayze, G.A., Arvidson, R.E., Bishop, J.L., Clark, R.N., Ehlmann, B.L., Green, R.O., Grotzinger, J.P., Morris, R.V., Murchie, S., Mustard, J.F., Weitz, C., and the CRISM Science Team, 2008, Opaline silica in young deposits on Mars: Geology, v. 36, no. 11, p. 847–850.

Swayze, G.A., Smith, K.S., Clark, R.N., Sutley, S.J., Pearson, R.N, Rust, G.S., Vance, J.S., Hageman, P.L., Briggs, P.H., Meier, A.L., Singleton, M.J., and Roth, S., 2000, Using imaging spectroscopy to map acidic mine waste: Environmental Science and Technology, v. 34, no. 1, p. 47–54.

Swayze, G.A., Desborough, G.A., Clark, R.N., Rye, R.O., Stoffregen, R.E., Smith, K.S., and Lowers, H.A., 2006, Detection of jarosite and alunite with hyperspectral imaging—Prospects for determining their origin on Mars using orbital sensors, in Martian sulfates as recorders of atmospheric-fluid-rock interactions: Lunar and Planetary Institute, 7072.pdf. available at *http://www.lpi.usra.edu/meetings/sulfates2006/pdf/7072.pdf* and accessed 07/22/08.

Chapter C: In-Situ Acid Weathering Reactions in Areas Affected by Large-Scale and Pervasive Hydrothermal Alteration in the Southern Rocky Mountains

by Dana J. Bove, Heather A. Lowers, Geoff S. Plumlee, and Philip L. Verplanck

Overview

Weathering of pyrite-rich, hydrothermally altered rocks can produce acidic, metal-rich waters. This study of large-scale, pervasively altered, unmined areas in Colorado and New Mexico documents the in-situ mineralogical changes of the hydrothermally altered rocks (altered protolith) in response to this acid weathering. Quantitative X-ray diffraction analyses document a decrease in the amount of chlorite, illite, pyrite ± plagioclase in the protolith as weathering progresses. The decreased abundance of these minerals is associated with a concurrent increase in smectite (a highly swelling clay), kaolinite, and jarosite. The data indicate that waters related to pyritic weathering are initially acidic and result in the precipitation of kaolinite. As solutions evolve locally to more neutral compositions, they precipitate and equilibrate with smectite. These in-situ mineralogical changes can decrease the strength of the rock and enhance physical weathering. Understanding the mineralogical evolution of these altered and mineralized rocks has implications as to mine-waste pile stability.

Introduction

Numerous studies during the past decade have documented the presence of acidic, metal-rich surface and ground waters derived from pervasively clay-altered rocks that were stripped of their original mineralogic constituents in the geologic past by caustic solutions. These hydrothermally altered rocks, called the "altered protolith," contain exceptionally high quantities of fine-grained pyrite. Weathering of the pyrite-rich altered protolith produces highly acidic water that is largely unbuffered owing to the general lack of calcite and other acid-neutralizing minerals. Even in the absence of human-induced disturbances such as mining or prospecting, waters draining these rocks are highly acidic (pH, 2 to 4) and contain aluminum, iron, and sulfate concentrations that far exceed aquatic-life standards.

Prior to our current work, the understanding of acid weathering reactions in hydrothermally altered rock has been largely based on theoretical models simulating mineral reactions. In contrast, our study documents the actual in-situ mineralogical response of the pyrite-bearing protolith due to attack by low temperature and highly acidic waters. During the course of various geoenvironmental investigations by the U.S. Geological Survey (USGS), we conducted studies in four principal areas (fig. 1) that hosted large expanses (1.7 to 20 km^2) of hydrothermally altered rock. Natural weathering in each of these areas produces low-pH and metal-rich water (fig. 2). These study areas include (1) Webster Pass, in the central Colorado Front Range, near Keystone, Colorado (Caine and others, 2006); (2) Prospect Gulch in the upper Animas River watershed, southwest Colorado (Bove and others, 2007); (3) Alum Creek, tributary to the upper Alamosa River, near Summitville Colorado (Bove and others, 1996); and (4) Straight Creek, near Questa and the Red River, New Mexico (Ludington and others, 2004).

The results of our studies demonstrate that the fundamental processes of acidic weathering of rocks are remarkably similar in each of these four hydrothermally altered areas. Although results from a compendium of these studies will be presented, we will specifically focus on our findings in Straight Creek, northern New Mexico, which provide an exceptional example of what we have observed elsewhere.

Results and Discussion of Weathering Studies

Gullies incised into the eroded slopes of the four study areas expose relatively unweathered (absence of recent and low-temperature alteration), pyrite-rich rocks. These characteristically light-gray, clay-rich rocks were hydrothermally altered millions of years ago by hot, caustic solutions driven by magmas rising high into the Earth's crust. In geologic terms, we classify the hydrothermally altered rock as the altered protolith. The altered protolith is classically characterized as quartz-sericite-pyrite (qsp)-altered because the original mineral constituents—rich in calcium, sodium, magnesium, and iron—were largely stripped of these elements during their transformation to an assemblage dominated by quartz, fine-grained muscovite (sericite), pyrite, and in some instances chlorite. In many instances, however, some of the original mineral components of the protolith remained partially intact during hydrothermal alteration; these include a variety of feldspars and rarely biotite. Recent weathering of pyrite in the qsp-altered protolith ultimately results in the formation of sulfuric acid, which initiates a cycle called "acid weathering." Quantitative analyses by X-ray diffraction (XRD) document a decrease in chlorite, illite, and pyrite ± plagioclase in the altered protolith as acid weathering progresses. The loss of these minerals during low-temperature weathering is associated with a correlated increase in smectite (a clay that swells when wet), kaolinite, and jarosite (formed from the alteration of pyrite). A spectacular rock sequence from the Straight Creek alteration "scar" (fig. 1*D*) exemplifies the progressive transformation of the altered protolith during the acid-weathering process (fig. 3). Scanning Electron Microscopic (SEM) observations support our quantitative mineralogical data that show an inversely linear decrease in chlorite (89-percent reduction) and pyrite (100-percent reduction) in the altered

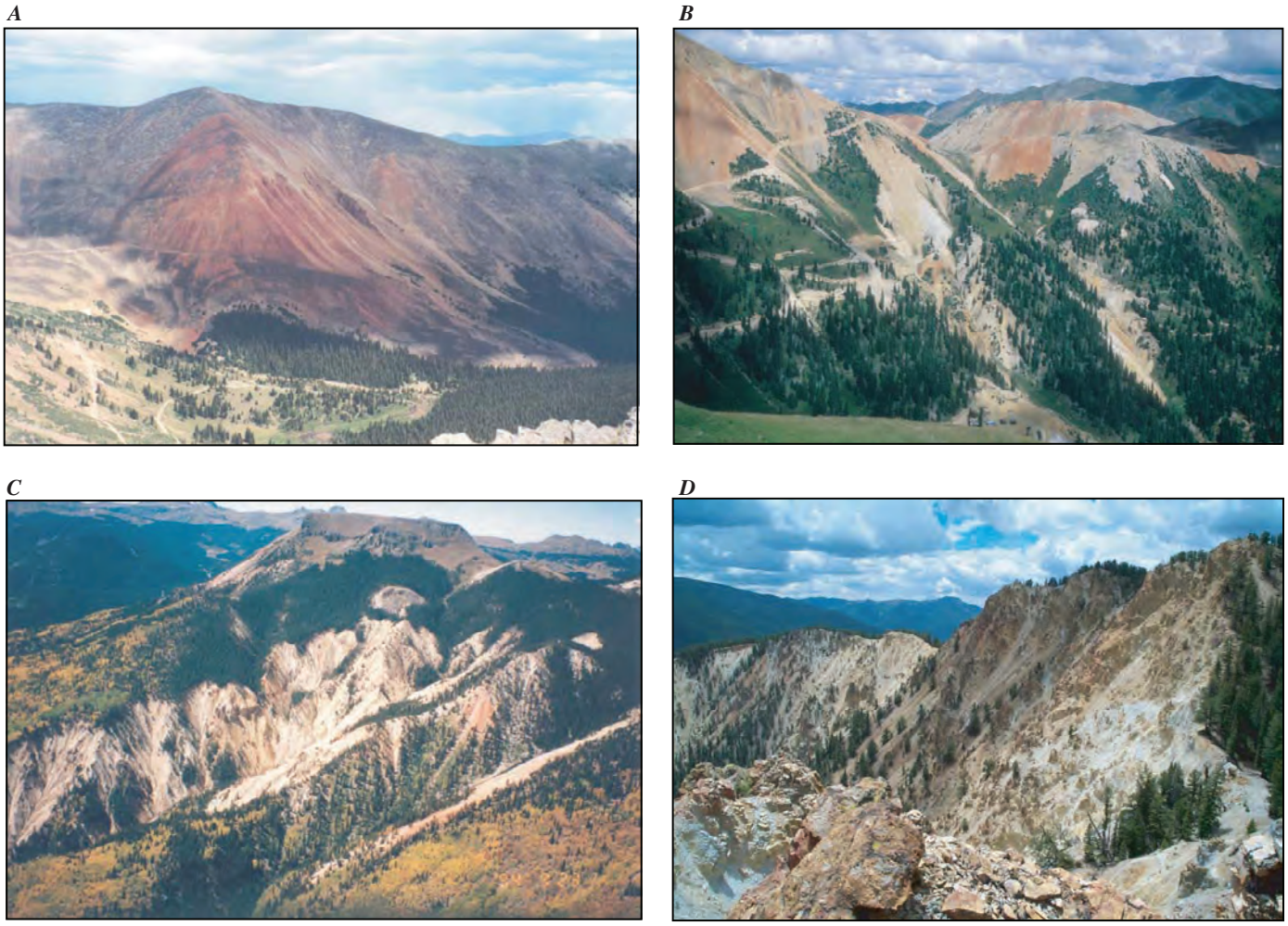

Figure 1. Large areas of hydrothermally altered rock in the four study areas. (*A*) Webster Pass, near Keystone, Colorado; (*B*) Prospect Gulch in the headwaters of the upper Animas River, near Silverton, Colorado; (*C*) Alum Creek, a tributary to the Alamosa River, near Summitville, Colorado; and (*D*) Straight Creek, near Questa, northern New Mexico.

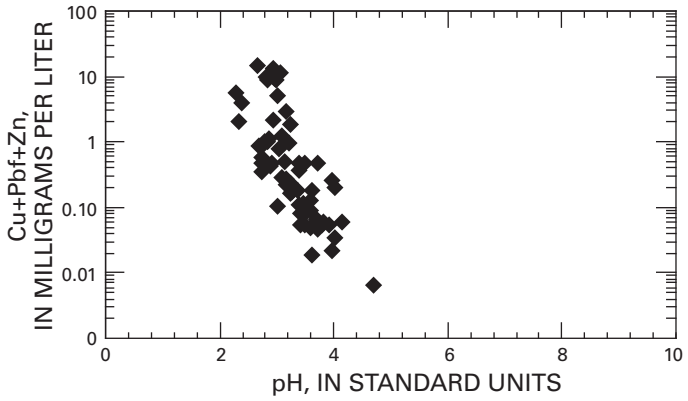

Figure 2. Plot of pH relative to sum of dissolved copper (Cu), lead (Pb), and zinc (Zn) for stream and spring samples in the four study areas. Data from Mast and others (2000); Verplanck and others (2006, 2007).

protolith with an increase in smectite ± kaolinite (fig. 4). Decreases in illite (32-percent reduction) and plagioclase feldspar (26-percent reduction) from altered protolith to the final weathering products are still considerable but have a less linear relationship with respect to increasing smectite (fig. 4). SEM textures and clay XRD studies suggest that smectite grew largely as newly formed crystals (fig. 5*A*). The precipitated smectite derived its elemental components from the concurrent dissolution of chlorite, illite, and plagioclase (fig. 5*B–D*). However, SEM data and mapping of elements by electron microprobe show zones of reaction around illite grains with a loss of potassium, magnesium, and iron. These reacted zones show the original illite crystal shapes, but chemical analyses suggest that some of the illite has been altered to smectite. Smectite and kaolinite are always the latest clays formed in the weathered rocks, and smectite always postdates kaolinite.

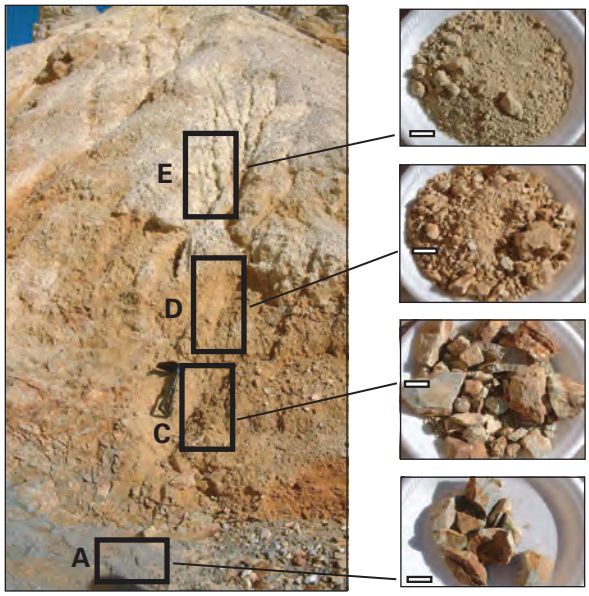

Figure 3. Acid-weathering sample sequence from a steeply incised gulley in Straight Creek, New Mexico. Sample A represents the quartz-sericite-pyrite-altered protolith that is relatively unaffected by low temperature weathering. Acid weathering increases upward from samples A through E. Quantitative XRD results from samples A, C, D, and E are presented in figure 4. Note shovel for scale in photograph on the right near sample site C. Scale bars on the left represent 2.5 centimeters. Figure modified from Ludington and others (2004).

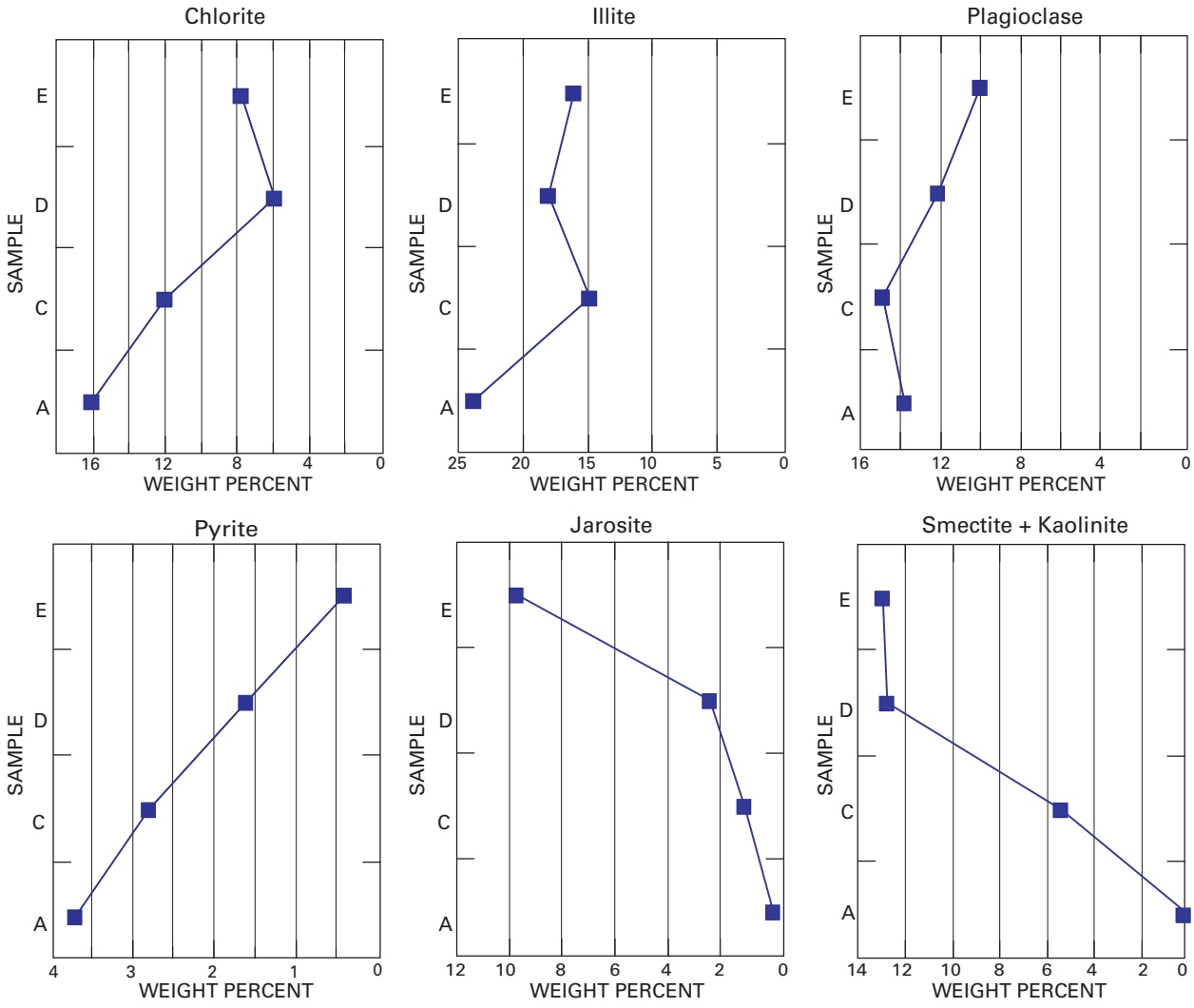

Figure 4. Quantitative XRD mineral analyses in weight percent for samples A, C, D, and E from the Straight Creek sequence (see figure 3). Methodology for XRD quantitative analyses described in Eberl (2003).

Simple reactions written from our data suggest that the weathering of pyrite forms goethite (iron hydroxide), which generates acidity that further drives the weathering reaction. Minerals in the altered protolith then react with the acid. Where the water is most acidic, kaolinite is formed. As fluids become less acidic and probably accumulate more solutes, smectite is formed. The more permeable pathways in the rock may conduct acidic waters and promote kaolinite formation. In low-permeability regions where solutions reside for a longer time, chlorite dissolution may locally increase the pH and cation concentrations, promoting smectite precipitation.

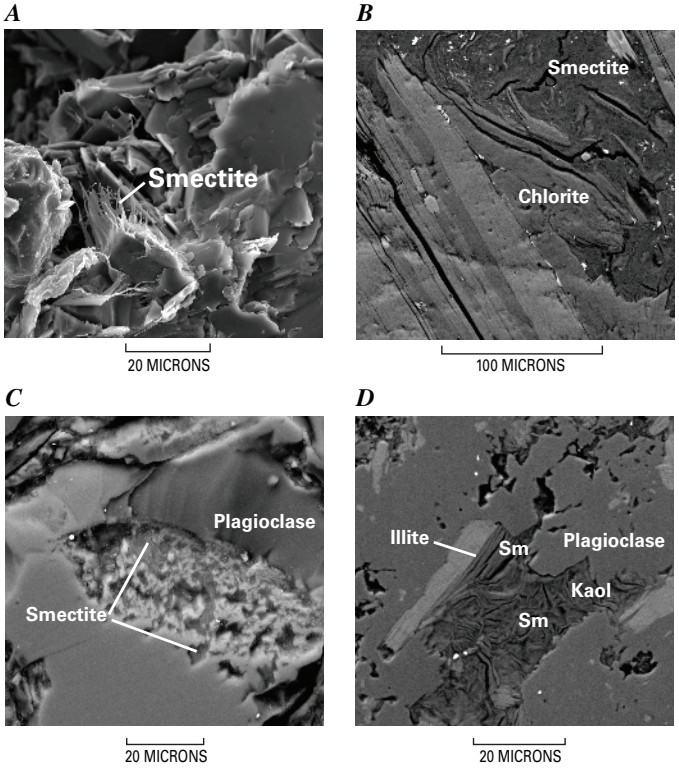

Figure 5. Scanning electron microscope photographs of samples from several study areas showing neoformed smectite morphology (*A*) and smectite that formed from the dissolution of chlorite (*B*), plagioclase (*C*), and illite and plagioclase (*D*). Note the opening of illite due to smectite alteration in figure B.

Conclusions and Implications

Although this study focuses on acidic rock weathering in natural settings, highly pyritic and altered rock of a very similar character typically compose a large portion of the material in mine-waste piles. Based on our studies, we suggest that mine waste that contains hydrothermally altered wall rock with abundant pyrite may undergo similar reactions and form smectite. Mine dump instability, a common problem on very steep slopes, may be exacerbated by the production of this highly swelling clay.

References Cited

Bove, D.J., Wilson, A.B., Barry, T.H., Hon, K., Kurtz, J., VanLoenen, R.E., and Calkin, W.S., 1996, Geology, alteration, and rock and water chemistry of the Iron, Alum, and Bitter Creek areas, upper Alamosa River, southwestern Colorado: U.S. Geological Survey Open-File Report 96–039, 34 p.

Bove, D.J., Mast, M.A., Dalton, J.B., Wright, W.G., and Yager, D.B., 2007, Major styles of mineralization and hydrothermal alteration and related solid- and aqueous-phase geochemical signatures, chap. E3, *in* Church, S.E., von Guerard, Paul, and Finger, S.E., eds., Integrated investigations of environmental effects of historical mining in the Animas River watershed, San Juan County, Colorado: U.S. Geological Survey Professional Paper 1651, p. 161–230.

Caine, J.S, Manning, A.H., Verplanck, P.L., Bove, D.J., Kahn, K.G., and Ge, S., 2006, Well construction information, lithologic logs, water level data, and overview of research in Handcart Gulch, Colorado—An alpine watershed affected by metalliferous hydrothermal alteration: U.S. Geological Survey Open-File Report 2006–1189, 15 p.

Eberl, D.D., 2003 User guide to RockJock—A program for determining quantitative mineralogy from X-ray diffraction data: U.S. Geological Survey Open-File Report 2003–78, 36 p.

Ludington, S., Plumlee, G.S., Caine, J.S., Bove, D., Holloway, J.M., and Livo, K.E., 2004, Questa baseline and pre-mining ground-water quality investigation 10. Geologic influences on ground and surface waters in the lower Red River watershed, New Mexico: U.S. Geological Survey Scientific Investigations Report 2004–5245, 41 p.

Mast, M.A., Evans, J.B., Leib, K.J., and Wright, W.G., 2000, Hydrologic and water-quality data at selected sites in the upper Animas River watershed, southwestern Colorado, 1997–99: U.S. Geological Survey Open-File Report 2000–53, 20 p.

Verplanck, P.L., McCleskey, R.B., and Nordstrom, D.K., 2006, Questa baseline and pre-mining ground-water quality investigation. 20. Water chemistry of the Red River and selected seeps, tributaries, and precipitation, Taos County, New Mexico 2000–2004: U.S. Geological Survey Scientific Investigations Report 2006–5028, 139 p.

Verplanck, P.L., Manning, A.H., Kimball, B.A., McCleskey, R.B., Runkel, R.L., Caine, J.S., Adams, Monique, Gemery-Hill, P.A., and Fey, D.L., 2007, Ground- and surface-water chemistry of Handcart Gulch, Park County, Colorado, 2003–2006: U.S. Geological Survey Open-File Report 2007–1020, 31 p.

Chapter D: Bacterial Processes Can Influence the Movement of Metal Contaminants in Wetlands that Have Been Affected by Acid Drainage

by Mark R. Stanton

Overview

Two important bacterial processes that can affect the removal (precipitation) or release (solubilization) of metal contaminants in wetlands affected by acid drainage are sulfate reduction resulting in metal-sulfide precipitation and bacterial iron oxidation potentially resulting in sulfide mineral dissolution. These processes were studied under natural and laboratory conditions by (1) characterizing metal-sulfide precipitates that formed in wetland sediments ("natural" sulfides) for total metal, acid-extractable metal, and total sulfide concentrations, and by number of sulfate-reducing bacteria, and (2) examining the potential function of iron-oxidizing bacteria in the release of metals from sulfide-bearing materials, specifically, fine-grained zinc sulfide (sphalerite, ZnS). The results confirm the importance of bacterial sulfate reduction as an agent for removal of metals as sulfide precipitates; the results also confirm that bacterial oxidation of iron in ZnS does not appear to greatly enhance ZnS dissolution over periods of several weeks.

Background

Many bacteria that live and bring about chemical changes in acid drainage environments are known as lithotrophs ("rock-eaters"). These microbes utilize just a few inorganic compounds or elements for energy or growth. Iron-oxidizing bacteria obtain energy by oxidizing ferrous iron (Fe^{2+}) to ferric iron (Fe^{3+}). The best-known lithotrophic iron oxidizer, *Acidithiobacillus ferrooxidans*, thrives in acidic (low pH) environments.

Bacteria that use organic compounds for energy or growth are known as heterotrophs ("diverse eaters"). Important heterotrophs are sulfate reducers that use sulfate (SO_4^{2-}), rather than oxygen as most bacteria do, to aid their decomposition of organic matter. The end product of this decomposition, sulfide (S^{2-}), is produced almost exclusively by sulfate-reducing bacteria (Widdell, 1988). Sulfide reacts to form $H_2S(g)$ (hydrogen sulfide gas), the compound that produces the odor of rotten eggs. The best-known sulfate-reducing bacteria are in the genus *Desulfovibrio*, but many other sulfate reducers are present in nature (Widdell, 1988; Ehrlich, 1990).

Bacterial processes involving iron and sulfate can be especially important in depositional sites such as wetlands that receive acid drainage. Sulfate is present in high concentration in acid drainage because of the oxidation of sulfide minerals. High sulfate and abundant organic matter promote sulfate-reducer growth (which in turn supports near-neutral [7.0] pH values). Sulfate reduction permits chemically reducing conditions to develop and persist in water-saturated, oxygen-poor portions of the sediment. Other areas of the sediment, such as areas at or near the surface, remain oxygenated. Thus, wetlands can have chemically reducing and chemically oxidizing zones in close proximity. In general, reducing conditions tend to immobilize metals and prevent them from moving in the surface-water/ground-water system, whereas oxidizing conditions tend to mobilize metals and allow them to move in the surface-water/ground-water system. The mobility of metals is important because metals usually are the source of toxicity in acid drainage.

Four of the most prominent metals in acid drainage are iron (Fe), copper (Cu), lead (Pb), and zinc (Zn). Under suitable geochemical conditions, aqueous sulfide produced by *Desulfovibrio* reacts with a dissolved metal to form a solid precipitate, for example, $Pb^{2+} + S^{2-} \rightarrow PbS_{(solid)}$. Amorphous iron sulfide ($FeS_{(am)}$), the most common metal-sulfide precipitate (Davison and others, 1992), is not soluble in waters of near-neutral pH (7.0) but tends to dissolve at about pH 5.0 or less (Pankow and Morgan, 1980). When iron-sulfide precipitates are dissolved in strong hydrochloric acid (6N HCl), they produce H_2S gas and hence are called "acid-volatile sulfide" (Berner, 1970); other strong HCl-soluble sulfides that might be present include Cu_2S (chalcocite), PbS (galena), and ZnS (sphalerite). Metal-sulfide precipitates formed by bacterial sulfide production are called "secondary" sulfides, whereas "primary" sulfides are those that are present in ore deposits.

Analytical Methods

The chemical composition of the natural sulfides and number of associated sulfate-reducing bacteria were determined from samples collected at the Forest Queen mine wetland near Silverton, Colorado (fig. 1). Details of the sampling, geochemistry, sedimentology, and hydrology of this site can be found in Stanton (2000) and Pavlik and others (1999).

Iron-sulfide-rich, black solids were present at depths to 3 meters in a matrix of silt and fine-grained sand or associated with organic matter. Orange-red iron oxides were present at the surface (fig. 2) and in the uppermost sections (0 to 60 cm depth) of the sediment column.

Complete separation of the black metal sulfides from other materials was not possible, and some samples contained an estimated 20–30 wt. % (weight percent) of silicate minerals (silt, sand, clay), plus traces of organic matter. The iron sulfides are in a complex matrix, but it is likely that the trapping of most metals had occurred because of the reducing (sulfidic) nature of the sediments. Filtered water samples were analyzed onsite to define the geochemical conditions under which the bacteria were living (fig. 3).

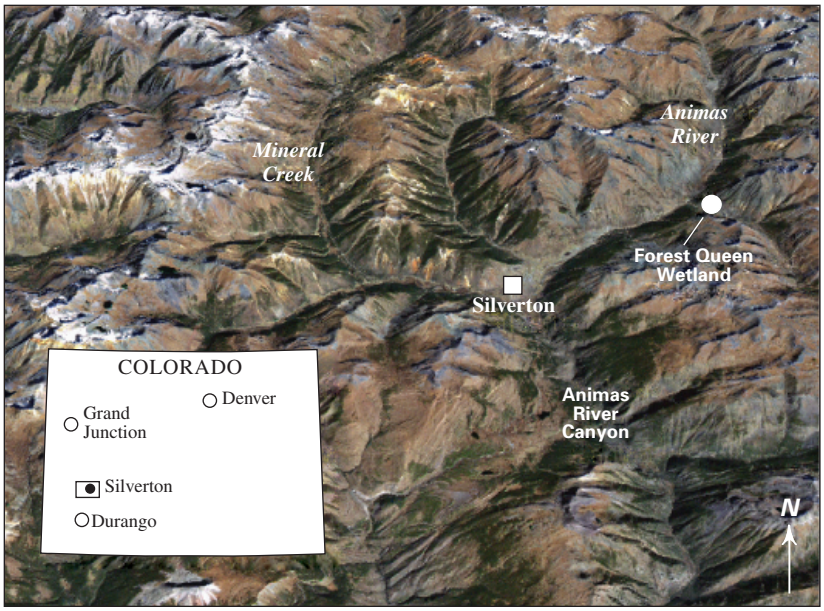

Figure 1. Location map of Forest Queen mine wetland, near Silverton, Colorado. (Topographic image from Douglas Yager, U.S. Geological Survey.)

The flowchart in figure 3 shows the procedures applied in this study. Water analyses included pH, dissolved oxygen (DO), specific conductivity (SpC), alkalinity, temperature, total iron (Fe[tot]), ferrous iron (Fe^{2+}), and ferric iron (Fe^{3+} = Fe[tot] – Fe^{2+}). Slight modifications of the acid volatile sulfide method described by Tuttle and others (1986) and Rice and others (1993) were made. Sulfide recovered from the strong acid (6N HCl) leach is reported as parts per million (ppm) total sulfide ($S^{2-}_{(tot)}$). Major and trace-element aqueous concentrations from the strong acid leach and dissolution experiments were obtained using atomic emission (Briggs, 2002) or mass spectrometric (Lamothe and others, 2002) methods, respectively (fig. 3). Metal concentrations are reported as parts per million in the solids and as micrograms or milligrams per liter (µg/L or mg/L) in the solutions. X-ray diffraction was used to evaluate the crystallinity of the natural sulfides and to characterize the mineralogy of the sulfides and reactant sphalerite.

Quantification of the sulfate-reducing bacteria in the natural sulfides was undertaken to see if there was any relation between the numbers of cells and the chemical composition (metals, sulfide). Similarly, numbers of iron oxidizers in the dissolution experiments were obtained to see if the ZnS dissolution rate was related to cell numbers. Methods to quantify the numbers of the sulfate-reducing and iron-oxidizing bacteria are based on standard microbiological culturing and staining techniques (Gerhardt and others, 1994; Atlas, 1995). The number of bacterial colonies grown on agar plates (or sometimes in liquid medium), adjusted by the appropriate dilution or concentration factor, produces the final number of cells in the original sample (cells per gram or cells per milliliter).

Experimental Dissolution of ZnS: Abiotic and Biotic Reactions

The sphalerite was powdered to an average particle size of approximately 10 µm (Stanton and others, 2008). This grain size is among the smallest mineral particle sizes that might be present in the wetland sediments, except for clays. The ZnS contained 6.7 wt.% Fe, 380 ppm Cu, 1,400 ppm Pb, and 61.8 wt.% Zn.

The *Acidithiobacillus* bacteria (maintained in culture medium at pH 4.5) and prepared ZnS were added to the acid solution (pH ≤ 4.0, 25°C) to begin the reaction. Three abiotic experiments (no bacteria) at starting pH values of pH 2, 3.3, and 4 were performed; a similar set of three experiments was run in the presence of the iron-oxidizing bacteria (biotic). All experiments were open to the air and used a high rate of stirring to permit oxygenation; most were maintained at constant pH by adding 0.1 N HCl as needed. Filtered samples for metal analysis were taken at about 48-hour intervals over a 2–3-week period; plate count samples were taken at approximately 100-hour intervals.

Figure 2. Forest Queen mine wetland (before remediation; looking north) showing the inflow of iron-bearing acid drainage. Core samples were collected in the green area between the red solids and road (top of picture).

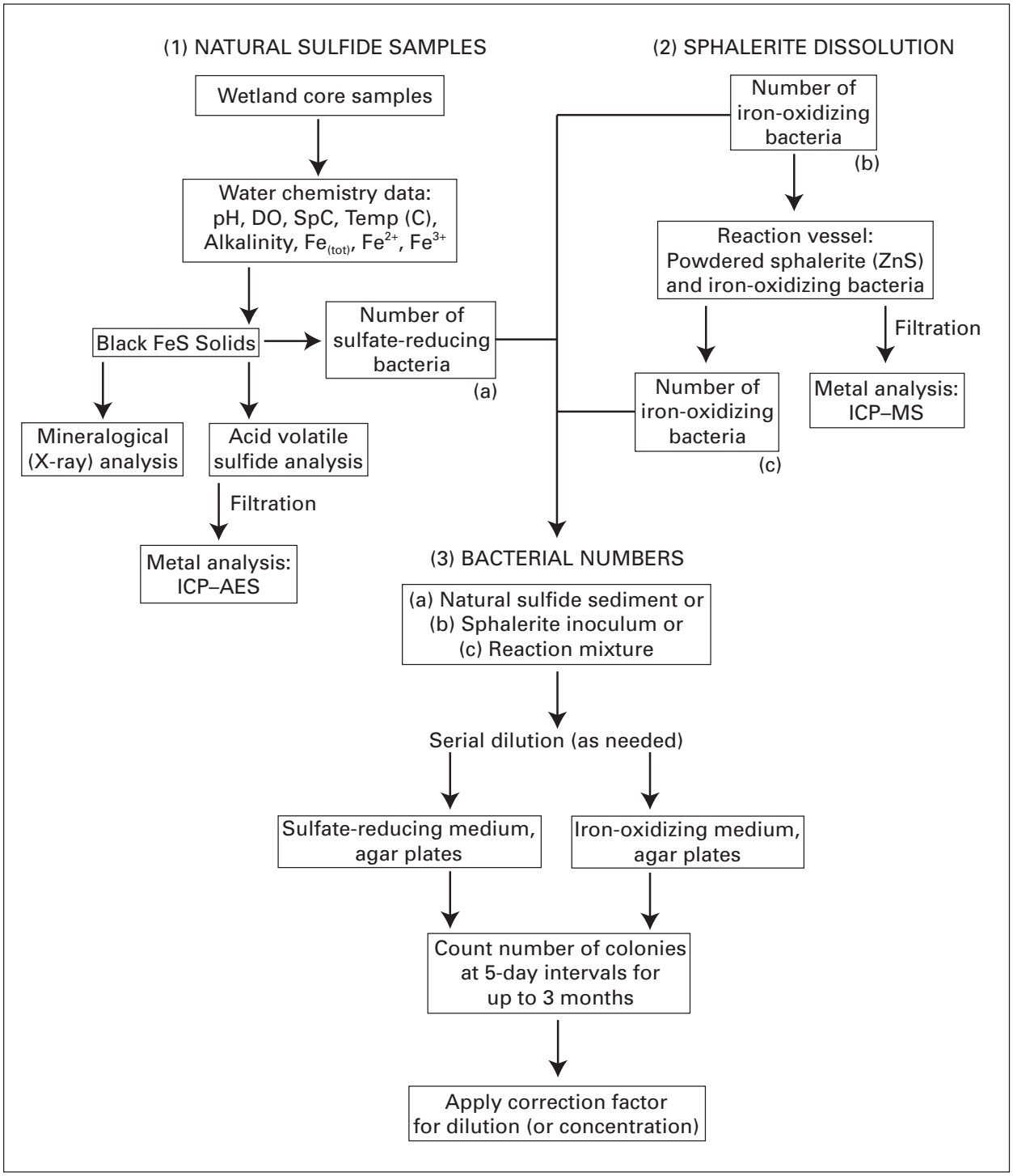

Figure 3. Flowchart showing the major sample treatment and analysis procedures used in this study.

Results and Discussion of Bacterial Studies

Natural Metal Sulfides

Acid-extractable metal concentrations and bacterial numbers in the natural iron sulfides showed little relation to each other or to total sulfide (fig. 4). The sulfides had a wide range of metal concentrations but generally low numbers of sulfate-reducing bacteria; in fact, 8 of the 20 samples produced no viable bacteria. The plate counts translate to cell numbers from zero up to about 3,000 per gram.

High values of total sulfide are not always found in samples with high metal concentrations (whether total or acid-extractable metals), and low values of total sulfide may have high metal concentrations (fig. 4). Strong HCl-extractable metal content is high even in samples containing less than 100 ppm $S^{2-}_{(tot)}$. Acid-extractable iron ranges from 10 to 100 times higher than total sulfide recovered. The metal-sulfide precipitates do not appear to amass metals in a consistent, predictable manner.

One likely reason for high metal content in samples lacking sulfide is that metals are sorbed onto silicates or undetectable (X-ray amorphous) ferric oxides. Solid-phase silica (Si) exhibits a pattern similar to leachable iron with respect to sulfide (fig. 5), suggesting metals are also bound by silicates within the sediment. The amount of metal associated specifically with the sulfide or silicate phase is unknown because of sample heterogeneity.

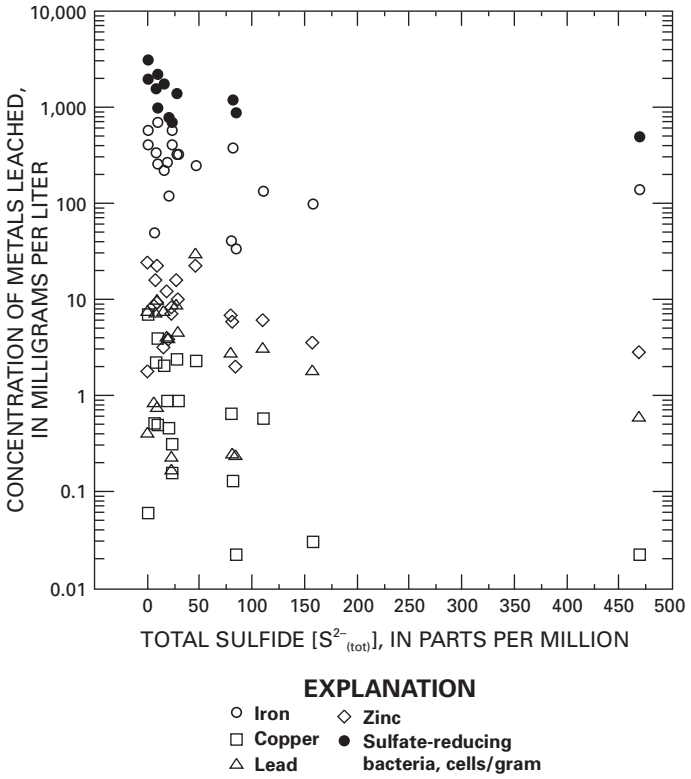

Figure 4. Acid-extractable (6N HCl) metal and numbers of sulfate-reducing bacteria plotted relative to total sulfide concentrations from natural sulfide samples.

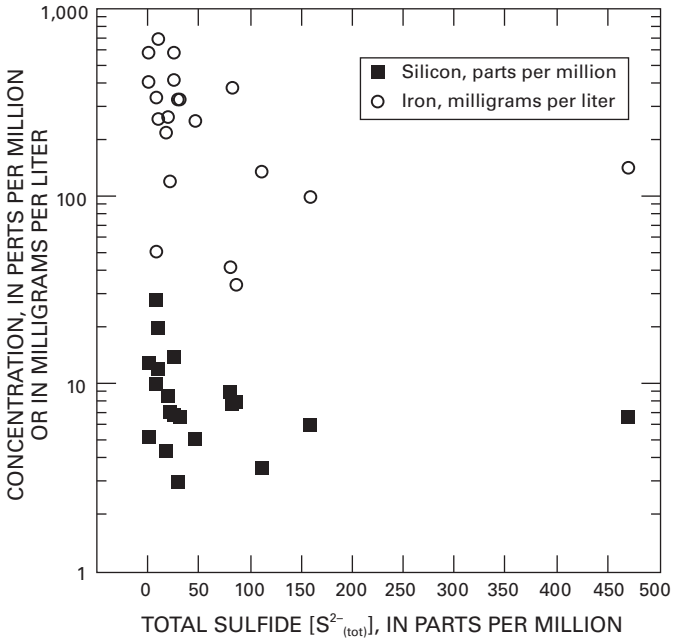

Figure 5. Solid-phase silica (Si), acid-extractable iron (Fe), and total sulfide concentrations from natural sulfide samples indicating the likelihood of metal being adsorbed onto silicate phases.

Another possible reason for the poor correspondence of metals and sulfide is that accumulation and enrichment of metals might occur over time. As ground or surface water move through the sediment column, preexisting metal sulfides may be able to adsorb more metals in concentrations greater than would be predicted on an ideal 1:1 ratio of metal to sulfide (for example, Fe:S).

Some sediments had low values of metals except iron, indicating there had been little or no copper, lead, and zinc available. Lack of a metal source, or location away from a metal source and flow path, is a potential reason for the samples having lower metal contents. Competition for metals by silicates or organic matter along a flow path might also contribute to low metal values in some sulfides.

Only slight differences in crystallinity were observed among the natural sulfides in that some had X-ray reflections indicative of a poorly crystalline FeS phase (possibly mackinawite); no other sulfides were detected. Pyrrhotite, a crystalline form of FeS, was found in trace amounts in the reactant ZnS.

Metal Release During Abiotic and Biotic ZnS Dissolution

The initial release of all metals in the biotic run was slightly higher than in the abiotic run, suggesting perhaps a slight increase in the ZnS dissolution rate by bacteria. Soluble total iron was slightly higher at all sampled intervals (fig. 6*A*), indicating the preference of iron oxidizers to release this metal. However, there was little change in metals released in the presence of iron-oxidizing microbes after about 48 hours (fig. 6*A*). The plot for zinc (fig. 6*B*) confirms that there was only minor variation between the abiotic and biotic reactions.

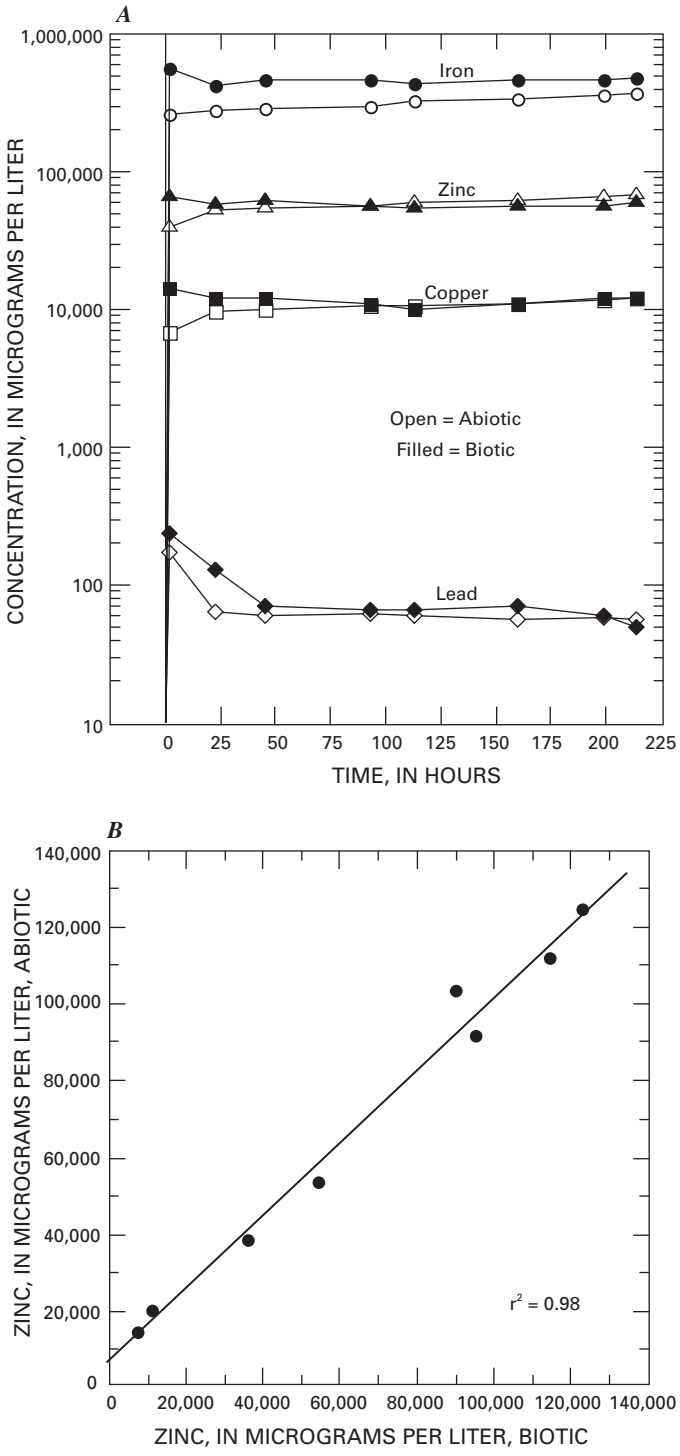

Figure 6. (*A*) Metal concentrations from acidic dissolution of zinc sulfide in the absence (abiotic) and presence (biotic) of iron-oxidizing bacteria (initial pH = 3.3). (*B*) Plot of zinc concentrations from the same abiotic and biotic zinc sulfide dissolution experiments shown in figure 6*A*.

The (ferric) iron concentration during the reaction apparently was not sufficient to promote faster decomposition through ferric iron oxidation (Perez and Dutrizac, 1991; de Giudici and others, 2002). Ferric iron did not become significant (that is, equal to the ferrous concentration) until about 100 hours of reaction time, and despite high oxygenation, the ferric iron and bacteria did not seem to accelerate the rate of dissolution of sphalerite during the time of the experiment. The bacteria may have enhanced the release of iron from pyrrhotite in the sphalerite, which might explain the higher total iron concentrations with little increase in other metals.

The results are in agreement with Fowler and Crundwell (1998), who noted that there were no direct microbial mechanisms involved in the short-term dissolution of ZnS. However, if the microbes were allowed sufficient time to produce significant quantities of ferric iron, perhaps they could enhance the rate of ZnS dissolution (Weisener and others, 2003) because Fe^{3+} is a known strong oxidant of ZnS (Rimstidt and others, 1994; Perez and Dutrizac, 1991). The fact that metal concentrations did not vary between the two types of experiments suggests the iron-oxidizing bacteria were incapable of directly solubilizing metals from the ZnS structure (at least in the time period of these experiments). The results with ZnS are in contrast to what is known about the important function of iron-oxidizing bacteria in the decomposition of pyrite (Berner, 1970; Nordstrom and Southam, 1997).

Plate counts indicated some difficulty in bacterial growth and viability during the reaction because cell numbers declined with increasing reaction time. The cells had been grown in a chemically defined medium prior to addition to the vessel and likely were unable to quickly adapt to the abrupt change of growing in a medium devoid of several nutrients. Thus, the cells were probably less viable at longer reaction times. Although the bacteria did not greatly accelerate the acid dissolution of ZnS, there were indications they may have done this in the earliest stages (0–48 hours) when their viability was highest.

Conclusions

In organic-rich, reducing sediments, many trace metals can be immobilized by precipitation as acid volatile sulfide; thus, bacteria that produce sulfide are geochemical agents in acid drainage environments. Relatively high concentrations of metal can be associated with the natural sulfides. However, the results indicate metal-sulfide formation is a process controlled primarily by inorganic (abiotic) geochemical factors and is not directly mediated by sulfate-reducing bacteria. Total sulfide and metal concentrations were independent of the sulfate-reducing bacteria cell numbers. One reason for this may be that in the natural samples, the bacteria are not continuously active or are active at different times. A sulfate-reducing bacterial population may be inactive (dormant) or perhaps absent from one precipitate for many reasons (exhaustion of nutrients, and so forth); cell numbers might vary greatly from an active population in another precipitate.

The metal sulfides are neither crystalline nor formed in proportions according to ideal chemical formulas. Aging of the natural sulfides rather than any direct microbial action likely is the dominant process for the FeS precipitates to become increasingly crystalline and exhibit ideal ratios of metal to sulfide. The enclosing sediments are young (less than 12,000 years before present; Stanton, 2000) and the sulfides have not had time to crystallize into more-ordered phases. Most of the metal leached from the sediment was probably immobilized as a result of the reducing conditions established by the sulfide, but the amount of metals associated with the silicates was not determined. And as noted earlier, the source location and transport of dissolved metals can influence the metal content of the sulfide precipitates.

Iron-oxidizing bacteria may have the potential to release metals during oxidative decomposition of ZnS, but the experimental results were not conclusive because of limited reaction time. Longer term experiments are likely needed to determine if bacterially mediated iron oxidation can contribute to enhanced dissolution of ZnS.

References Cited

Atlas, R.M., 1995, Handbook of media for environmental microbiology: Boca Raton, Fla., CRC Press, 540 p.

Berner, R.A., 1970, Sedimentary pyrite formation: American Journal of Science, v. 268, p. 1–23.

Briggs, P.H., 2002, The determination of forty elements in geological and botanical samples by inductively coupled plasma–atomic emission spectrometry, *in* Taggart, J.E., Jr., ed., Analytical methods for chemical analysis of geologic and other materials: U.S. Geological Survey Open-File Report 2002–0223–F, p. F1–F11.

Davison, W., Grime, G.W., and Woof, C., 1992, Characterization of lacustrine iron sulfide particles with proton-induced x-ray emission: Limnology and Oceanography, v. 37, p. 1770–1777.

de Giudici, Giovanni, Voltolini, Marco, and Moret, Massimo, 2002, Microscopic surface processes observed during the oxidative dissolution of sphalerite: European Journal of Mineralogy, v. 14, p. 757–762.

Ehrlich, H.L., 1990, Geomicrobiology: New York, Marcel Dekker, Inc., 646 p.

Fowler, T.A., and Crundwell, F.K., 1998, Leaching of zinc sulfide by Thiobacillus ferrooxidans—Experiments with a controlled redox potential indicate no direct bacterial mechanism: Applied and Environmental Microbiology, v. 65, p. 3570–3575.

Gerhardt, Philipp, Murray, R.G.E., Wood, W.A., and Krieg, N.R., eds., 1994, Methods for general and molecular bacteriology: Washington, D.C., American Society for Microbiology, 791 p.

Lamothe, P.L., Meier, A.M., and Wilson, S.A., 2002, The determination of forty-four elements in aqueous samples by inductively coupled plasma–mass spectrometry, *in* Taggart, J.E., Jr., ed., Analytical methods for chemical analysis of geologic and other materials: U.S. Geological Survey Open-File Report 2002–0223–H, p. H1–H11.

Nordstrom, D.K., and Southam, Gordon, 1997, Geomicrobiology of sulfide oxidation, *in* Banfield, J.F., and Nealson, K.H., eds., Geomicrobiology—Interactions between microbes and minerals: Mineralogical Society of America Reviews in Mineralogy, v. 345, p. 361–390.

Pankow, J.F., and Morgan, J.J., 1980, Dissolution of tetragonal ferrous sulfide (mackinawite) in anoxic aqueous systems; 2. Implications for the cycling of iron, sulfur, and trace metals: Environmental Science and Technology, v. 14, p. 183–186.

Pavlik, M.C., Kolm, K.E., Winkler, S., Emerick, J., Wildeman, T.R., and Robinson, Rob, 1999, Hydrogeologic controls on the geochemical function of the Forest Queen wetland, Colorado—Proceedings of 6th International Conference on Tailings and Mine Waste, Fort Collins, Colo., January 1999: Rotterdam, Balkema, p. 647–655.

Perez, I.P., and Dutrizac, J.E., 1991, The effect of iron content of sphalerite on its rate of dissolution in ferric sulphate and ferric chloride media: Hydrometallurgy, v. 26, p. 211–232.

Rice, C.A., Tuttle, M.L., and Reynolds, R.L., 1993, The analysis of forms of sulfur in ancient sediments and sedimentary rocks—Comments and cautions: Chemical Geology, v. 107, p. 83–95.

Rimstidt, J.D., Chermak, J.A., and Gagen, P.M., 1994, Reactions of sulfide minerals with Fe(III) in acidic solutions, *in* Alpers, C.N., and Blowes, D.W., eds., Environmental geochemistry of sulfide oxidation: ACS Symposium Series, American Chemical Society, Washington, D.C., p. 1–13.

Stanton, M.R., 2000, Trace metal and acid-volatile sulfide concentrations in sediments from the Forest Queen wetland near Silverton, Colorado—Implications for removal of metals from acid drainage waters: U.S. Geological Survey Open-File Report 2000–115, 43 p.

Stanton, M.R., Gemery-Hill, P.A., Shanks, W.C. III, and Taylor, C.D, 2008, Rates of zinc and trace metal release from dissolving sphalerite at pH 2.0–4.0: Applied Geochemistry, v. 23, p. 136–147.

Tuttle, M.L., Goldhaber, M.B., and Williamson, D.L., 1986, An analytical scheme for determining forms of sulfur in oil shale and associated rocks: Talanta, v. 33, p. 953–961.

Weisener, C.G., Smart, R.St.C., and Gerson, A.R., 2003, Kinetics and mechanisms of the leaching of low Fe sphalerite: Geochimica et Cosmochimica Acta, v. 67, p. 823–830.

Widdell, Friedrich, 1988, Microbiology and ecology of the sulfate- and sulfur-reducing bacteria, *in* A.J.B. Zehnder, ed., Biology of anaerobic microorganisms: New York, John Wiley and Sons, p. 469–585.

Chapter E: Simple Screening Tests to Determine the Potential Metal Toxicity of Mining-Waste Leachates

by LaDonna M. Choate, James F. Ranville, Eric P. Blumenstein, and Kathleen S. Smith

Overview

The leaching of metals from mining waste remaining after mining operations have ended can be toxic to aquatic organisms. Determination of water toxicity due to the presence of metals can be experimentally difficult. Standard aquatic toxicity tests also are expensive and time intensive. Therefore, development of screening methods that are experimentally simpler, cost effective, and more time efficient is beneficial. The results of our screening tests indicate that replacing the stock culture of a standard test species, *Ceriodaphnia dubia*, with hatched, dormant eggs (ephippia) of that species yields similar results while reducing cost, time, and labor required. MetPLATE™, which uses bacteria as a test organism, is also a promising screening tool to determine which disturbed sites require further investigation.

Introduction

Mine-waste leachates are assumed to be toxic to aquatic organisms if the pH value is less than 5 (Ohio River Valley Water Sanitation Commission, 1955; Wildeman and others, 2007), but toxicity is uncertain and must be tested above this pH threshold. Standard toxicity testing using *Ceriodaphnia dubia* (*C. dubia*, a type of water flea) requires maintaining a stock culture of the organism, making it time and labor intensive. The U.S. Geological Survey (USGS) has compared the use of stock *C. dubia* with the use of *C. dubia* ephippia, a dormant form that is rehydrated within a few days prior to the test. The 48-hour *C. dubia* test is a measure of acute toxicity, which is the toxicity determined by the percentage of mortality of the organisms (generally on the order of 20 individuals) after a single exposure. Acute toxicity commonly is reported as lethal concentration 50 (LC_{50}) or lethal dose 50 (LD_{50}), specifically the concentration or dose of a substance where 50 percent of the organisms die. Both standard *C. dubia* and ephippia-based tests are 48 hours long; however, the standard test usually requires long-term maintenance of a culture and is thus expensive to use in the screening of large numbers of samples and (or) sites. The USGS has also compared the 48-hour *C. dubia* toxicity test with the enzymatic assay MetPLATE™ (Bitton and others, 1996) for use as a screening tool. MetPLATE™ measures the acute toxicity of a substance where the endpoint is a sublethal effect such as abnormal development, growth, reproduction, behavior, and (or) other physiological or biological functions. Since the toxicity is based on factors other than mortality, it is reported as effected concentration 50 (EC_{50}) or effected dose 50 (ED_{50}), specifically the concentration or dose at which 50 percent of the organisms have been adversely affected. The USGS is also investigating nonlaboratory methods such as the Biotic Ligand Model (BLM) and the Mining Waste Decision Tree (MWDT). These methods use water-chemistry parameters, such as hardness, alkalinity, pH, and dissolved organic matter, to predict the aquatic metal toxicity and (or) determine potential toxic threats to aquatic organisms.

Ceriodaphnia dubia

Ceriodaphnia dubia (water flea) (fig. 1) is a freshwater zooplankton that is generally never larger than one millimeter (mm) in length. They are used in effluent toxicity testing because they are common among vegetation in shallow surface waters (that is lakes, ponds, and marshes) throughout most of the world (U.S. Environmental Protection Agency, 1993). With regard to metal toxicity, *C. dubia* are a relatively sensitive species. Standard U.S. Environmental Protection Agency (USEPA) test conditions were followed using both a stock cultured *C. dubia* and hatched *C. dubia* ephippia. Results of this comparison for copper toxicity in a number of simulated test waters are shown in figure 2. The

Figure 1. *Ceriodaphnia dubia* (water flea).

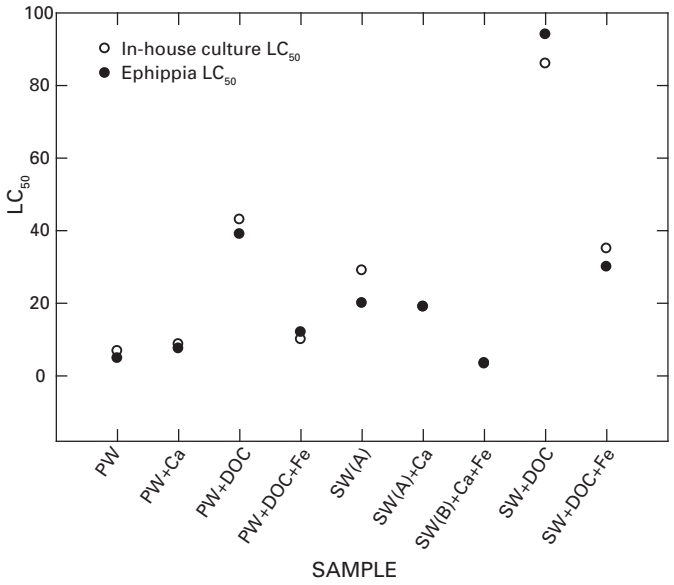

Figure 2. Lethal concentrations (LC_{50}) of copper (milligrams per liter) to *Ceriodaphnia dubia* for nine water samples: PW (pluton water), SW (sedimentary water), and PW or SW amended with Ca (calcium), DOC (dissolved organic carbon), and (or) Fe (iron).

simulated test waters PW and SW refer respectively to "pluton water," which is based upon the composition of stream-water samples collected from 10 Colorado stream-drainage basins underlain by plutonic (intrusive igneous) rocks, and "sedimentary water," which is based upon the composition of stream-water samples collected from 13 Colorado stream-drainage basins underlain by various sedimentary rocks associated with the Maroon and Morrison Formations. Figures 2 and 5 show the toxicity results of these simulated test waters amended with Ca (calcium), DOC (dissolved organic carbon), Fe (iron), or a combination of these. Figure 2 demonstrates that, for the simulated and amended simulated waters, the LC_{50} for copper varies but the results for the use of *C. dubia* stock culture and hatched ephippia are similar.

MetPLATE™

MetPLATE™ is an enzymatic bioassay kit where the toxicity is determined by the inhibition of the production of the enzyme β-galactosidase in *Escherichia coli* (*E. coli*) (fig. 3). When the *E. coli* bacteria are not stressed, they produce β-galactosidase, which cleaves the bonds of a colored substrate, causing the color of the solution to change. However, when the bacteria are stressed by the presence of metals, their production of enzyme is inhibited and less of the colored substrate is cleaved. The inhibition is determined by color (purple) measured as absorbance at 575-nanometer wavelength. Figure 4 is a developed MetPLATE™; columns 1 and 2 are controls, and columns 3 to 12 are samples. Each sample column is an individual sample with varying concentrations of a toxic substance, in this case copper. The copper concentration decreases going down the rows from A to H, and the inhibition (also referred to as toxicity) decreases with decreasing concentration. The less toxic the sample, the darker the color and the higher the absorbance measured. Absorbance is used to determine an EC_{50} for the *E. coli*. Comparison of this EC_{50} to the LC_{50} for the *C. dubia* is presented in figure 5. It can be seen from figure 5 that the EC_{50} for the *E. coli* is frequently higher than the LC_{50} for either *C. dubia*, but water-quality

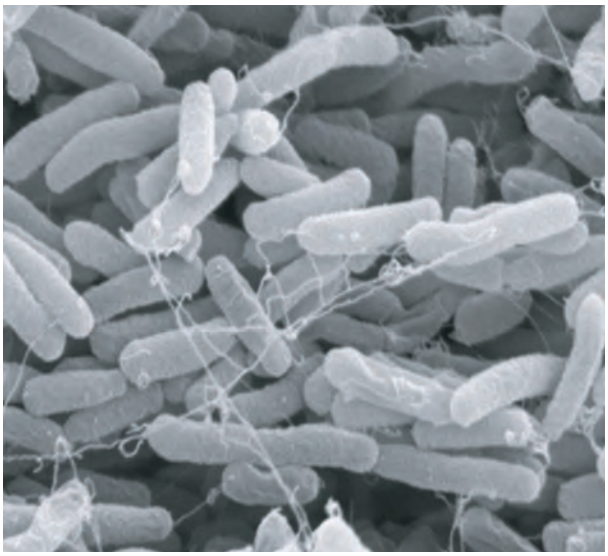

Figure 3. *Escherichia coli* (bacteria).

trends in the data are the same for both organisms, indicating that relative copper toxicity to *E. coli* also responds to water chemistry. Therefore, MetPLATE™ could be used as an initial screening tool to determine which samples would require more extensive toxicity testing and which samples are less toxic.

Other Approaches

Metal bioavailability and toxicity are a function of complex water chemistry (Sunda and Guillard, 1976). Historically, scientists have investigated the toxicity of individual metals. More recently the effects of other aqueous constituents, due to interactions with the metal and (or) organism, have been realized to be significant in metal toxicity. The Biotic Ligand Model is a computational approach that incorporates metal speciation and the protective effects of other chemicals in the water (Allen, 2002). The Biotic Ligand Model can be used to predict the potential toxicity of mining-waste leachates when they are released into the environment.

A simple decision tree (Mining Waste Decision Tree, MWDT) has been developed that uses simple physical and chemical tests to determine whether mine-waste material poses a potential toxicity threat to aquatic biota (Wildeman and others, 2007). The MWDT makes a distinction between leachates or waters with pH less than or greater than 5. The MWDT provides an inexpensive and reliable approach for preliminary assessment of the potential metal toxicity of mine-waste piles.

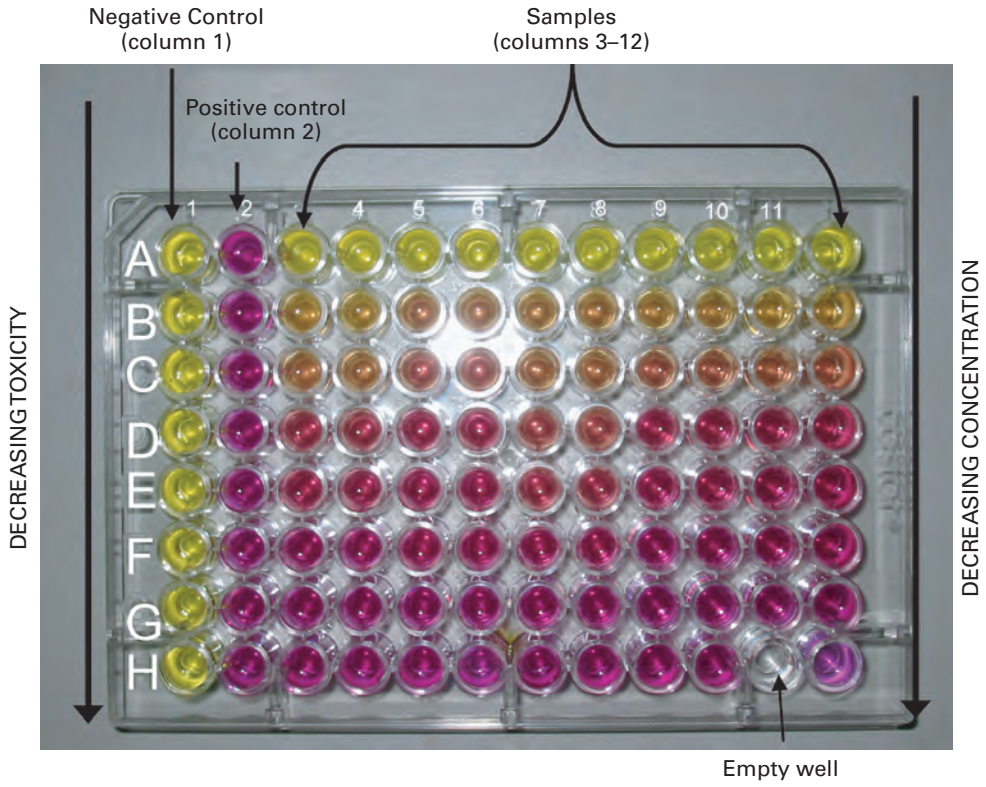

Figure 4. A developed 96-well MetPLATE™ bioassay, showing negative (toxic) and positive (nontoxic) controls and dilution series for several water samples.

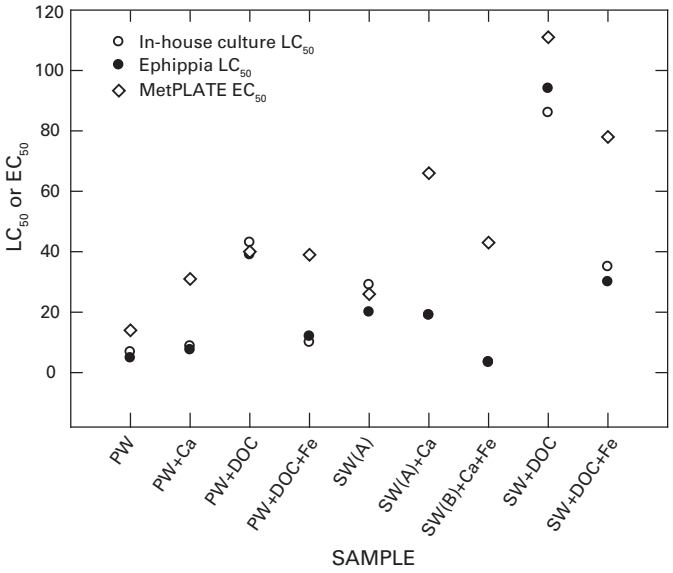

Figure 5. Lethal concentration (LC_{50}) of copper (milligrams per liter) to *Ceriodaphnia dubia* and effective concentration (EC_{50}) of copper (milligrams per liter) to *Escherichia coli* for nine water samples, PW (pluton water), SW (sedimentary water), and PW or SW amended with Ca (calcium), DOC (dissolved organic carbon), and (or) Fe (iron).

References Cited

Allen, H.E., 2002, The Biotic Ligand Model addresses effects of water chemistry on metal toxicity: Fact Sheet on Environmental Risk Assessment, no. 7, January 2002, London, International Council on Mining and Metals (ICMM), 5 p. *http://www.icmm.com/document/52* and accessed July 30, 2008.

Bitton, Gabriel, Garland, E., Kong, I-C., Morel, J.L., and Koopman, B., 1996, A direct solid-phase assay specific for heavy metal toxicity. I. Methodology: Journal of Soil Contamination, v. 5, no. 4, p. 385–394.

Ohio River Valley Water Sanitation Commission, Aquatic Life Advisory Committee, 1955, Aquatic life water quality criteria: Sewage Industrial Wastes, 27, p. 321–331.

Sunda, W.G., and Guillard, R.R.L., 1976, The relationship between cupric ion activity and the toxicity of copper to phytoplankton: Journal of Marine Research, v. 34, p. 511–529.

U.S. Environmental Protection Agency, 1993, Methods for measuring the acute toxicity of effluents and receiving waters to freshwater and marine organisms: U.S. Environmental Protection Agency /600/4–90/207F.

Wildeman, T.R., Smith, K.S., and Ranville, J.F., 2007, A simple scheme to determine potential aquatic metal toxicity from mining wastes: Environmental Forensics, v. 8, p. 119–128.

A second focus of this project was to investigate sources, pathways, and fate of metals and acidity at the watershed scale. An important aspect in evaluating the potential environmental effects of mineralized areas and abandoned mines is the determination of pathways and fluxes of metals from their sources to the receiving streams and ground water. In particular, integration of geological, geochemical, and geophysical techniques has led to substantial advances in our understanding of ground-water flow in alpine basins and waste-rock piles.

This section includes a variety of approaches that emphasize the need for understanding the factors controlling water quality in mineralized watersheds. Three studies of headwater catchments highlight the integration of geologic, geochemical, and geophysical data to develop conceptual models for the release and transport of metals. Two other studies describe the application of airborne geophysical and graphic information system (GIS) techniques to determine watershed attributes that may affect water quality.

Chapter F: Determination of Flow Paths and Metal Loadings from Mine Waste Using Geophysical and Geochemical Methods at the Waldorf Mine, Clear Creek County, Colorado

by David L. Fey, Robert R. McDougal, and Laurie Wirt

Overview

Mine waste, adit drainage, and mill tailings were studied at the Waldorf mine to determine water-flow paths and their relative contributions to contaminant loadings. Water draining from the adit and infiltrating through and under the waste pile, as well as shallow ground water flowing through the waste pile and through dispersed tailings, have affected nearby Leavenworth Creek with toxic metals, notably copper and zinc. The copper and zinc concentrations in the creek downstream from the mine-related inputs exceed standards for aquatic wildlife.

Geophysical and geochemical methods were applied to study waterflow through the mine waste and to assess metal sources and loads to Leavenworth Creek. Geophysical conductivity and resistivity surveys revealed two probable subsurface waterflow paths through the Waldorf mine waste. A geochemical tracer-dilution study delineated where contaminants were coming from, how and where they reached the creek, and their effect on water quality in the creek. Diversion of the adit drainage from the top to around the side of the mine-waste pile did not result in improved water quality of the creek.

Introduction

The Waldorf mine is located within the Colorado mineral belt near the Continental Divide in an alpine setting, near 3,540 meters (11,600 feet) elevation, in Clear Creek County, Colorado (fig. 1). Developed in the early part of the 20th century to mine polymetallic vein deposits for silver, lead, gold, copper, and zinc, the Waldorf mine is one of many thousands of inactive/abandoned hard-rock mines in the Western United States (Church and others, 2007) (fig. 2). Adit drainage and groundwater infiltration through waste material affect surface water in Leavenworth Creek, about 0.5 kilometer (0.3 mile) away.

Water Infiltration Through Waste Dump

The Waldorf mine and higher elevation, interconnected mine workings were drained by the Wilcox Tunnel, which is excavated about 1,200 meters (3,900 feet) into McClellan Mountain (Lovering, 1935). The drainage exits through a collapsed adit at the west end of the Waldorf waste pile; in July 2003, the discharge was 8 liters per second. The waste pile contains approximately 50,000 metric tons of material. There was at one time a 50-ton mill at the mine site (Lovering, 1935), and its tailings were dispersed some 800 meters to the northeast by a ditch; these tailings cover an area of about 12 hectares (30 acres) and are up to 1 meter in depth (McDougal and Wirt, 2007) (fig. 3). Previous to the first year of this study (2002), adit water had discharged across the top of the waste pile, where some of it infiltrated and some flowed across the face and into a wetland before flowing toward Leavenworth Creek.

After the first year's study, adit drainage was diverted through a culvert around the southwest side of the waste pile. Water samples from seeps at the toe of the dump were collected to see whether any surface drainage had infiltrated through the mine waste. A sodium chloride solution added to the adit discharge before the diversion traveled 92 meters through the dump and was detected at some of the seeps within 24 hours (McDougal and Wirt, 2007). However, surface infiltration of rainwater and snowmelt appears to be limited by a hardened crust, as evidenced by long-standing pools (generally lasting days) of water observed on the dump after summer rainstorms.

To determine possible waterflow paths, two kinds of geophysical techniques were applied to the waste pile, both involving the measurement or calculation of apparent conductivity. Electrical conductivity is a property of earth materials that varies with rock type, porosity, and the quality and quantity of subsurface water. Higher conductivity generally implies poor-quality subsurface water, that is, water with high dissolved-solids concentrations (McDougal and Wirt, 2007). Thus, higher conductivity zones or trends can be inferred as waterflow paths in the waste. An electromagnetic (EM) survey based on a grid on the top of the dump yielded a model with two horizontal layers, depicting apparent conductivity at about 7 and 15 meters below ground surface (fig. 4). Warmer colors denote more conductive areas. The surface topography of the waste pile is shown above the geophysical layers; the EM stations are depicted as dots. The upper layer shows an inferred water pathway from points B to B' and B''. The outer base of the waste pile (B' to B'') coincides with a conductive zone, which is interpreted as seepage of ground water containing relatively high dissolved-solids concentrations. Chemical analyses of water from these seeps confirmed that they are low in pH and high in dissolved metals (Fey and Wirt, 2007).

In the second year of the study, after the adit discharge was diverted, some seeps continued to issue low-quality water, implying that infiltration from the surface of the waste pile was not the only source of water, but that shallow ground water was infiltrating through the waste pile below the surface and (or) mine drainage was flowing down and through the dump before exiting the adit. The 15-meter EM layer revealed a deeper water pathway, A to A' (fig. 4).

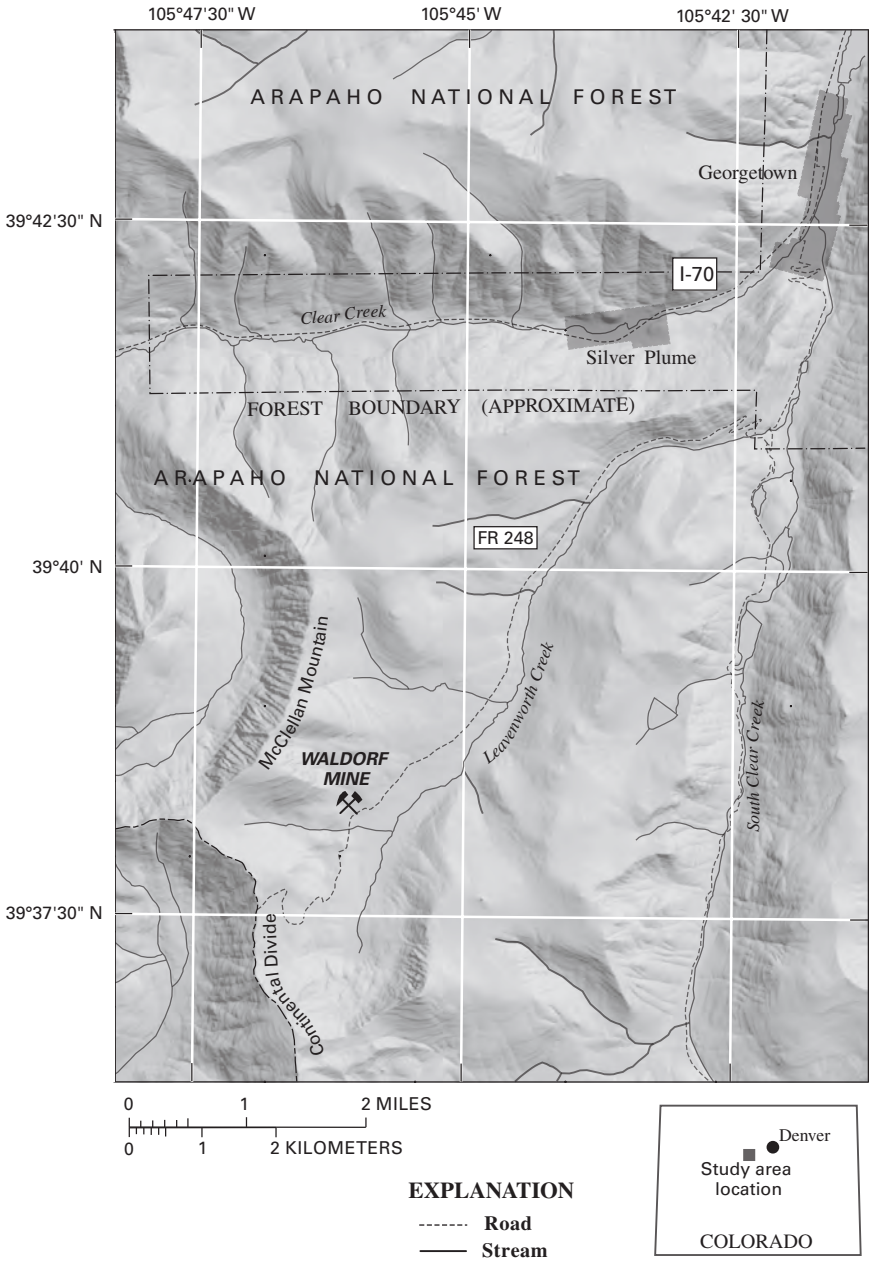

Figure 1. Location map of the Waldorf mine site and surrounding area.

Utilizing results from the second geophysical technique (a resistivity survey), we produced an apparent-conductivity model (inverted from resistivity) in four vertical cross sections (fig. 5; lines 1 through 4 shown in fig. 4). Connecting the inferred conductive zone at depth between lines 1, 2, and 3 (gray arrows in fig. 5) showed similar subsurface hydraulic pathways to the horizontal conductivity model. Line 4 was located away from the toe of the waste pile on a flat, water-saturated former railroad bed. The conductive zone shown on the surface of line 4 (fig. 5) indicates conductive water that collects there after issuing from the mine-waste pile and before it flows toward Leavenworth Creek.

Sources, Loads, and Transport to Leavenworth Creek

To determine the loadings of different chemical constituents to the creek and to locate inflows, whether point surface or diffuse ground water, a tracer-dilution study was conducted along about 1 kilometer of Leavenworth Creek, beginning about 300 meters upstream from where mine-affected water enters (Fey and Wirt, 2007). A nonreactive, conservative tracer (LiBr) was injected into the creek and allowed to reach

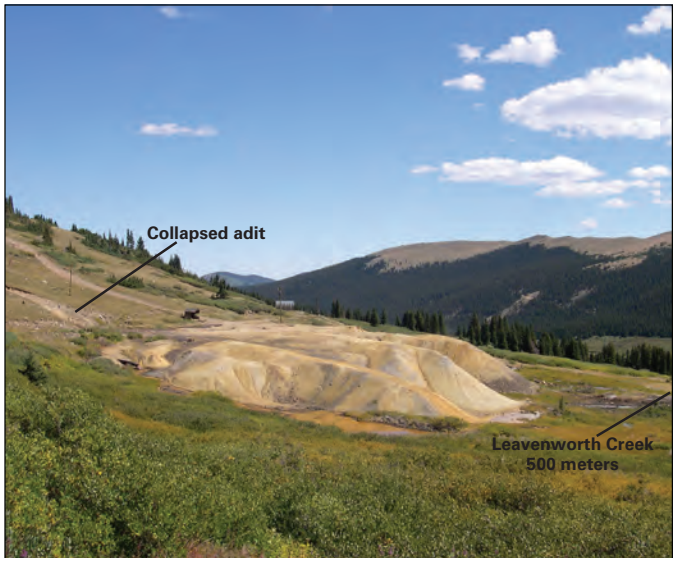

Figure 2. View of the Waldorf waste pile from south. Collapsed adit is at center left margin; drainage visible flowing around lobes of waste pile from left to right. Leavenworth Creek is 0.5 kilometer off to right.

steady-state conditions throughout the stream reach. Within a short timeframe (about 2 hours), 25 water samples were collected along the length of the reach and from identified surface tributaries. The downstream concentration of the tracer varies inversely proportionally to the increasing discharge; therefore, with a known, measured stream discharge at the beginning of the reach, subsequent discharges of the stream can be calculated from the analyzed water samples (Kimball and others, 2002). The discharges of tributaries are determined by the difference of the main stem upstream and downstream from each inflow. Unsampled ground-water inflow is determined by an increase in main-stem flow where tributaries are absent. The loads of various constituents (for example, copper, zinc, and sulfate) at every sampling point are calculated by multiplying discharge by measured concentration, giving the mass per day flowing past a given point. This calculation results in a loading profile, from which one can identify the locations both of surface and subsurface inputs.

At about 300 meters downstream from the uppermost site, the pH of the creek decreased and specific conductance increased, as did the concentrations of deposit-related constituents (for example, copper, lead, zinc, cadmium, and sulfate) due to the input of the surface drainage, which flows about 0.5 kilometer downslope from the mine site (arrow 1 in fig. 6). Comparing the loads of the adit with the loads of Leavenworth Creek just downstream from the mine-drainage input showed attenuation along the path from the waste pile (about 75 percent for copper and zinc), implying that some of the dissolved constituents were being sequestered in the wetland slope. Downstream about 200 meters, a small surface drainage introduces a mix of adit water and shallow ground water that has infiltrated through the area of dispersed mill tailings (arrow 2 in fig. 6). The concentrations and loads of copper and zinc in Leavenworth Creek increased slightly. At the end of the study reach, another surface discharge introduced mining-affected water. Its geochemical signature indicated that it was almost wholly composed of shallow ground water that had infiltrated downward through a large area of the dispersed tailings (arrow 3 in fig. 6). The magnitude of the zinc load of this tributary was larger than the load issuing at the site of the collapsed adit. There appeared to be some loading between sources 2 and 3 by input of unsampled diffuse ground water that had infiltrated through the area of dispersed tailings (arrow 4 in fig. 6; Fey and Wirt, 2007).

Comparing Sources and Loads Between Two Years

The purpose of the second year's efforts was to determine whether the diversion of the adit drainage around the waste pile had reduced loadings to Leavenworth Creek. In the second year of the study, the adit flow, waste-pile seeps, and Leavenworth Creek and its inputs were again sampled. In place of conducting another tracer study, manual

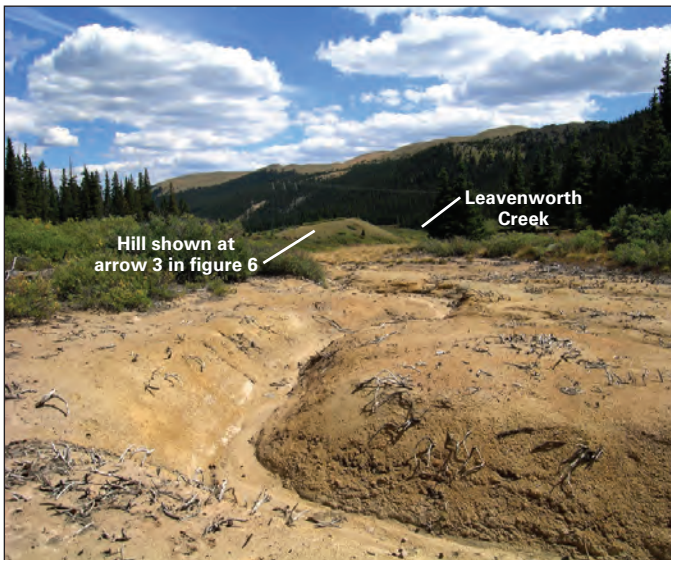

Figure 3. Photograph of dispersed mill tailings to the northeast of the Waldorf mine. These tailings are from a few centimeters to more than 1 meter thick. Rainwater runoff, snowmelt, and shallow ground water flow down these rills and enter Leavenworth Creek near the base of the hill in the center of photograph.

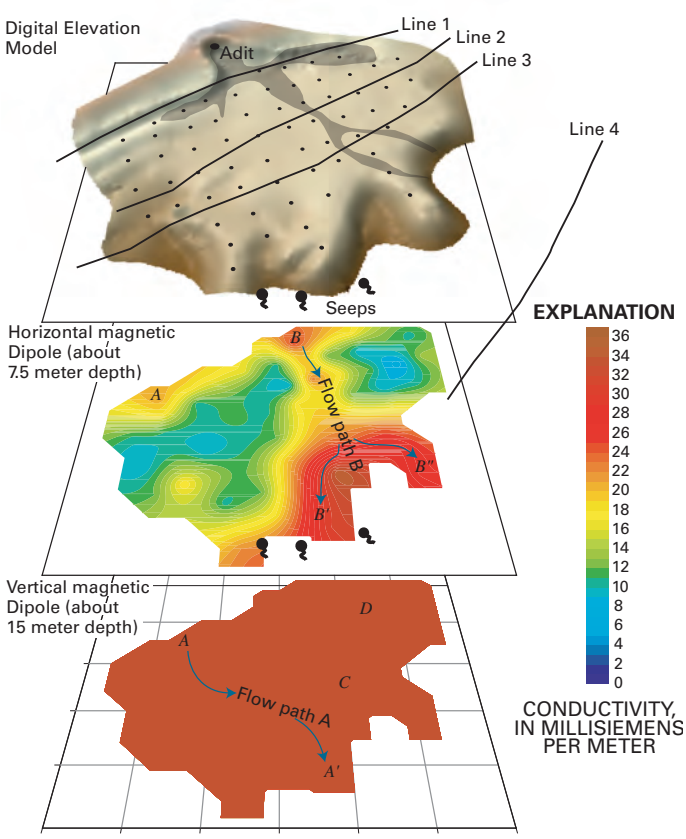

Figure 4. Digital Elevation Model of the waste-pile surface (top), Horizontal Magnetic Dipole conductivity contour map (middle), and Vertical Magnetic Dipole conductivity contour map (bottom).

measurements were made along the creek to determine discharge. The discharge of Leavenworth Creek was substantially higher in 2003 than in 2002 due to increased precipitation and snowpack of the previous winter (Fey and Wirt, 2007). The discharge of Leavenworth Creek at the most upstream part of the study reach was 100 liters per second in 2003 and 14 liters per second in 2002. Tributary inflows also were higher by varying amounts. The result of these different conditions is that any potential relative reduction of loading from the adit discharge was masked by increased discharges of all sources. The loadings of Leavenworth Creek at the downstream part of the study reach were all higher than the previous year, and the percent contributions of loadings from the adit discharge were also actually higher in 2003. This latter finding may have resulted from the dispersed mill tailings having been flushed of soluble salts during the wetter spring of 2003, yielding lower relative loadings from them (and higher relative loadings from the adit discharge) compared to the previous year (Fey and Wirt, 2007). Figure 7 shows these results in a graphical representation.

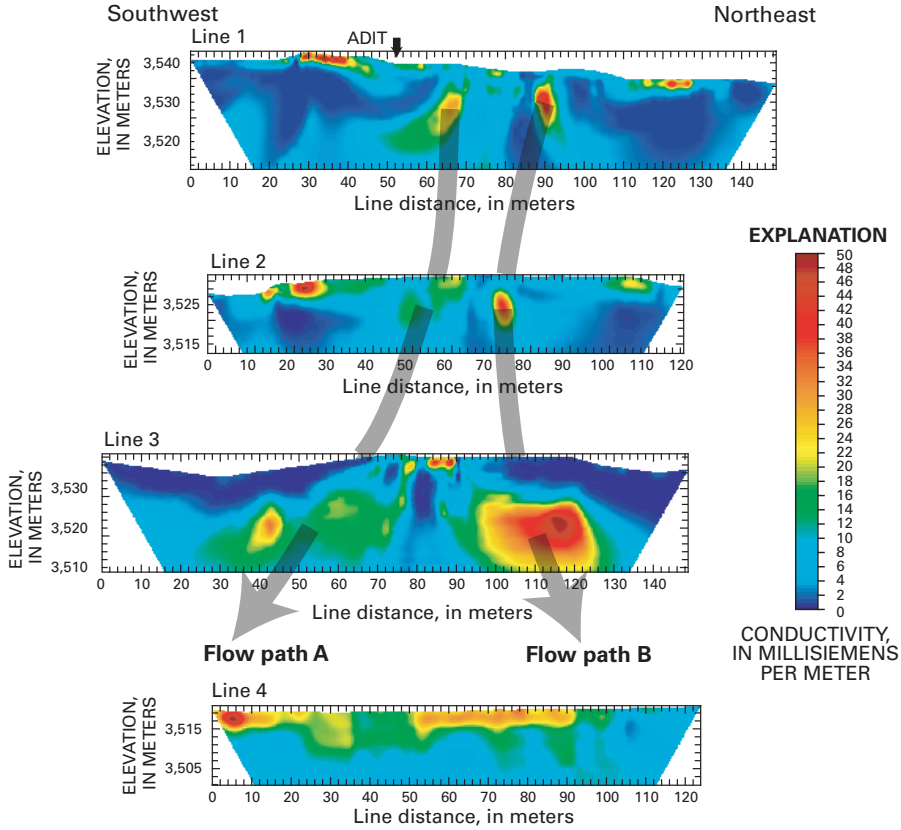

Figure 5. Conductivity profiles converted from DC resistivity profiles. Flow paths A and B refer to same in figure 4.

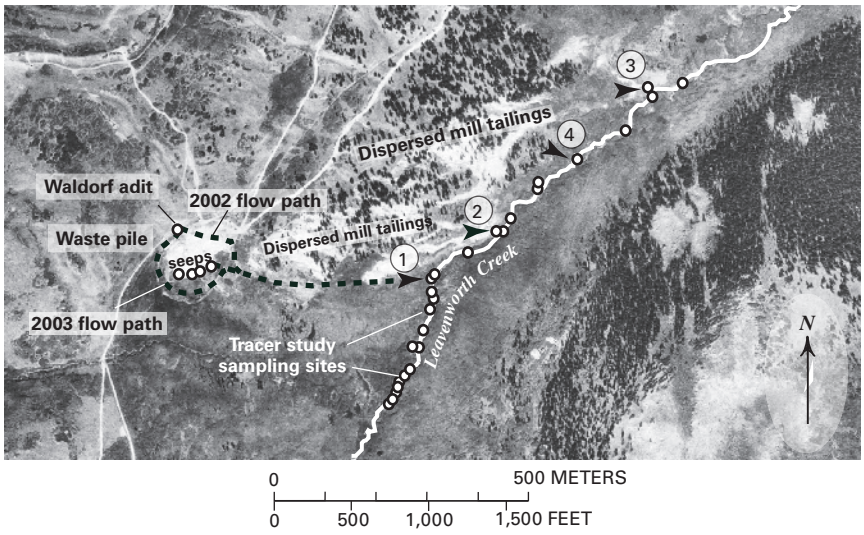

Figure 6. Aerial photograph of the Waldorf mine and Leavenworth Creek area. Arrows indicate surface flow of affected water. Affected shallow ground water enters creek between (2) and (3). Arrow (3) is location of the hill in figure 3.

Metal Concentrations and Comparison to Aquatic-Life Standards

Elevated concentrations of certain metals in stream water can adversely affect fish health and (or) potentially contaminate their food sources. Copper is toxic to fish, and zinc and cadmium are toxic to the benthic macroinvertebrates (caddisflies and mayflies). Acute and chronic aquatic-life toxicity standards, developed by the U.S. Environmental Protection Agency (USEPA), can be calculated based on hardness (calcium and magnesium content) of site water (Colorado Department of Public Health and Environment [CDPHE], 2007) and compared with site trace-element concentrations. Such standards have been developed for copper, zinc, nickel, lead, cadmium, and manganese. In this study, copper and zinc proved to exceed the standards at numerous sites.

Table 1 shows copper and zinc concentrations for six different sampling sites and the calculated chronic and acute toxicity standards. Upstream from the study reach, the copper concentration in Leavenworth Creek water is only at about 25 percent of the standards. The zinc concentration is already near the acute and chronic limits (about 85 percent). This may be due to an elevated background of this deposit-related element in rock and soil. Not surprisingly, the mine drainage that enters the creek from the wetland (TR–295) greatly exceeds the standards (6–10 times for copper and 12–14 times for zinc). As a result, Leavenworth Creek water (LC–325) reaches the toxicity standard for copper and exceeds the zinc standard by a factor of 4 just downstream from this drainage.

At the most downstream part of the study reach, 600 meters downstream from the first mine inputs, additional inputs from the sources previously discussed maintain the copper concentrations near the chronic and acute standards and increase the zinc concentration by a factor of six over the zinc standards. The copper concentration is diluted/attenuated to below standards at the mouth of Leavenworth Creek where it enters South Fork Clear Creek, 7 kilometers downstream. The zinc concentration at the mouth, however, is still at twice the chronic and acute standards.

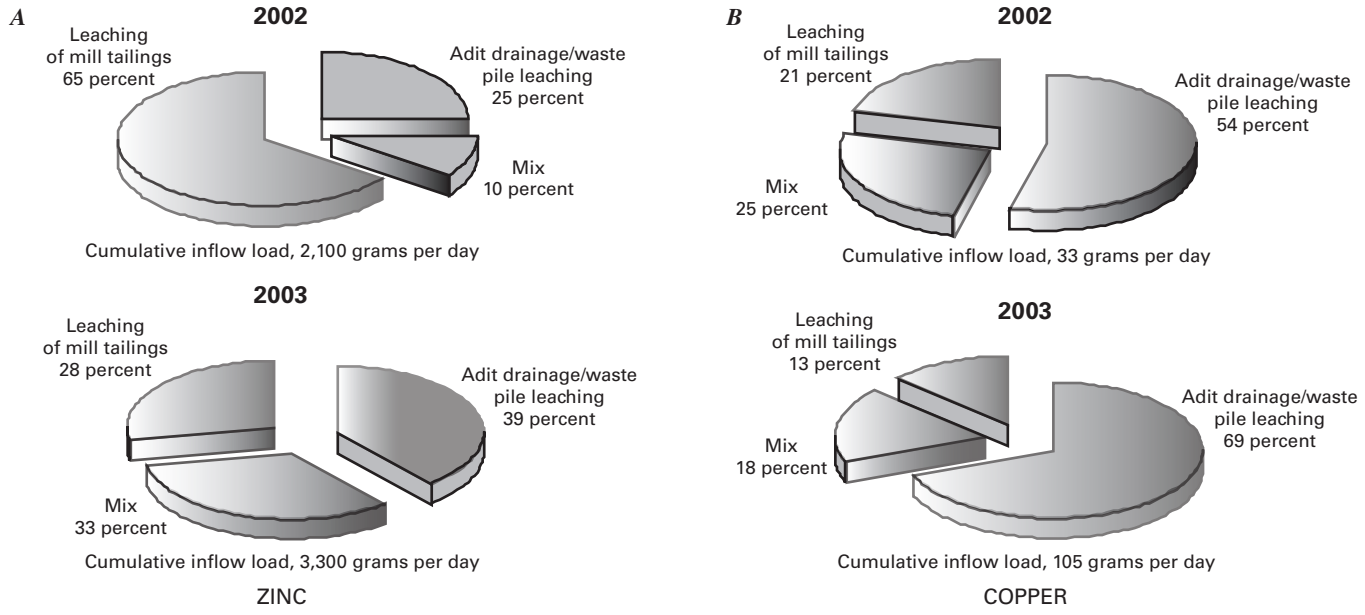

Figure 7. Pie charts illustrating relative contributions of zinc and copper to Leavenworth Creek in 2002 and 2003. Note higher loads in 2003 compared to 2002.

Table 1. Dissolved concentrations and hardness-based and chronic aquatic standards for copper and zinc, Leavenworth Creek and inflows.

[µg/L, micrograms per liter; L, Leavenworth]

Field number		Dissolved copper (µg/L)	Hardness-based chronic copper standard (µg/L)	Site copper/chronic standard (percent)	Hardness-based acute copper standard (µg/L)	Site copper/acute standard (percent)
Adit drainage	Adit	190	20	960	32	590
LC–200	L. Creek	0.54	2.7	20	3.5	15
TR–295	Tributary	160	15.4	1,040	24	660
LC–325	L. Creek	3.5	3.4	102	4.7	74
TR–902	Tributary	49	4.6	1,070	6.4	770
LC–930	L. Creek	5.2	3.7	140	5.1	100

Field number		Dissolved zinc (µg/L)	Hardness-based chronic zinc standard (µg/L)	Site zinc/chronic standard (percent)	Hardness-based acute zinc standard (µg/L)	Site zinc/acute standard (percent)
Adit drainage	Adit	7,440	270	2,700	320	2,300
LC–200	L. Creek	30	34	88	39	76
TR–295	Tributary	2,580	190	1,400	220	1,200
LC–325	L. Creek	175	44	390	51	340
TR–902	Tributary	2,780	67	4,900	58	4,800
LC–930	L. Creek	288	47	510	55	520

Conclusions

Geophysical and geochemical tools were used to identify ground-water flow paths and sources of metals and acidity to a receiving stream from a mine site. Integrating results from various techniques was essential in determining the hydrogeochemistry at this complex site. Adit water from the Waldorf mine flows around, under, and through the waste pile and enters Leavenworth Creek. Ground water also flows through dispersed mill tailings and into the creek. Concentrations of copper and zinc exceed aquatic-life standards along much of Leavenworth Creek.

References Cited

Church, S.E., Owen, J.R., von Guerard, P.B., Verplanck, P.L., Kimball, B.A., and Yager, D.B., 2007, The effects of acidic mine drainage from historical mines in the Animas River watershed, San Juan County, Colorado—What is being done and what can be done to improve water quality?, *in* DeGraff, J.V., ed., Understanding and responding to hazardous substances at mine sites in the Western United States: Geological Society of America Reviews in Engineering Geology, v. XVII, p. 47–83.

Colorado Department of Public Health and Environment (CDPHE), Water Quality Control Commission, 2007, Regulation 31, The basic standards and methodologies for surface water (5CCR 1002–31): Accessed November 8, 2007, at *http://www.cdphe.state.co.us/regulations/wqccregs/index.html*

Fey, D.L., and Wirt, L., 2007, Mining-impacted sources of metal loading to an alpine stream based on a tracer-injection study, Clear Creek County, Colorado, *in* DeGraff, J.V., ed., Understanding and responding to hazardous substances at mine sites in the Western United States: Geological Society of America Reviews in Engineering Geology, v. XVII, p. 85–103.

Kimball, B.A., Runkel, R.L., Walton-Day, K., and Bencala, K.E., 2002, Assessment of metal loads in watersheds affected by acid mine drainage by using tracer injection and synoptic sampling, Cement Creek, Colorado, USA: Applied Geochemistry, v. 17, no. 9, p. 1183–1207.

Lovering, T.S., 1935, Geology and ore deposits of the Montezuma quadrangle, Colorado: U.S. Geological Survey Professional Paper 178, 119 p.

McDougal, R.R., and Wirt, L., 2007, Characterizing infiltration through a mine-waste dump using electrical geophysical and tracer-injection methods, Clear Creek County, Colorado, *in* DeGraff, J.V., ed., Understanding and responding to hazardous substances at mine sites in the Western United States: Geological Society of America Reviews in Engineering Geology, v. XVII, p. 9–23.

Chapter G: Geologic Controls on Metal Transport in Ground Water Within an Alpine Watershed Affected by Historical Mining

by Raymond H. Johnson

Overview

In the upper Animas River watershed in southwestern Colorado, ground-water discharge to streams is a significant pathway for surface-water metal loading from both acid-mine drainage and acid-rock drainage. However, the delineation of metal transport through ground water is difficult in fractured-rock terrain. Prospect Gulch, a small alpine catchment in San Juan County, Colorado, was selected for study because of (a) a high degree of mineral alteration, (b) effects from historical mining, and (c) preexisting multidisciplinary data sets. Data on the hydrogeology of the Prospect Gulch system include geologic mapping, rock core analyses, multilevel ground-water monitoring wells, geochemistry of ground and surface water, stream tracer-dilution studies, and ground-water modeling. An integrated-science approach was taken to assemble these multiple datasets and provide a detailed conceptual model of the geologic controls on metal transport in ground water of Prospect Gulch.

Data analysis provided the following insights: (a) the presence of shallow and deep ground-water flow with distinct pathways, residence times, and geochemistry, which affect metal concentrations throughout the year, (b) distinct ground-water flow paths that can be delineated using geochemistry and modeling, and (c) the presence of different recharge and discharge zones for ground water and surface water due to structural control in the bedrock. This detailed conceptual model provides information that may assist stakeholders in making science-based decisions regarding long-term monitoring and remediation activities in Prospect Gulch.

Introduction

Although most mining activity in San Juan County, Colorado, and the upper Animas River watershed ceased by the 1990s, the effects of historical mining continue to release metals to ground water and surface water. These increased metal concentrations degrade stream-water quality and can be toxic to fish and other aquatic organisms. As a result, viable fish and aquatic habitat is now more limited than what existed before mining (Besser and others, 2007). Streams in this area have naturally low pH and elevated metal loads due to acid-rock drainage, but the effects of acid-mine drainage from historical mining activity have degraded preexisting ground-water and surface-water quality (Church and others, 2007). Ground-water discharge has been identified as a significant pathway for the loading of metals to surface water both from acid-mine drainage and from acid-rock drainage (Church and others, 2007; Kimball and others, 2002; Kimball and others, 2007; Paschke and others, 2005). Understanding the ground-water flow and dissolved-metal transport is essential in determining whether sampled metal loads to streams are related to acid-mine drainage or acid-rock drainage, and thus, whether or not an identified source of metal loading should be remediated. The ultimate objective of this research is to provide the necessary scientific information for public land managers to select effective remedial approaches that will improve water quality in the watershed.

In an effort to understand the ground-water flow system in the upper Animas River watershed, we selected Prospect Gulch (fig. 1) for further study because of the amount of existing multidisciplinary data in and around that particular watershed (Church and others, 2007). These data include stream tracer-dilution studies (Kimball and others, 2002; Wirt and others, 2001) that provide detailed streamflow and geochemistry information and detailed maps of the hydrothermal alteration in the bedrock (Bove and others, 2007b). In addition, Prospect Gulch has several inactive mines that are on land managed by the Bureau of Land Management (BLM).

An integrated-science approach was taken to address surface-water metal contributions from mining and the interaction of hydrothermally altered, sulfide-rich, volcanic rock with ground water. Three-dimensional geologic data include mineral analyses of rock cores (Bove and others, 2007a), maps of mineral alteration and structural features (Bove and others, 2007b), and seismic and ground-conductivity surveys (McDougal, 2006). For this study, the flow and geochemistry

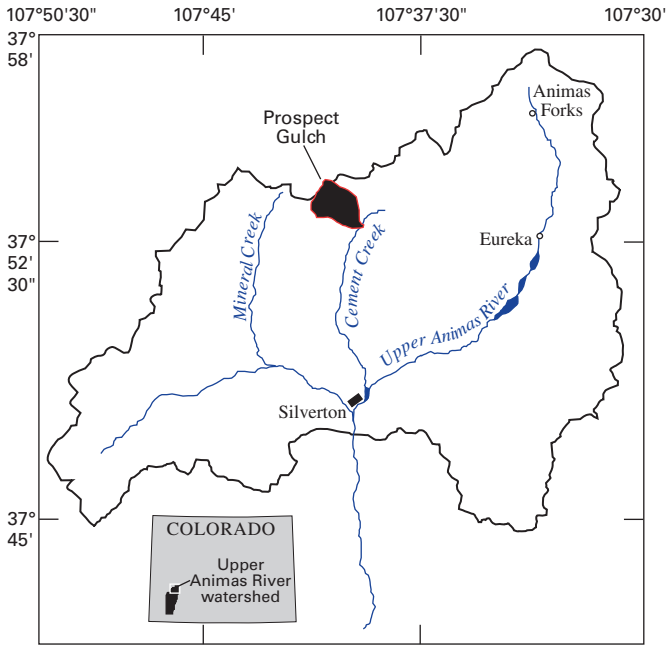

Figure 1. Location of Prospect Gulch in the upper Animas River watershed in southwestern Colorado.

of ground and surface water were defined through additional stream-tracer dilution studies (Johnson and others, 2007), the installation of ground-water monitoring wells (Johnson and Yager, 2006), and ground-water flow modeling (Johnson, 2007). This research integrates these multiple datasets to develop a detailed conceptual model of the geologic controls on metal transport in ground water.

Field Investigations

Bedrock in Prospect Gulch is composed of volcanic rocks that have been hydrothermally altered (fig. 2). As a result of this alteration, these rocks contain pyrite, which oxidizes and produces acidic ground water that can have high concentrations of iron and sulfate. A combination of impurities in the pyrite, oxidation of other sulfide minerals, and dissolution of buffering minerals also provides a source of other metals, such as copper, zinc, and aluminum (which are all toxic to fish at low concentrations). Sulfide oxidation occurs naturally in the mountain block (acid-rock drainage, fig. 3) and can be enhanced by mining activities through underground shafts and adits and the placement of sulfide-rich waste rock at the surface (acid-mine drainage, fig. 3). To monitor the resulting metal transport processes in Prospect Gulch, an intensive field investigation was initiated.

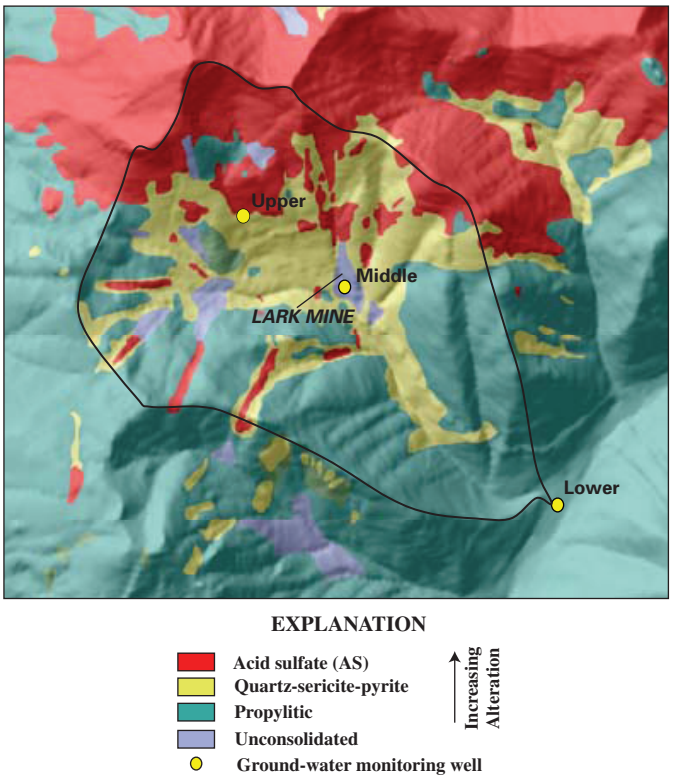

Figure 2. Map of altered bedrock in Prospect Gulch with the location of three ground-water monitoring wells.

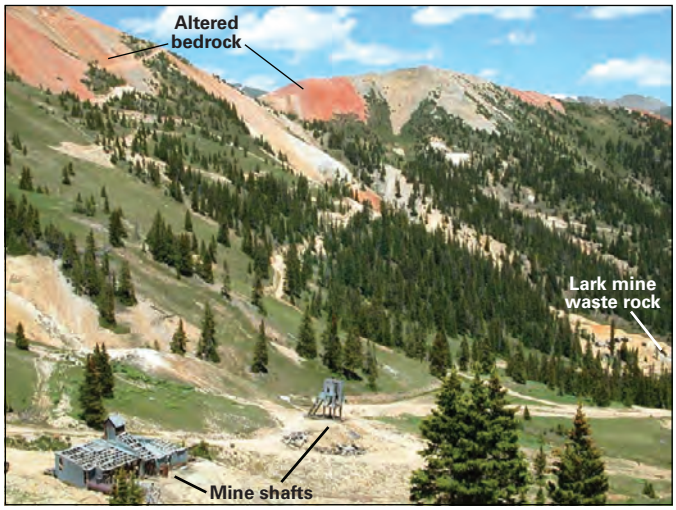

Figure 3. View of Prospect Gulch, looking north, with abandoned mines (acid-mine drainage) and areas with altered bedrock (acid-rock drainage).

Multilevel ground-water monitoring wells with sampling points at several depths were drilled in three locations (fig. 2) to determine (1) ground-water quality, (2) ground-water flow conditions, and (3) geology/mineralogy with depth. Bedrock cores were collected to a depth of 150 to 200 feet below land surface. Pyrite content up to 20 weight percent was measured in these cores (Bove and others, 2007a), indicating a large capacity for acid-rock drainage and an existing natural source of acidity and metals. The monitoring wells were located at upper, middle, and lower elevations (fig. 2) to capture ground water above, near, and below the mining-affected areas, which are in the middle elevations of Prospect Gulch. Water levels in the monitoring wells were measured year-round, when accessible. Additional geochemistry data were provided from sampling springs and the installation of shallow ground-water sampling points. Detailed sampling of surface-water quantity and quality using stream-tracer dilution studies provided companion data to the ground-water sampling. The complete details on methods and data collected during this project are summarized in three U.S. Geological Survey (USGS) Open-File Reports (Johnson and Yager, 2006; Johnson and others, 2007; and Bove and others, 2007a). Additional data collected before this project as part of the USGS Abandoned Mine Lands Initiative (Church and others, 2007) were also used as needed to assist in interpretations.

Improved three-dimensional stratigraphy was determined using geophysical techniques as companion data to bedrock cores collected during drilling. Core data provided a ground truth that allowed for a more unique interpretation of the geophysics. Companion geophysical profiles from seismic and ground-conductivity methods (fig. 4) were collected at several locations (McDougal, 2006). Interpretations from the

geophysical data were confirmed and (or) enhanced by data from cores and multilevel ground-water sampling in companion monitoring wells. Data from the middle well indicate a perched water table based on water levels within the monitoring well, the seismic profile indicates the depth to bedrock, and the conductivity profile highlights conductive ground-water plumes near the Lark Mine with high concentrations of dissolved solids and metals (fig. 4).

Conceptual Model

Data from the geophysics, monitoring well installations, and hydraulic and geochemical testing were used to develop a conceptual model of the hydrogeology at Prospect Gulch. A conceptual cross section from the top of Red Mountain #3 to the base of Prospect Gulch, with an elevation drop of 2,500 feet, is shown in figure 5. The conceptual model of the ground-water flow is characterized by shallow, intermediate, and deep ground-water flow lines. These ground-water flow paths have longer residence times with depth as confirmed by helium/tritium age dating (Johnson and others, 2007). The interaction of the ground-water flow with the geology produces distinct zones of geochemistry (fig. 5). The shallow ground water is highlighted by zone A, which has low pH, elevated copper (Cu) concentrations, and low iron (Fe) concentrations. Zone B represents an intermediate flow path with little geochemical difference from the shallower zone, except for slightly higher Fe concentrations. In zones A and B, sulfide oxidation is releasing iron and copper, but the oxygenated system allows for the precipitation of iron oxyhydroxides, whereas the copper remains in solution. As ground water moves with depth (zone C), sulfide oxidation continues to release iron and copper and consume oxygen. The consumption of oxygen allows for iron to remain in solution, but copper is precipitated. These oxidation-reduction controls are also seen with other metal concentrations (Johnson and others, 2007). The ground-water geochemistry created by mine waste rock is characterized by distinct plumes with even lower pH and very high concentrations of iron, copper, and other metals (exceeding background) that generally occur only in the shallow ground water (zone D).

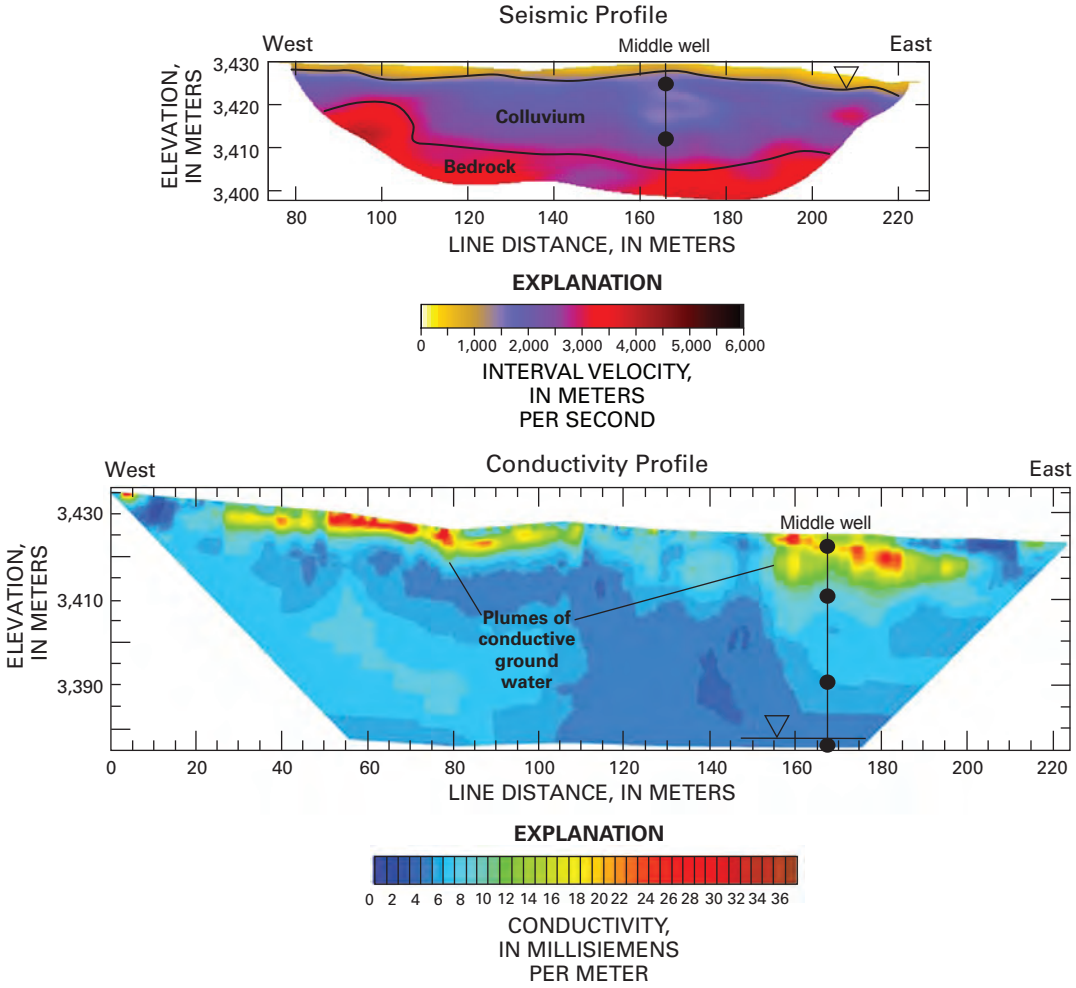

Figure 4. Companion geophysical profiles near the middle well. Triangles indicate the top of the shallow (on seismic profile) and deep (on conductivity profile) water tables. Note that the seismic profile is not as deep as the conductivity profile. Black circles indicate depth of sampling point within the multilevel monitoring well.

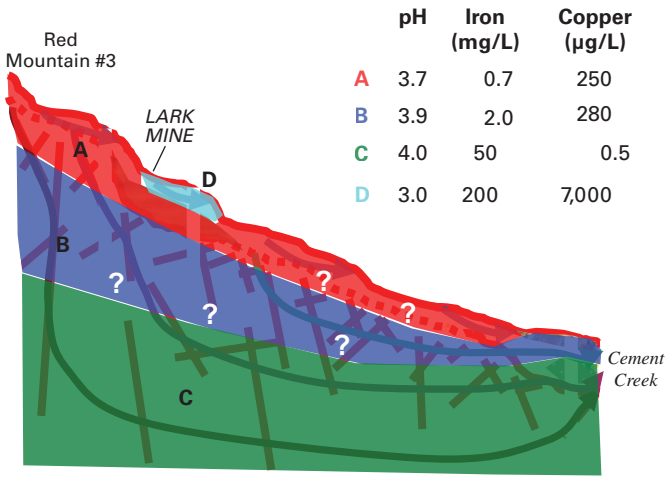

Figure 5. Conceptual cross section with geochemical zones. µg/L, micrograms per liter; mg/L, milligrams per liter.

Discharge of ground water to the surface creates distinct geochemistry in stream water. A snapshot of surface-water geochemistry is shown in figure 6, where samples representing detailed geochemistry of the stream water were collected at low-flow conditions (October 2004). This figure highlights the deep and shallow ground-water flow and the effects of mine-affected, shallow ground waters.

The mine-affected waters result in iron and copper loading to Prospect Gulch near the Lark mine. Downstream from the central portion of Prospect Gulch, the shallow and intermediate depth ground water discharges to the stream with low iron and high copper concentration; hence, the dilution of iron and maintenance of high copper concentrations within the stream. At the base of Prospect Gulch and in Cement Creek downstream from the confluence with Prospect Gulch, the discharge of the deep ground water to surface water substantially increases iron and decreases copper concentrations.

The results of stream monitoring at the mouth of Prospect Gulch indicate how the shallow and deep ground water affects the seasonal surface-water geochemistry (fig. 7). After recharge events, such as spring snowmelt or late summer rains, the larger contribution of shallow ground water creates a higher concentration of copper at the mouth of Prospect Gulch. In contrast, during the winter months when streamflow is supported by deep ground-water discharge, the highest iron concentrations and lowest copper concentrations occur. Surface-water data provide a valuable tool in understanding the seasonal and spatial complexity of ground-water flow and geochemistry within Prospect Gulch.

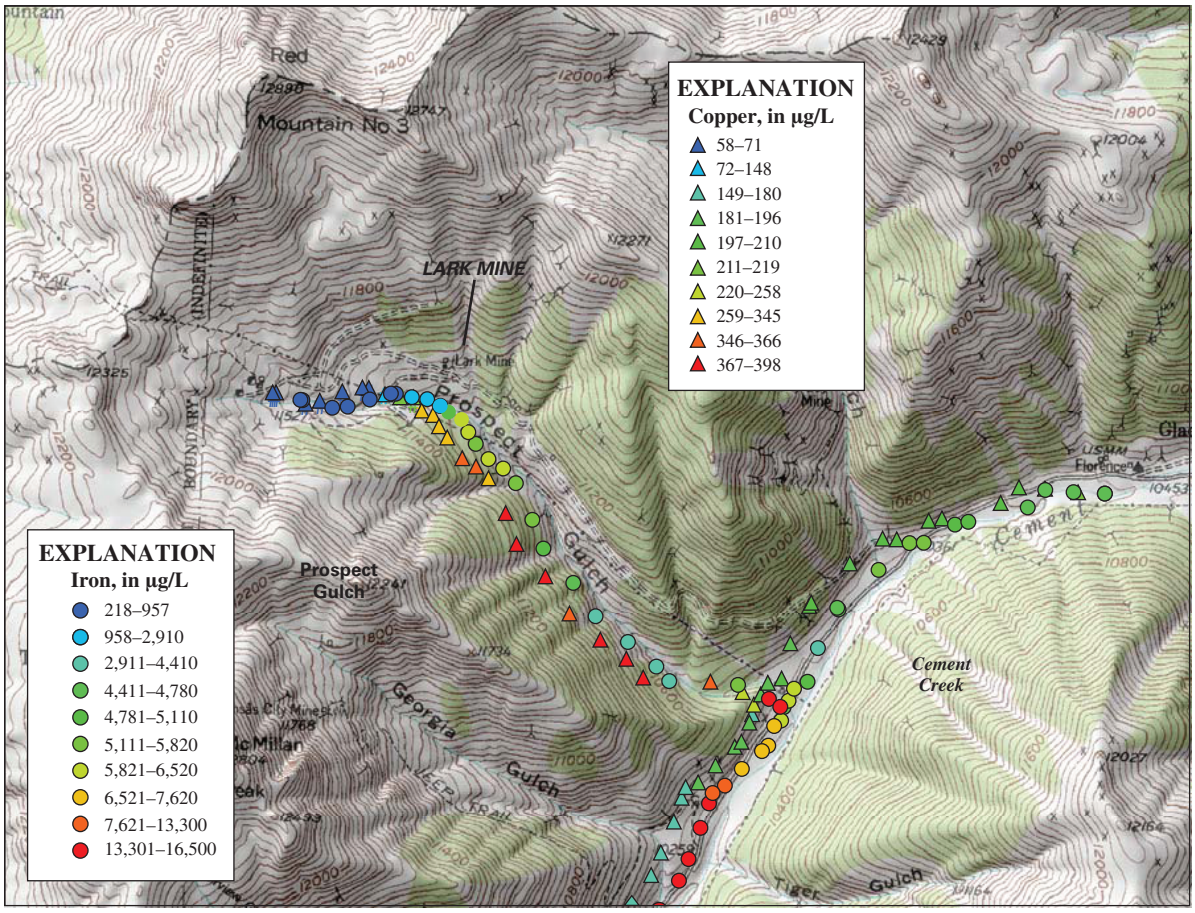

Figure 6. Downstream variation of dissolved copper and iron. µg/L, micrograms per liter.

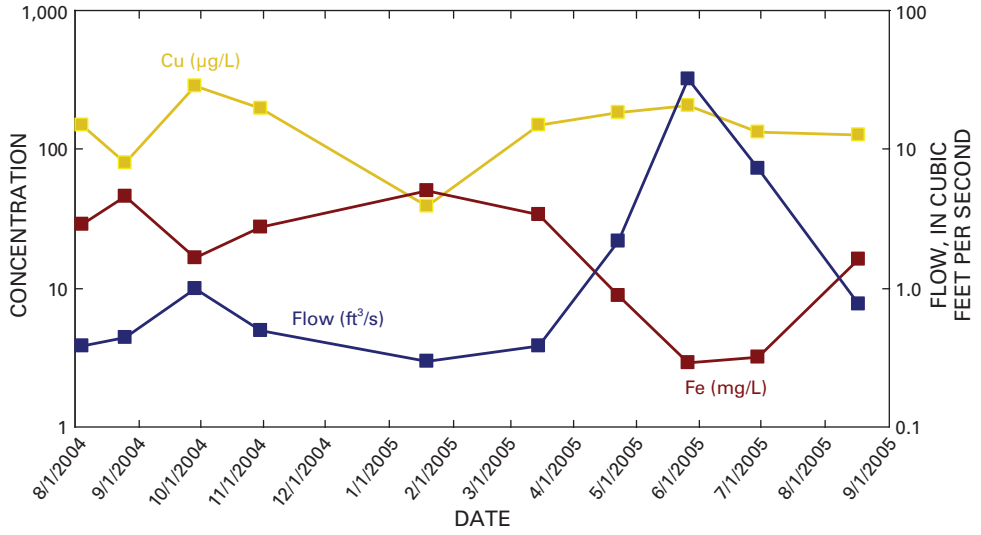

Figure 7. Temporal stream flow and concentrations of dissolved copper and iron measured at the mouth of Prospect Gulch. ft^3/s, cubic feet per second; µg/L, micrograms per liter; mg/L, milligrams per liter; Cu, copper; Fe, iron.

Ground-Water Flow Modeling

Three steady-state ground-water flow simulations were created for the area surrounding Prospect Gulch by using MODFLOW-2000 (Harbaugh and others, 2000) to evaluate the conceptual model of deep ground-water flow. These simulations considered steady-state conditions for the deep ground water and expand upon simulations completed before the field investigations were initiated, where sensitivity analyses were performed to guide field-data collection (Johnson, 2007). The three simulations all have the same boundary conditions and calibration data (streamflow and hydraulic head) but evaluate the following three conceptual models: (1) homogeneous hydraulic conductivity with depth, (2) decreasing hydraulic conductivity with depth, and (3) decreasing hydraulic conductivity with depth with the addition of structural controls. Structural control was provided by using a horizontal flow barrier that followed alignments similar to mapped veins and faults and boundaries provided by airborne magnetic data. Decreasing hydraulic conductivity with depth provides a large improvement in matching the observed hydraulic heads when compared to a homogeneous simulation but does not improve the match to streamflow. The additional structural control (fig. 8) improves the match to the observed streamflows. This structural control drains an upper portion of the model domain across a surface-water divide, directing ground water to the base of Prospect Gulch instead of the upper reaches of Cement Creek. This improvement in calibration demonstrates the need for some structural control in the fractured bedrock, but the use of hydraulic barriers is not a unique solution, as other conceptual models of structural features may also give reasonable calibration results.

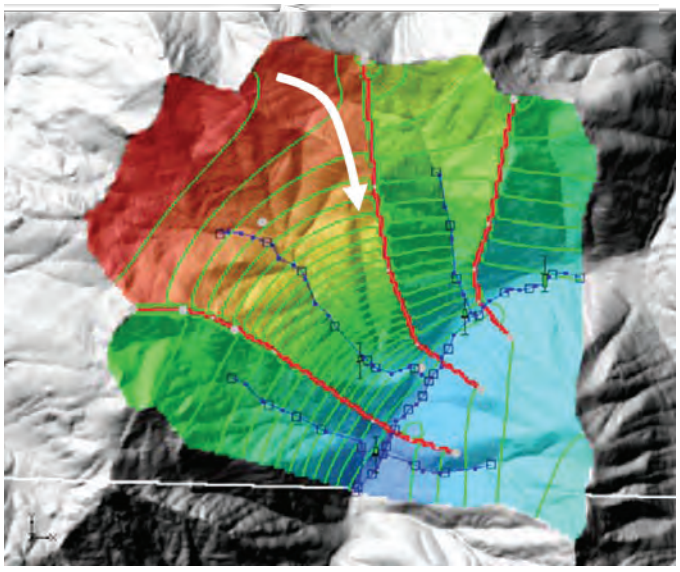

Figure 8. Simulated hydraulic head contours for conceptual model with decreasing hydraulic head with depth and structural control. Hydraulic barriers are in red, and the redirected flow path is in white arrow.

Conclusions

In Prospect Gulch, an interdisciplinary approach has demonstrated the occurrence of shallow and deep ground-water flow with distinct pathways, residence times, and geochemistry and has provided a conceptual model of ground-water flow and metal transport. The distinct geochemistry of the ground water is created by changing redox conditions, local geology, and mining effects. The discharge of ground water to nearby streams affects the concentrations of metals observed in the surface water in spatial and temporal patterns. These patterns highlight

the discharge of shallow, deep, and mine-affected ground water because of their unique geochemical signatures. Ground-water flow modeling identifies areas where surface-water and ground-water recharge and discharge zones may differ, with ground water crossing a surface-water divide. The combined use of geochemical data, conceptual model development, and ground-water flow modeling has delineated distinct ground-water flow pathways and identified the presence of structural control, all of which demonstrate effects on metal transport in ground water within Prospect Gulch. This framework and modeling approach can be used in Prospect Gulch and other areas in a predictive mode to determine how possible remedial scenarios may affect the discharge of metals to surrounding streams. This approach can provide stakeholders and land managers with a scientific-based conceptual model that can be used as a decisionmaking tool in proceeding with the remediation of abandoned mine lands.

Acknowledgments

As an integrated-science project, this research is a compilation of work completed by many, through data collection and assistance in figure preparation. Geophysical research was completed by Michael Powers, Bethany Burton, and Robert McDougal. Geologic research was completed by Dana Bove and Douglas Yager, and the stream tracer-dilution research was completed by Laurie Wirt, David Fey, and Kenneth Leib. Funding for this research was provided by the USGS Mendenhall Postdoctoral Research Program, the USGS Mineral Resources Team, and the Bureau of Land Management.

References Cited

Besser, J.M., Finger, S.E., and Church, S.E., 2007, Impacts of historical mining on aquatic ecosystems—An ecological risk assessment, *in* Church, S.E., von Guerard, Paul, and Finger, S.E., eds., Integrated investigations of environmental effects of historical mining in the Animas River watershed, San Juan County, Colorado: U.S. Geological Survey Professional Paper 1651.

Bove, D.J., and Johnson, R.H., and Yager, D.B, 2007a, Mineralogy from cores in Prospect Gulch, San Juan County, Colorado: U.S. Geological Survey Open-File Report 2007–1095 *http://pubs.usgs.gov/of/2007/1095/*

Bove, D.J., Mast, M.A., Dalton, J.B., Wright, W.G., and Yager, D.B, 2007b, Major styles of mineralization and hydrothermal alteration and related solid- and aqueous-phase geochemical signatures, *in* Church, S.E., von Guerard, Paul, and Finger, S.E., eds., Integrated investigations of environmental effects of historical mining in the Animas River Watershed, San Juan County, Colorado: U.S. Geological Survey Professional Paper 1651, 1096 p., 2 volumes.

Church, S.E., von Guerard, Paul, and Finger, S.E., eds., 2007, Integrated investigations of environmental effects of historical mining in the Animas River Watershed, San Juan County, Colorado: U.S. Geological Survey Professional Paper 1651, 1096 p., 6 plates, 1 DVD.

Harbaugh, A.W., Banta, E.R., Hill, M.C., and McDonald, M.G., 2000, MODFLOW-2000, the U.S. Geological Survey modular ground-water model—User guide to modularization concepts and the ground-water flow process: U.S. Geological Survey Open-File Report 2000–92, 121 p.

Johnson, R.H., 2007, Ground water flow modeling with sensitivity analyses to guide field data collection in a mountain watershed: Ground Water Monitoring and Remediation, v. 27, no. 1, p. 75–83.

Johnson, R.H., Wirt, L., Manning, A.H., Leib, K.J., Fey, D.L., and Yager, D.B., 2007, Geochemistry of surface and ground water in Cement Creek from Gladstone to Georgia Gulch and in Prospect Gulch, San Juan County, Colorado: U.S. Geological Survey Open-File Report 2007–1004, 140 p. *http://pubs.usgs.gov/of/2007/1004/*

Johnson, R.H., and Yager, D.B., 2006, Completion reports, core logs, and hydrogeologic data from wells and piezometers in Prospect Gulch, San Juan County, Colorado: U.S. Geological Survey Open-File Report 2006–1030, 32 p. *http://pubs.usgs.gov/of/2006/1030/*

Kimball, B.A., Runkel, R.L., Walton-Day, Katherine, and Bencala, K.E., 2002, Assessment of metal loads in watersheds affected by acid mine drainage by using tracer injection and synoptic sampling—Cement Creek, Colorado, USA: Applied Geochemistry, v. 17, p. 1183–1207.

Kimball, B.A., Walton-Day, Katherine, and Runkel, R.L., 2007, Quantification of metal loading by tracer injection and synoptic sampling, 1996–2000, *in* Church, S.E., von Guerard, Paul, and Finger, S.E., eds., Integrated investigations of environmental effects of historical mining in the Animas River Watershed, San Juan County, Colorado: U.S. Geological Survey Professional Paper 1651, 1096 p., 2 volumes.

McDougal, R.R., 2006, Electrical resistivity surveys in Prospect Gulch, San Juan County, Colorado: U.S. Geological Survey Open-File Report 2006–1171 *http://pubs.usgs.gov/of/2006/1171/*

Paschke, S.S., Kimball, B.A., and Runkel, R.L., 2005, Quantification and simulation of metal loading to the upper Animas River, Eureka to Silverton, San Juan County, Colorado, September 1997 and August 1998: U.S. Geological Survey Scientific Investigations Report 2005–5054, 73 p.

Wirt, Laurie, Leib, K.J., Bove, D.J., and Melick, R., 2001, Metal loading assessment of point and non-point sources in a small alpine sub-basin characterized by acid drainage—Prospect Gulch, upper Animas River watershed, Colorado: U.S. Geological Survey Open-File Report 2001–0258.

Chapter H: Electrical Geophysical Characterization of a Mining-Affected Subbasin, Prospect Gulch, Colorado

by Robert R. McDougal

Overview

Prospect Gulch is a major source of naturally occurring and mining-related metals to Cement Creek, a tributary of the upper Animas River in southwestern Colorado. Efforts to improve water quality in the watershed have focused on Prospect Gulch because many of its abandoned mines are located on Federal lands. Information on sources and pathways of metals and related ground-water flow will be useful to help prioritize and develop remediation strategies. It has been shown that the occurrence of sulfate, aluminum, iron, zinc, and other metals associated with historical mining and the natural weathering of pyritic rock is substantial. In this study, direct current resistivity surveys were conducted to determine the subsurface resistivity distribution and to identify faults and fractures that may act as ground-water conduits or barriers to flow. Five profiles of resistivity data were collected in the vicinity of Prospect Gulch, and cross-section profiles were constructed from the field data using a two-dimensional inversion algorithm. The conductive anomalies in the profiles are most likely caused by wet or saturated rocks and sediments, clay-rich deposits, or ground water with high concentrations of dissolved solids. Resistive anomalies are likely bedrock, dry surficial and subsurface deposits, or deposits of ferricrete.

Introduction

As a tributary of the upper Animas River in southwestern Colorado, Prospect Gulch is a major source of naturally occurring and mining-related metals to Cement Creek. In this highly mineralized subbasin it has been shown that the presence of sulfate, aluminum, iron, zinc, copper, and other metals associated with historical mining is substantial but relatively insignificant compared to contributions from areas of natural weathering of highly altered, pyritic rock (Wirt and others, 2001). While many of the streams in the area have low pH and elevated metal loads caused by acid-rock weathering, acid-mine drainage from historical mining has contributed to the degradation of ground and surface water (Church and others, 2007). Efforts to improve water quality in the watershed have focused on Prospect Gulch because many of its abandoned mines and waste-rock piles are located on land managed by the Bureau of Land Management (BLM). Information on sources and pathways of metals and related ground-water flow will be useful to the BLM to help develop and prioritize remediation strategies. Several mine adits and large waste dumps are located on BLM property in the drainage. These are associated with the Lark, Henrietta, and Joe and John mines. Other notable historical mines include the Hercules and Galena Queen mines (fig. 1).

The direct current (dc) resistivity method is a geophysical technique that measures subsurface electrical resistivity to help characterize subsurface features related to geologic structure and ground-water geochemistry. The dc resistivity surveys presented in this study were conducted to determine the subsurface resistivity distribution and to identify faults and fractures that may act as conduits or barriers to ground-water flow. The results of the electrical geophysical surveys presented here are part of an integrated effort, including seismic surveys, drilled core and monitoring wells, stream-tracer injection studies, and geochemical analyses, to characterize and model ground-water flow in Prospect Gulch.

Geology and Physical Setting of Prospect Gulch

Prospect Gulch is located on the margin of the historic Red Mountain mining district, near the northwest structural margins of the San Juan and Silverton calderas. Rocks in Prospect Gulch formed following formation of the 28.2-million-year-old San Juan Caldera and are coincident with and (or) postdate formation of the 27.8-million-year-old Silverton caldera (Yager and Bove, 2002). The igneous sequence, referred to as the Silverton Volcanics, formed from lavas and volcaniclastic sediment that infilled the San Juan caldera over an area of 14 km^2 to a thickness of nearly a kilometer (Lipman and others, 1973). Following caldera formation, and simultaneous with Silverton Volcanics deposition, regional alteration occurred throughout much of the study area. Several small-volume plugs and dikes intruded along the structural margins of the calderas long after caldera activity ceased. Based on the isotopic ages of the intrusions near Prospect Gulch, the intrusions formed several million years after the eruption of the Silverton Volcanics lavas during the Miocene Epoch (Lipman and others, 1973). The intrusions are thought to have provided the heat source for the hydrothermal alteration and mineralization of the Red Mountain mining district (Lipman and others, 1976; Bove and others, 2001).

A number of alteration types are found in Prospect Gulch and vary substantially from north to south across the subbasin (Bove and others, 2007a; Bove and others, 2007b). Near Red Mountain No. 3 (fig. 1), acid sulfate mineralization is exposed and is associated with pervasive silicification that formed resistant ridges. The acid sulfate mineralization is characterized by high sulfate content and includes the mineral assemblage of quartz, alunite, pyrophyllite (qap), and pyrite. More easily

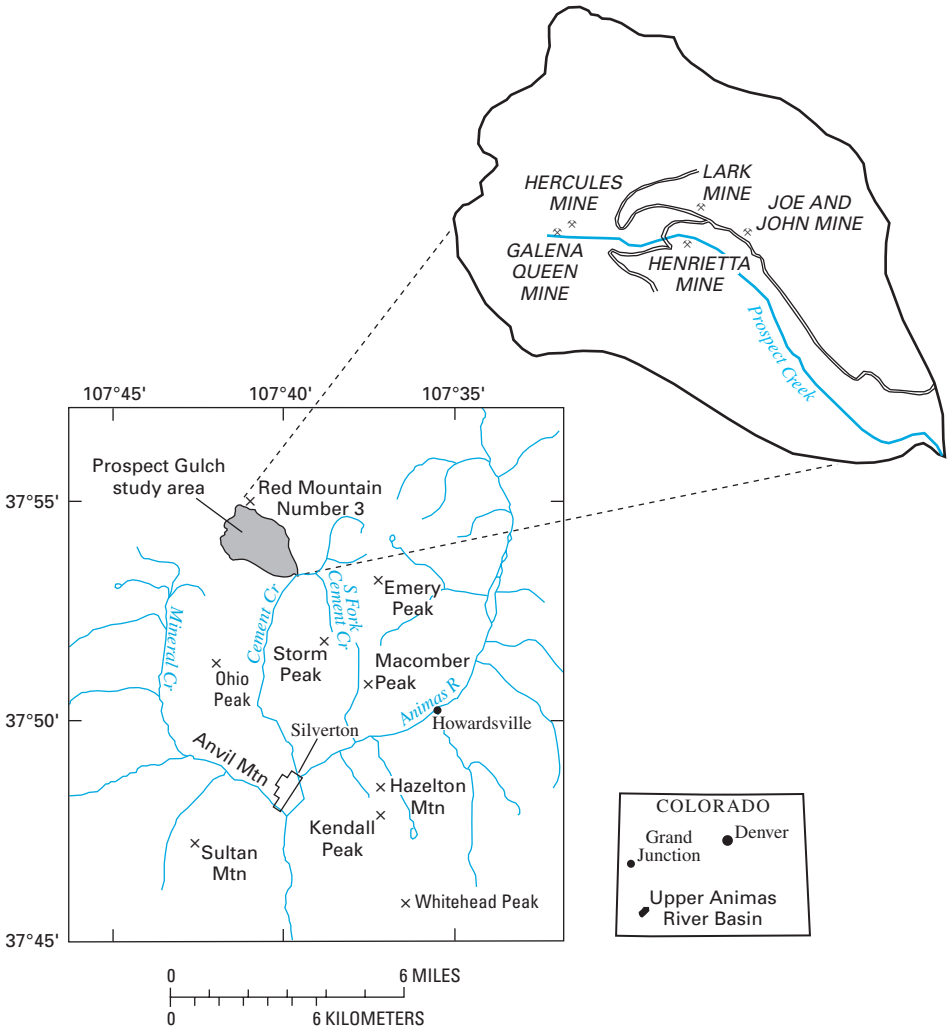

Figure 1. Location map of the Prospect Gulch study area in the upper Animas River watershed.

weathered argillic alteration occurs on the margins of the qap assemblage. The most abundant alteration assemblage in Prospect Gulch is the quartz-sericite-pyrite (qsp), locally containing 10 to 20 volume percent pyrite. In the lower part of the subbasin, regional propylitic alteration is dominant.

Structural interpretation of mapped veins in the subbasin indicates that general trends of northwest, north, and northeast are predominant. Evidence suggests that these veins may have formed coincident with mineralization along structural zones of weakness. East-west-trending veins, although uncommon, do occur in Prospect Gulch (Bove and others, 2007a; Bove and others, 2007b).

Prospect Gulch is a steep-gradient alpine to subalpine mountain subbasin that drains the southern flank of Red Mountain No. 3 (fig. 1). The stream in Prospect Gulch has an elevation change of 800 m along its 2.4-km length. Much of Prospect Gulch is above tree line, which is approximately 3,500 m at this latitude. Nonforested areas primarily consist of alpine vegetation, poorly developed soils, talus, and exposures of bedrock.

Electrical Properties of Earth Materials

Electrical resistivity, which can be expressed inversely as electrical conductivity, is a fundamental property of all earth materials. The degree of resistance or conductance varies with rock or sediment type, porosity, clay mineral type and content, and the quantity and quality of water. Poorer quality ground water (that is, water with higher concentrations of dissolved solids) or sediments with higher clay content are usually more

conductive than "clean" water (Zohdy and others, 1974). The presence of electrically conductive minerals such as metallic sulfides can also result in higher conductivity values.

Resistivity units are ohm-meters. Often, in geophysical studies associated with ground-water characterization, it is useful to convert values of resistivity to conductivity to identify or emphasize conductive anomalies or zones. To convert resistivity to conductivity, the following formula is used:

$$1{,}000/\text{ohm-meters} \rightarrow \text{millisiemens/meter}$$

Because of the many factors that affect terrain conductivity, interpretation of geophysical surveys can often result in a nonunique explanation for a conductive or resistive anomaly. Therefore, in this study, the availability of information from drilled core samples (Johnson and Yager, 2006) aided in the interpretation of the resistivity data.

Collection of Resistivity Data

Five resistivity profiles were collected on and downgradient from the alluvial fan at the base of Prospect Gulch (fig. 2). Profile 1, paralleling Cement Creek Road, starts at the north end of the Prospect Gulch alluvial fan, crosses Prospect Creek, and ends at the southern extent of the fan. Profiles 2 and 3 coincide with the location of two seismic profiles collected contemporaneously with the resistivity. Profile 4 extends from the southern extent of the alluvial fan past an iron bog adjacent to Cement Creek. Profile 5 was located below the Lark mine on an old road grade composed of waste rock from the Henrietta mine (fig. 2).

The dc resistivity equipment used in this study records lateral and vertical resistivity variations in the subsurface. This multielectrode system has the capability of recording many channels of data simultaneously and allows for the collection of very dense dc resistivity data in a relatively short amount of time. The electrode array consisted of 76 dual mode switches in contact with the ground using stainless-steel stakes driven into the ground along a relatively straight profile. The dual mode electrodes are automatically switched to allow each to operate as either current or potential electrodes in the array. Equidistant spacing between each electrode was varied, depending upon the desired line length, depth of investigation, and data resolution.

The data collected in the field indicated the apparent resistivity of the subsurface. These data were then converted to true resistivity as a function of depth using a numerical inversion method (Advanced Geosciences, Inc., 2006). The result of the inversion process is a true resistivity cross section corrected for changes in topography along the profile by using elevation and position data.

Results

The inverted data were used to construct profiles of subsurface resistivity profiles of the Prospect Gulch alluvial fan, the area along the Cement Creek road from Prospect Gulch to Georgia Gulch, and the waste rock below the Lark mine (fig. 2). Resistivity values in ohm-meters obtained from the inversion program were converted to conductivity values in millisiemens per meter to emphasize conductive anomalies as previously described. Data grids were calculated using the minimum curvature gridding method and plotted as contoured profile maps ranging in value from 0 to 37 millisiemens per meter.

The conductive anomalies in these profiles are most likely caused by wet or saturated rocks, clay-rich sediments, or ground water with high concentrations of dissolved solids. Resistive anomalies are likely bedrock, dry surficial and subsurface deposits, or deposits of ferricrete. Identification of these conductive and resistive zones is important to help characterize ground-water flow in the subbasin and help constrain ground-water modeling efforts.

Profile 1 (fig. 3) was positioned to identify conductive anomalies that are possibly related to ground water discharging to Cement Creek from Prospect Gulch. The highest conductivity values are interpreted as wet or saturated alluvium when recorded near the surface, and wet or saturated bedrock when recorded at depth, although the alluvium/bedrock interface is not well defined. Conductive anomalies occurring in bedrock may be associated with fracture-controlled ground-water flow, and conductive anomalies in the alluvium may be associated with increased clay content. A well-core log from an exploration well drilled near Profile 1 shows that bedrock (Silverton Volcanics) in this area is highly fractured and hydrothermally altered (Johnson and Yager, 2006).

The location of Profile 2 (fig. 4) was selected to correspond with the position of a contemporaneous seismic survey profile. As with Profile 1, Profile 2 is characterized by high resistivity at the surface, which is the result of dry surficial deposits and ferricrete. In some areas near the center of the profile, ferricrete was exposed at the surface. The very hard nature of the ferricrete made placement of the electrodes difficult and resulted in very high contact resistance and degraded signal quality.

The location of Profile 3 (fig. 5) was also coincident with a seismic survey profile. The relative depth of conductive features in this profile indicates that the saturated alluvial zone is deeper near the bottom of the alluvial fan and may also indicate the changing depth of clay-rich sediments. The conductive zone at the surface is near an area of saturated ground observed to be associated with an iron bog. The thin, resistive layer beneath this conductive zone is interpreted as a ferricrete confined unit between the conductive shallow ground water and the deeper conductive ground water.

Profile 4 (fig. 6) was positioned to identify conductive zones downgradient from Prospect Gulch that might be associated with an iron bog along Cement Creek. The profile is generally resistive at the surface along its length, resulting from ferricrete and dry soil and surficial deposits. The highly resistive surface layer at the northeast end of the profile coincides with the resistivity high at the southwest end of Profile 1 and results from ferricrete and dry surficial deposits.

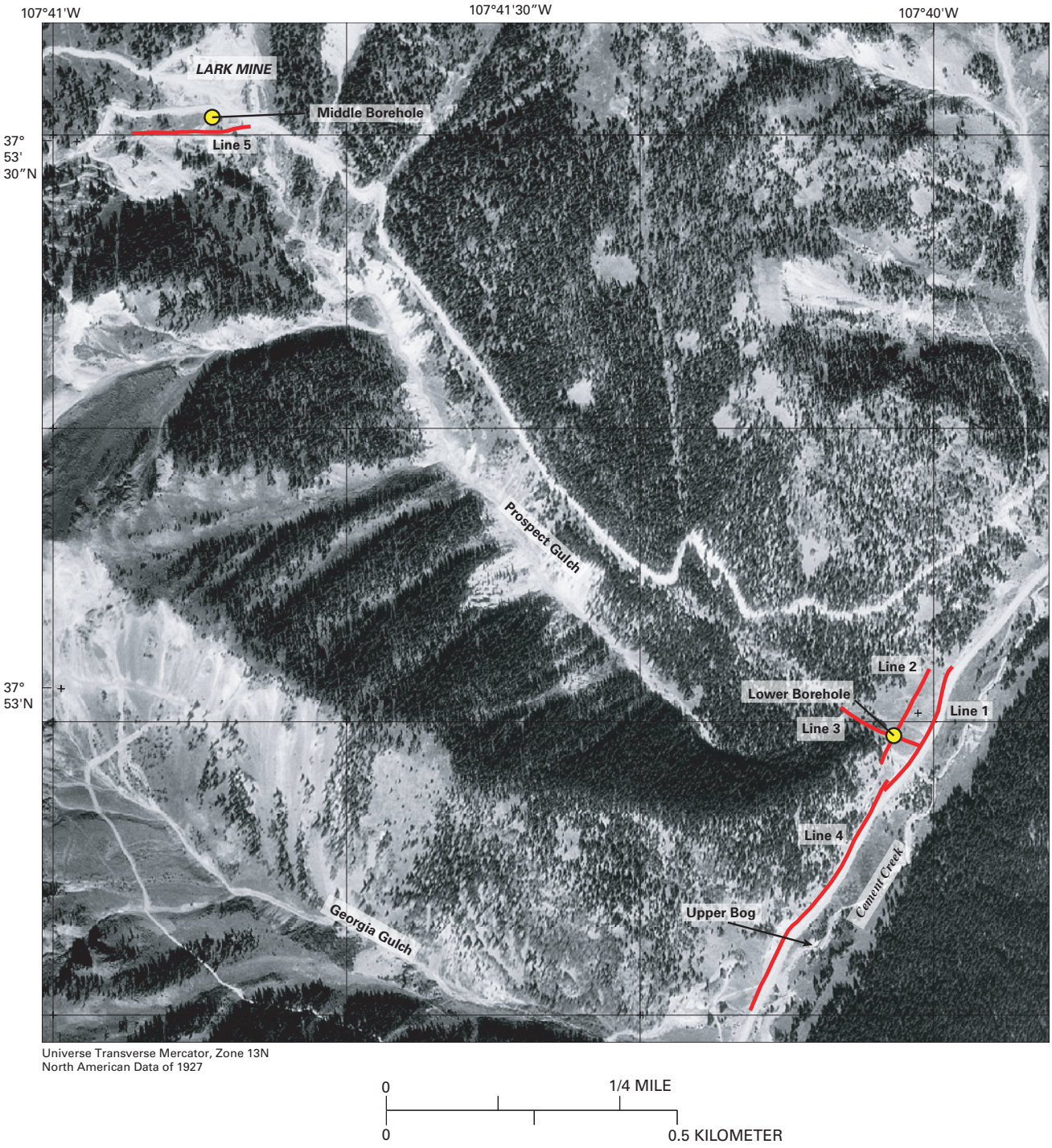

Figure 2. Location of resistivity survey lines and boreholes within the study area (digital orthophoto quad base image).

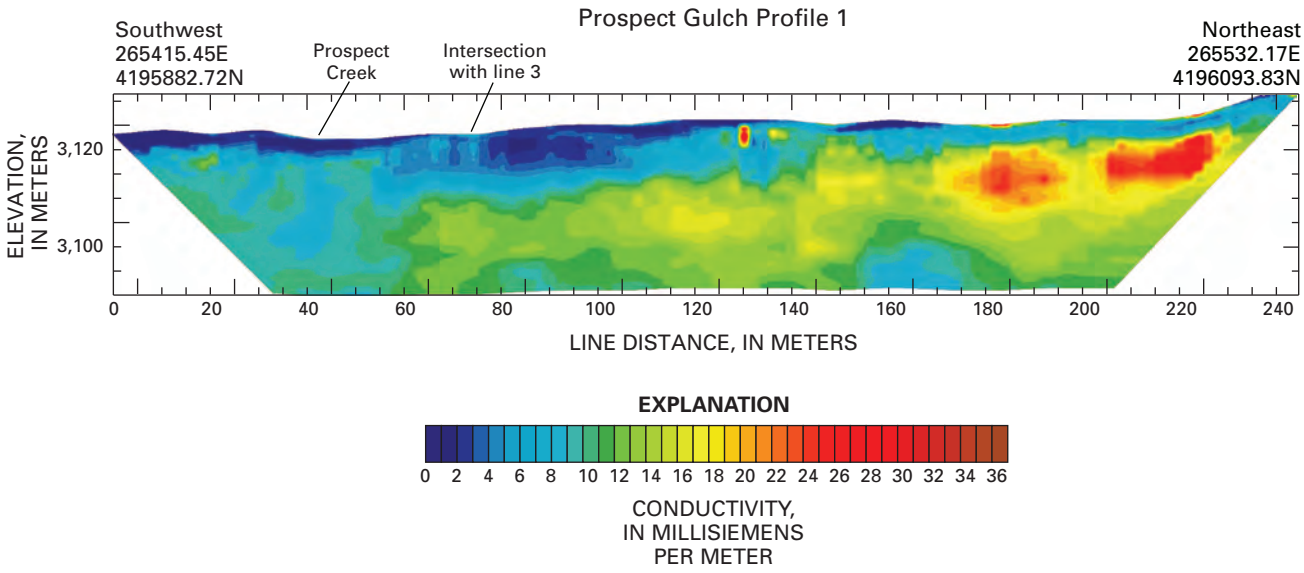

Figure 3. Conductivity Profile 1. m, meters.

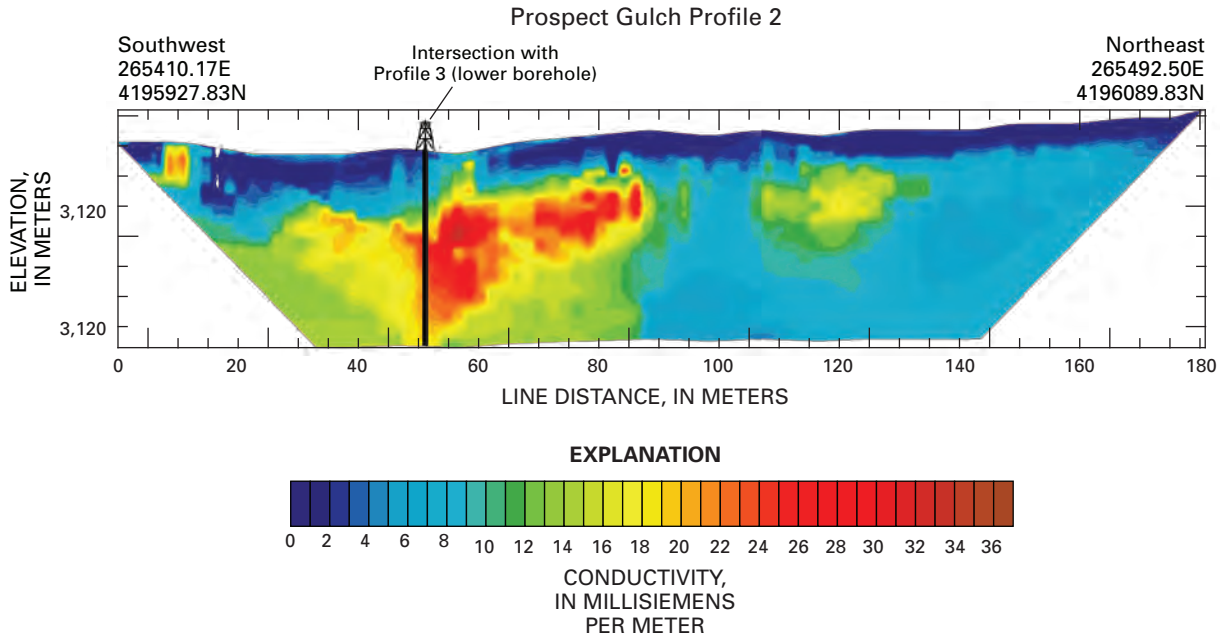

Figure 4. Conductivity Profile 2. m, meters.

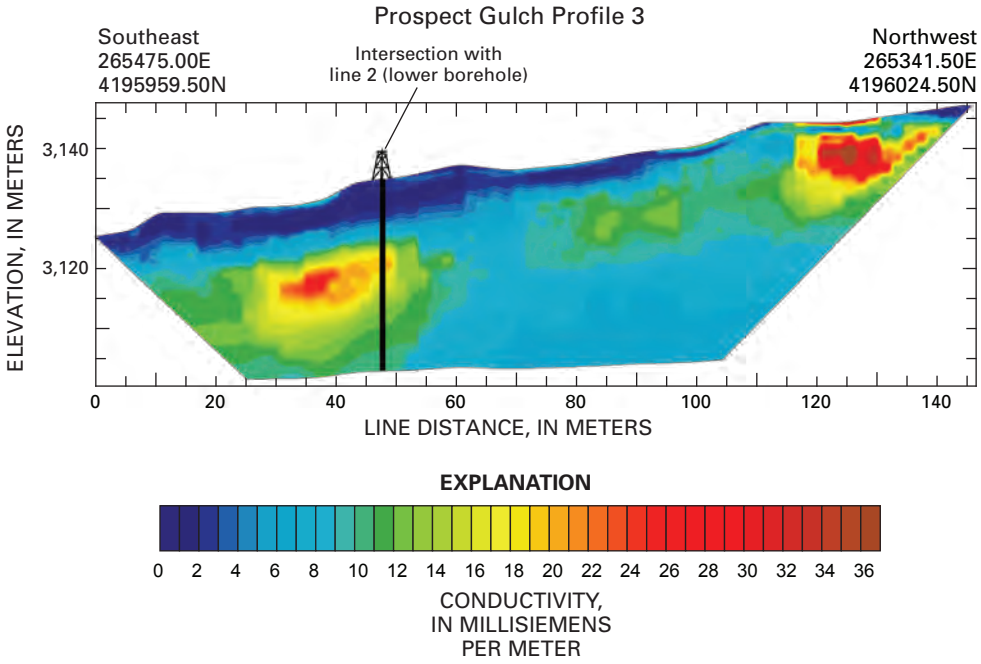

Figure 5. Conductivity Profile 3. m, meters.

The shallow conductive layer extending from 260 to 430 m is interpreted as wet clay and alluvium eroded off the ridge between Prospect Gulch and Georgia Gulch. The resistive zone below this layer is likely bedrock that becomes more conductive downgradient to the southwest.

We conclude that deep circulating ground-water flow is likely influenced by the resistive structure near the Upper Iron Bog and that the near-surface layer of ferricrete acts as a confining layer. The highly conductive anomaly between 40 and 110 m is interpreted as the result of ground water with high concentrations of dissolved solids that is mantled and confined by the ferricrete. This zone could also contain clay-rich sediments, but this alternate interpretation cannot be confirmed without direct core data.

Profile 5 (fig. 7) was positioned to intersect ground water draining from the tailings and waste rock associated with the Lark mine to record preremediation subsurface conditions. Several seeps and springs were observed below the embankment to the north of the profile, some having orange-colored water with iron precipitate.

The near-surface conductive anomaly between 155 and 200 m along the profile is coincident with seeps and saturated surface soils. This zone is interpreted as a plume of conductive shallow ground water draining from the Lark mine waste rock. The sharp interface between conductive and resistive zones suggests that ground water at 200 m along the profile is perched on a resistive surface of ferricrete and (or) bedrock.

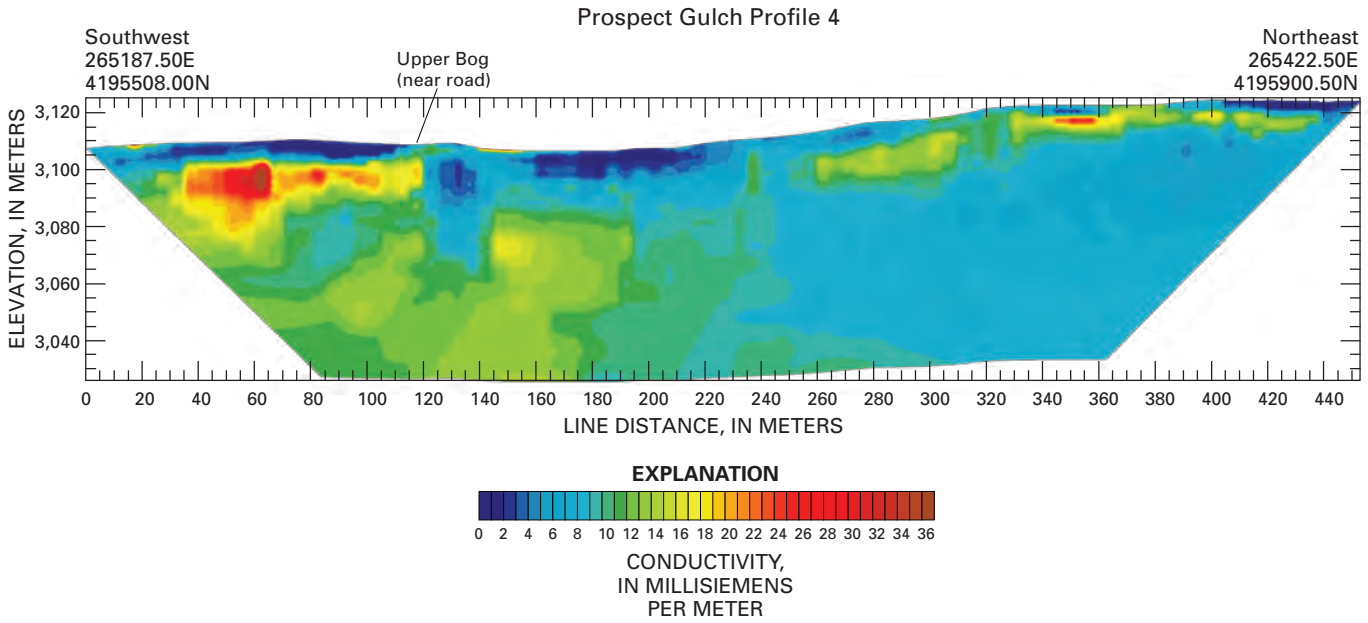

Figure 6. Conductivity Profile 4. m, meters.

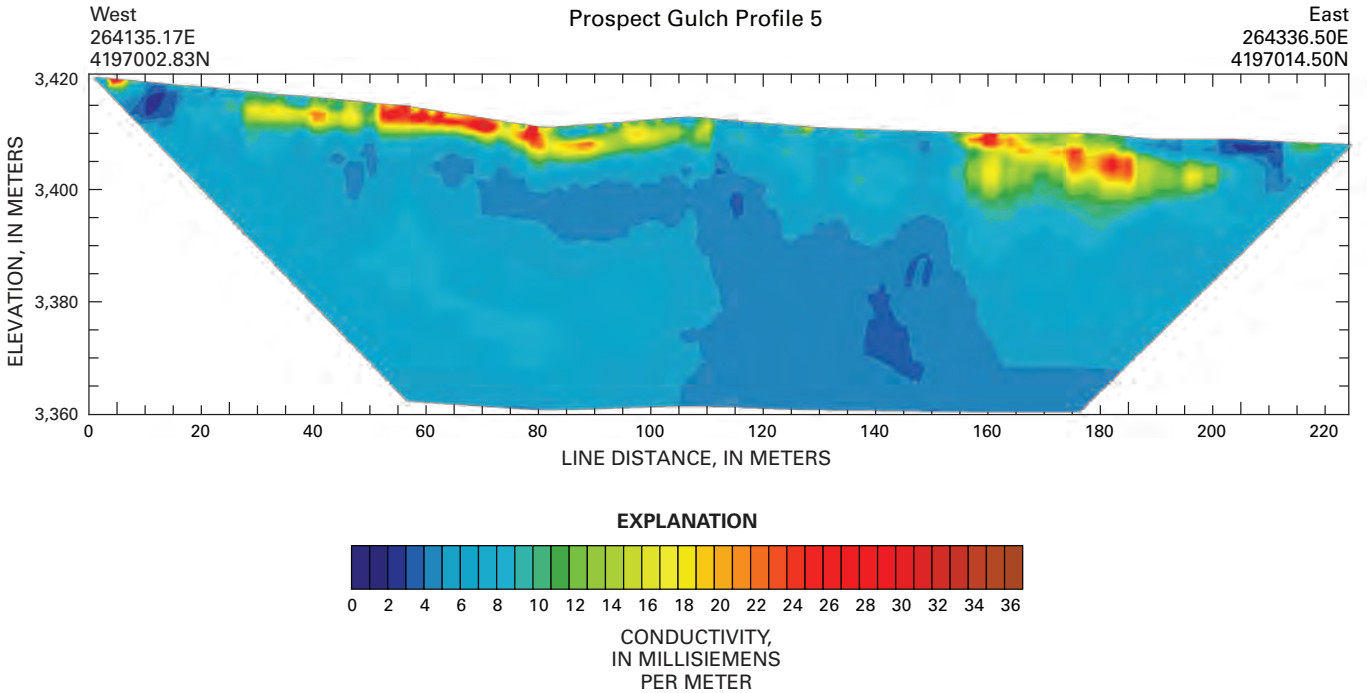

Figure 7. Conductivity Profile 5. m, meters.

Conclusions

The conductivity profiles presented in this study generally identify zones of varying near-surface geology (for example, clay-rich sediments and ferricrete) as well as zones of conductive ground water. Conductive zones at depth indicate the presence of ground water that is either in saturated layers of clay and alluvium or in faults and fractures in bedrock. Where ground water is associated with mine waste, the subsurface conductivity is generally high, suggesting poor water quality.

This study illustrates the utility of combining geophysical investigations with available well-core logs to expand the interpretation and understanding of the ground-water and geologic systems in complex mountainous terrains. By correlating well and piezometer data with the conductivity profiles, the often nonunique interpretation of the geophysical data can be improved.

References Cited

Advanced Geosciences, Inc., 2006, EarthImager 2D, ver. 2.1.8 (build 507): Austin, Texas.

Bove, D.J., Hon, Ken, Budding, K.E., Slack, J.F., Snee, L.W., and Yeoman, R.A., 2001, Geochronology and geology of late Oligocene through Miocene volcanism and mineralization in the western San Juan Mountains, Colorado: U.S. Geological Survey Professional Paper 1642, 30 p.

Bove, D.J., Mast, M.A., Dalton, J.B., Wright, W.G., and Yager, D.B., 2007a, Major styles of mineralization and hydrothermal alteration and related solid- and aqueous-phase geochemical signatures, *in* Church, S.E., von Guerard, Paul, and Finger, S.E., eds., Integrated investigations of environmental effects of historical mining in the Animas River Watershed, San Juan County, Colorado: U.S. Geological Survey Professional Paper 1651, 1096 p.

Bove, D.J., Yager, D.B., Mast, M.A., and Dalton, J.B., 2007b, Alteration map showing major faults and veins and associated water-quality signatures of the Animas River watershed headwaters near Silverton, southwest Colorado: U.S. Geological Survey Scientific Investigations Map 2976, 18-p. pamphlet, 1 plate, scale 1:24,000.

Church, S.E., Mast, M.A., Martin, E.P., and Rich, C.L., 2007, Mine inventory and compilation of mine-adit chemistry data, Chapter E5 *in* Church, S.E., von Guerard, Paul, and Finger, S.E., eds., Integrated investigations of environmental effects of historical mining in the Animas River Watershed, San Juan County, Colorado: U.S. Geological Survey Professional Paper 1651, 1096 p.

Johnson, R.H., and Yager, D.B., 2006, Completion reports, core logs, and hydrogeologic data from wells and piezometers in Prospect Gulch, San Juan County, Colorado: U.S. Geological Survey Open-File Report 2006–1030, 32 p.

Lipman, P.W., Steven, T.A., Luedke, R.G., and Burbank, W.S., 1973, Revised volcanic history of the San Juan, Uncompahgre, Silverton, and Lake City calderas in the western San Juan Mountains, Colorado: U.S. Geological Survey Journal of Research, v. 1, 627–642.

Lipman, P.W., Fisher, F.S., Mehnert, H.H., Naeser, C.W., Luedke, R.G., and Steven, T.A., 1976, Multiple ages of mid-Tertiary mineralization and alteration in the western San Juan Mountains, Colorado: Economic Geology, v. 71, 571–588.

Wirt, Laurie, Leib, J.L., Melick, Roger, and Bove, D.J., 2001, Metal loading assessment of a small mountainous sub-basin characterized by acid drainage—Prospect Gulch, Upper Animas River Watershed, Colorado: U.S. Geological Survey Open-File Report 2001–0258, 36 p.

Yager, D.B., and Bove, D.J., 2002, Generalized geologic map of part of the upper Animas River watershed and vicinity, Silverton, Colorado: U.S. Geological Survey Miscellaneous Field Studies Map MF–2377, 1:48.000.

Zohdy, A.A.R., Eaton, G.P., and Mabey, D.R., 1974, Application of surface geophysics to ground-water investigations: U.S. Geological Survey Techniques of Water-Resources Investigations, book 2, chap. D1, 116 p.

Chapter I: U.S. Geological Survey Research in Handcart Gulch, Colorado—An Alpine Watershed Affected by Metalliferous Hydrothermal Alteration

by Jonathan Saul Caine, Andrew H. Manning, Philip L. Verplanck, Dana J. Bove, Katherine Gurley Kahn, and Shemin Ge

Overview

Handcart Gulch is an alpine watershed along the Continental Divide. It contains an unmined mineral occurrence composed primarily of pyrite with trace metals including copper and molybdenum. Although the geology of Handcart Gulch is typical of many hydrothermal mineral deposits in the intermountain West, the area is unique because of a set of deep and shallow wells used to conduct an integrated study of the processes involved with the liberation, transport, and fate of naturally occurring acid-rock drainage in a mountain watershed. Commonly, mountainous watersheds are underlain by complexly deformed crystalline rocks where the occurrence, storage, and flow of ground water are poorly understood. These environments also are characterized by high to extreme hydraulic gradients and heterogeneous networks of fractures and faults that control the ground-water flow system and contaminant transport. Integrating geological, hydrological, geochemical, and geophysical data in a series of numerical flow models, we find that ground-water flow at the watershed scale can be conceptualized using a relatively simple equivalent porous media approach. We also find that ground water accounts for a significant component of discharge to the trunk stream, about 37 percent of the total annual streamflow. The work to date (2008) suggests that, in spite of low bulk permeability and various geologic complexities, hydrologic contributions from fractured crystalline bedrock rock should be carefully considered when evaluating alpine ground-water flow systems.

Introduction

Handcart Gulch provides a unique opportunity to study how a variety of complex geological characteristics control the hydrology in an alpine watershed containing an unmined, metallic mineral occurrence. The occurrence can be characterized as a copper-molybdenum porphyry system in which pyrite is the most abundant metallic mineral. Although pyrite is of little economic value, it has had a major effect on the Handcart Gulch watershed. The study arose out of the need to better understand the liberation, transport, and fate of natural contaminants related to the weathering of pyrite in mountain watersheds, especially the function of ground water in transporting these contaminants to the surface-water system. The study area is unique because there is a network of shallow and deep boreholes that the USGS has converted to ground-water research and monitoring wells. Such wells exist in few alpine environments worldwide and, as such, provide the opportunity to more fully understand the hydrogeological system as a whole.

The motivation to complete an integrated study of the geology and hydrology of Handcart Gulch is multifold and was a collaborative effort between the U.S. Geological Survey Geologic and Water Resources Disciplines as well as the Mendenhall Program, the University of Colorado, and the Colorado Geological Survey. There is growing recognition that mountains occupy a critical place in the hydrologic cycle in many parts of the world. They capture precipitation by orographic effect, store water in snowpack and in mountain aquifers, are a primary source of surface water in arid regions, and serve as recharge zones for local and regional aquifers. Rapidly increasing population in mountainous areas has led to a greater utilization of mountain aquifers and a need to better understand their production capacity and vulnerability to contamination. Mineral deposits are common in mountain environments and are the source of natural and mining-related acid and trace-metal loading to alpine surface and ground waters. However, identifying transport pathways and specific local sources of contamination has remained a challenge (for example, Runnells and others, 1992; Kimball and others, 2002; Mast and others, 2007). The growing demand to improve water quality in affected mountain streams and develop scientifically based remediation strategies for affected waters has created a need to better understand the ground-water systems feeding mountain streams. Additionally, the potential for hydraulic gradients in mountainous terrain to drive ground-water flow to considerable depth within the Earth's upper crust is poorly understood. Such deep flow likely contributes significantly to the formation of mineral deposits, seismicity, and other geologic processes. Mountains commonly exist in environments underlain by complex geology, and important questions regarding the potential effects of geology on ground-water flow in mountainous settings include the following:

(1) To what degree do discrete fracture networks and (or) fault zones control preferred ground-water flow paths, and at what scale might the bulk permeability structure be treated as a continuum?

(2) Is the bulk permeability of fractured bedrock sufficiently low, as is commonly assumed, to ignore contributions of bedrock-hosted ground water to streams? If not, is this component of flow typically high enough to demand the inclusion of bedrock waters in watershed hydrologic models?

(3) How does bedrock permeability vary spatially, and does this type of heterogeneity need to be incorporated in numerical ground-water flow models?

(4) What geologic factors control the concentrations and fluxes of acid and metals in mountain ground-water flow systems?

This chapter provides an overview of U.S. Geological Survey research in Handcart Gulch and a brief synopsis of preliminary results from the site. More detailed information can be found in the following publications: Caine and others (2006), Manning and Caine (2007), Kahn and others (2007), Verplanck and others (2007), and Verplanck and others (in press).

Overview of Handcart Gulch Research

Geology, Mineral Deposit, Hydrothermal Alteration, and Contaminant Sources

Handcart Gulch is located in central Colorado within the Colorado Mineral Belt (figs. 1 and 2; Tweto and Sims, 1963). The mineral occurrence in Handcart is hosted within complexly folded and fractured Precambrian metamorphic bedrock. The bedrock consists of gneisses, schists, amphibolites, and granites that have been intruded by small, Tertiary-age, porphyritic igneous stocks that likely account for the metallic mineralization (figs. 2 and 3). T.S. Lovering originally mapped the area in 1935 and identified what he called "iron bog" along the bed of the trunk stream along most of its course. This material is ferricrete, iron-hydroxide-cemented alluvium and colluvium. Another geological unit in the watershed with hydrological significance is a rock glacier (figs. 2 and 3).

The Montezuma mining district, to the north of Handcart Gulch, has a long mining history starting with an initial discovery of silver in 1864 (fig. 1; Lovering, 1935). Metals mined in the district include silver, lead, zinc, copper, and molybdenum (Botinelly, 1979). As in Handcart Gulch, these metals are associated with disseminated and veinlet-hosted pyrite (FeS_2) in large zones of hydrothermal alteration related to Tertiary intrusions (figs. 2 and 3). Pyrite at the near surface of the Earth is unstable in the presence of oxygenated waters and thus breaks down into its principal chemical components by weathering processes. The primary components include iron and any trace metals such as copper that commonly occur with pyrite, as well as sulfur, usually in the form of sulfuric acid. Acidified and metal-laden waters are transported from zones of oxidation by infiltrating precipitation into the ground-water flow system or by runoff and (or) ground-water

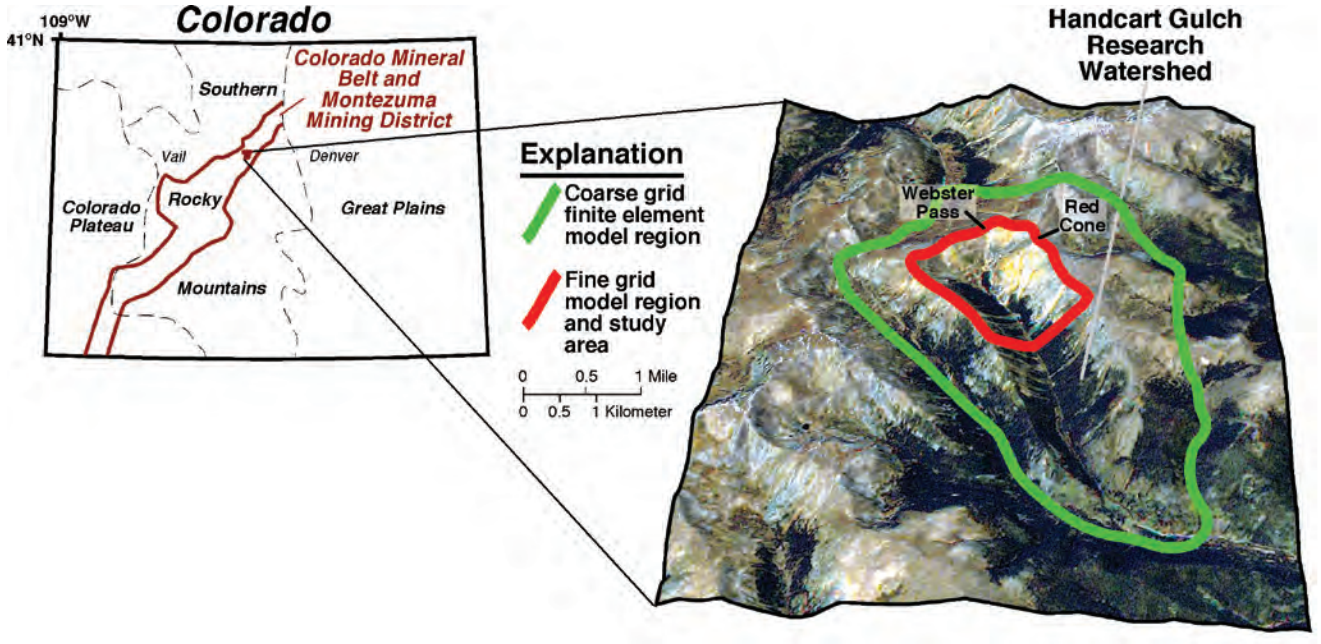

Figure 1. Location of Handcart Gulch with major physiographic province boundaries and the location of the study area within the Colorado Mineral Belt and Montezuma Mining District, which is characteristic of many such districts in the Mineral Belt. Also shown is a visible satellite image draped on a tilted digital elevation model. The image shows the extreme topographic relief (over 800 meters with a gradient of about 0.1) and the red-orange weathering of the unmined mineral occurrence. The study area (red) and numerical ground-water flow model domains (red and green) are also shown. Webster Pass and Red Cone Mountain are shown for reference.

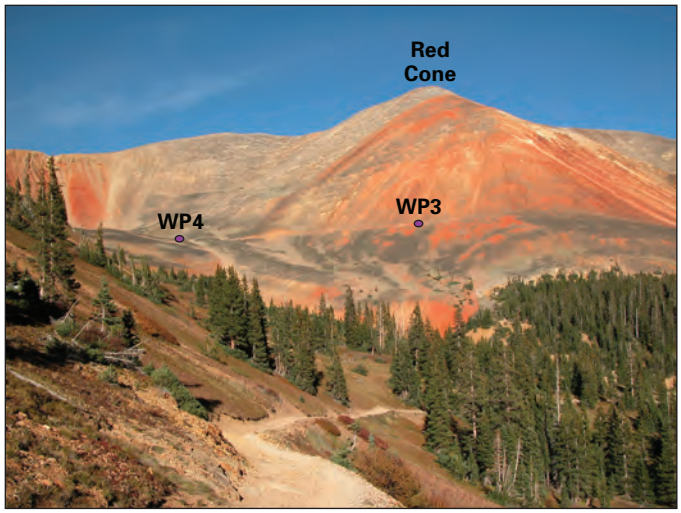

Figure 2. Red Cone, altitude 3,900 meters, in the upper reaches of Handcart Gulch in Colorado. Note the red staining from the oxidation of pyrite at concentrations of nearly 8 percent of the rock mass. This is the primary and natural source of low-pH water in the watershed. The locations of the mineral exploration holes WP3 and WP4 are shown as purple ovals.

base-flow discharge into stream channels or other surface-water bodies. These processes cause the Handcart Gulch trunk stream to be naturally acidic (pH 2.6–4.6) with elevated metal concentrations. Because no mining has occurred in Handcart Gulch, the watershed also provides a unique opportunity to evaluate and monitor a natural acid-rock-drainage system and associated processes that liberate, transport, and deposit contaminants.

Wells and Field Data

In the summers of 2001 and 2002 a private mineral exploration company (Mineral Systems, Inc.) drilled and cored four deep, mineral exploration boreholes in Handcart Gulch (deep wells; fig. 3). The wells are located in the upper part of the watershed, the highest one at Webster Pass on the Continental Divide at an altitude of 3,690 meters, and range in depth from 366 to 1,067 meters (fig. 3). Mineral Systems, Inc., donated the boreholes to the U.S. Geological Survey, who reconditioned them for use as research and monitoring wells. The deep wells were supplemented with nine new shallow wells (3 to 52 meters deep) located in five well nests adjacent to the trunk stream (shallow wells; fig. 3; Caine and others, 2006).

During the field seasons of 2003 to 2005, a variety of data were collected in the boreholes and from the watershed, including (1) basic geologic, fracture network, and fault data as well as rock samples for alteration mineralogy, elemental geochemistry, and thin-sectioning; (2) a tracer-dilution study in the trunk stream; (3) continuous hourly stream discharge and temperature data from the trunk stream for water year 2005; (4) geophysical borehole-logging data (caliper, optical and acoustic imaging, heat-pulse flow metering, temperature, water conductivity, gamma, specific potential, and magnetic susceptibility); and (6) single-well, aquifer hydraulic test data. Ground- and surface-water samples were collected and analyzed for major and trace elements, multiple isotopes (Sr, S, O, and H), dissolved noble gases (including ^{3}He), tritium, chlorofluorocarbons, and ^{13}C and ^{14}C—the latter three for water age determinations.

Preliminary Results and Discussion

Research is ongoing in Handcart Gulch, and the site, wells, and installed instrumentation are intended for long-term monitoring. The following is a list of results and a sample of associated publications to date.

(1) Outcrop and well-log data indicate that the bedrock is complexly deformed and primarily consists of tightly folded felsic and mafic Precambrian metamorphic rocks (figs. 3 and 7). Geologic structures include the Montezuma ductile shear zone (fig. 4), cut by a few brittle, small-displacement faults, and high-intensity joint networks. Down-hole televiewer and flow-meter data indicate that the high intensity, open-joint networks persist to depth. However, the percentage of fractures that are hydraulically conductive is small (fig. 7). There also are a few discrete, polymetallic veins in the watershed. Of all these structures, only the open-joint networks have a significant function in ground-water processes.

The dominant hydrothermal alteration assemblage is quartz-sericite-pyrite (qsp) commonly found in felsic lithologies with an average concentration of about 8 weight-percent fine-grained, disseminated pyrite and quartz-pyrite veinlets. These are the primary source rocks for natural contamination to surface and ground waters. The intensity of hydrothermal alteration decreases away from Webster Pass and Red Cone and transitions outward from qsp, to propylitic alteration (particularly in mafic amphibolites), to relatively unaltered rocks (figs. 2, 3, and 4).

The pervasive hydrothermal qsp alteration extends to as much as 1,000-m depth from the ground surface. Beneath this depth, rocks are generally more weakly to propylitically altered, particularly in amphibolitic lithologies. On the basis of the four WP and four HC bedrock wells, zones of pyrite oxidation related to infiltrating ground water appear to generally reflect a fracture-controlled unsaturated zone, ranging in depth from about 100 m below surface at higher elevations to just a few meters near the base of the study area (Caine and others, 2006).

(2) A tracer-dilution study (Kimball and others, 2002) was conducted in the upper 2 kilometers of the Handcart Gulch trunk stream to quantify stream discharge and to delineate locations of metal loading. Data indicated that discharge, acidity, and loading of zinc and copper increase in the downstream direction, and zinc and copper concentrations exceed aquatic-life standards (fig. 5).

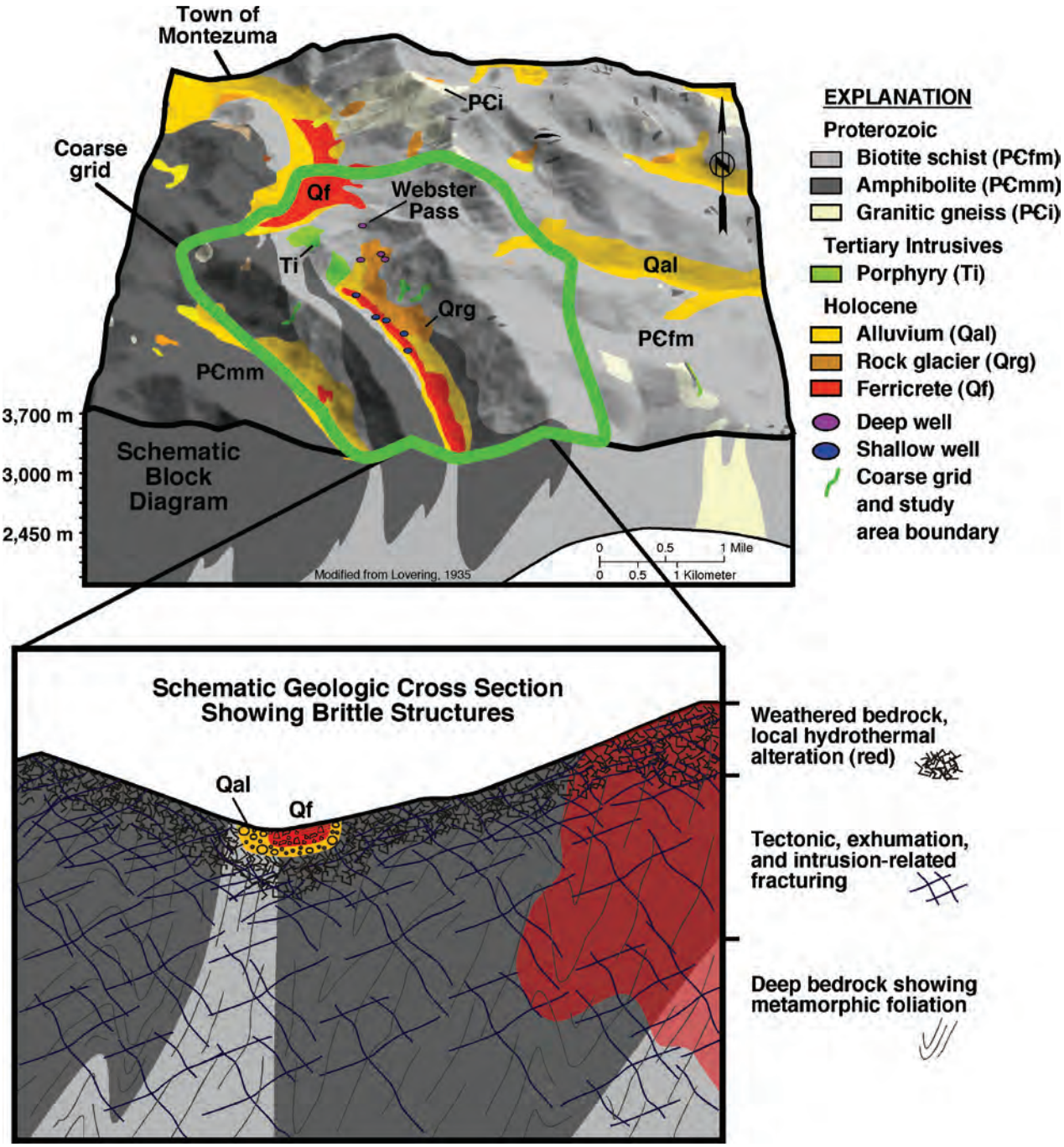

Figure 3. Simplified geologic map (modified from Lovering, 1935), block diagram, and cross section of the Handcart Gulch study area draped on a digital elevation model showing the location of the research wells. Also shown is a geological conceptual model in cross section depicting the major features that might control the ground-water flow system and associated contaminant sources.

(3) Ground-water samples from Handcart Gulch are Ca-SO_4 type and range in pH from 2.5 to 6.8. Most samples (75 percent) have pH values between 3.3 and 4.3 (Verplanck and others, 2007). Surface-water samples are also Ca-SO_4 type and have a narrower range in pH (2.7 to 4.0). Ground- and surface-water samples vary from relatively dilute (specific conductance of 68 µS/cm) to concentrated (2,000 µS/cm). Compared to other unmined, porphyry-mineralized areas in the Southern Rocky Mountains, dissolved copper concentrations in Handcart Gulch ground and surface waters are relatively high and dissolved zinc concentrations are relatively low (fig. 6; Verplanck and others, in press).

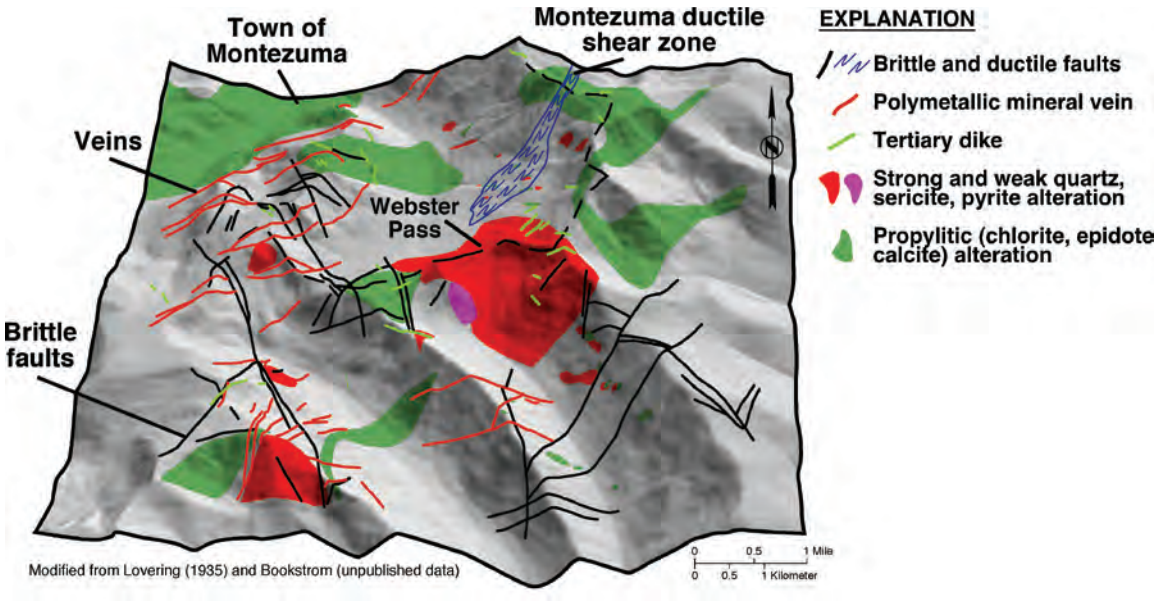

Figure 4. Hydrothermal alteration and geologic structure map draped on a digital elevation model as shown in figure 3. Note: Webster Pass is at the headwaters of Handcart Gulch and the northwest edge of the study area for reference.

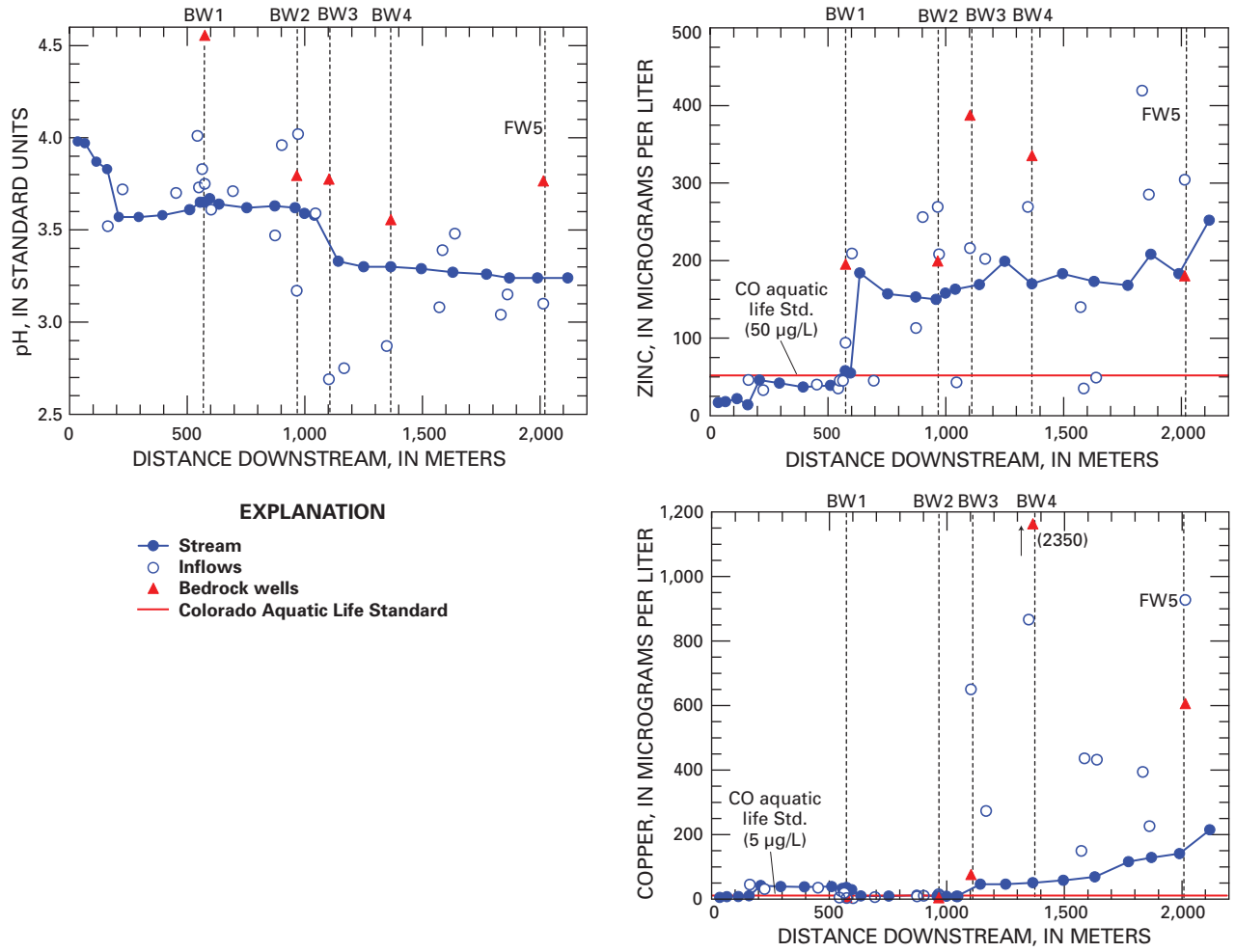

Figure 5. Examples of pH and dissolved constituent load data for zinc (Zn) and copper (Cu) as a function of downstream distance along the trunk stream in Handcart Gulch. Constituent concentrations for springs (inflows) and bedrock wells (BW) are also shown.

(4) Up to 13 meters of well-indurated ferricrete forms a confining unit, resulting in artesian conditions in the bedrock near the trunk stream. Measured static water levels in the bedrock under the stream were as much as 3 meters above ground surface. Sustained or seasonal artesian flow occurs in many of the bedrock wells adjacent to the trunk stream (with a maximum flow of 76 liters or about 20 gallons per minute, Caine and others, 2006). Because the ferricrete impedes ground-water discharge to the stream, much of the bedrock ground water may flow down-drainage underneath the stream, making its discharge location uncertain.

(5) Temperature-depth profiles from the deep wells become nearly linear at depths greater than about 100 meters below the water table (greater than about 200 meters below ground surface), suggesting that active ground-water circulation does not exceed these depths (see Manning and Caine, Chapter J, this volume).

(6) Tritium/helium ($^3H/^3He$) ground-water age results indicate increasing ground-water age with depth (Manning and Caine, 2007, and chap. J, this volume). Mean ages from integrated bedrock ground-water samples collected near the trunk stream are very similar. These data are consistent with a relatively simple representation of the flow system in which recharge and circulation depth are constant throughout the drainage (see Manning and Caine, Chapter J, this volume, for details). This in turn supports a conceptual model where the watershed aquifer system can be represented as equivalent porous media in spite of the complexities in the geology and fracture networks.

(7) Seasonal water-table fluctuations in the upper part of the watershed are very large (up to about 45 meters) indicating significant seasonal cycles of saturation and oxygenation in the thick unsaturated zone in the upper reaches of the watershed. This may be an important mechanism controlling pyrite oxidation and the liberation of acidity and metals to ground and surface waters.

(8) Geological, geophysical, hydrological, water age, and thermal data were used as input for constructing a series of numerical ground-water flow models and a water budget (Kahn and others, 2007). Single-well aquifer-test data were numerically modeled with MODFLOW-2000 (Harbaugh and others, 2000) to estimate hydraulic conductivities (K) and specific storage values (S) for the surface deposits and bedrock. Model-derived K and S values for the surficial deposits are about 10^{-6} to 10^{-5} m/s and about 10^{-4} to 10^{-3} per meter, respectively, and values for the bedrock are about 10^{-9} to 10^{-6} m/s and about 10^{-5} to 10^{-4} per meter, respectively. These results indicate ground-water flow rates through fracture networks can be high in the bedrock aquifer, particularly near the trunk stream. Therefore, bedrock ground water is a nontrivial component of the hydrologic system.

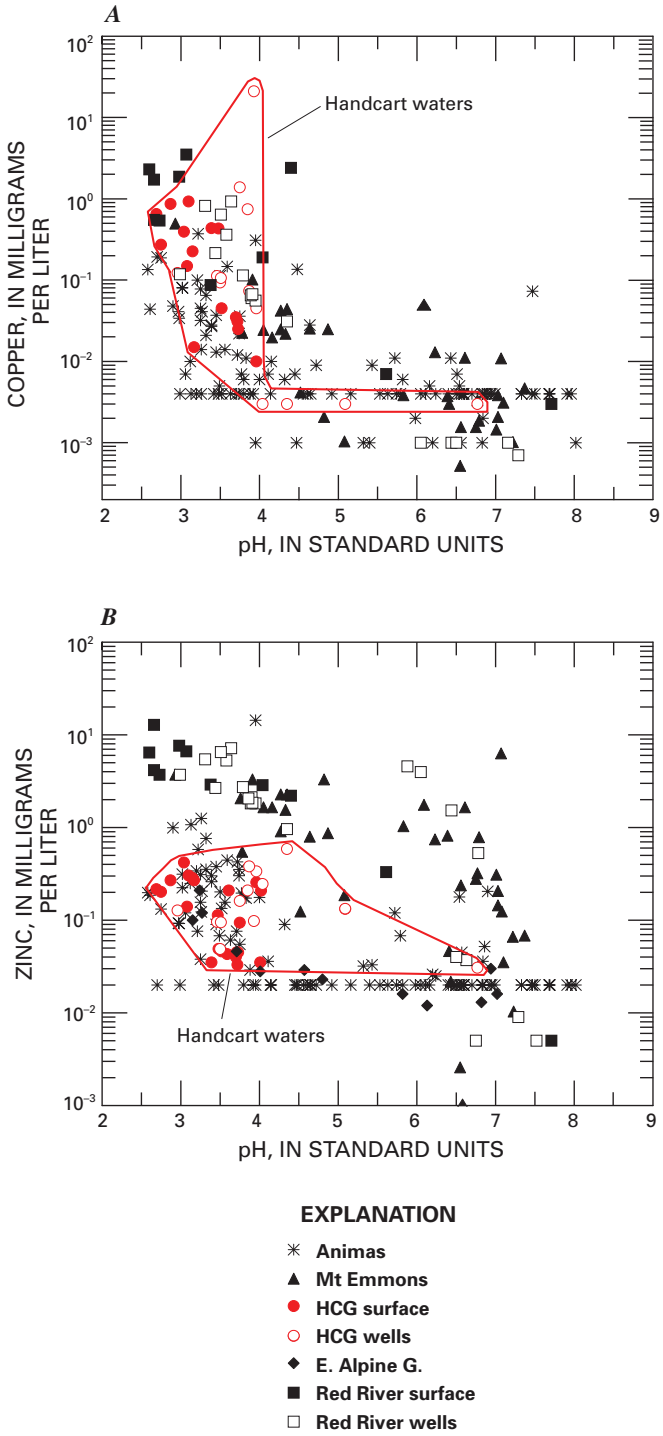

Figure 6. Variation in pH and dissolved copper (*A*) and zinc (*B*) concentration of ground and surface waters from five porphyry mineralized areas. HCG = Handcart Gulch waters are indicated in red.

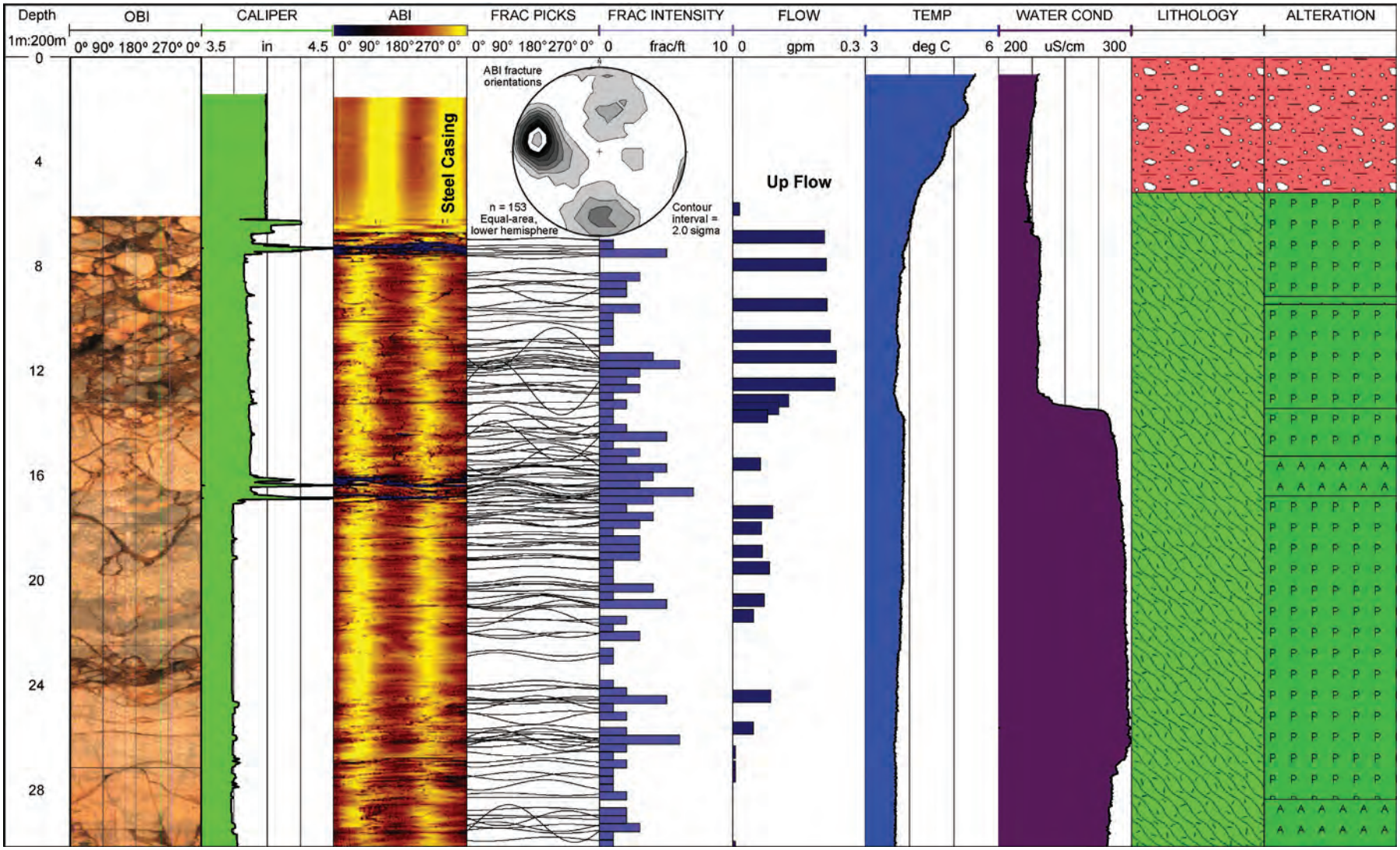

Figure 7. An example of composite geophysical and lithological logs from Handcart Gulch wells. Optical televiewer image (OBI) shows surface deposits/bedrock interface and sinusoidal traces of open fractures in WP4 (all other logs from shallow HCBW1 next to the trunk stream). Fracture orientations derived from the acoustic televiewer image (ABI) plotted on an equal area projection are consistent with outcrop and regional fracture orientations. Heat-pulse flow meter (HPFM data shown as FLOW) indicates flow direction and magnitude in the well and does not correlate with fracture orientation or fracture intensity. Inflow does correlate with temperature and conductivity. Lithology and hydrothermal alteration log data are also shown for HCBW1 shallow bedrock well (red layered material is ferricrete, green diagonal pattern is amphibolite; P = propylitic alteration and A = quartz-sericite-pyrite or argillic alteration). See Caine and others (2006) for details. gpm, gallons per minute; μS/cm, microsiemens per centimeter; frac/ft, fractures per foot; deg C, degrees Celsius; m, meter.

A coupled heat, mass, and fluid-transport finite-element model of the watershed incorporates the water-age and temperature-depth data. Successful calibration to observed heads and temperatures required specifying permeabilities similar to those derived from the aquifer-test data, decreasing permeability with depth, applying a recharge rate of 10–20 cm/yr to the bedrock aquifer, and using relatively high flow velocities under the stream in the downstream direction (Manning and Caine, 2007).

A MODFLOW-2000 watershed-scale finite-difference model was also constructed using stream discharge, precipitation, and other climate data from an adjacent watershed to estimate a water budget for Handcart Gulch. During water year 2005, precipitation in the watershed was 2.16×10^{-3} km^3 and total stream discharge was 1.28×10^{-3} km^3 of which base flow accounted for about 4.73×10^{-4} km^3 (Kahn and others, 2007). Estimated base flow for the year equates to about 1.25×10^8 gallons of water, about 22 percent of precipitation, and about 37 percent of total stream discharge. Modeling components of the water budget suggest that, under normal climatic conditions, water is available to recharge the ground-water flow system (Kahn and others, 2007).

Acknowledgments

This work would not have been possible without the generosity of Dr. Charles S. Robinson of Mineral Systems, Inc., who donated the deep boreholes in the study area for research purposes. Cooperation with the USDA Forest Service and the Colorado Geological Survey is much appreciated. Numerous field partners whose time and efforts we greatly appreciate conducted and assisted with various types of field work: Briant Kimball, Katherine Walton-Day, Robert Runkel, Richard Wanty, Greg O'Neill, and others. We thank Cliff Taylor and Carma San Juan of the USGS for constructive reviews of this report. This work was funded by the U.S. Geological Survey's Mineral Resources and Mendenhall Postdoctoral Fellowship Programs.

References Cited

Botinelly, Theodore, 1979, Mineralogy as a guide for exploration in the Montezuma District, central Colorado: U.S. Geological Survey Open-File Report 79–1177, 18 p.

Caine, J.S., Manning, A.H., Verplanck, P.L, Bove, D.J., Kahn, K.G., and Ge, S., 2006, Well construction information, lithologic logs, water-level data, and overview of research in Handcart Gulch, Colorado—An alpine watershed affected by metalliferous hydrothermal alteration: U.S. Geological Survey Open-File Report 2006–1189, 14 p. *http://pubs.usgs.gov/of/2006/1189/*

Harbaugh, A.W., Banta, E.R., Hill, M.C., and McDonald, M.G., 2000, MODFLOW-2000, the U.S. Geological Survey modular ground-water model—User guide to modularization concepts and the ground-water flow process: U.S. Geological Survey Open-File Report 2000–92, 121 p.

Kahn, K.G., Ge, S., Caine, J.S., and Manning, A.H., 2007, Characterization of the shallow groundwater system in an alpine watershed, Handcart Gulch, Colorado: Journal of Hydrogeology: DOI: 10.1007/s10040–007–0225–6.

Kimball, B.A., Runkel, R.L., Walton-Day, K., and Bencala, K.E., 2002, Assessment of metal loads in watersheds affected by acid mine drainage by using tracer injection synoptic sampling—Cement Creek, Colorado, USA: Applied Geochemistry, v. 17, p. 1183–1207.

Lovering, T.S., 1935, Geology and ore deposits of the Montezuma quadrangle, Colorado: U.S. Geological Survey Professional Paper 178, 119 p.

Manning, A.H., and Caine, J.S., 2007, Groundwater noble gas, age, and temperature signatures in an alpine watershed—Valuable tools in conceptual model development: Water Resources Research, v. 43, W04404, DOI: 10.1029/2006WR005349.

Mast, M.A., Verplanck, P.L., Wright, W.G., and Bove, D.J., 2007, Characterization of background water quality in the upper Animas River watershed, Chapter E7 *in* Church, S.E., von Guerard, Paul, and Finger, S.E., eds. Integrated investigations of environmental effects of historical mining in the Animas River watershed, San Juan County, Colorado: U.S. Geological Survey Professional Paper 1651, 1096 p., p. 347–386.

Runnells, D.D., Shepherd, T.A., and Angino, E.E., 1992, Metals in water-determining natural background concentrations in mineralized areas: Environmental Science and Technology, v. 26, p. 2316–2323.

Tweto, Ogden, and Sims, P.K., 1963, Precambrian ancestry of the Colorado Mineral Belt: Geological Society of America Bulletin, v. 74, p. 991–1014.

Verplanck, P.L., Manning, A.H., Kimball, B.A., McCleskey, R.B., Runkel, R.L., Caine, J.S., Adams, M., Gemery-Hill, P.A., and Fey, D.L., 2007, Ground- and surface-water chemistry of Handcart Gulch, Park County, Colorado, 2003–2006: U.S. Geological Survey Open-File Report 2007–1020.

Verplanck, P.L., Nordstrom, D.K., Bove, D.J., Plumlee, G.S., and Runkel, R.L., in press, Naturally acidic surface and ground waters draining porphyry-related mineralized areas of the southern Rocky Mountains, Colorado and New Mexico: Applied Geochemistry.

Chapter J: Developing a Conceptual Model of Ground-Water Flow in an Alpine Watershed

by Andrew H. Manning and Jonathan Saul Caine

Overview

Understanding how ground water transports metals and acid to mountain streams is critical in order to effectively manage mountain watersheds affected by acid-rock and acid-mine drainage. The transport of dissolved constituents in ground water is best represented by a coupled numerical ground-water flow and solute-transport model. Building such a numerical model requires first developing a conceptual model of the ground-water flow system that includes its most fundamental characteristics. This chapter describes the development of a conceptual model of ground-water flow in Handcart Gulch, an alpine watershed in the Front Range of Colorado affected by acid-rock drainage. New applications of ground-water age and temperature data that utilize the site's unique monitoring-well network were essential in this process and resulted in a conceptual model considerably more accurate and defensible than what could have been developed using standard hydrologic and chemical data alone.

Introduction

Many acid-rock and acid-mine drainage sites are located in mountainous terrain. A growing number of studies indicate that ground-water inputs exert a major influence on stream-water chemistry in mountain watersheds (Soulsby and others, 2000; Kimball and others, 2001, 2002; Liu and others, 2004); ground water may compose a substantial fraction of the total annual streamflow (20–50 percent; Tiedeman and others, 1998; Uhlenbrook and others, 2002; Kosugi and others, 2006) and commonly has considerably higher concentrations of dissolved constituents than precipitation returned rapidly to the stream as surface runoff. Therefore, understanding how streams become contaminated by low-pH, metal-rich water in many cases requires understanding the ground-water flow system feeding the stream.

The transport of dissolved constituents in ground water is best represented by a coupled numerical ground-water flow and solute-transport model. Building such a numerical model requires first developing a conceptual model of the ground-water flow system that includes its most fundamental characteristics, such as the location of its boundaries, the location of recharge and discharge, and the distribution of zones of similar hydraulic conductivity (hydrogeologic framework). Unfortunately, in all but the rarest cases, ground-water data from mountain watersheds are insufficient to develop a defensible conceptual model, let alone to construct and calibrate a numerical model with any real confidence. Data from monitoring wells in mountain watersheds are particularly scarce, especially near the uppermost parts of watersheds. Thus, mountain ground-water flow systems remain poorly understood. Conceptual models of these systems that rely upon simple assumptions are dubious because these systems are potentially highly complex; they commonly involve structurally complex rocks, extreme head gradients (ground-slope angles of 10–40°), and extremely fluctuating recharge due to seasonal snowmelt.

A primary motivation for developing the Handcart Gulch study site was to obtain sufficient ground-water data to build a numerical ground-water flow and solute-transport model of an alpine watershed affected by acid-rock drainage (Caine and others, Chapter I, this volume). Wells with depths ranging from 3 to 342 m were installed along the trunk stream and in upper parts of the watershed, the highest well being located directly on the Continental Divide at 3,688 meters above sea level (fig. 1). This chapter describes the development of a conceptual model of ground-water flow in the watershed, the first critical step in building a numerical flow and transport model. New applications of ground-water age and temperature data were essential in this process and resulted in a conceptual model that is considerably more defensible than what could have been developed using standard hydrologic data alone.

Methods

Detailed descriptions of the physiography, geology, climate, and general hydrology of Handcart Gulch are provided in Caine and others (Chapter I, this volume) and Manning and Caine (2007). Hydraulic head measurements, aquifer tests, core logging, outcrop mapping, borehole geophysical logging, and other data types from the site reveal several important general aspects of the ground-water flow system (Caine and others, 2006; Kahn and others, 2008). The two fundamental characteristics addressed specifically in this chapter include (1) the depth to which ground-water flow actively occurs (aquifer thickness); and (2) the degree to which aquifer thickness, recharge rate (probably controlled in part by permeability), and porosity vary throughout the watershed. The latter is particularly uncertain given the limited well coverage. These two pieces of information are essential components of any conceptual model of a ground-water flow system and had to be attained using nontraditional applications of ground-water temperature and age data.

We determined aquifer thickness (envisioned as a watershed-scale average thickness) using temperature-depth profiles from borings that transect the entire thickness of the aquifer. The concept that bedrock ground-water flow in mountains dominantly occurs in a shallow, higher permeability

zone (active zone) that overlies a deeper, lower permeability zone hosting little flow (inactive zone) has been described by several workers (Snow, 1973; Robinson and others, 1974; Mayo and others, 2003). Higher permeability at shallower depth is generally attributed to a greater degree of weathering and (or) smaller overburden loads allowing more fractures to remain open. Temperature-depth profiles serve as a direct and continuous measure of the change in flow rate with depth because ground temperatures are sensitive to ground-water flow rates. The transition between linear temperature-depth profiles with gradients similar to the local conductive geothermal gradient (conductive profiles) and nonlinear temperature-depth profiles associated with advective heat transport from ground-water flow (disturbed profiles) should occur at Darcy flow velocities of roughly 1 cm/yr in mountain watersheds (Domenico and Palciauskas, 1973; Forster and Smith, 1989). Estimated recharge rates in alpine watersheds are typically tens of centimeters per year (Hely and others, 1971; Wasiolek, 1995). Therefore, flow velocities in the active zone generally should be high enough to result in disturbed profiles, and flow velocities in the inactive zone generally should be low enough (less than 10 percent of the recharge rate) to result in conductive profiles.

Temperature-depth profiles presented here were measured in wells WP1 and WP2 (fig. 1), which are located in the upper part of the watershed and have total depths of 336 m and 236 m, respectively (Caine and others, Chapter I, this volume). Profiles were measured in 2004 by using a standard downhole temperature/conductivity logging tool following procedures detailed in Manning and Caine (2007).

We evaluated potential watershed-scale variations in aquifer thickness, recharge rate, and porosity by comparing the mean age of ground water discharging to the stream at different locations along the stream. Haitjema (1995) demonstrated that the mean age of ground water discharging to a stream should be constant throughout a watershed if aquifer thickness (z), recharge rate (R), and porosity (n) are constant throughout that watershed (fig. 2*A*). Therefore, if ground-water samples can be collected at multiple locations along a stream such that each sample integrates all ground water discharging to the stream at that location (flow-weighted sample), then the mean age of these different flow-weighted samples should reflect watershed-scale variation in z, R, and n. More specifically, if z, R, and n are constant, then the mean age of flow-weighted samples should be constant (fig. 2*A*). Conversely, if z, R, and n vary significantly on a watershed scale due to geological complexities such as major fault zones intersecting the stream and lithologic variations, then the mean age of flow-weighted samples should also vary significantly (fig. 2*B*). Herein, the former case is referred to as a "uniform flow system" and the latter case as a "complex flow system." Observing uniform mean ages of flow-weighted samples along a stream, of course, does not prove the presence of a uniform flow system. Nonetheless, such uniform mean ages still serve as supporting evidence that these parameters either are relatively constant or vary in a systematic way on a watershed scale and that a relatively simple equivalent porous-media model (which represents the system as a continuum without discrete features) might represent the ground-water flow system sufficiently well to provide useful information about watershed-scale flow and transport processes.

Ground-water age was determined using the tritium/helium-3 method (see Solomon and Cook [2000] for a comprehensive review). Tritium (^{3}H) is a radioactive isotope of hydrogen that occurs in water and decays to ^{3}He (a dissolved noble gas) with a half-life of 12.32 years. The age of a ground-water sample is determined by measuring both ^{3}H and tritium-derived

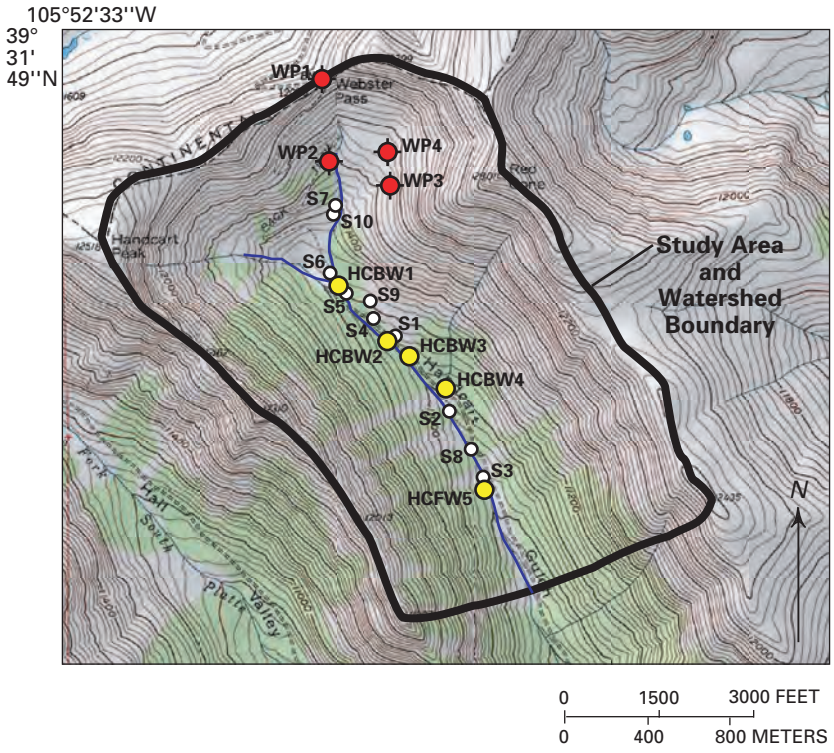

Figure 1. Topographic map of Handcart Gulch study area showing locations of deep wells (WP1–4, in red), bedrock wells near trunk stream (HCBW1–4 and HCFW5, in yellow), and springs (S1–10, in white). Base map from U.S. Geological Survey Montezuma quadrangle, 1:24,000 (1958).

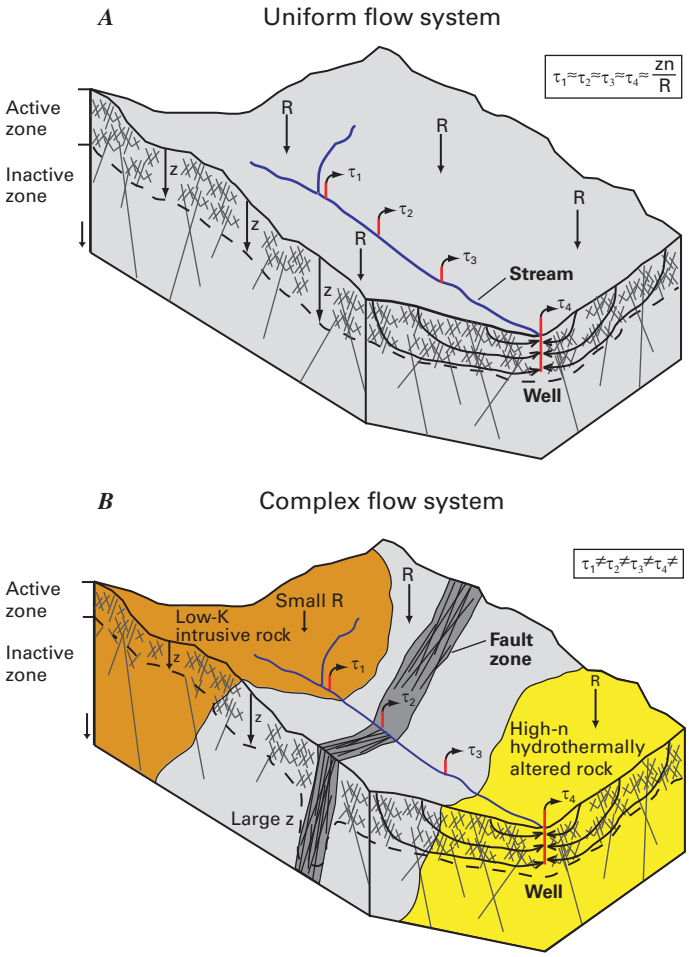

Figure 2. Schematic diagrams illustrating two different conceptual models of ground-water flow in an alpine watershed underlain by fractured crystalline rock. (*A*) Uniform flow system in which aquifer thickness, z, recharge rate, R, and porosity, n, are relatively uniform throughout the watershed. Mean residence times, τ, of samples from wells along the creek that integrate all flow paths to the creek (flow-weighted samples) are uniform and equal to zn/R (Haitjema,1995). (*B*) Complex flow system in which z, R, and n vary throughout the watershed, resulting in variations in τ along the creek. K, hydraulic conductivity.

(tritiogenic) ^{3}He concentrations and then using their ratio along with the radioactive decay equation to compute the time elapsed since the sampled water entered the saturated zone. The method can be used to date water less than 50 years old.

Samples discussed here were collected from 10 springs and 5 bedrock wells in late summer and fall of 2003 and were analyzed for dissolved gases and tritium. Details regarding sampling procedures, analytical techniques, and ^{3}H/^{3}He age calculations are available in Manning and Caine (2007).

All sampled springs and wells are located next to the stream except HCBW4, which is set back 60 m from the stream. Wells HCBW1–4 (fig. 1) are completed exclusively in bedrock and have total depths of 30–52 m. Well HCFW5 (total depth of 7 m) is completed in both bedrock and overlying ferricrete but is considered a bedrock well because significant artesian flow was encountered when the bedrock was penetrated during drilling. All five bedrock wells are open throughout the bedrock interval. Additional well information is provided by Caine and others (2006).

Two types of samples were collected from the bedrock wells: discrete and integrated. Discrete samples were collected from near the bottom of the well in order to characterize ground water at deeper levels of the bedrock aquifer. Integrated samples were collected from above the well screen. Four of the five bedrock wells are artesian, HCBW4 being the exception. The artesian flow means that the integrated samples should integrate a broad spectrum of flow paths in the bedrock en route to the stream, thereby approximating a flow-weighted sample. The integrated sample from HCBW4 was collected using a submersible pump and pumping at a high flow rate. Given the well's long screen (29 m) and relatively close proximity to the stream, the integrated sample from HCBW4 should also approximate a flow-weighted sample.

Results

Temperature-depth profiles from WP1 and WP2 are relatively smooth and do not suggest the presence of large, discrete inflows and outflows (fig. 3). Both profiles have an upper curved segment and a lower linear segment. Curved segments are concave upward, indicative of downward flow (recharge) and (or) lateral flow from higher elevations. Linear segments in WP1 and WP2 have slopes of 21°C/km and 28°C/km, respectively, consistent with expected conductive geotherms for the Front Range (20–25°C/km; Birch, 1950; Decker, 1969). In WP1, the profile becomes conductive at a depth of about 210 m, or about 100 m below the water table. In WP2, the profile becomes conductive at a depth of about 130 m, or about 110 m below the water table. Therefore, profiles from WP1 and WP2 are consistent with diffuse flow in the active zone associated with pervasive fractures and suggest a maximum circulation depth of about 200 m, or about 100 m below the water table. A maximum active zone thickness of about 200 m is consistent with estimates by Robinson and others (1974) and by Snow (1968) for nearby areas of the Front Range and with most estimates (100–200 m) for bedrock aquifers in other mountainous areas (Tiedeman and others, 1998; Desbarats, 2002; Mayo and others, 2003).

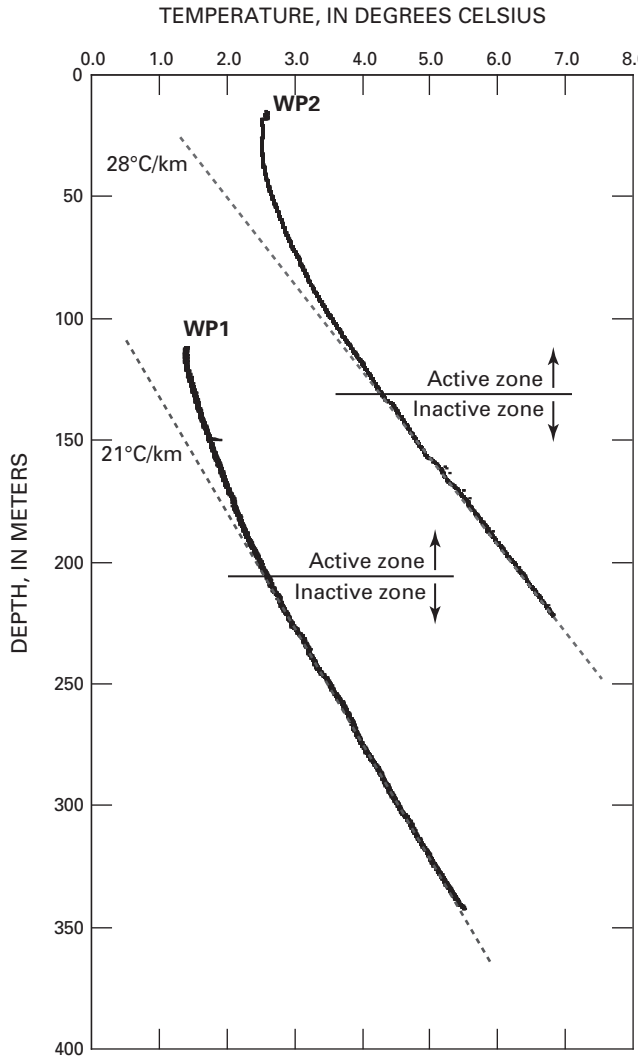

Figure 3. Temperature-depth profiles from WP wells. Both start at the water table. Dashed line is conductive geothermal gradient inferred from the lower linear portion of the profile. km, kilometers; °C, degrees Celsius.

Computed $^{3}H/^{3}He$ ages are plotted relative to distance down the stream in figure 4. The ages range from 0.1 to 35.9 years and generally have an uncertainty of 0.5–2.0 years. The integrated well samples presumably contain a mixture of waters of varying age. Therefore, the ages shown in figure 4 for these samples are mean ages computed from the ^{3}H and ^{3}He measurements, assuming that the samples contain an exponential age distribution (Vogel, 1967; Cook and Böhlke, 2000).

The $^{3}H/^{3}He$ ages indicate that ground-water age in the vicinity of the stream increases with depth, as expected in a uniform flow system. Spring samples collected at the surface are the youngest (mainly less than 3 years old), discrete well samples collected from the bottom of the wells are the oldest (19–36 years), and integrated well samples containing water from a range of intermediate depths are of intermediate age.

The ages of the integrated well samples from HCBW2 downstream to HCFW5 are remarkably uniform, ranging from 8 to 11 years (fig. 4). The similarity in the age of these flow-weighted samples is consistent with a uniform flow system downstream from HCBW2, which includes most of the study area. The $^{3}H/^{3}He$ ages of both discrete and integrated well samples collected from HCBW1 indicate that bedrock ground water is older at this location than at other locations in the watershed. Ground-water temperatures at depths greater than 10 m (below the zone of seasonal oscillation) are warmer in HCBW1 (3.6°–3.9°C) than in the other bedrock wells (2.3°–3.1°C), which also is consistent with water in HCBW1 being anomalously old. The reason for the older water at HCBW1 is not clear and requires further investigation.

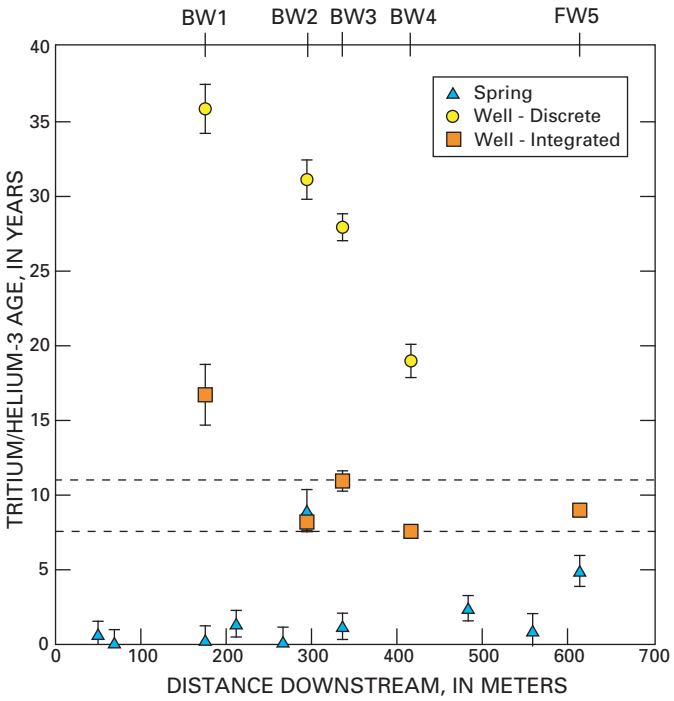

Figure 4. Distance downstream relative to $^{3}H/^{3}He$ age for springs and bedrock well samples. BW1–4 and FW5 along top axis indicate well locations. Samples collected from springs are the youngest. Discrete well samples, collected from the bottom of the well screen, are the oldest. Integrated well samples, collected from the entire well screen, are of intermediate age. Dashed lines indicate the relatively narrow zone of variation of mean ages for integrated well samples (HCBW1 excepted). One sigma error bars are displayed on symbols.

Conclusions

Temperature-depth profiles indicate active ground-water circulation to a maximum depth (aquifer thickness) of about 200 m, or about 100 m below the water table in the study area. Borehole temperature logging is a reliable method of identifying aquifer thickness in alpine watersheds underlain by fractured crystalline rock because linear profiles with slopes similar to the conductive geothermal gradient are reliable indicators of very low flow velocities characteristic of the underlying inactive zone.

The ages of integrated bedrock samples, assumed to be approximately flow weighted due to artesian flow, are remarkably consistent along the stream, four of five being from 8 to 11 years old. This result, in combination with other hydrologic and geologic data, supports a simple watershed-scale conceptual model of ground-water flow in which permeability is primarily a function of depth, and where recharge, aquifer thickness, and porosity are relatively uniform throughout most of the watershed. The conceptual model's simplicity is surprising given the geological complexity of the study area. A flow system of this sort could be reasonably well represented with an equivalent porous-media model calibrated with limited data, and such a model may be used to simulate solute transport and to explore chemical mass balance and fluxes within the watershed.

References Cited

Birch, Francis, 1950, Flow of heat in the Front Range, Colorado: Bulletin of the Geological Society of America, v. 61, p. 567–630.

Caine, J.S., Manning, A.H., Verplanck, P.L., Bove, D.J., and Kahn, K.G., and Ge, Shemin, 2006, Well construction information, lithologic logs, water-level data, and overview of research in Handcart Gulch, Colorado—An alpine watershed affected by metalliferous hydrothermal alteration: U.S. Geological Survey Open-File Report 2006–1189, 14 p.

Cook, P.G., and Böhlke, J.K., 2000, Determining timescales for groundwater flow and solute transport, *in* Cook, P.G., and Herczeg, A.L., eds., Environmental tracers in subsurface hydrology: New York, Kluwer Academic Publishers, p. 1–30.

Decker, E.R., 1969, Heat flow in Colorado and New Mexico: Journal of Geophysical Research, v. 74, p. 550–559.

Desbarats, A.J., 2002, A lumped-parameter model of groundwater influx to a mine adit in mountainous terrain: Water Resources Research, v. 38, no. 11, doi:10.1029/2001WR001058.

Domenico, P.A., and Palciauskas, V.V., 1973, Theoretical analysis of forced convective heat transfer in regional ground-water flow: Geological Society of America Bulletin, v. 84, p. 3803–3814.

Forster, Craig, and Smith, Leslie, 1989, The influence of groundwater flow on thermal regimes in mountainous terrain—A model study: Journal of Geophysical Research, v. 94, p. 9439–9451.

Haitjema, H.M., 1995, On the residence time distribution in idealized groundwatersheds: Journal of Hydrology, v. 172, p. 127–146.

Hely, A.G., Mower, R.W., and Harr, C.A., 1971, Water resources of Salt Lake County, Utah: Utah Department of Natural Resources Technical Publication 31, 192 p.

Kahn, K.G., Ge, Shemin, Caine, J.S., and Manning, A.H., 2008, Characterization of the shallow groundwater system in an alpine watershed—Handcart Gulch, Colorado: Hydrogeology Journal, v. 16, p. 103–121.

Kimball, B.A., Runkel, R.L., and Gerner, L.J., 2001, Quantification of mine drainage inflows to Little Cottonwood Creek, Utah, using a tracer-injection and synoptic-sampling study: Environmental Science and Technology, v. 40, p. 1390–1404.

Kimball, B.A., Runkel, R.L., Walton-Day, Katherine, and Bencala, K.E., 2002, Assessment of metal loads in watersheds affected by acid mine drainage by using tracer injection and synoptic sampling, Cement Creek, Colorado, USA: Applied Geochemistry, v. 17, p. 1183–1207.

Kosugi, Ken'ichirou, Katsura, Shin'ya, Katsuyama, Masanori, and Mizuyama, Takahisa, 2006, Water flow processes in weathered granitic bedrock and their effects on runoff generation in a small headwater catchment: Water Resources Research, v. 42, W02414, doi:10.1029/2005WR004275.

Liu, Fengjing, Williams, M.W., and Caine, Nel., 2004, Source waters and flow paths in an alpine catchment, Colorado Front Range, United States: Water Resources Research, v. 40, W090401, doi:10.1029/2004WR003076.

Manning, A.H., and Caine, J.S., 2007, Groundwater noble gas, age, and temperature signatures in an alpine watershed—Valuable tools in conceptual model development: Water Resources Research, v. 43, W04404, doi:10.1029/2006WR005349.

Mayo, A.L., Morris, T.H., Peltier, Steven, Petersen, E.C., Payne, Kelly, Holman, L.S., Tingey, David, Fogel, Tamara, Black, B.J., and Gibbs, T.D., 2003, Active and inactive groundwater flow systems—Evidence from a stratified, mountainous terrain: Geological Society of America Bulletin, v. 115, p. 1456–1472.

Robinson, C.S., Lee, F.T., Scott, J.H., Carroll, R.D., Hurr, R.T., Richards, D.B., Mattei, F.A., Hartmann, B.E., and Abel, J.F., 1974, Engineering geologic, geophysical, hydrologic and rock-mechanics investigations of the Straight Creek Tunnel site and pilot bore, Colorado: U.S. Geological Survey Professional Paper 815, 158 p.

Snow, D.T., 1968, Hydraulic character of fractured metamorphic rocks of the Front Range and implications to the Rocky Mountain Arsenal well: Golden, Colorado School of Mines Quarterly, v. 63, p. 167–199.

Snow, D.T., 1973, Mountain groundwater supplies: The Mountain Geologist, v. 10, p. 19–24.

Solomon, D.K., and Cook, P.G., 2000, ^{3}H and ^{3}He, *in* Cook, P.G., and Herczeg, A.L., eds., Environmental tracers in subsurface hydrology: New York, Kluwer Academic Publishers, p. 397–424.

Soulsby, Chris, Malcolm, Rob, and Malcolm, I.A., 2000, Groundwater in headwaters—Hydrological and ecological significance: Geological Society Special Publication, no. 182, p. 19–34.

Tiedeman, C.R., Goode, D.J., and Hsieh, P.A., 1998, Characterizing a ground water basin in a New England mountain and valley terrain: Ground Water, v. 36, p. 611–620.

Uhlenbrook, Stefan, Frey, Markus, Leibundgut, Christian, and Maloszewski, Piotr, 2002, Hydrograph separations in a mesoscale mountainous basin at event and seasonal timescales: Water Resources Research, v. 38, no. 6, doi:10.1029/2001WR000938.

Vogel, J.C., 1967, Investigation of groundwater flow with radiocarbon, *in* Isotopes in hydrology, IAEA–SM–83/7: Vienna, International Atomic Energy Agency, p. 355–369.

Wasiolek, Maryann, 1995, Subsurface recharge to the Tesuque aquifer system from selected drainage basins along the western side of the Sangre de Cristo Mountains near Santa Fe, New Mexico: U.S. Geological Survey Water-Resources Investigations Report 94–4072, 72 p.

Chapter K: Environmental Rock Properties at Abandoned Mine Lands that Generate or Neutralize Acid Drainage, Silverton, Colorado

by Douglas B. Yager

Overview

Land managers are interested in the environmental rock properties, net acid production (NAP), and acid-neutralizing capacity (ANC) of local bedrocks that are host to base- and precious-metal mineralization. This study addresses these properties for igneous rocks near Silverton, Colorado, and has identified volcanic units that are currently used by land managers to help mitigate the effects of acid drainage at mine sites. This work has implications for reducing hauling costs if local ANC rocks could be used in combination with or in place of limestone, the rock type traditionally transported to mine sites to neutralize acid drainage. Detailed studies including field work, mineralogy, geochemical analyses, rock physical properties (magnetic susceptibility), and laboratory investigations (acid titration experiments) aid in understanding the characteristic rock properties that contribute to generating or neutralizing acid drainage.

Introduction

This study is focused on the historical mining area of Silverton, Colorado, in the western San Juan Mountains, a region affected by two caldera-forming events that occurred about 28 million years ago. The calderas (collapsed volcanoes) were infilled by a nearly 1-km-thick accumulation of lava flows that were subsequently hydrothermally altered and locally mineralized with base metals (copper-lead-zinc) and precious metals (gold-silver). Acid water that formed from natural weathering processes emanated from hydrothermally altered and mineralized rocks in the Silverton area long before any mining activity. Historical observations in the region by Spanish expeditions in 1776 describe springs that "flowed red in color" and were "hot and ill-tasting" (Vélez de Escalante, 1792). The Hayden expedition in 1874 documented poor water quality in the study area, referring to Mineral Creek as "so strongly impregnated with mineral ingredients as to be quite unfit to drink" (Rhoda, 1876). These explorers' descriptions indicate there was some natural acid drainage in the area prior to mining. Since the 1870s when mining began, large volumes of mine-waste rock containing acid-generating minerals were concentrated at the surface, adding to the acid and metal burden to streams already affected by natural weathering processes.

Today, Federal and State land managers and private stakeholders throughout the Western United States are actively involved in the cleanup of watersheds affected by metal mines that have been essentially abandoned by previous mine owners. Many of these abandoned mines are affected by acid drainage that is caused by weathering of acid-generating minerals; principal among these minerals is pyrite (FeS_2). In the presence of oxygen and water, pyrite and other sulfide minerals react to yield sulfuric acid (H_2SO_4), which can lower stream pH, leach toxic metals, and substantially degrade water quality (fig. 1). Weathering of mine waste and consequent acid drainage has overwhelmed the acid-neutralizing capacity (ANC) of some streams already affected by natural weathering of pyritic country rocks (Yager and others, 2000; Mast and others, 2007).

Country rocks that host mineralization provide clues as to possible reclamation strategies that might be used to alleviate acid-mine drainage issues. This is due to the presence of acid-neutralizing minerals, such as calcite ($CaCO_3$), that form in some altered igneous country rocks. Limestone is nearly pure calcite and is commonly transported from long distances to reclamation sites that require a substance that can effectively neutralize acidity. If a local source of acid-neutralizing country rock can be identified, this could lessen the need to haul limestone to mine sites, thus reducing reclamation costs and perhaps providing a potential source of jobs for communities that are in transition from a mining-based economy once mining ceases. The purpose of this study was, therefore, to identify the local source rocks that can aid in mine-waste cleanup.

A map and database that identify the acid-neutralizing capacity (ANC) for 59 samples were generated as a result of this study (fig. 2). This map and accompanying data (Yager and others, 2005, 2008) can guide local land managers to outcrops with a high net acid production (NAP) and to high-ANC rocks suitable for remediation of acid drainage.

Methods Used to Determine Environmental Rock Properties

Two important environmental rock properties of igneous country rocks that can be measured and quantified are NAP and ANC. A field sampling effort was completed to collect representative examples from all igneous rock types in the study area; NAP and ANC were subsequently determined for all samples. In addition, rocks were analyzed for major- and trace-element chemical compositions, CO_2, carbon from carbonate, quantitative mineralogy, and physical properties (magnetic susceptibility and resistivity) (Yager and others, 2005, 2008). NAP and ANC are correlated with rock chemical composition and mineralogy; therefore, it was useful to quantify these rock characteristics. In addition, rock physical properties were determined as ground-truth verification of airborne geophysical datasets (Yager and others, 2005, 2008).

A

B

Figure 1. (*A*) U.S. Geological Survey scientist measuring the acidity (pH) of a ground-water seep on the bank of Cement Creek near Prospect Gulch. Such acidic seeps and acidic surface water are toxic to aquatic life. No fish live in Cement Creek. (*B*) Abandoned mine southwest of Silverton, Colorado, along Mineral Creek.

This was done to determine whether correlations among physical and environmental properties of rock could enable regional mapping of outcrops with varying NAP and ANC by using airborne geophysical datasets (McCafferty and others this volume, Chapter L). The following sections define acidity, discuss how acid can be neutralized, and relate how NAP and ANC are measured.

Acidity and How It Is Neutralized

Acidity is a function of the concentration of H^+ in solution. Acidity is measured with a pH probe that detects and records the exponential quantity of H^+ ions. A one-unit change in pH is 10 times different than the previous whole unit. It is recorded on a logarithmic scale between pH 1 (acid) and pH 14 (alkaline) with pH 7 being neither acid nor alkaline but neutral. Drinking water is commonly pH 7.

The concentration of H^+ needs to be reduced to decrease acidity and increase pH. One way to increase pH is to expose acid solutions to rocks that contain acid-neutralizing minerals that consume H^+. Minerals in Silverton-area igneous rocks that react with H^+ are calcite and chlorite [$(Mg, Fe, Al)_6(Si, Al)_4O_{10}(OH)_8$] and to a lesser extent epidote [$Ca_2(Al, Fe)_3(SiO_4)_3(OH)$]. Calcite reacts with H^+ to eventually form free calcium and carbonic acid (H_2CO_3). Carbonic acid is a weak acid, and it is only slightly acid under normal atmospheric conditions. The negatively charged hydroxyl group (OH^-) in chlorite reacts with the positively charged hydrogen ion in an acid solution to form water. Chlorite reactions are slow compared to calcite reactions. However, this could be beneficial from a remediation standpoint as it appears that chlorite may be able to decrease acidity long after calcite has been consumed. We are currently (2008) investigating the utility of using rocks containing both calcite and chlorite in remediation projects.

Measuring Net Acid Production (NAP)

NAP tests were done with a method described by Lapakko and Lawrence (1993) that uses a titration procedure to determine the amount of sodium hydroxide (NaOH), a strong alkaline base that would be required to neutralize acid generated by rocks. The test uses boiling hydrogen peroxide (H_2O_2) to dissolve all sulfides in the sample available for sulfuric acid production. Once a powdered rock sample is dissolved in the hydrogen pyroxide solution, NaOH solution is added to the sample—the larger the volume of NaOH needed to raise the pH to neutral, the more the sample has the capacity to generate acid due to the quantity of dissolved sulfides. The amount of base added is calculated as calcium carbonate ($CaCO_3$) equivalents measured in kilograms per ton. Calcium

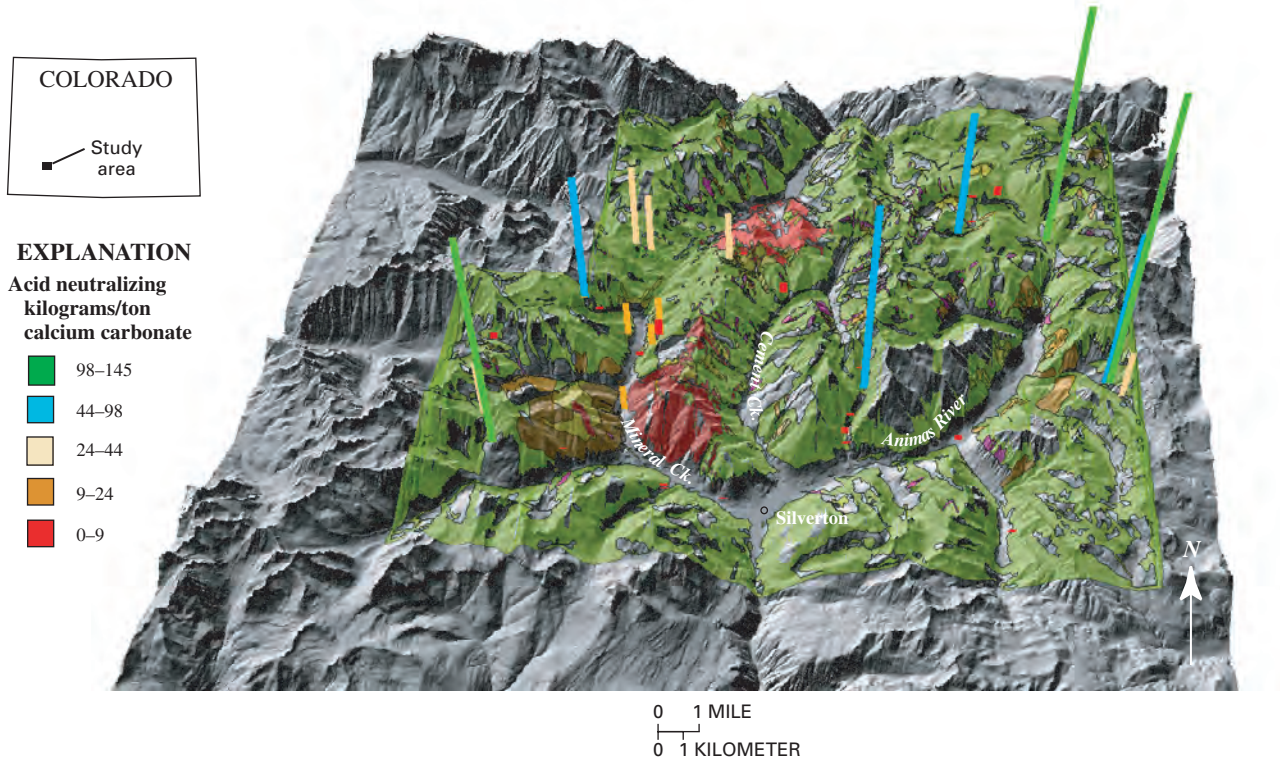

Figure 2. Map showing 59 ANC sites. Vertical bars are proportionate to acid-neutralizing capacity in kilograms per ton calcium carbonate equivalent. Note that some vertical bar symbols are obscured by topography. Alteration assemblages (Bove and others, 2007) are draped on USGS DEM hillshade image (2 X vertical exaggeration). Green areas represent the propylitic alteration assemblage that affects most of the study area; rocks portrayed in red, brown, and yellow represent areas of late-stage intense alteration containing abundant pyrite and other sulfides that locally obliterate the acid-neutralizing capacity supplied by the propylitic assemblage.

carbonate equivalents are calculated because mine-waste remediation projects commonly use limestone to neutralize acidity. This test is a useful screening tool to eliminate high-NAP samples from further ANC study and to determine those samples that are acid producers.

Measuring Acid-Neutralizing Capacity (ANC)

Laboratory experiments were also used to determine the ANC of igneous rocks. These experiments involved combining crushed (<2 mm) samples with deionized water in a glass beaker (fig. 3). The rock/water mixture is titrated by adding small amounts of sulfuric acid (the main acid in mine drainage) to the rock/water mixture to quantify the amount of acid added to reach the titration endpoint (pH 2). The calcium carbonate equivalent (in kilograms per ton) is calculated and recorded as "instantaneous ANC" (see Yager and others, 2005, for details of this calculation). The term instantaneous ANC is used because ANC reactions in this study occur over a duration of hours and not weeks, or in the case of remediation projects, years (Gustavson

Figure 3. Laboratory ANC test apparatus. Glass beaker contains water and rock fragments (gray). Acid is added to the sample through the red tube; probe (center of beaker) monitors pH.

others, 2007). Rocks that contain the mineral mixtures calcite and chlorite with ANC properties can neutralize or sequester greater amounts of acid and have a greater acid-remediation potential compared to those rocks that lack these minerals.

Application to the Silverton Study Area

Several of the Silverton ANC igneous rock units (for example, the San Juan Formation, Eureka Member of the Sapinero Mesa Tuff, and pyroxene andesite member of the Silverton Volcanics have pervasive calcite and chlorite that make these units ideal for neutralizing acid drainage (fig. 4). In contrast to the highly altered red, yellow, and bleached-white mineralized rocks in figure 5, volcanic rocks with high ANC properties range in hue from pale grey, to green, to nearly black in outcrop (fig. 6). Outcrop color is an indicator of the types of ANC minerals present (calcite, chlorite, epidote) that formed during a regional propylitic alteration event (Bove and others, 2007). Propylitic alteration in the study area is thought to have formed during the period 28.2 Ma to about 27.6 Ma, as the nearly 1-kilometer sequence of Silverton Volcanics lavas that infilled the San Juan caldera cooled, and in the process of cooling, degassed volatile constituents. Large quantities of carbon dioxide (CO_2), perhaps the primary rock-altering volatile component, among others such as water (H_2O) and sulfur dioxide (SO_2), were released during cooling, altering the original minerals and matrix of the country rock (Burbank, 1960; Bove and others, 2007).Where rocks are overprinted by more intense, higher temperature alteration, the greenish hue of the propylitic assemblage is obliterated, bleached to white, and replaced with NAP minerals.

The current use of local ANC igneous rocks in Bureau of Land Management and USDA Forest Service remediation projects, such as at the Brooklyn mine in Browns Gulch north of Silverton, and at the U.S. Environmental Protection Agency's Idarado mine-tailings Superfund site near Red Mountain Pass, north of the study area, has helped to alleviate the need to haul limestone from distant quarries, reducing both material and hauling costs, and has helped create local, low environmental-impact mining jobs. Identification of high-ANC rocks prior to mining will allow reclamation managers to develop plans that layer or mix ANC material with NAP mine wastes as they accumulate, to minimize or eliminate acid mine drainage, and to decrease the cost of postmining remediation. Data presented here help support mine cleanup efforts and permit land managers and stakeholders to identify rocks that (1) confound mine-cleanup efforts by generating acidity or (2) are beneficial mine-waste materials that can neutralize acid mine drainage.

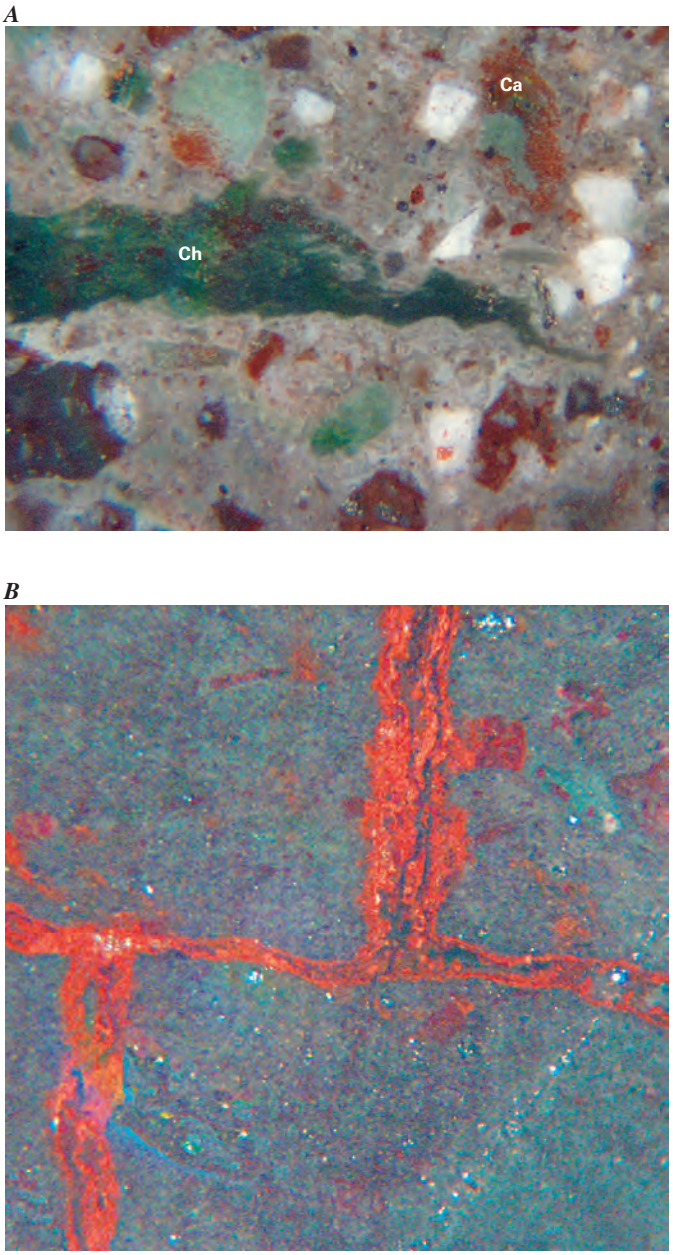

Figure 4. High-ANC samples: *A*, Eureka Member of the Sapinero Mesa Tuff; Ch is chlorite-filled pumice, red areas are calcite (Ca) that has been stained with "alizarin red," *B*, pyroxene andesite member of the Silverton volcanics with alizarin red-stained calcite in veinlets and replaced crystals; matrix has abundant chlorite that imparts a greenish hue.

Figure. 5. Hydrothermally altered and mineralized igneous bedrock north of Silverton, Colorado; red-yellow and brown hues are caused by oxidation of pyrite and other sulfide minerals that produce acid rock drainage.

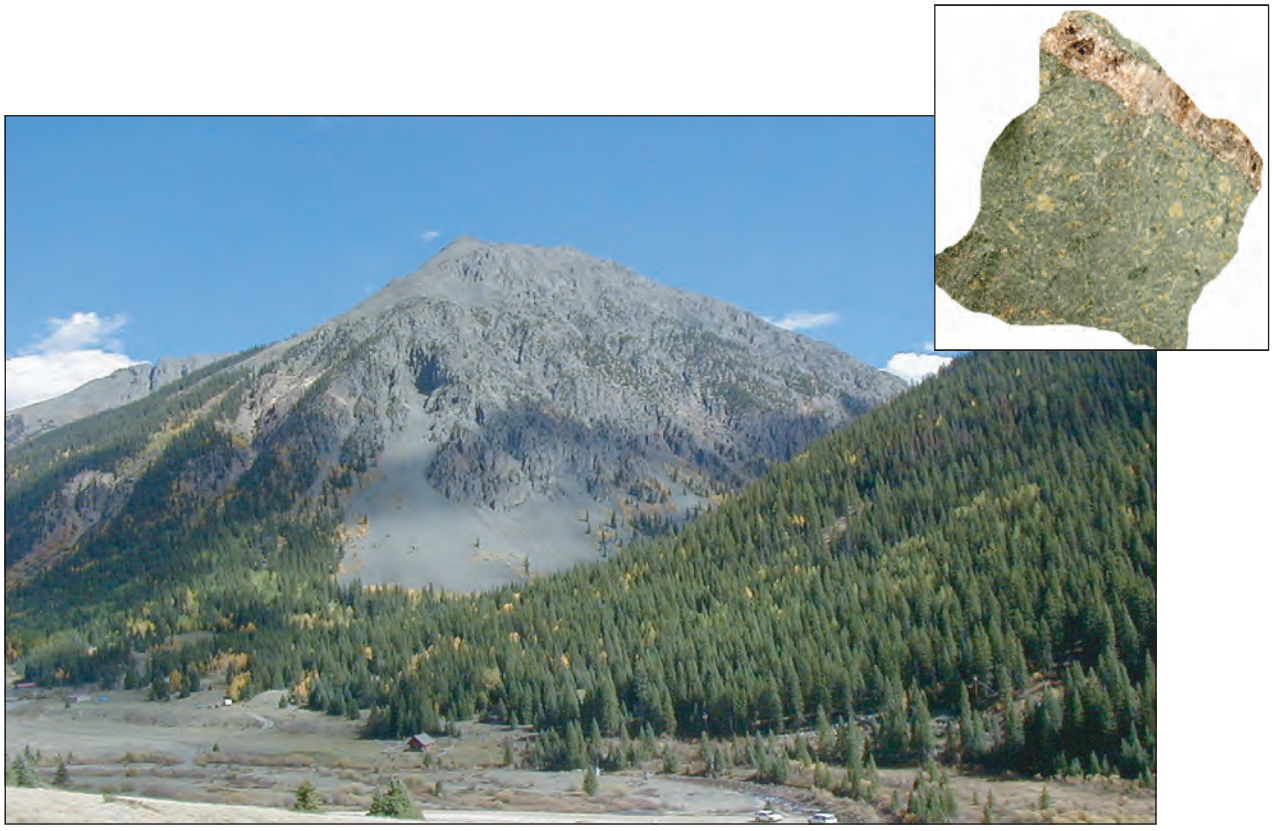

Figure 6. Greenish-gray ANC rocks southeast of Silverton. The greenish-gray hue is caused by the minerals chlorite and epidote. Inset is a sample (6 centimeters across) of the Burns Member of Silverton Volcanics.

References Cited

Bove, D.J., Yager, D.B., Mast, M.A., and Dalton, J.B., 2007, Alteration map showing major faults and veins and associated water-quality signatures of the Animas River watershed headwaters near Silverton, southwest Colorado: U.S. Geological Survey Scientific Investigations Map 2976, 18-page pamphlet, 1 plate, scale 1:24,000.

Burbank, W.S., 1960, Pre-ore propylization, Silverton Caldera, Colorado, *in* Geological Survey Research 1960: U.S. Geological Survey Professional Paper 400–B, article 6, p. B12–B13.

Gustavson, K.E., Barnthouse, L.W., Brierley, C.L., Clark, E.H. II, and Ward, C.H., 2007, Superfund and mining megasites: Environmental Science and Technology, v. 41, p. 2667–2672.

Lapakko, Kim, and Lawrence, R.W., 1993, Modification of the net acid production (NAP) test, *in* Proceedings of the Seventeenth Annual British Columbia Mine Reclamation Symposium, May 4–7, 1993: Port Hardy, British Columbia, p. 145–159.

Mast, M.A., Verplanck, P.L., Wright, W.G., and Bove, D.J., 2007, Characterization of background water quality, Chapter E7 *in* Church, S.E., von Guerard, Paul, and Finger, S.E., eds., Integrated investigations of environmental effects of historical mining in the Animas River watershed, San Juan County, Colorado: U.S. Geological Survey Professional Paper 1651, p. 351–386.

Rhoda, F., 1876, Report on the topography of the San Juan country, *in*, Hayden, F.V., annual report of the United States Geological Survey of the territories, embracing Colorado and parts of adjacent territories; being a report of progress of the exploration for the year 1874: 515 p.

Vélez de Escalante, Silvestre, 1792, The Dominguez—Escalante journal—Their expedition through Colorado, Utah, Arizona, and New Mexico in 1776: translated by Fray Angelico Chavez, edited by Ted J. Warner, 1995, Salt Lake City, University of Utah Press, 153 p.

Yager, D.B., Choate, LaDonna, and Stanton, M.R., 2008, Net acid production, acid neutralizing capacity, and associated mineralogical and geochemical characteristics of Animas River watershed igneous rocks near Silverton, Colorado: U.S. Geological Survey Scientific Investigations Report 2008–5063, 63 p.

Yager, D.B., Mast, M.A., Verplanck, P.L., Bove, D.J., Wright, W.G., and Hageman, P.L., 2000, Natural versus mining-related water quality degradation to tributaries draining Mount Moly, Silverton, Colorado: Proceedings of the Fifth International Conference on Acid Rock Drainage, Littleton, Colorado Society for Mining, Metallurgy, and Exploration, Inc., May 21–24, 2000, v. 1, p. 535–547.

Yager, D.B., McCafferty, A.E., Stanton, M.R., Diehl, S.F., Driscoll, R.L., Fey, D.L., and Sutley, S.J., 2005, Net acid production, acid neutralizing capacity, and associated geophysical, mineralogical, and geochemical characteristics of Animas River watershed rocks near Silverton, Colorado: U.S. Geological Survey Open-File Report 2005–1433, 75 p.

Chapter L: Connecting Airborne Geophysical Data to Geologic Structures in the Upper Animas River Watershed, Silverton, Colorado

by Anne E. McCafferty and Robert R. McDougal

Overview

High-resolution magnetic and electromagnetic survey data collected during helicopter flights were used to characterize the geophysical signatures and directional trends of geologic structures in the upper Animas River watershed study area. Geologic structures include faults and mineralized and nonmineralized veins. Many of the structures have localized mineralization or provide connectivity for ground-water movement, or both. In some cases, faults act as conduits for migration of ground water or movement of fluids and alteration of the host-rock mineralogy. In other cases, faults and veins may act as barriers to flow, such as where they are annealed with quartz. We use the airborne geophysical data and their derivative products to provide an understanding of how physical properties of magnetization and resistivity relate to and typify mapped geologic structures; specifically, faults, fractures, and mineralized veins.

Introduction

Our investigation uses a number of approaches to define the magnetic and electrical characteristics of mineralized and nonmineralized faults and veins in the study area. We use the results to infer the locations of exposed and concealed geologic structures in the watershed. Specifically, the airborne geophysical survey data were enhanced and analyzed to:

- identify major geophysical gradient trends that correspond with mapped structures,
- characterize electrical and magnetic properties of the structures, and
- interpret concealed crustal structures not mapped at the surface.

This paper summarizes interpretation of airborne geophysical data presented in McDougal and others (2007).

Airborne Geophysical Data

Magnetic and electromagnetic (EM) data were collected during helicopter flights over the upper Animas River watershed study area (fig. 1) in 1996 (Smith and others, 2007). Data were acquired along north-south flight lines at a 200-m spacing for the western one-half of the watershed and every 400 m for the eastern one-half. The electromagnetic response of the Earth was measured with three frequencies that included 984, 4,310, and 33,000 Hz. Data were collected at approximately 30 m above the ground surface, and measurements were taken every 3 m along the flight lines. Values of apparent resistivity were subsequently computed for each measurement point. A comprehensive discussion of the geophysical data acquisition and processing is in Smith and others (2007). The geophysical interpretations presented here were produced from grids of the magnetic and electromagnetic data.

In order to relate geophysical interpretations to geologic structure, we applied data-enhancement techniques to the gridded magnetic data, which transformed anomalies into forms that we could correlate to geologic structures. First, application of a reduction-to-pole (RTP) filter produced a grid (fig. 2*A*) in which magnetic anomalies are correctly positioned over their causative sources. Next, gradient trends of the magnetic anomalies were calculated from the RTP data (fig. 2*B*). Finally, we analyzed the gradient trends considering the mapped geologic structural trends. We increased the resolution of the small-scale anomalies by using a matched filter. Because of their high spatial frequency, these anomalies are directly related to near-surface magnetic sources. The high-frequency RTP magnetic data were used to determine the magnetic characteristics of surface geologic structures by using a statistical probability approach.

The midfrequency 4,310 Hz-data (fig. 3*A*) were used to investigate the resistivity characteristics of structures located from 0 m to between 30 to 50 m below the surface. The structures in this depth range are likely those that would be associated with shallow to mid-depth, structurally controlled vein deposits and geologic features controlling ground-water flow paths. Specifically, using data from the grid of the 4,310-Hz resistivity data, we applied filters to extract resistivity gradient trends so they could be related to mapped structural trends (fig. 3*B*) and to determine the electrical properties associated with the geologic structures.

Geophysical Gradient Trends Related to Shallow Crustal Geologic Structures

Geophysical gradient trends are defined as distinct linear and curvilinear elements that can be mapped from contours in geophysical maps. Magnetic and resistivity gradients result from contrasts in magnetic and electrical properties of rocks, respectively, and map the boundaries between rocks with dissimilar physical properties. These boundaries frequently correlate to mapped geologic structures and trends associated with

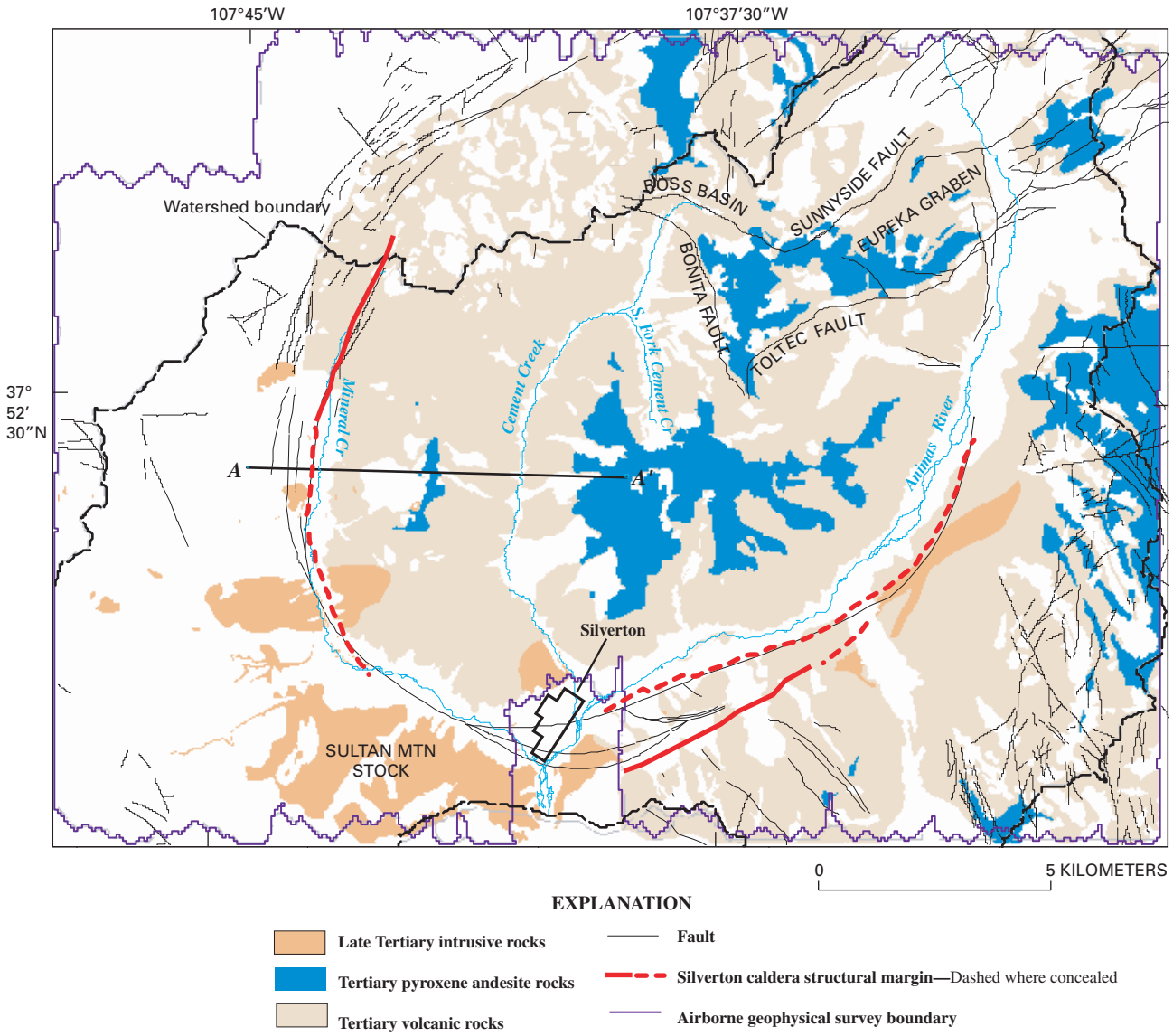

Figure 1. Location of airborne geophysical survey and selected geographic and geologic features in the Animas River watershed study area. Modified from Yager and Bove (2002). Profile *A–A′* in figure 4.

rock-unit (formational) contacts. The planimetric orientations of mapped structures and mineralized veins were compared to orientations of geophysical gradients. The orientations were calculated from the RTP magnetic data (fig. 2) and from the mid-frequency 4,310-Hz resistivity data (fig. 3) using methodology described in McDougal and others (2007). Evidence that many of the magnetic and resistivity gradients are related to geologic structures can be seen by comparing the rose diagrams from the geophysical data and the geologic data. Results show that good agreements between the orientations of geophysical gradients are colinear with east-west, northerly, and northwesterly geologic structure trends.

Magnetic and Electrical Signature of Geologic Structures

Do the geologic structures within the watershed have characteristic magnetic or electrical signatures? If so, can we determine these signatures from the airborne survey data and use this information to locate unmapped structures? We explored these questions using a predictive modeling approach that objectively determines the statistical likelihood (probability) that a range of values within the magnetic or apparent resistivity data characterize geologic structures (Lee and others, 2001). Results show that:

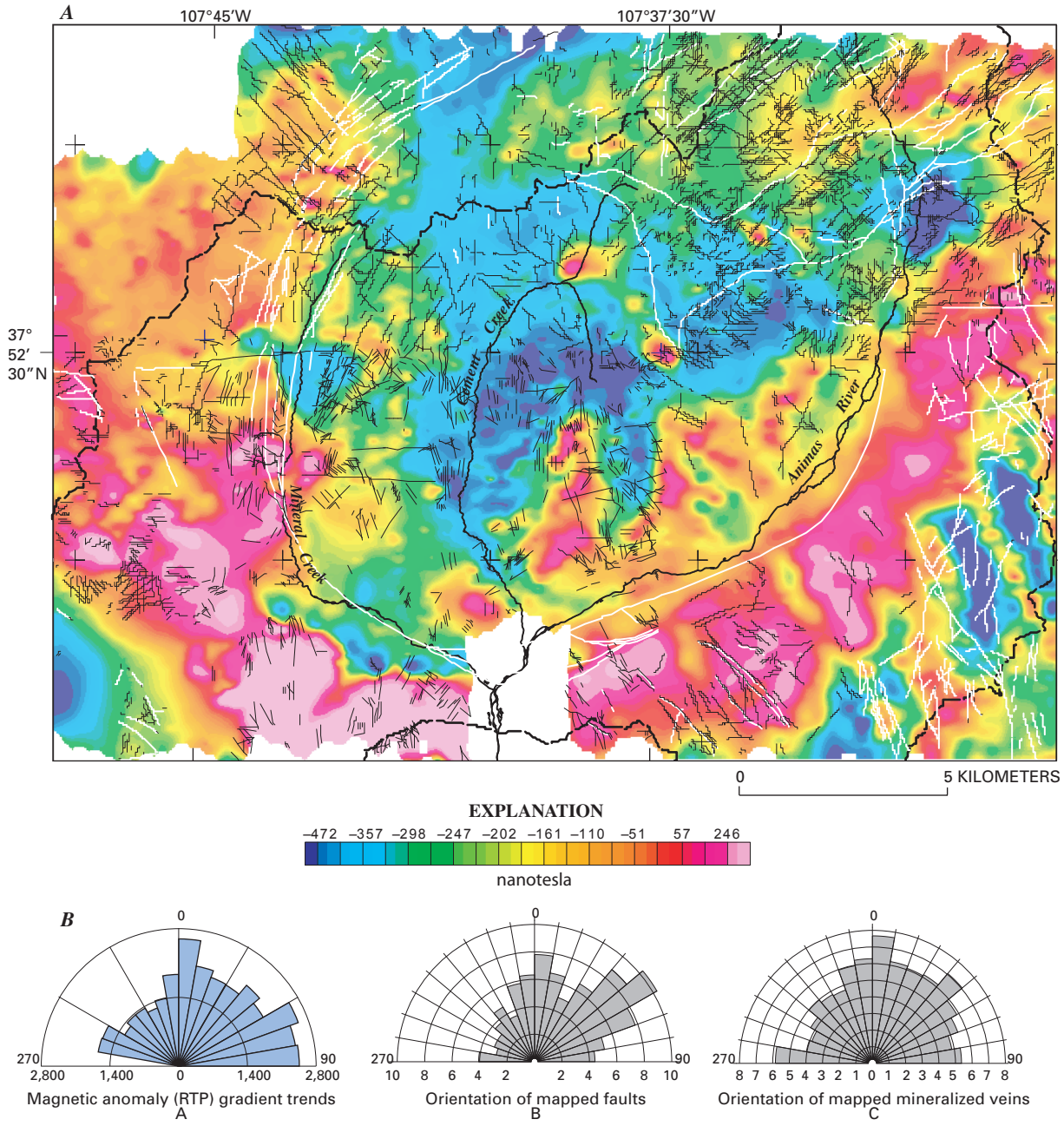

Figure 2. (*A*) Reduced-to-pole magnetic anomaly map. Data from this map were filtered to enhance magnetic anomalies and gradient trends associated with shallow geologic structures. Faults and veins from Yager and Bove (2007) are overlain on the magnetic data map. (*B*) Magnetic gradient trends (A) compared to planimetric orientation of mapped faults (B) and veins (C). Rose diagrams of mapped structures were calculated as class percentages; rose diagrams of geophysical gradients were calculated as number per class.

- Faults and veins have characteristic magnetic and apparent resistivity signatures within discrete data value ranges.
- Magnetically, the faults and veins are mostly characterized by extremely low magnetizations that are associated with the magnetite-poor mineralogy of the silicic vein material.
- Less typically, some faults and veins are characterized by moderately high magnetizations.
- Mapped faults and veins are characterized by moderately high electrical resistivity consistent with the silicic mineralogy of the vein material and silica-rich phases within the Silverton Volcanics.
- The predictive models give high probability values that correlate accurately with many known structures; but, more interestingly, high probability values are also present that indicate areas that are devoid of structures that likely predict the locations of potentially unmapped structures.

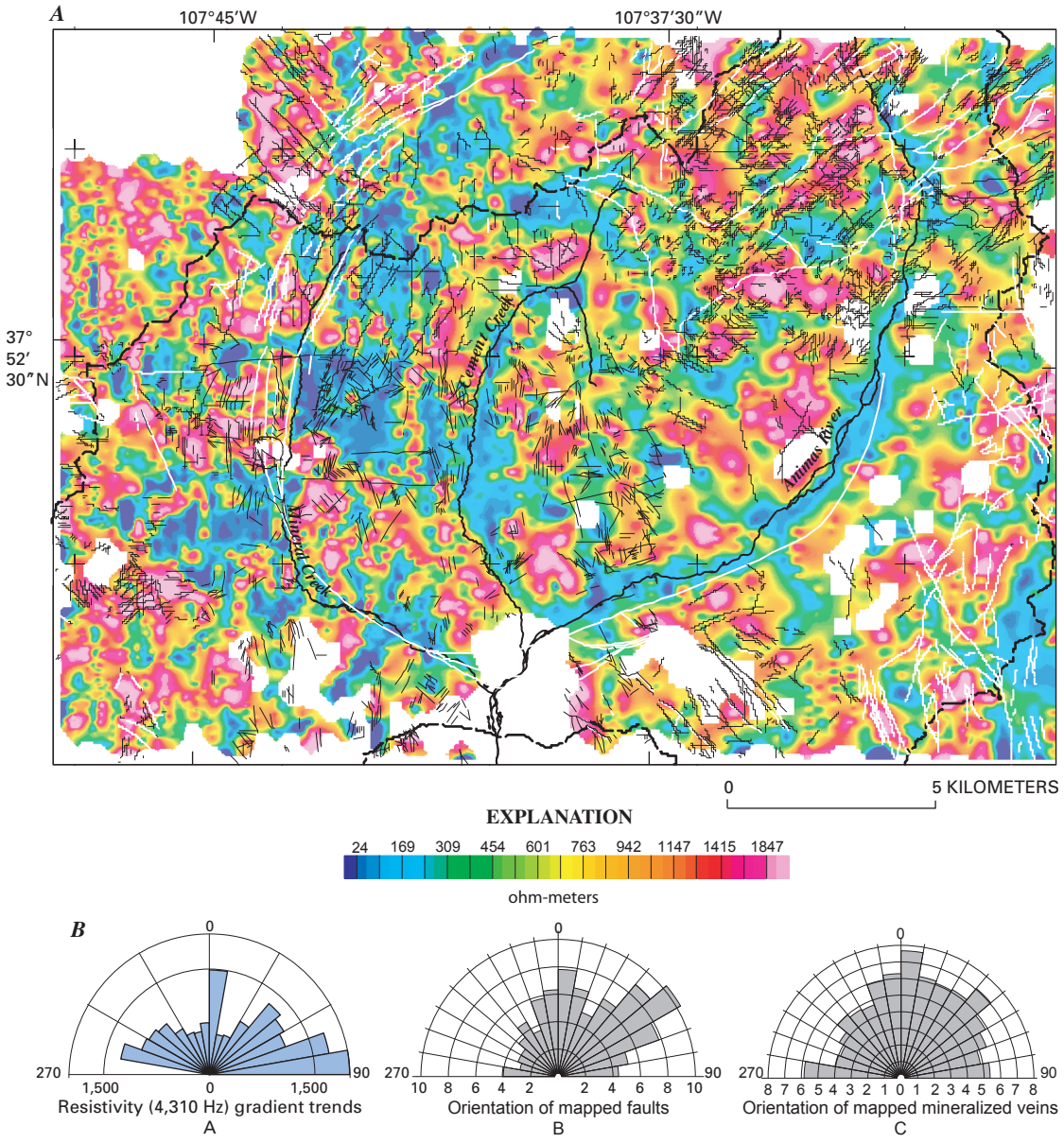

Figure 3. (*A*) Map of 4,310 hertz apparent resistivity data showing lateral variations in the electrical resistivity of rocks from topographic surface to depths 30 to 50 meters. Data from this map were used to define the resistivity properties of geologic structures. Faults and veins from Yager and Bove (2007) are overlain on the resistivity map. (*B*) Resistivity gradient trends (A) compared to planimetric orientation of mapped faults (B) and veins (C). Rose diagrams of mapped structures were calculated as class percentages; rose diagrams of geophysical gradients were calculated as number per class.

We plotted the predicted locations of geologic structures from the geophysical data in a geologic cross section (Luedke and Burbank, 2000), shown as profile *A*–*A′* (fig. 4). The geologic cross section runs from west to east, begins north of Middle Fork Mineral Creek, ends southwest of Storm Peak, and is entirely within the Silverton caldera. Probabilities associated with the predicted locations are shown as histogram bars beneath the magnetic or apparent resistivity profile. The variable bar heights indicate the relative strength of positive probabilities; therefore, the higher the bar height, the higher the probability that a particular geophysical characteristic will have a strong spatial association with a geologic structure. Where both magnetic and electromagnetic models predict structures, we consider this as very strong evidence that these locations identify unmapped structures. To highlight these occurrences, geologic structures that have a predicted location in both the magnetic and resistivity models have been projected onto the geologic cross section as blue dashed lines.

Both the magnetic and apparent resistivity predictive models show a number of predicted structures coincident with mapped structures and locations of predicted new structures. For

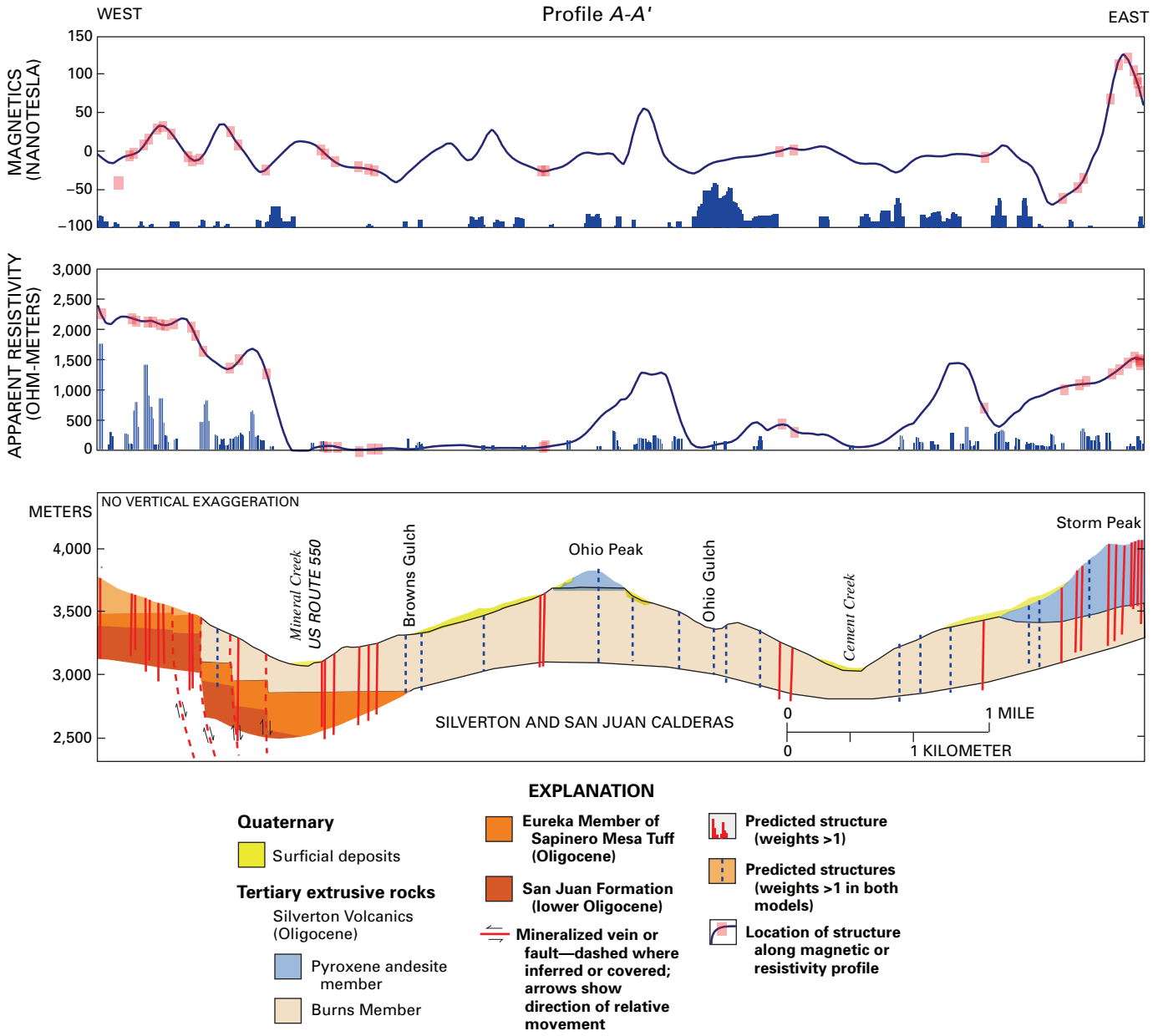

Figure 4. Magnetic (RTP) and apparent resistivity (4,310 hertz) over geologic cross section (Luedke and Burbank, 2000). Boxes on profiles (□) map locations of mineralized veins or faults (red). Locations of predicted structures from modeling are shown as bar charts below the profile. Predicted structures with coincident locations in both models are shown as blue dashed lines. Modified from McDougal and others (2007). The airborne geophysical models predict approximately 46 percent more structures than are mapped.

example, of the 14 mapped structures between the west end of profile *A–A'* and Mineral Creek, the magnetic model located 8 (57 percent) and the resistivity model located 12 (86 percent). In total, 35 structures are mapped along the profile. An additional 16 new structures are predicted from the magnetic and resistivity models, resulting in an increase of 46 percent more predicted than mapped. Many of the predicted, but unmapped, structures are located in areas of surficial deposits and may map the locations of faults or veins that would be covered.

Summary and Conclusions

This investigation was conducted to define and analyze the geophysical characteristics of faults and veins within the study area. We use this information to predict permissive areas for unmapped geologic structures in the watershed based on probability. Magnetic and electrical attributes were quantified for geologic structures, and the statistical method used identified target areas for further investigation. For example, the

predictive models could be considered in remediation planning or used as an exploration tool for ground-water or mineral-resource applications. The methods and approaches we used here can be applied to other watersheds with similar structural and volcanic regimes containing acid-generating historical mines or source rocks.

The predictive geophysical models showing high probabilities accurately locate many known structures. More interesting, the models suggest structures in areas where they had not been mapped. Many of the permissive areas lie in places of restricted access, limited outcrop, and thick alluvial soil or vegetation cover.

The planimetric orientation of electrical resistivity gradients identifies a prominent east-west orientation that correlates with one trend of unmapped structures. In terms of structurally controlled ground-water flow, faults and veins of this orientation would be least likely to provide flow paths. The resistive geophysical signature suggests that these structures are quartz filled and extend to a depth of at least 50 m. In areas where quartz-filled structures have secondary or younger fracturing, secondary permeability may be considerable. Magnetically, the faults and veins are characterized by either extremely low magnetizations or moderately high magnetizations. Faults and veins both are associated with moderately steep magnetic gradients.

Buried or covered geologic structures not mapped at the surface are suggested by both the magnetic and electromagnetic data. Faults and veins are characterized by moderately high electrical resistivities and may point to more silica-rich phases within the Silverton Volcanics. The predictive model calculated from the electrical resistivity characteristics of structures identifies areas where faults and veins are resistive at depth and, as previously discussed, least likely to be structurally controlled ground-water conduits, except where significantly fractured.

The predictive models presented here could be used to guide further geologic mapping and investigation, incorporated in hydrologic applications, or considered in remediation planning. The implication that significantly more mineralized and nonmineralized faults and veins, approximately 36 percent on average (McDougal and others, 2007), may exist in the watershed than previously mapped might be important in terms of estimating fracture permeability that would be included in ground-water modeling efforts.

The methods and approaches used in this study can be applied to other watersheds with similar structural and volcanic regimes containing acid-generating historical mines or source rocks. Further investigations may benefit from integration of the geophysical, topographic, and mineralogical characterization of structures presented here, with geochemical and geologic analysis to identify discrete ground-water flow paths and structurally controlled inflows to streams.

References Cited

Lee, G.K., McCafferty, A.E., Alminas, H.V., Bankey, Viki, Frishman, David, Knepper, D.H., Jr., Kulik, D.M., Marsh, S.P., Phillips, J.D., Pitkin, J.A., Smith, S.M., Stoeser, D.B., Tysdal, R.G., and Van Gosen, B.S., 2001, Montana geoenvironmental explorer: U.S. Geological Survey Digital Data Release DDS–65.

Luedke, R.G., and Burbank, W.S., 2000, Geologic map of the Silverton and Howardsville quadrangles, southwestern Colorado: U.S. Geological Survey Geologic Investigations Map I–2681, scale 1:24,000, 11 p.

McDougal, R.R., McCafferty, A.E., Smith, B.D., and Yager, D.A., 2007, Topographic, geophysical, and mineralogical characterization of geologic structures using a statistical modeling approach, *in* Church, S.E., von Guerard, Paul, and Finger, S.E., eds., Integrated investigations of environmental effects of historical mining in the Animas River watershed, San Juan County, Colorado: U.S. Geological Survey Professional Paper 1651, chap. E13, p. 643–688.

Smith, B.D., McDougal, R.R., Deszcz-Pan, M., and Yager, D.B., 2007, Helicopter electromagnetic and magnetic surveys, *in* Church, S.E., von Guerard, Paul, and Finger, S.E., eds., Integrated investigations of environmental effects of historical mining in the Animas River watershed, San Juan County, Colorado: U.S. Geological Survey Professional Paper 1651, chap. E4, p. 231–254.

Yager, D.B., and Bove, D.J., 2002, Generalized geologic map of part of the upper Animas River watershed and vicinity, Silverton, Colorado: U.S. Geological Survey Miscellaneous Field Studies Map 2377.

Yager, D.B., and Bove, D.J., 2007, Geologic framework, *in* Church, S.E., von Guerard, Paul, and Finger, S.E., eds., Integrated investigations of environmental effects of historical mining in the Animas River watershed, San Juan County, Colorado: U.S. Geological Survey Professional Paper 1651, chap. E1, p. 107–140.

Chapter M: Using a Geographic Information System (GIS) to Determine the Physical Factors that Affect Water Quality in the Western San Juan Mountains, Silverton, Colorado

by Douglas B. Yager, Raymond H. Johnson, and Bruce D. Smith

Overview

A cooperative, U.S. Geological Survey–Federal Land Management Agency study of abandoned mine lands in the western San Juan Mountains, Silverton, Colorado, was undertaken to evaluate water quality. The resulting comprehensive digital data base included GIS layers that were analyzed in this followup study by using a GIS and statistical approach to determine the most prominent physical factors that influence water quality. The GIS-statistical approach identified areas of quartz-sericite-pyrite alteration among the most important assemblages that adversely affect water quality in the study area. Ground-water quantity and quality were addressed using detailed hydrologic and geophysical conductivity surveys that enable the identification of ground-water inflows. These data correspond to stream inflows that are useful in inferring possible metal contaminant loading that could be associated with ground water. These findings are important to land managers and local stakeholders involved in land-use decisions and abandoned mine cleanup.

Introduction

During 1996 to 2001, the U.S. Geological Survey along with multiple Federal, State, and local stakeholders, completed an Abandoned Mine Lands Initiative (AMLI) study of the Animas River watershed near Silverton, Colo. (von Guerard and others, 2007). These AMLI datasets are a result of one of the most comprehensively studied watersheds affected by metallic mining in the world and consist of geologic, geophysical, geochemical, hydrologic, biologic, remote sensing, and base cartographic digital information (Yager and Bove, 2007; Smith and others, 2007; Kimball and others, 2007; Bove and others, 2007; Dalton and others, 2005). This region was the site of base- and precious-metal hard rock mining from the late 1870s to 1991. An extensive legacy of mining has left behind thousands of mines and prospects. Weathering of mine waste and hydrothermally altered bedrock, which hosts metallic mineral deposits, produces acidic drainage that adversely affects the environment. Federal land managers and the local Animas River Stakeholders Group are actively involved in abandoned mines cleanup in the study area.

The principal goal of this study is to analyze the extensive digital AMLI datasets summarized in Sole and others (2007) to advance understanding of the factors that control water quality. Our analysis of AMLI datasets combined a Geographical Information System (GIS) and a statistical-based approach to identify both mining and nonmining sources of metals and acidity to surface water and ground water (Yager and others, 2002; Yager and Caine, 2003).

Geology of the Study Area

The geology of the western San Juan Mountains study area is exceptional in that many diverse rock types representing every geologic era from the Proterozoic to Cenozoic are preserved. It is an area that was extensively glaciated during the Pleistocene and has high topographic relief, providing excellent bedrock exposures. The general stratigraphy of the San Juan Mountains near Silverton consists of Precambrian crystalline basement overlain by Paleozoic to Tertiary sedimentary rocks and a voluminous Oligocene volcanic cover (Yager and Bove, 2007). Two caldera-forming eruptions, together with subsequent postcaldera-collapse intrusive activity and volcanism affected much of the study area. Structures that developed during and after caldera collapse focused hydrothermal fluids during several episodes of alteration and base- with precious-metal mineralization that formed in the Tertiary volcanic assemblage. Today, an arcuate drainage network delineates the structural margins of each caldera (fig. 1). Weathering of pervasively altered igneous bedrocks and surficial deposits derived from them is a critical factor that influences water quality. Thus, much of this study has focused on the physical and chemical attributes of the Tertiary igneous sequence.

Geographic Information System (GIS) and Statistical Methods

GIS Overlays

While naturally altered and unmined areas have affected water quality, mining has concentrated acid-generating minerals and leachable metals in waste piles and in fluvial tailings on the surface, adding to the premining geochemical baseline metal concentrations in streams. Inspection of multiple GIS layers was used to qualitatively distinguish areas where surface water or ground water is affected by natural and (or) anthropogenic sources of contaminants. Prospect Gulch is a

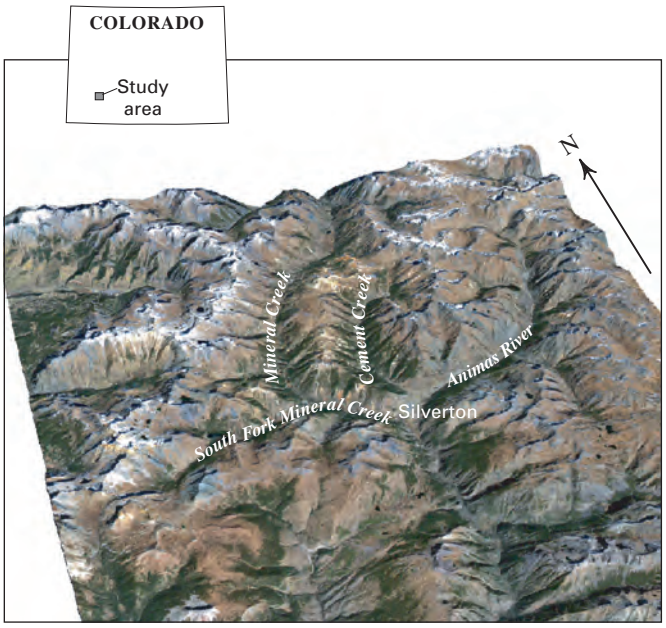

Figure 1. Landsat thematic mapper remote sensing scene draped on digital terrain model of study area. Arcuate drainages of Mineral Creek and Animas River follow the structural margins of two collapsed volcanoes (calderas) that formed during the Oligocene.

good example that shows the combined mining and nonmining factors that affect water quality in a well-studied, heavily altered and mined catchment (fig. 2). These methods are especially effective for quickly and easily communicating scientific data to audiences with varying backgrounds and experience.

Geomorphometric Methods

Geomorphometric analysis involves extracting quantitative measurements for topographic surfaces as well as for hydrologic networks. A surface-hydrology modeling tool, the GIS Weasel (Viger and others, 1998), was used to analyze a 10-m-resolution USGS digital elevation model and extract basinwide geomorphometric data (for example, slope, aspect, flow direction, flow accumulation, drainage network, and Strahler stream order). GIS Weasel also interfaces with ArcGrid™ to delineate modeling response units, or subbasin hydrologic catchments, referred to as catchments in this study (fig. 3).

Once catchments were delineated, ArcGrid™ GIS Weasel parameterization routines were used to compile characteristics of each catchment such as areas of altered rock and corresponding areas of nonvegetated rock or soil. These physical factors were evaluated for similarities and differences between catchments and associated water-quality signatures. One physical factor important to our study is the area of acid-generating alteration types that contain pyrite among other acid-generating minerals in each catchment. Pyrite in the presence of oxygen and water dissolves to produce sulfuric acid that degrades water quality and is toxic to aquatic life. Each of the 98 catchments delineated has varying proportions of acid-generating or acid-neutralizing bedrocks (fig. 4) and associated water-quality signatures (fig. 5).

GIS analysis also was used to determine the nonvegetated areas of catchments (figs. 6 and 7). Where acid-generating rock types are exposed due to lack of vegetative cover, erosion from precipitation and surface runoff can increase and have an effect on water quality (Ritter and others, 1995). These types of analyses identified the subbasins that are most likely to be affected by weathering of acid-generating alteration types that degrade water quality.

Statistics

Linear regression analysis was used to determine correlations between areas of alteration types determined by GIS analysis for each catchment and the water-quality parameters measured in streams at the mouths of the catchments. The Kendall's Tau method of regression (Kendall, 1975) was used to calculate the strength of correlation between the dependent and independent variables of interest, for example, area of quartz-sericite-pyrite (qsp), and pH determined by field measurement. Regression analysis results identified a correlation between catchment area of qsp alteration and pH (fig. 8), in addition to correlations with other water-quality variables such as aluminum concentration. Compared with other study-area alteration types, qsp alteration was determined to be one of the most important alteration types that adversely affects water quality. This method can be used to rank catchments that have the highest potential to affect water quality and adversely affect riparian habitat.

Ground Water in the Study Area

The AMLI study did not specifically evaluate the effect of inflowing ground-water quality and quantity on surface water in detail. However, an extensive data set exists with the quantity, quality, and location of ground-water discharge to surrounding streams (Kimball and others, 2007). In addition, geophysical data can be useful in inferring the location and quality of ground-water discharge where drill-hole, piezometer, or other direct measurement and sampling of ground water are lacking.

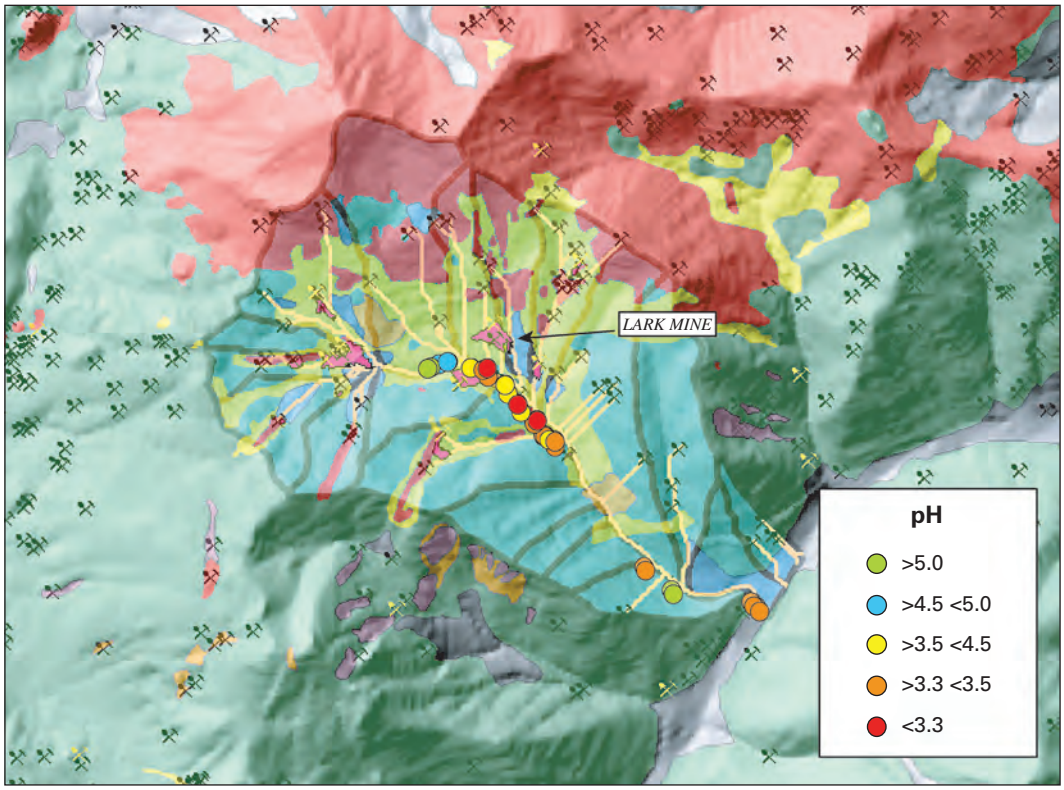

Figure 2. Alteration types draped on shaded relief model of Prospect Gulch, and pH from water-quality samples collected on September 29, 1999; pick and hammer symbols represent mines and prospects. Note that pH is greater than 5.0 near head of basin (green circles), left center of catchment. Acidity increases downstream (right of image) as weathering of mine waste and alteration assemblages affects water quality. Acid sulfate alteration (red) and quartz-sericite-pyrite alteration (yellow). Propylitic rocks (green) near mouth of catchment at one sampling site may be neutralizing acidity. Alteration from Bove and others, 2007; pH values from Johnson and others, 2007.

In stream tracer-dilution studies (Kimball and others, 2007), all visible surface-water inflows observed along a stream segment are recorded and measured for flow, quantity, and quality. When the upstream flow plus added inflows do not sum to the downstream total, an unsampled ground-water discharge is inferred as causing the increased surface-water flow. This inferred ground-water discharge, in addition to sampled springs and seeps, provides the total amount of ground-water contribution to the stream at specified locations (fig. 9). Interpretation of the source, flow path, and quality of ground water required evaluating geologic, topographic, geochemical, hydrologic, and geomorphic variables. A GIS-based approach helped in evaluating the multiple variables that influence this complex system.

Initial research is aiding in understanding the complexities of the ground-water system starting with locations, quantity, and quality of ground-water discharge as stream inflows (fig. 9). Geochemical data collected from water-quality sampling sites (inset box, fig. 9*A*) indicated the ground-water discharge in this area has compositions that are dissimilar to surface-water quality in the immediate vicinity, suggesting that the ground-water recharge did not occur locally. Understanding the movement of ground water, the subsequent transport of metals, and the final discharge to surface water is important for water quality in studies of catchments in mountainous terrain (Caine and others, 2004). Our studies, in combination to those reported in Johnson and others (2007) and Kimball and others (2007), identified that ground-water discharge in the study area occurs (1) where surface gradients decrease, (2) where there is an abrupt change in rock type, for example, near the Tertiary volcanic and Precambrian bedrock contact; (3) where landslides or alluvial fans with high clay content cause reduced ground-water flow beneath the stream; or (4) where geologic structures focus ground-water flow (Smith and others, 2007).

Geophysical conductivity profiles (Smith and others, 2007) constructed along stream segments with known ground-water discharge also provide an indication of ground-water quality. High conductivity can be indicative of high metal concentrations (fig. 9*B*). When several GIS layers such as alteration type, geologic structure, geophysics, and bedrock and surficial geology are combined, more detailed interpretations are possible that consider the quality of ground water, flow paths, source material (for example, surficial deposit or altered bedrock), and the resulting water quality.

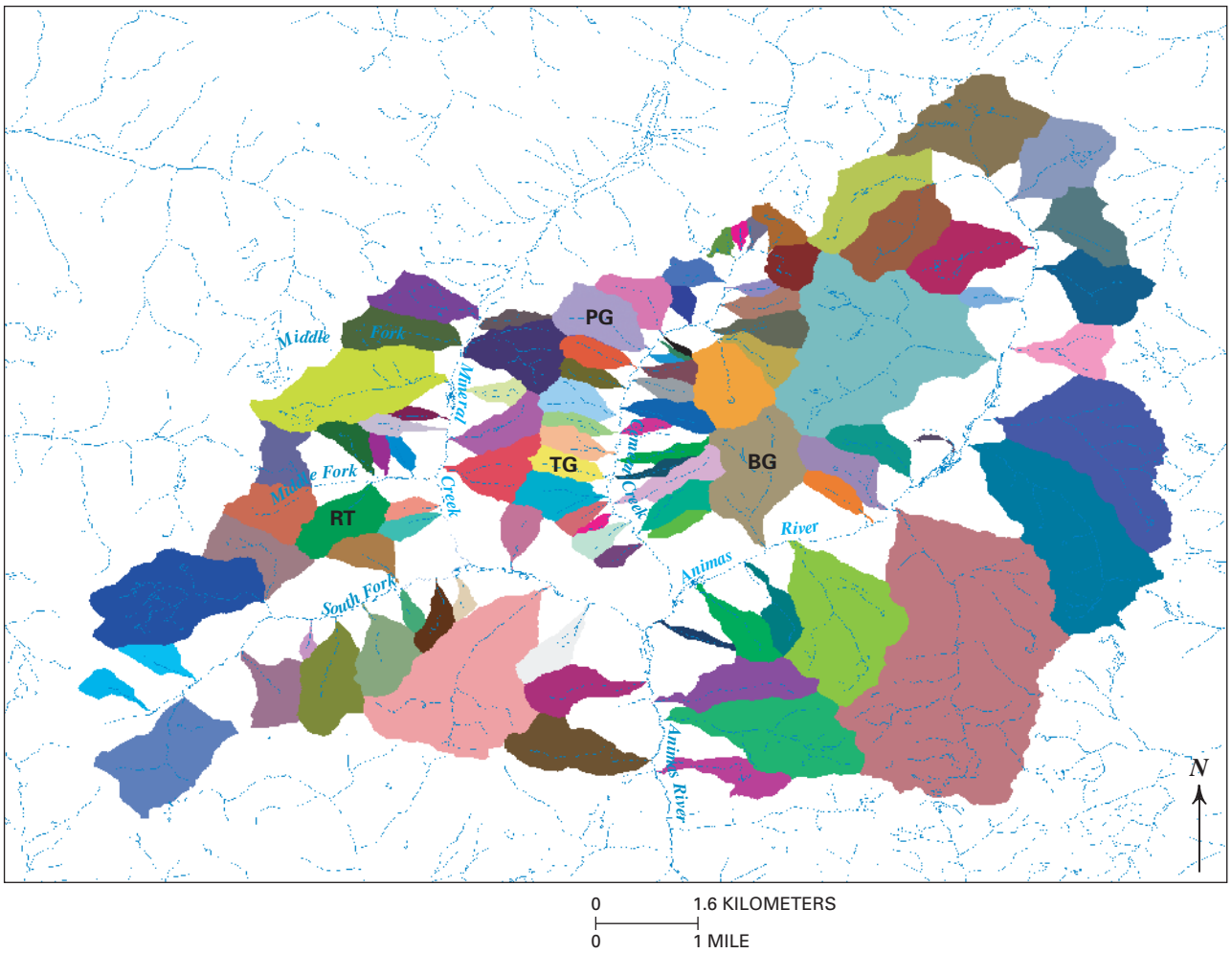

Figure 3. Subbasins delineated using the GIS Weasel. The subbasins form the principal modeling response units of interest in this study. Quantitative data for multiple physical factors such as area of alteration types were acquired for subbasins and compared with water-quality "signals" at the mouths of each subbasin catchment. Labeled catchments discussed elsewhere are RT, Red Tributary; TG, Topeka Gulch; PG, Prospect Gulch; and BG, Boulder Gulch.

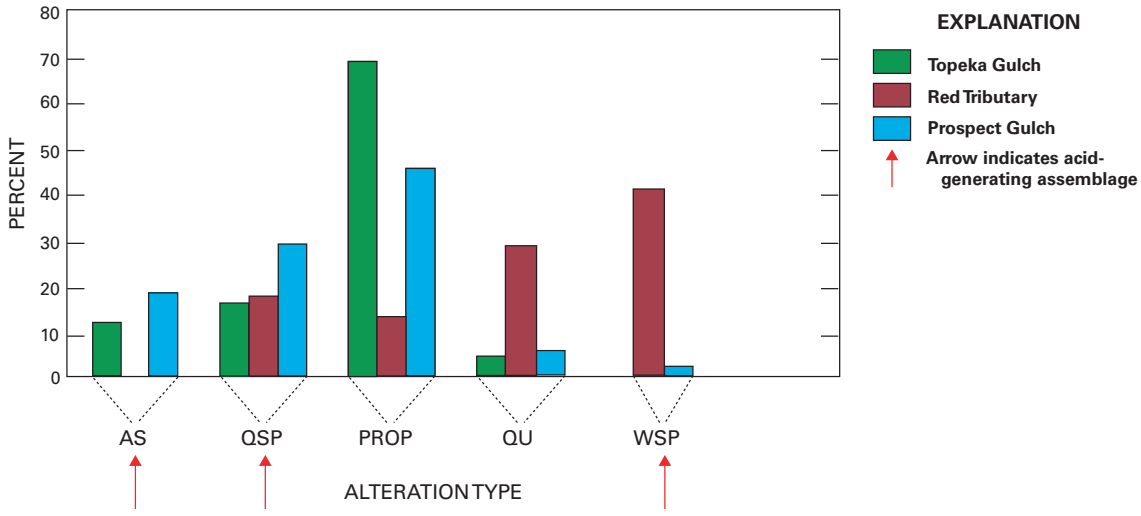

Figure 4. Alteration types determined for three catchments (areas in percent). Alteration types: AS, acid sulfate; QSP, quartz-sericite-pyrite; PROP, propylitic; QU, Quaternary undifferentiated; and WSP, weak sericite-pyrite. Alteration types described in Bove and others (2007) and Yager and Bove (2007).

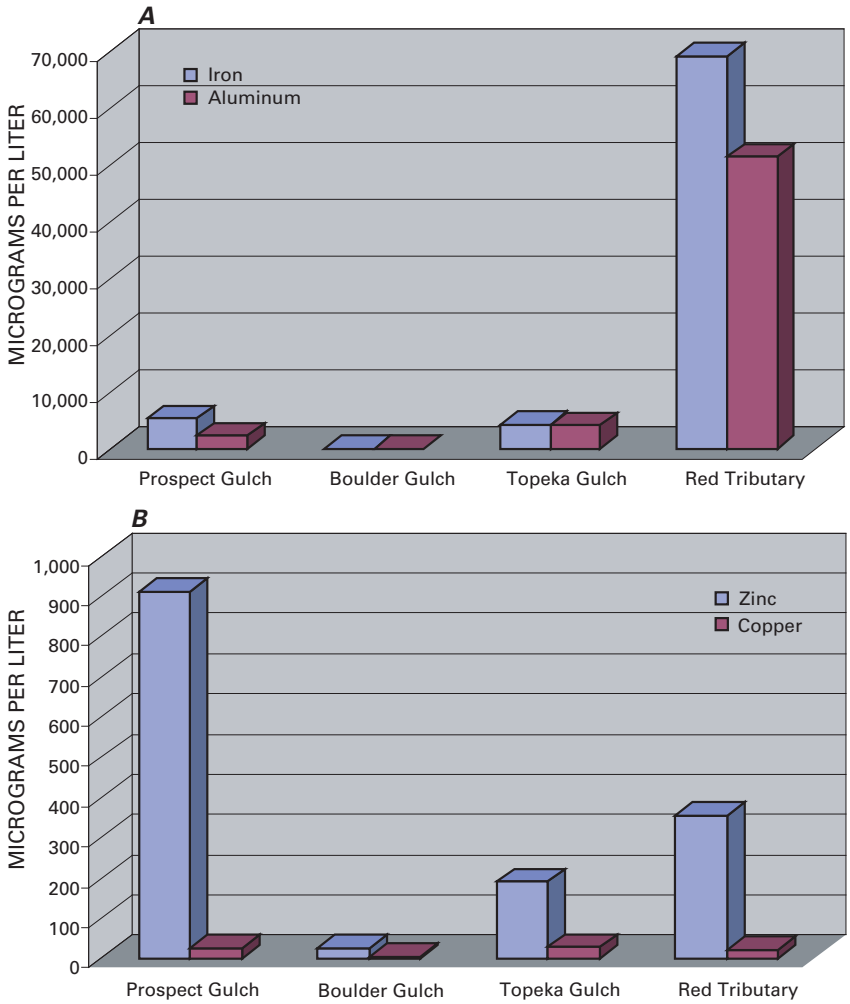

Figure 5. Surface-water-quality data for catchments in figures 4 and 7. (*A*) Iron (Fe) and aluminum (Al) data); (*B*) zinc (Zn) and copper (Cu) data. Data were collected during base-flow conditions during the fall after most snow had melted. Surface-water-quality data for Boulder Gulch (composed of over 82 percent propylitic alteration and having some acid neutralizing capacity, Yager, Chapter K, this volume; Yager and others, 2005) shown for comparison with other more highly altered catchments. Water-quality data from Johnson and others, 2007; Mast and others, 2007.

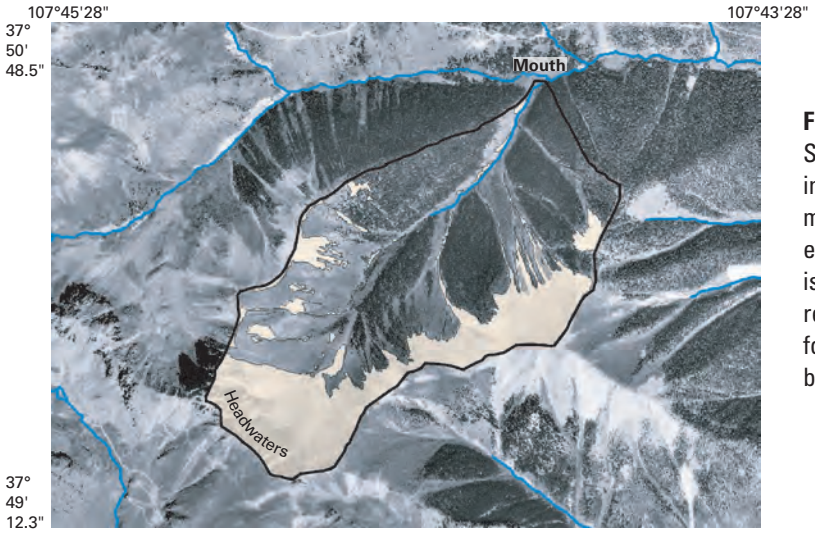

Figure 6. Red Tributary catchment located west of Silverton in Middle Fork Mineral Creek subbasin. Areas in tan indicate sparsely vegetated slopes that have minimal precipitation interception capacity and a high erosion potential. Top of digital orthophoto quadrangle is to the north. Subbasin outline in black; blue lines represent streams. Dark areas in subbasin are spruce forest. Area covered by image is about 4.5 kilometers by 3.7 kilometers.

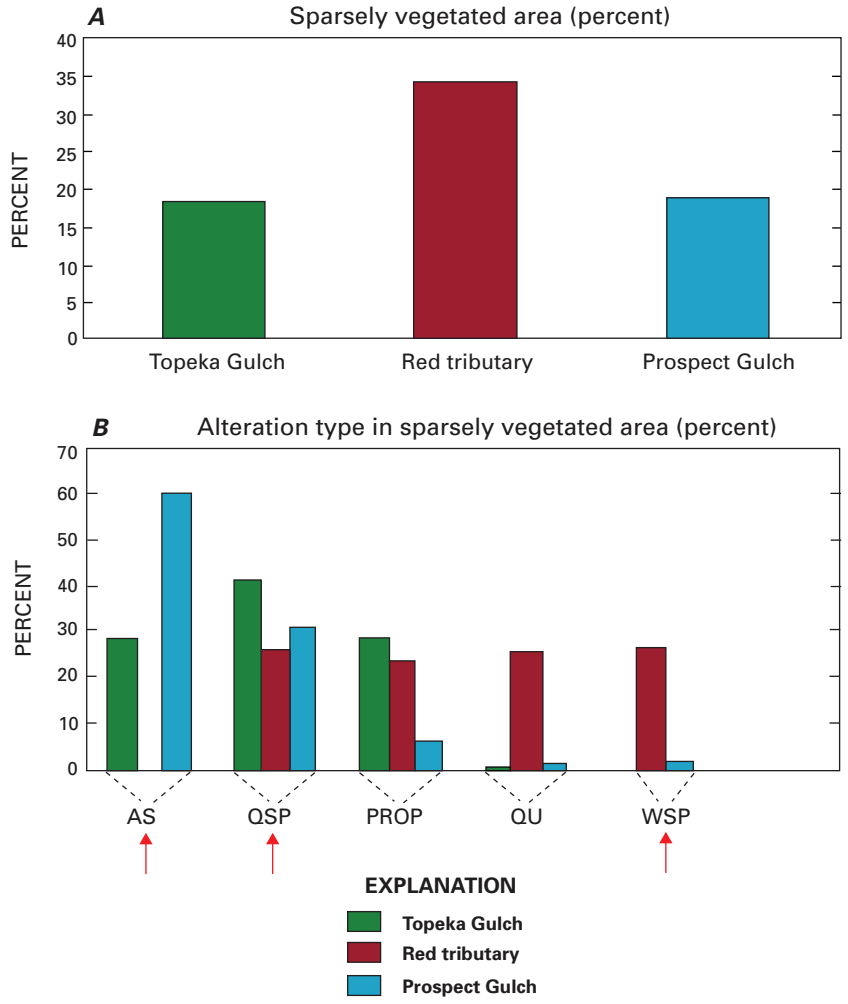

Figure 7. (*A*) Areas of sparse vegetation (in percent) determined by GIS analysis of AVIRIS mapping (Dalton and others, 2005), and (*B*) corresponding catchment areas that are both nonvegetated and also have corresponding areas of various alteration types (in percent).

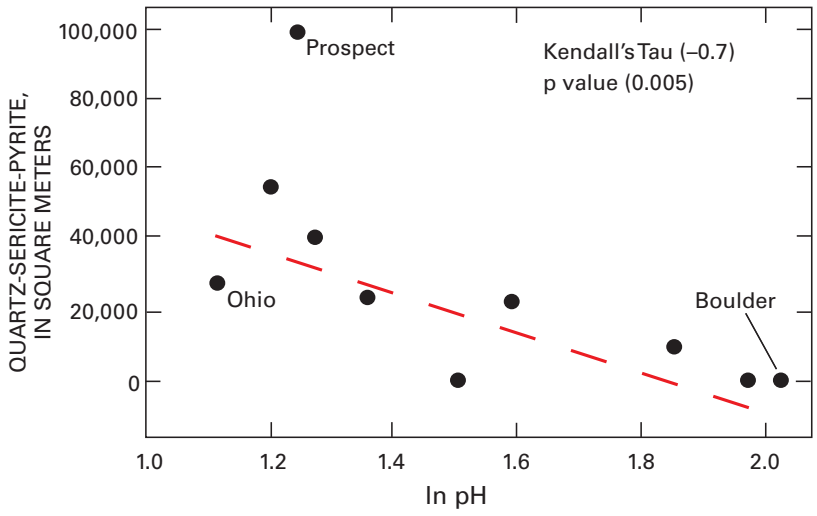

Figure 8. Linear regression results showing the correlation between catchment area of quartz-sericite-pyrite alteration and pH. Kendall's Tau negative correlation of –0.7 and low "P" value indicates that lower pH (more acidic water quality) is correlative with increasing area of quartz-sericite-pyrite alteration. Note that Boulder Gulch has less acidic water quality and contains rocks with a high acid-neutralizing capacity (see Yager, Chapter K, this volume).

A

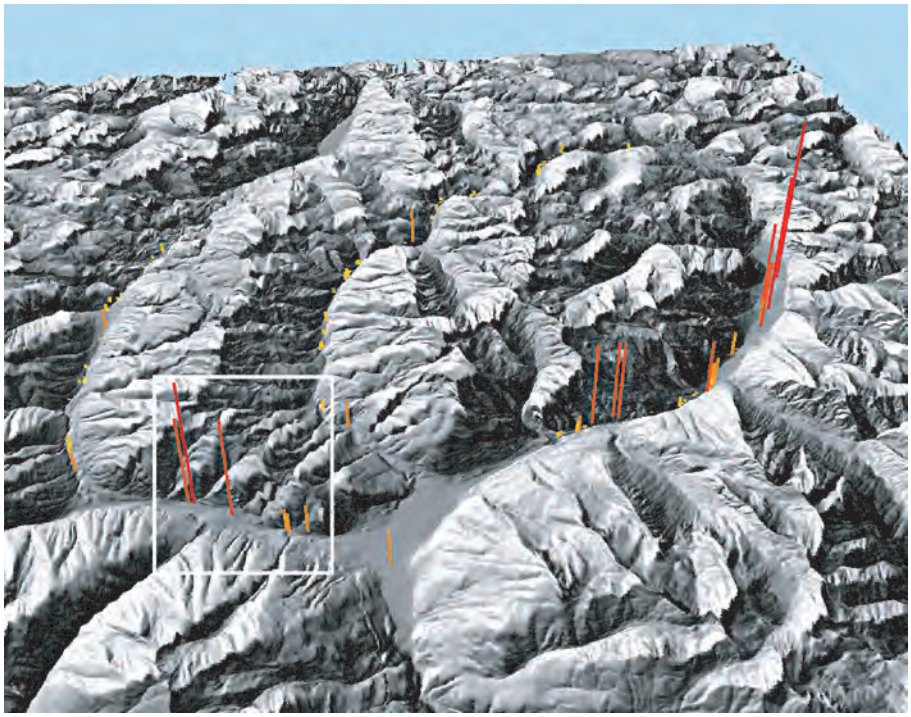

B

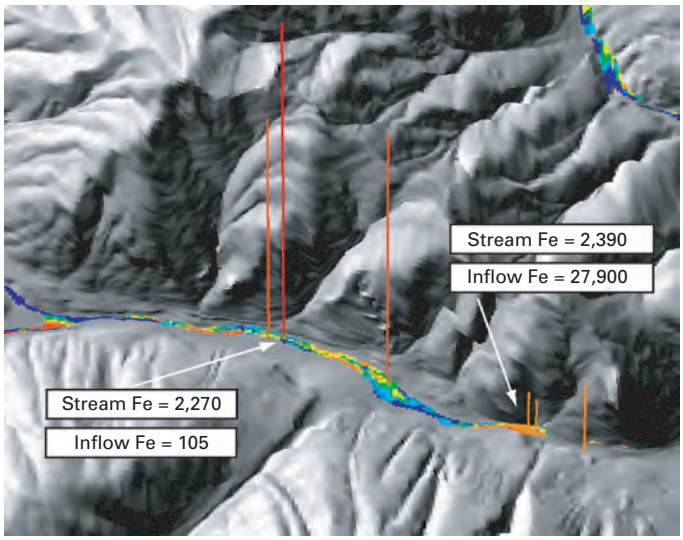

Figure 9. Ground-water inflows determined by tracer injection studies. Height of lines (*A*) are proportional to quantity of ground-water inflows that range from 0 to 0.9 cubic foot per second (yellow) to 7 cubic feet per second (red). White box (*A*) corresponds to the area in (*B*). Conductivity profiles (from airborne geophysics) and corresponding ground-water inflows shown in (*B*) along Mineral Creek. Bright colors (yellow-orange-red) correlate with increasing conductivity along the stream. White arrows point to low-conductivity ground-water inflows (left), and higher conductivity ground-water inflows (right). Iron concentrations (Fe, in micrograms per liter) shown for corresponding surface-water and ground-water inflows.

Conclusions

Multiple anthropogenic and natural catchment physical factors in each catchment combine to influence water quality. A GIS and statistical approach that evaluates the correlation between percentage of areas of geologic substrate and water-quality signals determined at the mouths of study-area catchments provides an effective way to evaluate and identify the important factors that have the greatest influence on water quality. Simultaneous statistical analysis of several physical factors, using multiple linear regression analysis, can now be used to determine how combinations of factors synergistically affect catchment water quality.

Ground-water studies commonly are limited by few direct observations of the ground-water flow system; for example, drilling or piezometers. Data from detailed surface-water and ground-water sampling and geophysical conductivity profiles helped to infer ground-water discharge areas to streams along with associated water-quality changes. By combining these data along with other GIS, AMLI geodatasets, more detailed interpretations can be made regarding ground-water quality, quantity, and flow paths. GIS approaches such as this can help land managers identify and prioritize abandoned mine areas for cleanup that will have the greatest positive effects on downstream water quality.

References Cited

Bove, D.J., Yager, D.B., Mast, M.A., and Dalton, J.B., 2007, Alteration map showing major faults and veins and associated water-quality signatures of the Animas River watershed headwaters near Silverton, southwest Colorado: U.S. Geological Survey Scientific Investigations Map 2976, 18-page pamphlet, 1 plate, scale 1:24,000.

Caine, J.S., Bove, D.J., Manning, A.H., and Verplanck, P.L., 2004, Preliminary characterization of geological controls on groundwater flow and solute transport in an alpine hydrothermal metal deposit—Handcart Gulch, Montezuma Mining district, Colorado Rocky Mountain Front Range: Geological Society of America Abstracts with Programs, v. 36, p. 539.

Dalton, J.B., Bove, D.J., and Mladinich, C.S., 2005, Remote sensing characterization of the Animas River watershed, southwestern Colorado, by AVIRIS imaging spectroscopy: U.S. Geological Survey Scientific Investigations Report 2004–5203, 49 p.

Johnson, R.H., Wirt, L., Manning, A.H., Leib, K.J., Fey, D.L., and Yager, D.B., 2007, Geochemistry of surface and ground water in Cement Creek from Gladstone to Georgia Gulch and in Prospect Gulch, San Juan County, Colorado: U.S. Geological Survey Open-File Report 2007–1004, 140 p.

Kendall, M.G., 1975, Rank correlation methods, 4th edition: Charles Griffin, London, 202 p.

Kimball, B.A., Walton-Day, Katherine, and Runkel, R.L., 2007, Quantification of metal loading by tracer injection and synoptic sampling, 1996–2000, *in* Church, S.E., von Guerard, Paul, and Finger, S.E., eds., Integrated investigations of environmental effects of historical mining in the Animas River watershed, San Juan County, Colorado: U.S. Geological Survey Professional Paper 1651, chap. E9, p. 417–495.

Mast, M.A., Verplanck, P.L., Wright, W.G., and Bove, D.J., 2007, Characterization of background water quality, *in* Church, S.E., von Guerard, Paul, and Finger, S.E., eds., Integrated investigations of environmental effects of historical mining in the Animas River watershed, San Juan County, Colorado: U.S. Geological Survey Professional Paper 1651, chap. E7, p. 347–386.

Ritter, D.F., Kochel, R.C., and Miller, J.R., 1995, Process geomorphology, 3d ed.: New York, McGraw-Hill Professional Publishing, 560 p.

Smith, B.D., McDougal, R.R., Deszcz-Pan, Maryla, and Yager, D.B., 2007, Helicopter electromagnetic and magnetic surveys, *in* Church, S.E., von Guerard, Paul, and Finger, S.E., eds., Integrated investigations of environmental effects of historical mining in the Animas River watershed, San Juan County, Colorado: U.S. Geological Survey Professional Paper 1651, chap. E4, p. 231–254.

Sole, T.C., Grannito, Matthew, Rich, C.L., Litke, D.W., and Pelltier, R.T., 2007, Digital databases and CD–ROM for the Animas River watershed, *in* Church, S.E., von Guerard, Paul, and Finger, S.E., eds., Integrated investigations of environmental effects of historical mining in the Animas River watershed, San Juan County, Colorado: U.S. Geological Survey Professional Paper 1651, chap. G, p. 1079–1096.

Viger, R.J., Markstrom, S.L., and Leavesley, G.H., 1998, The GIS Weasel—An interface for the treatment of spatial information used in watershed modeling and water resource management: Proceedings of the First Federal Interagency Hydrologic Modeling Conference April 19–23, 1998, Las Vegas, Nevada, v. II, chap. 7, p. 73–80.

von Guerard, Paul, Church, S.E., Yager, D.B., and Besser, J.M., 2007, The Animas River watershed, San Juan County, Colorado, *in* Church, S.E., von Guerard, Paul, and Finger, S.E., eds., Integrated investigations of environmental effects of historical mining in the Animas River watershed, San Juan County, Colorado: U.S. Geological Survey Professional Paper 1651, chap. B, p. 17–38.

Yager, D.B., and Bove, D.J., 2007, Geologic framework, *in* Church, S.E., von Guerard, Paul, and Finger, S.E., eds., Integrated investigations of environmental effects of historical mining in the Animas River watershed, San Juan County, Colorado: U.S. Geological Survey Professional Paper 1651, chap. E1, p. 107–140.

Yager, D.B., and Caine, J.S., 2003, GIS analysis of the fundamental geologic, topographic, and mining-related factors that influence water quality: Geological Society of America Abstracts with Programs, v. 35, no. 5, p. 6.

Yager, D.B., Caine, J.S., Bove, D.J., Church, S.E., Smith, B.D., McDougal, R.R., Wirt, Laurie, Mast, M.A., Kimball, B.A., and Walton-Day, Katherine, 2002, A GIS data viewer for physical and geochemical characterization of abandoned mine lands—An example from the Animas River watershed, Silverton, Colorado: Geological Society of America Abstracts with Programs, v. 34, no. 6, p. 145.

Yager, D.B., McCafferty, A.E., Stanton, M.R., Diehl, S.F., Driscoll, R.L., Fey, D.L., and Sutley, S.J., 2005, Net acid production, acid neutralizing capacity, and associated geophysical, mineralogical, and geochemical characteristics of Animas River watershed rocks near Silverton, Colorado: U.S. Geological Survey Open-File Report 2005–1433, 75 p.

Part 3—Postremediation Recovery of Stream Ecosystems

After metals and acidity have been mobilized from their sources and transported to receiving streams, determining their fate and effect on the ecosystem is important to the understanding the potential effects of abandoned mines and mineralized but unmined areas. The effects of metals and acidity on ecosystems have been closely monitored by mining companies, land managers, and government regulators involved in mine sites. It has been determined that different factors contribute to the movement of metals and acidic water through our environment. This section presents time-series data collected as part of the downstream monitoring effort at three mine sites to evaluate the changes in water chemistry that affect the recovery of the aquatic ecosystem.

Chapter N: Recovery of Aquatic Life in Surface Streams Affected by Mining Following Remediation

by Stanley E. Church

Overview

Documentation of the successful recovery of aquatic life downstream from remediated mine sites has been examined at three sites: the Animas River watershed in Colorado, the Boulder River watershed in Montana, and the Gila River in Arizona. The first two sites were studied extensively during the U.S. Geological Survey Abandoned Mine Lands Initiative (AMLI, 1997–2002). These data show that recovery of both the riparian habitat and aquatic life in the immediate downstream reach is highly dependent upon many variables: geologic setting, rock types present in the watershed, the topographic relief in the watershed and geomorphology of the stream reaches affected, nature and extent of hydrothermal alteration in the watershed, metals released and their residence time in various media, pH of the water in the receiving stream, and extent to which adequate financial resources were available for the remedial activities. One outcome from the AMLI studies has been the development of a decision tree to be used to determine what scientific studies are most useful in watershed characterization (Kimball and others, 2006). Examples of successful restoration activities are documented for the Boulder River watershed, and remediation work in the Animas River watershed has perhaps resulted in some small downstream improvement of water and sediment quality.

Work at the third site, downstream from the Morenci mine site in Arizona, has demonstrated that mitigation resulted in improved water and sediment quality. The environmental contamination resulted from poor management of mine-site runoff. Corrective action by Phelps Dodge, the operator at the time, resulted in immediate downstream improvement in water and sediment quality in the San Carlos Reservoir.

Introduction

The effect of mining on water quality has been examined in detail by many workers (Nimick and others, 2004; Church, von Guerard, and Finger, 2007, and numerous references therein). These studies have shown that the processes resulting in acidic drainage are multiple, and the remedial solutions are often quite complex. It is necessary to separate the effects of weathering of hydrothermally altered rock from the additional effects resulting from mining. Furthermore, it is necessary to carefully define the goals of any remedial work done on the watershed to improve aquatic-life habitat. The terms remediation, reclamation, rehabilitation, and restoration all have differing ecological goals (Finger, Church, and von Guerard, 2007). Using the watershed approach defined in the Abandoned Mine Land Initiative (Buxton and others, 1997), the U.S. Geological Survey recommended to the Bureau of Land Management (BLM) and to the U.S. Department of Agriculture (USDA) Forest Service that the most cost-effective approach to achieving ecological goals was to focus on those sites within a watershed where the largest effect could be achieved with the remediation efforts (Nimick and others, 2004; Church, von Guerard, and Finger, 2007). A summary of the scientific methods developed, data obtained, and critical information developed from these different studies was presented in Kimball and others (2006). This summary can be used by Federal and State land-management agencies, private entities, and stakeholder groups as guidelines for evaluating the scientific information needed before developing a site or watershed remediation plan. At a recent conference, Federal land-management agencies summarized a decade of watershed remedial work (USDA Forest Service and Bureau of Land Management, 2007). Successful remediation (removal of contaminants and improvement of water quality downstream as a result of work on a site), reclamation (recontouring and reestablishing of vegetation at a site), and restoration (reestablishment of the ecological function of the site as shown by self-sustaining fish populations and a healthy riparian zone) have occurred on Federal lands throughout the Western United States (Finger and others, 2004, 2007). One of the fundamental issues that has been poorly documented in the scientific literature is the length of time necessary to achieve restoration given a set of starting conditions and the scope of remedial work undertaken.

During the course of this project, we have had the opportunity to evaluate remedial work undertaken by Federal and State agencies and by private industry at three sites: the Boulder River watershed in Montana, the Animas River watershed in Colorado, and in the San Carlos Reservoir on the Gila River downstream from the Morenci copper mine in Arizona (fig. 1). The necessary monitoring data to support aquatic recovery at other remediated sites probably exists in a fragmented state for many other remediated mine sites or watersheds, but generally these data reside in unpublished reports by various consultants used during the course of remediation and are neither available to the public nor in the scientific literature. In order to demonstrate the success of recovery of aquatic life, we need to have thorough documentation of the conditions prior to remediation and monitoring data collected during and following the remediation for a substantial period of time (Finger and others, 2004, 2007). Our results, discussed more fully in this chapter, show that recovery of aquatic life downstream from the remediated sites is highly dependent upon the geologic setting, rock types present in the watershed, topographic relief in the watershed and geomorphology of the stream reaches affected, the nature and extent of hydrothermal

alteration in the watershed, metals released and their residence time in various media, pH of the water in the receiving stream, and extent to which adequate financial resources were available for the remedial activities. In two of the three sites studied, the recovery of aquatic life downstream from these remediated sites appears to require more time than anticipated. Results from three case studies will be discussed in this report:

- Recovery of the Boulder River downstream from a small historical polymetallic vein mining district in west-central Montana;
- Recovery downstream on the Animas River in southwestern Colorado, an extensive hydrothermally altered and heavily mined watershed; and
- Recovery of the Gila River and in San Carlos Reservoir downstream from a point source at the Morenci porphyry copper mine in eastern Arizona.

Three additional sites were investigated in anticipation of future remedial activities to establish preremediation baseline geochemical data; however, remedial action has not been initiated. Fey and others (2002) reported baseline sediment and water-quality results from the Snake River watershed in central Colorado. This basin is being considered for remedial work under the U.S. Environmental Protection Agency (USEPA) Brownfields program (*http://www.epa.gov/brownfields/*). Church, Fey, and Marot (2005) investigated the geochemical effect on stream sediment of the Red River both during active mining and the premining period downstream from the Questa porphyry molybdenum mine to provide documentation to the State of New Mexico for anticipated mine-site closure. Church, Kirschner, and others (2007) investigated the premining and background data in the Blue Creek watershed downstream from the Midnite uranium mine in Stevens County, Washington. Remedial action is anticipated at this site over the next decade.

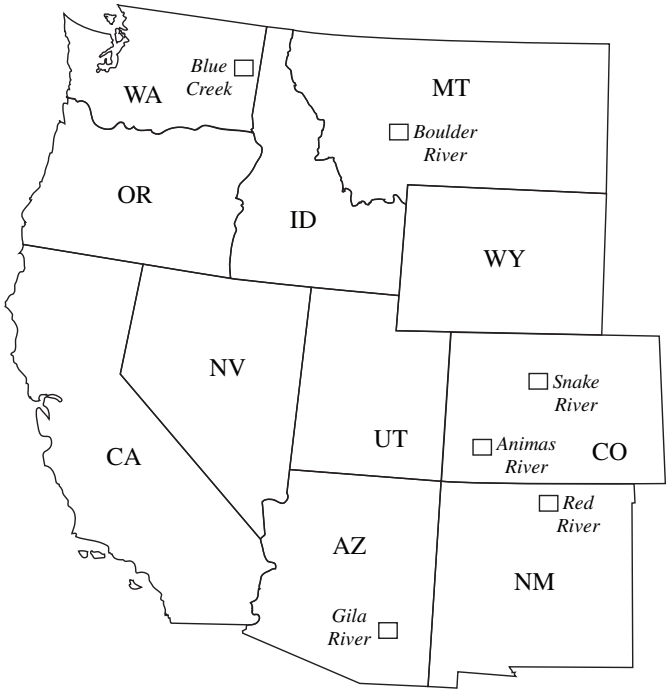

Figure 1. Index map showing study areas discussed in text.

Boulder River Watershed, Montana

Sampling of water and sediment in the Boulder River downstream from historical mine sites before remediation was documented in the U.S. Geological Survey Abandoned Mine Lands Initiative (AMLI) (Finger and others, 2004; Church and others, 2004; Nimick and Cleasby, 2004; Farag and others, 2007). Postremedial monitoring data are summarized in (Unruh and others, in press). This study shows that improvement has resulted immediately downstream from some, but not all, remediated mine sites. Overall, remedial work in the tributary basins (figs. 2 and 3) has resulted in small changes in water and sediment geochemistry over a 5-year timeframe. Historical mining in the districts was from polymetallic vein deposits in the granitic rocks in the Boulder batholith (O'Neill and others, 2004). The district produced copper, lead, silver, and zinc with minor gold from 1868 through 1958. An open pit at the Comet mine on High Ore Creek was a major source of sediment contamination (Fey and Church, 1998; Church and others, 2004) in the Boulder River, whereas dissolved constituents from Cataract Creek (Nimick and Cleasby, 2004) were the primary source of aqueous contaminants to the Boulder River (*http://ecorestoration.montana.edu/mineland/histories/metal/comet/default.htm*). The Comet mine site was remediated by the State of Montana and BLM in 1998 (Gelinas and Tupling, 2004). Monitoring work by the USGS took place over the following 5-year period. Additional monitoring work is reported in an unpublished report prepared for the BLM, Butte, Mont. (J.D. Belanger-Woods, Butch Gerbrandt, and J.P. Madison, 2003, High Ore Creek postremediation surface water sampling data summary report, 101 p.). Data from the monitoring work show:

- Temporal trends of dissolved and total concentrations of metals in water have changed in some stream reaches downstream since the remediation phase began (fig. 2).
- Extensive restoration by the State of Montana and the BLM in the High Ore Creek tributary at and downstream from the Comet mine site (Gelinas and Tupling, 2004) has resulted in restoration of High Ore Creek as a viable trout fishery with an excellent riparian zone (fig. 3; Mike Browne, written commun., 2007).

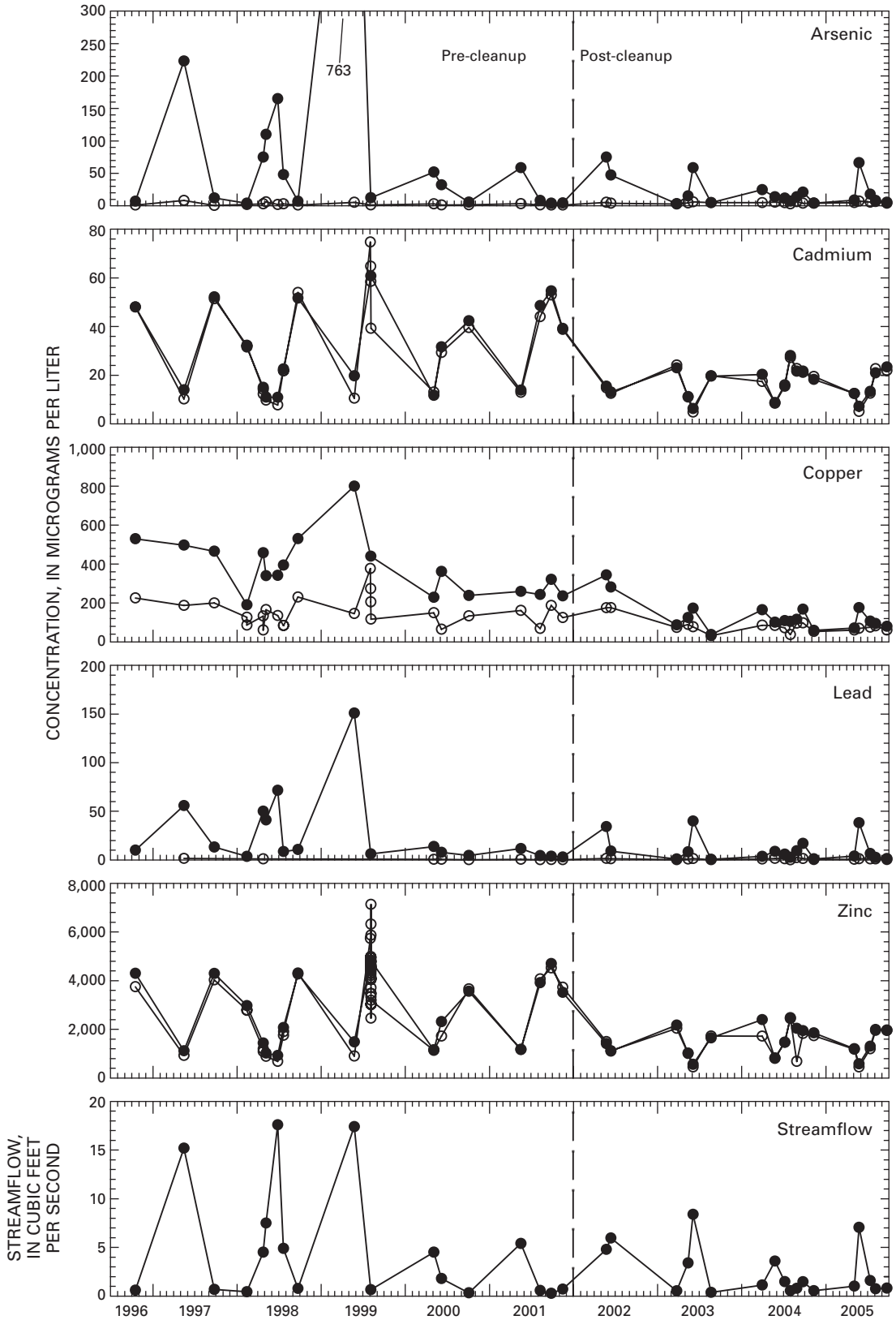

Figure 2. Temporal trends of streamflow and concentrations of dissolved (open circles) and total (closed circles) trace elements in water, Uncle Sam Gulch, 1996–2005, a contaminated tributary of Cataract Creek in the Boulder River watershed study area (Unruh and others, in press). Upstream remediation work shutting off surface water flowing into the Crystal mine was completed in 2002 (dashed line in figure) and resulted in a reduction in the amount of copper and zinc released.

Figure 3. High Ore Creek photographs showing changes in the riparian zone before and after restoration by Bureau of Land management in 2002. Photographs provided by Mike Browne (2007).

- Removal actions have been conducted by the USDA Forest Service in the Basin and Cataract Creek tributaries (fig. 4), but little improvement in sediment quality or aquatic life has been demonstrated downstream in the Boulder River (Rhea and others, 2006; Unruh and others, in press).
- Stream response to remedial actions (1998–2001) was demonstrated in the water-quality sampling, but no measurable improvement is indicated by the sediment or biological data in the Boulder River downstream from the tributaries where restoration has been conducted (Unruh and others, in press).
- The recovery curve for biota in the Boulder River is projected to be a decadal response function unless contaminated sediment is removed from the Boulder River.

Animas River Watershed, Colorado

The Animas River watershed is a heavily mineralized and highly altered area (Church, von Guerard, and Finger, 2007). Fish habitat is limited; food supply is limited by high dissolved concentrations of cadmium and zinc, and fish are limited by high dissolved concentrations of copper (Besser and others, 2001, 2007). Remediation costs in the Animas River watershed by all sources through 2004 have exceeded $20 million (Church, Owen, and others, 2007). Monitoring of sediment and water has shown very little improvement although some benthic macroinvertebrates have reappeared in stream reaches on lower Mineral Creek that were previously barren (Anderson, 2007; William Simon, oral commun., 2006). The following summary is largely from Church, Owen, and others (2007):

- Remediation work in the headwaters of Mineral Creek has lowered the dissolved loads of zinc and copper associated with historical mining of breccia pipe deposits in the Red Mountain district in the headwaters of Mineral Creek.
- Remediation work in the headwaters of Cement Creek has lowered the dissolved concentrations of manganese and sulfate.
- During the period from April 1996 through April 1999, the water-treatment plant operating at Gladstone by the Sunnyside Gold Corporation lowered the dissolved copper and zinc load in Cement Creek relative to preremediation conditions (Kimball and others, 2002; fig. 5).
- Extensive remediation of mill wastes disposed of in the Animas River has resulted in small changes in dissolved metal concentrations: copper and zinc have improved slightly, manganese concentrations have elevated substantially, and sulfate concentrations are somewhat elevated above the preremediation baseline concentrations, possibly because of the remediation work that disturbed the streambed and exposed new material (Kimball and others, 2007; Church, Owen, and others, 2007; fig. 6).
- Analysis of aerial photography from the upper Animas River over a 50-year period (Vincent and

Figure 4. Buckeye mill site in the upper reaches of Basin Creek, showing site before and after reclamation. The mill tailings (white waste pile on the flood plain, top photograph) released metals and contaminated sediment to the stream during high-flow runoff (Cannon and others, 2004). Photographs from Nimick (2004).

Elliott, 2007) showed a slow rate of recovery of willows in the riparian zone downstream from the Sunnyside mill. Without implementation of riparian zone restoration like that in High Ore Creek, recovery of the riparian habitat downstream from the Eureka mill will likely require many decades, if not centuries, to restore the riparian ecological function of this reach to premining conditions (Vincent and Elliott, 2007).

- Dissolved concentration data from the compliance point downstream from the confluence of the two major tributaries with the Animas River show little change over the decade of monitoring and ongoing remediation (fig. 6). Remediation in this ecosystem will be measured in several decades, if not centuries (Church, Owen, and others, 2007).

San Carlos Reservoir Downstream from the Morenci Copper Mine, Gila and San Francisco Rivers, Arizona

Sediment cores from the San Carlos Reservoir clearly document the release of copper from the Morenci porphyry copper mine site over time (fig. 7). The age of sediment in the core was dated using ^{137}Cs and ^{210}Pb methods. Core geochemistry was correlated with historical documentation of contamination at the mine site (Church, Fey, and Marot, 2005). The data show:

- When open-pit mining began at Morenci in the late 1930s, the copper concentration in sediment in the San Carlos Reservoir was at about the crustal abundance concentration for copper (CA_{Cu} = 68 parts per million; Fortescue, 1992), that is, about half of the probable-effects sediment quality guideline concentration for copper (SQG_{Cu} = 149 ppm; MacDonald and others, 2000). At this concentration, the SQG_{Cu} accurately predicts a toxic effect 90 percent or more of the time for sediment-dwelling organisms (n = 347).
- About the year 1957, there was a one-time release of copper that greatly exceeded SQG (245-cm depth, core 04SCR112). This event was accompanied by a zinc release that also exceeded SQG (SQG_{Zn} = 459 ppm, MacDonald and others, 2000). Recovery was essentially instantaneous, but the release would have resulted in massive acute aquatic exposure and probably death. Unfortunately, no biological data are available from that time period.
- Further development at the mine site and lapse in environmental monitoring at the mine site resulted in a long period of elevated copper release beginning about 1967.
- The Morenci copper mine entered into a cease-and-desist consent decree with the USEPA in 1986 (Chase Creek Consent Decree, U.S. Department of Justice and Phelps Dodge Corporation, August 25, 1986, filed with the U.S. District Court in Arizona) and immediately instituted surface-runoff controls on the mine site. The result downstream was essentially instantaneous: copper concentrations dropped to near the SQG where they have remained ever since.
- Open-pit mining over the past 70 years has resulted in doubling the copper concentration in the sediment in the San Carlos Reservoir, near the point at which many aquatic organisms would be affected (fig. 7; Church and others, 2005).
- BLM has granted Freeport-McMoRan, the current operator, a NO-RELEASE permit to develop the Dos Pobres and Safford porphyry copper open-pit mines downstream from the Morenci copper mine, but upstream from the San Carlos Reservoir.

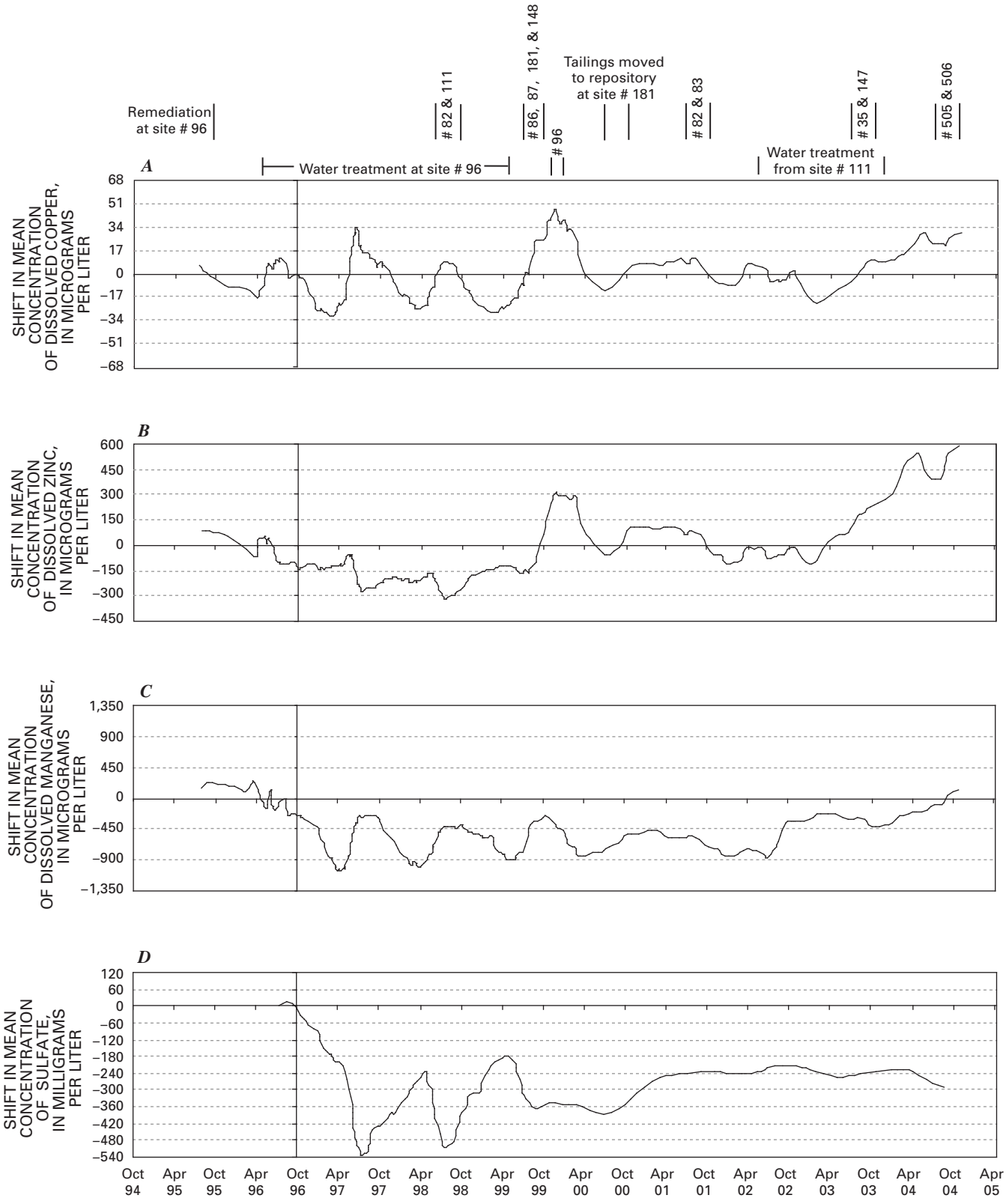

Figure 5. Time-series plots showing 12 sample moving-average concentrations of dissolved copper (*A*), zinc (*B*), manganese (*C*), and sulfate (*D*) in Cement Creek. Water sampled at USGS gage (09358550) on Cement Creek. Baseline monitoring data collected from 1994 to 1996. Remediation at mine sites and period of operation of the water-treatment plant at Gladstone are shown at top of figure. See Church, Owen, and others (2007) for details.

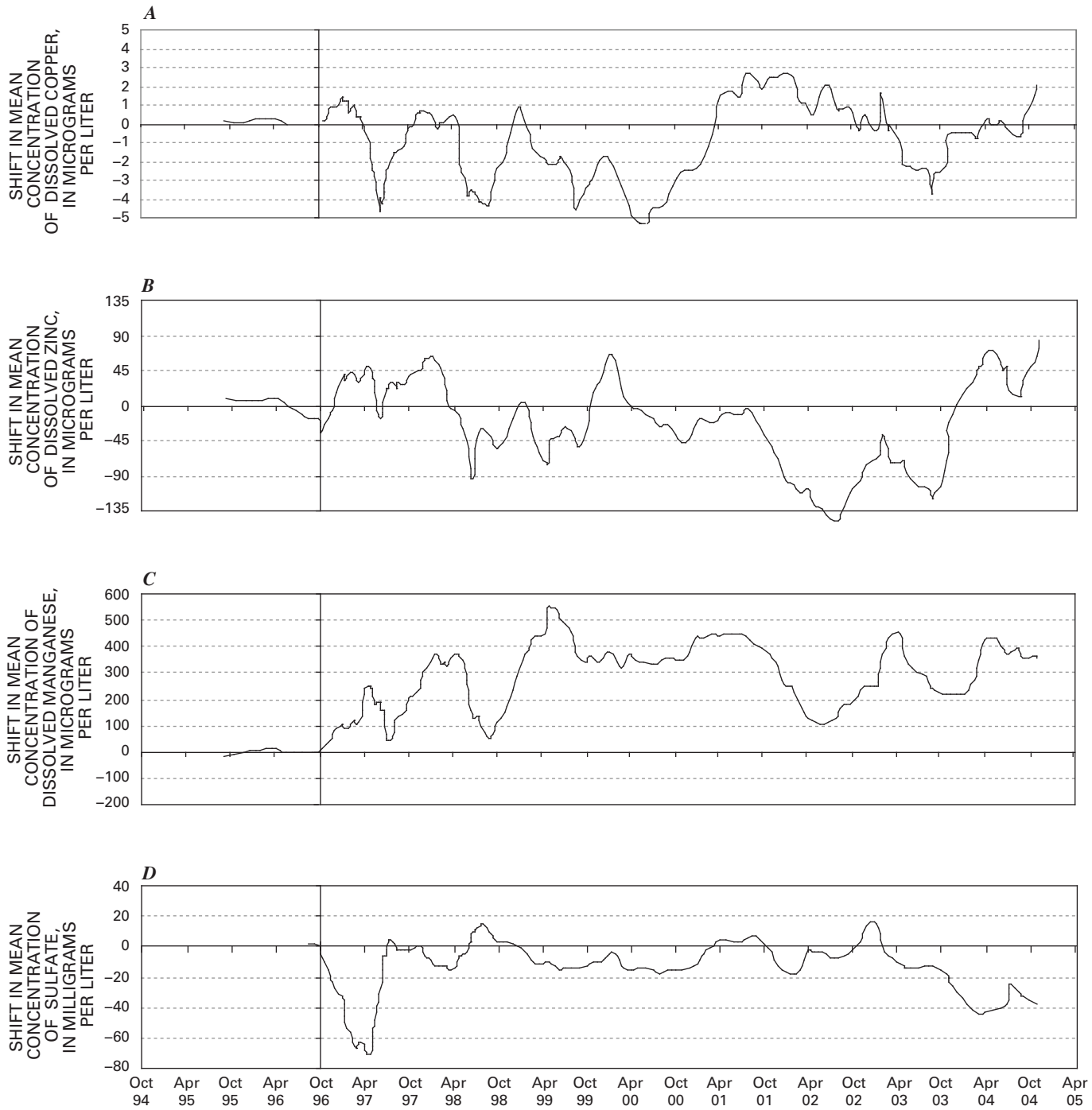

Figure 6. Time-series plots showing 12 sample moving-average concentrations of dissolved copper (*A*), zinc (*B*), manganese (*C*), and sulfate (*D*) at the compliance site downstream from the confluence of Mineral Creek with the Animas River. Water sampled at the USGS gage (09359020). Baseline monitoring data collected from 1991 to 1996. See Church, Owen, and others (2007) for details.

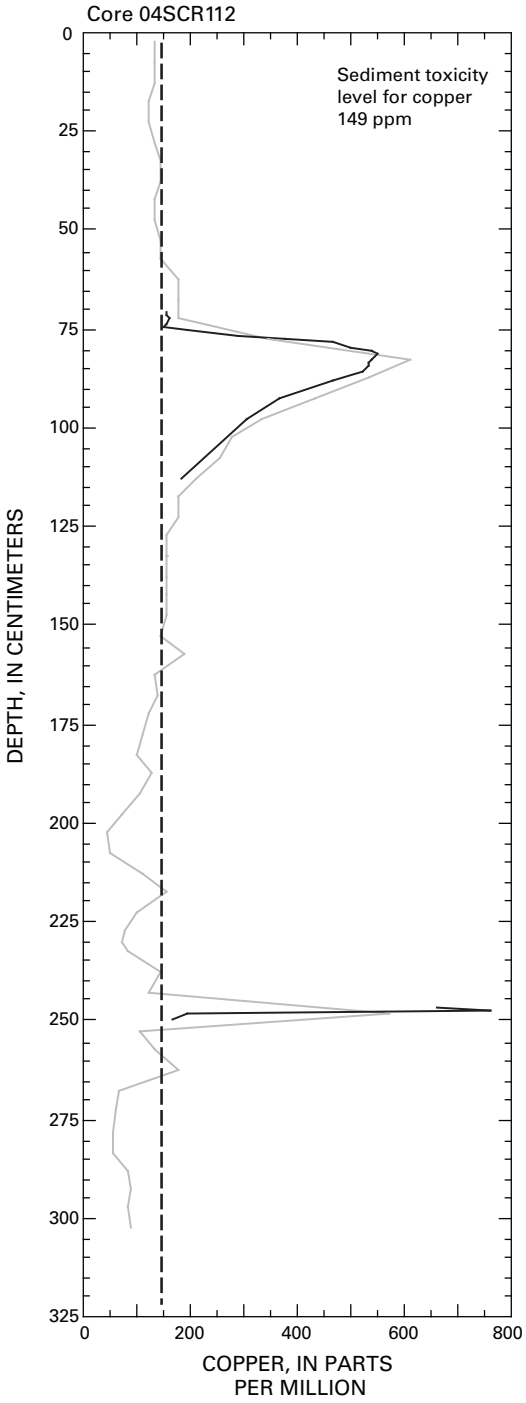

Figure 7. Variation of concentration of copper in sediment with depth, core 04SCR112, San Carlos Reservoir (gray line; Church, Choate, and others, 2005). Two large copper spikes are preserved in the sediment core and record uncontrolled releases that occurred at the Morenci copper mine. Analysis of the contaminant peaks was undertaken in 2007 at 1-centimeter intervals (black line). These new analyses confirm the instantaneous nature of the release at 243 centimeters that took place in about the year 1957. The second was a prolonged release from the mine site that began in 1978 and lasted through 1983 (124–72 centimeter depth). The dashed line is the SQG_{Cu} concentration (149 parts per million; MacDonald and others, 2000).

Summary

Our studies of aquatic recovery downstream from remediated mine sites show that, at active mine sites, release of metal contaminants to surface streams can be controlled with onsite engineering remedies and controls, and that the downstream response can be essentially immediate once those remedies are implemented. The Morenci copper mine is one example of such a success story. Comparison of the concentrations of copper, lead, and zinc measured in the active stream channel of the San Francisco and Gila Rivers downstream from the Morenci mine site to San Carlos Reservoir in 1990 and 2004 shows very similar results and does not appear to indicate that sediment in the active downstream channel in the Gila and San Francisco Rivers constitutes a long-term sink of contaminated sediment (fig. 7). Likewise, a spill, probably of molybdenum product at the Questa mine site, also showed an immediate response to the cleanup of the spill in sediment cored from Eagle Rock Lake on the Red River (Church, Fey, and Marot, 2005).

In a watershed where there is little hydrothermal alteration, the primary source of metals is mine-waste piles, mill tailings, and acidic water generated at the mine sites. In this case, the cleanup of the largest contributing sites in the watershed will result in an improvement of the water and sediment quality in the immediate downstream reach, but stored fluvial tailings and mine waste in sediment traps such as overbank deposits, stream meanders, and oxbow lakes must also be removed to achieve recovery of aquatic life and restoration of a functional riparian zone. Excellent results are shown by the remediation on the Buckeye mine site in upper Basin Creek and the Comet mine site in High Ore Creek (figs. 3 and 4).

In watersheds where the geology is more complex and hydrothermal alteration extensive (Bove and others, 2007), determination of premining water and sediment quality is more difficult (Church, Fey, and Unruh, 2007). Defining remedial objectives that are financially achievable may not result in restoration of aquatic life in the immediate downstream reach, but the improvement in water and sediment quality achieved will improve aquatic habitat to the point where aquatic life may return to previously dead downstream reaches. This has been the goal of the Federal and State land managers and the local stakeholders group in the Animas River watershed. It is especially important to recognize that some stream reaches in these watersheds may not have supported aquatic life prior to mining (Besser and others, 2007; Church, Fey, and Unruh, 2007).

References Cited

Anderson, C.R., 2007, Effects of mining on benthic macroinvertebrate communities and monitoring strategy, *in* Church, S.E., von Guerard, Paul, and Finger, S.E., eds., Integrated investigations of environmental effects of historical mining in the Animas River watershed, San Juan County, Colorado: U.S. Geological Survey Professional Paper 1651, p. 851–872.

Besser, J.M., Brumbaugh, W.G., May, T.W., Church. S.E., and Kimball, B.A., 2001, Bioavailability of metals in stream food webs and hazards to brook trout (Salvelinus fontinalis) in the upper Animas River watershed, Colorado: Archives of Environmental Contamination and Toxicology, v. 40, p. 48–59.

Besser, J.M., Finger, S.E., and Church, S.E., 2007, Impacts of historical mining on aquatic ecosystems—An ecological risk assessment, *in* Church, S.E., von Guerard, Paul, and Finger, S.E., eds., Integrated investigations of environmental effects of historical mining in the Animas River watershed, San Juan County, Colorado: U.S. Geological Survey Professional Paper 1651, p. 87–106.

Bove, D.J., Yager, D.B., Mast, M.A., and Dalton, J.B., 2007, Alteration map showing major faults and veins and associated water-quality signatures of the Animas River watershed headwaters near Silverton, southwest Colorado: U.S. Geological Survey Scientific Investigations Map 2976, 18-page pamphlet, 1 plate, scale 1:24,000.

Browne, Mike, 2007, Montana abandoned mine land program ten-year anniversary, Presentation made at the BLM and Forest Service meeting, Silverton, Colo., September 27, 2007.

Buxton, H.T., Nimick, D.A., von Guerard, Paul, Church, S.E., Frazier, Ann, Gray, J.R., Lipin, B.R., Marsh, S.P., Woodward, Daniel, Kimball, Briant, Finger, Susan, Ischinger, Lee, Fordham, J.C., Power, M.S., Bunck, Christine, and Jones, J.W., 1997, A science-based, watershed strategy to support effective remediation of abandoned mine lands: Proceedings of the Fourth International Conference on Acid Rock Drainage, Vancouver, B.C., May 31–June 6, 1997, p. 1869–1880.

Cannon, M.R., Church, S.E., Fey, D.L., McDougal, R.R., Smith, B.D., and Nimick, D.A., 2004, Understanding trace-element sources and transport to upper Basin Creek in the vicinity of the Buckeye and Enterprise mines, *in* Nimick, D.A., Church, S.E., and Finger, S.E., eds., Integrated investigations of environmental effects of historical mining in the Basin and Boulder mining districts, Boulder River watershed, Jefferson County, Montana: U.S. Geological Survey Professional Paper 1652, p. 401–455.

Church, S.E., Choate, L.M., Marot, M.E., Fey, D.L., Adams, Monique, Briggs, P.H., and Brown, Z.A., 2005, Geochemical assessment of metals and dioxin in sediment from the San Carlos Reservoir and the Gila, San Carlos, and San Francisco Rivers, Arizona: U.S. Geological Survey Scientific Investigations Report 2005–5086, 61 p. (*http://pubs.usgs.gov/sir/2005/5086/*)

Church, S.E., Fey, D.L., and Marot, M.E., 2005, Questa baseline and pre-mining ground-water quality investigation 8—Lake-sediment geochemical record from 1960 to 2002, Eagle Rock and Fawn Lakes, Taos County, New Mexico: U.S. Geological Survey Scientific Investigations Report 2005–5006, 47 p. *http://pubs.usgs.gov/sir/2005/5006/*

Church, S.E., Fey, D.L., and Unruh, D.M, 2007, Trace elements and lead isotopes in modern streambed and terrace sediment—Determination of current and premining geochemical baselines, *in* Church, S.E., von Guerard, Paul, and Finger, S.E., eds., Integrated investigations of environmental effects of historical mining in the Animas River watershed, San Juan County, Colorado: U.S. Geological Survey Professional Paper 1651, p. 571–642. *http://pubs.usgs.gov/pp/1651/*

Church, S.E., Kirschner, F.K., Choate, L.M., Lamothe, P.J., Budahn, J.R., and Brown, Z.A., 2007, Geochemical premining background study of the Blue Creek drainage, Stevens County, Washington: U.S. Geological Survey Scientific Investigations Report 2007–5262, 177 p. *http://pubs.usgs.gov/sir/2007/5262/*

Church, S.E., Owen, J.R., von Guerard, Paul, Verplanck, P.L., Kimball, B.A., and Yager, D.B., 2007, The effects of acidic mine drainage from historical mines in the Animas River watershed, San Juan County, Colorado—What is being done and what can be done to improve water quality? *in* DeGraff, J.V., ed.: Geological Society of America Reviews in Engineering Geology, v. XVII, p. 47–83.

Church, S.E., Unruh, D.M., Fey, D.L., and Sole, T.C., 2004, Trace elements and lead isotopes in streambed sediment in streams affected by historical mining, *in* Nimick, D.A., Church, S.E., and Finger, S.E., eds., Integrated investigations of environmental effects of historical mining in the Basin and Boulder mining districts, Boulder River watershed, Jefferson County, Montana: U.S. Geological Survey Professional Paper 1652, p. 279–336.

Church, S.E., von Guerard, Paul, and Finger, S.E., eds., 2007, Integrated investigations of environmental effects of historical mining in the Animas River watershed, San Juan County, Colorado: U.S. Geological Survey Professional Paper 1651, 6 plates, 1 DVD, 1096 p.

Farag, A.M., Kimball, B.A., Nimick, D.A., Church, S.E., and Brumbaugh, W.G., 2007, Concentrations of metals in water, sediment, biofilm, benthic macroinvertebrates and fish in the Boulder River Watershed, Montana, and the role of colloids in metal uptake: Archives of Environmental Contamination and Toxicology, v. 46, p. 397–409.

Fey, D.L., and Church, S.E., 1998, Analytical results for 42 fluvial tailings cores and 7 stream-sediment samples from High Ore Creek, northern Jefferson County, Montana: U.S. Geological Survey Open-File Report 98–215, 49 p.

Fey, D.L., Church, S.E., Unruh, D.M., and Bove, D.J., 2002, Water and sediment study of the Snake River watershed, Colorado, Oct. 9–12, 2001: U.S. Geological Survey Open-File Report 2002–330, 41 p. *http://pubs.er.usgs.gov/usgspubs/ofr/ofr02330*

Finger, S.E., Church, S.E., and Nimick, D.A., 2004, Evaluating the success of restoration in the Boulder River watershed, *in* Nimick, D.A., Church, S.E., and Finger, S.E., eds., Integrated investigations of environmental effects of historical mining in the Basin and Boulder mining districts, Boulder River watershed, Jefferson County, Montana: U.S. Geological Survey Professional Paper 1652, p. 495–502.

Finger, S.E., Church, S.E., and von Guerard, Paul, 2007, Potential for successful ecological restoration, remediation, and monitoring, *in* Church, S.E., von Guerard, Paul, and Finger, S.E., eds., Integrated investigations of environmental effects of historical mining in the Animas River watershed, San Juan County, Colorado: U.S. Geological Survey Professional Paper 1651, p. 1065–1078.

Fortescue, J.A.C., 1992, Landscape geochemistry—Retrospect and prospect—1990: Applied Geochemistry, v. 7, p. 1–54.

Gelinas, S.L., and Tupling, Robert, 2004, Monitoring remediation—Have mine-waste and mill-tailings removal and flood-plain restoration been successful in the High Ore Creek valley?, *in* Nimick, D.A., Church, S.E., and Finger, S.E., eds., Integrated investigations of environmental effects of historical mining in the Basin and Boulder mining districts, Boulder River watershed, Jefferson County, Montana: U.S. Geological Survey Professional Paper 1652, p. 457–473.

Kimball, B.A., Church, S.E., and Besser, J.M., 2006, Lessons learned from the U.S. Geological Survey Abandoned Mine Lands Initiative—1997–2002, *in* Proceedings from the Seventh International Conference on Acid Rock Drainage, St. Louis, Missouri, March 26–30, 2006, p. 944-963.

Kimball, B.A., Runkel, R.L., Walton-Day, Katherine, and Bencala, K.E., 2002, Assessment of metal loads in watersheds affected by acid mine drainage by using tracer injection and synoptic sampling, Cement Creek, Colorado, USA: Applied Geochemistry, v. 17, p. 1183–1207.

Kimball, B.A., Walton-Day, Katherine, and Runkel, R.L., 2007, Quantification of metal loading by tracer injection and synoptic sampling, 1996–2000, *in* Church, S.E., von Guerard, Paul, and Finger, S.E., eds., Integrated investigations of environmental effects of historical mining in the Animas River watershed, San Juan County, Colorado: U.S. Geological Survey Professional Paper 1651, p. 417–496.

MacDonald, D.D., Ingersoll, C.G., and Berger, T.A., 2000, Development and evaluation of consensus-based sediment quality guidelines for freshwater ecosystems: Archives of Environmental Contamination and Toxicology, v. 39, p. 20–31.

Nimick, D.A., 2004, Environmental effects of historical mining in the Boulder River watershed, southwestern Montana: U.S. Geological Survey Fact Sheet 2005–3148, 2 p. *http://pubs.usgs.gov/fs/2005/3148/*

Nimick, D.A., Church, S.E., and Finger, S.E., eds., 2004, Integrated investigations of environmental effects of historical mining in the Basin and Boulder mining districts, Boulder River watershed, Jefferson County, Montana: U.S. Geological Survey Professional Paper 1652, 524 p. *http://pubs.er.usgs.gov/pubs/pp/pp1652*

Nimick, D.A., and Cleasby, T.E., 2004, Trace elements in water in streams affected by historical mining, *in* Nimick, D.A., Church, S.E., and Finger, S.E., eds., Integrated investigations of environmental effects of historical mining in the Basin and Boulder mining districts, Boulder River watershed, Jefferson County, Montana: U.S. Geological Survey Professional Paper 1652, p. 155–190.

O'Neill, J.M., Lund, Karen, Van Gosen, B.S., Desborough, G.A., Sole, T.S., and DeWitt, E.H., 2004, Geologic framework, *in* Nimick, D.A., Church, S.E., and Finger, S.E., eds., Integrated investigations of environmental effects of historical mining in the Basin and Boulder mining districts, Boulder River watershed, Jefferson County, Montana: U.S. Geological Survey Professional Paper 1652, p. 49–88.

Rhea, D.T., Harper, D.D., Farag, A.M., and Brumbaugh, W.G., 2006, Biomonitoring in the Boulder River watershed, Montana, USA—Metal concentrations in biofilm and macroinvertebrates, and relations with macroinvertebrate assemblage: Environmental Monitoring Assessment, v. 115, p. 381–393.

Unruh, D.M., Church, S.E., Nimick, D.A., and Fey, D.L., in press, Metal contamination and post-remediation recovery in the Boulder River watershed, Jefferson County, Montana: Geochemistry: Exploration, Environment, Analysis.

U.S. Department of Agriculture, Forest Service, and U.S. Department of Interior, Bureau of Land Management, 2007, Abandoned mine lands—A decade of progress reclaiming hardrock mines: Forest Service Publication No. FS–891, 33 p.

Vincent, K.R., and Elliott, J.G., 2007, Response of the upper Animas River downstream from Eureka to discharge of mill tailings, *in* Church, S.E., von Guerard, Paul, and Finger, S.E., eds., Integrated investigations of environmental effects of historical mining in the Animas River watershed, San Juan County, Colorado: U.S. Geological Survey Professional Paper 1651, p. 889–941.

Publishing support provided by:
Denver Publishing Service Center, Denver, Colorado
Manuscript approved for publication, August 13, 2008
Edited by Mary A. Kidd
Graphics and layout by Joy Monson

For more information concerning this publication, contact:
Team Chief Scientist, USGS Central Mineral Resources
Box 25046, MS 973
Denver, CO 80225
(303) 236-1562

Or visit the Central Mineral Resources Team Web site at:
http://minerals.cr.usgs.gov/

This publication is available online at:
http://pubs.usgs.gov/cir/1328/